NORSAR

AD-A268 619

‖‖‖‖‖‖‖‖‖‖‖‖‖‖‖‖‖‖

①

NORSAR Scientific Report No. 1-92/93

Semiannual Technical Summary

1 April — 30 September 1992

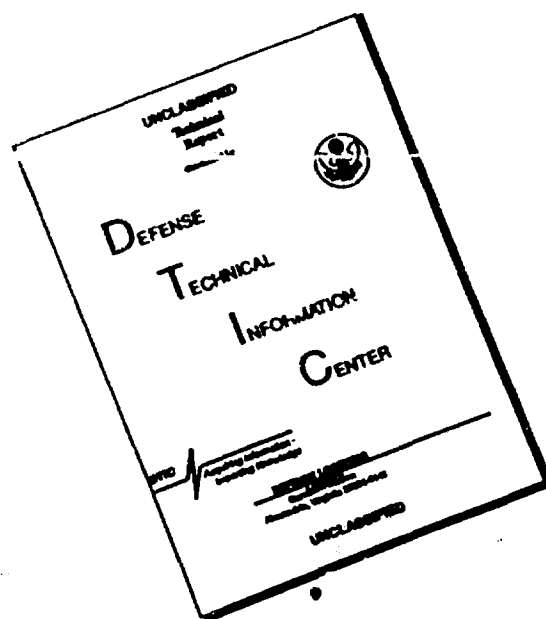Kjeller, November 1992

DTIC
ELECTE
AUG 2 5 1993
S E D

93-19874
‖‖‖‖‖‖‖‖‖‖‖‖

93 8 24 208

DISCLAIMER NOTICE

THIS DOCUMENT IS BEST QUALITY AVAILABLE. THE COPY FURNISHED TO DTIC CONTAINED A SIGNIFICANT NUMBER OF PAGES WHICH DO NOT REPRODUCE LEGIBLY.

NORSAR Scientific Report No. 1-92/93

Semiannual Technical Summary

1 April - 30 September 1992

Kjeller, November 1992

Accesion For		
NTIS CRA&I		☒
DTIC TAB		☐
U announced		☐
Justification		
By		
Distribution /		
Availability Codes		
Dist	Avail and / or Special	
A-1		

REPORT DOCUMENTATION PAGE

1a. REPORT SECURITY CLASSIFICATION **UNCLASSIFIED**		1b RESTRICTIVE MARKINGS **NOT APPLICABLE**		
2a. SECURITY CLASSIFICATION AUTHORITY **NOT APPLICABLE**		3. DISTRIBUTION / AVAILABILITY OF REPORT **APPROVED FOR PUBLIC RELEASE**		
2b. DECLASSIFICATION / DOWNGRADING SCHEDULE **NOT APPLICABLE**		**DISTRIBUTION UNLIMITED**		
4. PERFORMING ORGANIZATION REPORT NUMBER(S) Scientific Report 1-92/93		5. MONITORING ORGANIZATION REPORT NUMBER(S) Scientific Report 1-92/93		
6a. NAME OF PERFORMING ORGANIZATION NTNF/NORSAR	6b. OFFICE SYMBOL *(If applicable)*	7a. NAME OF MONITORING ORGANIZATION HQ/AFTAC/TTS		
6c. ADDRESS *(City, State, and ZIP Code)* Post Box 51 N-2007 Kjeller, Norway		7b. ADDRESS *(City, State, and ZIP Code)* Patrick AFB, FL 32925-6001		
8a. NAME OF FUNDING /SPONSORING ORGANIZATION Defense Advanced Research Projects Agency	8b. OFFICE SYMBOL *(If applicable)* NMRO	9. PROCUREMENT INSTRUMENT IDENTIFICATION NUMBER		

8c. ADDRESS *(City, State, and ZIP Code)* 3701 N. Fairfax Dr. #717 Arlington, VA 22203-1714	10. SOURCE OF FUNDING NUMBERS			
	PROGRAM ELEMENT NO **R&D**	PROJECT NO. **NORSAR** **Phase 3**	TASK NO **SOW** **Task 5.0**	WORK UNIT ACCESSION NO. **Seq.no. 003A2**

11. TITLE *(Include Security Classification)* SEMIANNUAL TECHNICAL SUMMARY, 1 APRIL - 30 SEPTEMBER 1992 (UNCLASSIFIED)

12. PERSONAL AUTHOR(S)

13a. TYPE OF REPORT Scientific Summary	13b. TIME COVERED FROM 1 Apr 92 TO 30 Sep 92	14. DATE OF REPORT *(Year, Month, Day)* Nov 1992	15. PAGE COUNT 132

16. SUPPLEMENTARY NOTATION **NOT APPLICABLE**

17.	COSATI CODES		18. SUBJECT TERMS *(Continue on reverse if necessary and identify by block number)*
FIELD	GROUP	SUB-GROUP	**NORSAR, Norwegian Seismic Array**
8	11		

19. ABSTRACT *(Continue on reverse if necessary and identify by block number)*

This Semiannual Technical Summary describes the operation, maintenance and research activities at the Norwegian Seismic Array (NORSAR), the Norwegian Regional Seismic Array (NORESS) and the Arctic Regional Seismic Array (ARCESS) for the period 1 April - 30 September 1992. Statistics are also presented for additional seismic stations, which through cooperative agreements with institutions in the host countries provide continuous data to the NORSAR Data Processing Center (NPDC). These stations comprise the Finnish Experimental Seismic Array (FINESA), the German Experimental Seismic Array (GERESS), and two 3-component stations in Poland: Ksiaz and Stary Folwark.

(cont.)

20. DISTRIBUTION / AVAILABILITY OF ABSTRACT ☐ UNCLASSIFIED / UNLIMITED ☐ SAME AS RPT. ☐ DTIC USERS	21. ABSTRACT SECURITY CLASSIFICATION	
22a. NAME OF RESPONSIBLE INDIVIDUAL Mr. Michael C. Baker	22b. TELEPHONE *(Include Area Code)* (407) 494-7665	22c. OFFICE SYMBOL AFTAC/TTS

DD FORM 1473, 84 MAR 　　83 APR edition may be used until exhausted.　　SECURITY CLASSIFICATION OF THIS PAGE
All other editions are obsolete.　　**UNCLASSIFIED**

Abstract (cont.)

This Semiannual Report also presents statistics from operation of the Intelligent Monitoring System (IMS). The IMS has been operated in an experimental mode, and the performance has been very satisfactory. Since October 1991, a new version of the IMS that accepts data from an arbitrary number of arrays and single 3-component stations has been operated.

The NORSAR Detection Processing system has been operated throughout the period with an average uptime of 96.7% as compared to 99.6% for the previous reporting period. A total of 2056 seismic events have been reported in the NORSAR monthly seismic bulletin. The performance of the continuous alarm system and the automatic bulletin transfer by telex to AFTAC has been satisfactory. The system for direct retrieval of NORSAR waveform data through an X.25 connection has been tested successfully for acquiring such data by AFTAC. Processing of requests for full NORSAR and regional array data on magnetic tapes has progressed according to established schedules. There have been no modifications made to the NORSAR data acquisition system.

On-line detection processing and data recording at the NORSAR Data Processing Center (NDPC) of NORESS, ARCESS, FINESA and GERESS data have been conducted throughout the period. Data from the two stations in Poland have been recorded and processed in an experimental mode. As of the end of the reporting period (30 Sep 1992) data acquisition from these two stations was terminated, in accordance with the terms of the contract. Monthly processing statistics for the arrays as well as results of the IMS analysis for the reporting period are given.

Maintenance activities in the period comprise preventive/corrective maintenance in connection with all the NORSAR subarrays, NORESS and ARCESS. In addition, the maintenance center has been involved with occasional maintenance of equipment for FINESA and work in connection with the two stations in Poland. Other activities have involved testing of the NORSAR communications systems, and establishment of experimental small-aperture arrays at sites in Spitsbergen and the Kola Peninsula (see Section 7.1).

Starting 1 October 1991, an effort has begun to carry out a complete technical refurbishment of the NORSAR array. This project is funded jointly by AFTAC, DARPA and NTNF. During the reporting period, efforts have focused upon evaluation and laboratory testing of technical options for field instrumentation, in particular state-of-the-art A/D converters, data acquisition and synchronization devices. During the next few months, we plan to test several such systems under realistic operating conditions in the field. Initial testing of some systems has already started. When these studies have been completed, a recommendation for a system to be installed will be presented to the funding agencies.

Summaries of seven scientific contributions are presented in Chapter 7 of this report.

Section 7.1 gives a technical description of the most recent extensions of the Northern Europe Regional Array Network. Two new small-aperture arrays have been established; one near Apatity, Russia, and one on the Arctic island of Spitsbergen. The Apatity array was installed in September 1992 as part of an agreement on scientific cooperation between

NORSAR and the Kola Science Centre of the Russian Academy of Sciences. This 9-element array comprises a center site and two concentric rings, and has an aperture of approximately 1 km. All sites are equipped with a short-period vertical seismometer of type Geotech S-500, and the site at the center of the array has in addition two horizontal seismometers of the same type. Data are transmitted to Apatity by radio link. A dedicated full duplex 64 Kbps satellite link, based on Norwegian Telecom's NORSAT B system, has been installed between NORSAR and the Kola Regional Seismology Centre in Apatity. A computer-to-computer Ethernet link connects the two data centers.

During late October/early November 1992 a small-aperture array very similar to the Apatity array was installed on the island of Spitsbergen, east of Longyearbyen. Data from this array are transmitted by radio and terrestrial link to Norwegian Telecom's satellite hub station at Isfjord Radio, from where a dedicated simplex 64 Kbps satellite link is used for transmission of the continuous data to Norway. The Spitsbergen array deployment is supported financially by Norwegian oil companies, and the integration of this array into the IMS (Intelligent Monitoring System) is sponsored by DARPA.

Section 7.2 presents initial processing results from the Apatity array. The noise level is found to be similar to that of ARCESS at frequencies below 2 Hz, and slightly higher than ARCESS at higher frequencies. This is consistent with the expectations. Diurnal noise variation at Apatity is similar to that seen at NORESS. The Apatity array appears to provide excellent noise suppression ($\sqrt{N}$ or better) at frequencies above 2.5 Hz. Initial event processing shows that frequency-wavenumber processing gives well-defined peaks in the F-K diagram both for P and S type phases. A particularly noteworthy feature is the excellent stability in azimuth determination of local events using the low-frequency Rg phases. It is emphasized that these results are preliminary and that more definite conclusions must await analysis of more extensive data sets.

Section 7.3 discusses the use of regionalized wave propagation characteristics in automatic global phase association. This is basically an attempt to establish a strategy for retrieving and organizing regionally dependent propagation parameters that are useful for generalized beamforming of global network data. Examples from the GSETT-2 data base are used to illustrate features such as the distance-dependent occurrence of seismic phases, the reliability of phase labels reported by NDCs and the accuracy of one-station event locations.

Section 7.4 presents and compares two techiques for construction of a uniform grid system covering the earth's surface. The first technique deploys equidistant grid points along equidistant latitude circles. The second method uses triangulation of icosaeders. The second technique is recommended for application in the generalized beamforming process because it gives more effective coverage and provides a well-defined pointer structure from each point to its neighbors. The latter property is important for beampacking, since it enables us to refine a given grid in a straightforward manner.

Section 7.5 outlines some of the fundamental concepts for using the generalized beamforming (GBF) method to conduct phase association and event location on a global scale. Using the icosaeder-based method described in Section 7.4, a global grid of beam-steering

points is defined. Formulas for time tolerances and slowness vector tolerances are developed, taking into account both the tolerance required to compensate for the grid spacing and the tolerances due to effects of sampling rates, earth inhomogeneities, estimation uncertainties and other random errors. A step-by-step description for a global GBF algorithm is outlined. An example of processing a 1-hour time interval of GSETT-2 detection data is presented. This interval includes a small earthquake in Tadjikistan, and this earthquake is correctly processed by the GBF method using either 162, 642 or 2562 global grid steering points. The location precision is illustrated by color contour maps, and is naturally highest for the highest point density. However, it is noteworthy that an acceptable solution is found even with only 162 steering points. This indicates that the method is very robust as long as parameter tolerances are adjusted to reflect the density of the beam deployment.

Section 7.6 reviews available NORSAR detection data for an event in Ukraine on 16 Sep 1979, which was recently reported in Izvestiya to have been a nuclear explosion of 1/3 kt yield, detonated next to a Ukrainian coal mine. Using the location of the mining town as an assumed epicenter, we found an entry in the NORSAR automatic detection list that is consistent with an origin time exactly at noon (Moscow time) and a location approximately as given in the press report. The automatically calculated magnitude was $m_b = 3.3$. Some implications of this case study for seismic monitoring are discussed.

Section 7.7 is a review of induced seismicity caused by mining activities in the Khibiny Massif, Kola Peninsula. It is demonstrated that the extraction of large volumes of rock mass has led to a significant increase in earthquakes and rockbursts in recent years. Although earthquakes have been found to be triggered by explosions in many cases, it is too early to give a definite conclusion abut the triggering mechanism. The array recently installed near Apatity is located close to the Khibiny Massif, and will provide useful data for further investigation of the source characteristics of earthquakes and mining explosions in this area.

AFTAC Project Authorization	:	T/9141/B/PKP
ARPA Order No.	:	4138 AMD # 16
Program Code No.	:	0F10
Name of Contractor	:	Royal Norwegian Council for Scientific and Industrial Research (NTNF)
Effective Date of Contract	:	1 Oct 1988
Contract Expiration Date	:	30 Sep 1993
Project Manager	:	Frode Ringdal (06) 81 71 21
Title of Work	:	The Norwegian Seismic Array (NORSAR) Phase 3
Amount of Contract	:	$ 9,954,194
Contract Period Covered by Report	:	1 April - 30 September 1992

NORSAR Contribution No. 478

Table of Contents

1   Summary

This Semiannual Technical Summary describes the operation, maintenance and research activities at the Norwegian Seismic Array (NORSAR), the Norwegian Regional Seismic Array (NORESS) and the Arctic Regional Seismic Array (ARCESS) for the period 1 April - 30 September 1992. Statistics are also presented for additional seismic stations, which through cooperative agreements with institutions in the host countries provide continuous data to the NORSAR Data Processing Center (NPDC). These stations comprise the Finnish Experimental Seismic Array (FINESA), the German Experimental Seismic Array (GERESS), and two 3-component stations in Poland: Ksiaz and Stary Folwark.

This Semiannual Report also presents statistics from operation of the Intelligent Monitoring System (IMS). The IMS has been operated in an experimental mode, and the performance has been very satisfactory. Since October 1991, a new version of the IMS that accepts data from an arbitrary number of arrays and single 3-component stations has been operated.

The NORSAR Detection Processing system has been operated throughout the period with an average uptime of 96.7% as compared to 99.6% for the previous reporting period. A total of 2056 seismic events have been reported in the NORSAR monthly seismic bulletin. The performance of the continuous alarm system and the automatic bulletin transfer by telex to AFTAC has been satisfactory. The system for direct retrieval of NORSAR waveform data through an X.25 connection has been tested successfully for acquiring such data by AFTAC. Processing of requests for full NORSAR and regional array data on magnetic tapes has progressed according to established schedules. There have been no modifications made to the NORSAR data acquisition system.

On-line detection processing and data recording at the NORSAR Data Processing Center (NDPC) of NORESS, ARCESS, FINESA and GERESS data have been conducted throughout the period. Data from the two stations in Poland have been recorded and processed in an experimental mode. As of the end of the reporting period (30 Sep 1992) data acquisition from these two stations was terminated, in accordance with the terms of the contract. Monthly processing statistics for the arrays as well as results of the IMS analysis for the reporting period are given.

Maintenance activities in the period comprise preventive/corrective maintenance in connection with all the NORSAR subarrays, NORESS and ARCESS. In addition, the maintenance center has been involved with occasional maintenance of equipment for FINESA and work in connection with the two stations in Poland. Other activities have involved testing of the NORSAR communications systems, and establishment of experimental small-aperture arrays at sites in Spitsbergen and the Kola Peninsula (see Section 7.1).

Starting 1 October 1991, an effort has begun to carry out a complete technical refurbishment of the NORSAR array. This project is funded jointly by AFTAC, DARPA and NTNF. During the reporting period, efforts have focused upon evaluation and laboratory testing of technical options for field instrumentation, in particular state-of-the-art A/D converters, data acquisition and synchronization devices. During the next few months, we

plan to test several such systems under realistic operating conditions in the field. Initial testing of some systems has already started. When these studies have been completed, a recommendation for a system to be installed will be presented to the funding agencies.

Summaries of seven scientific contributions are presented in Chapter 7 of this report.

Section 7.1 gives a technical description of the most recent extensions of the Northern Europe Regional Array Network. Two new small-aperture arrays have been established; one near Apatity, Russia, and one on the Arctic island of Spitsbergen. The Apatity array was installed in September 1992 as part of an agreement on scientific cooperation between NORSAR and the Kola Science Centre of the Russian Academy of Sciences. This 9-element array comprises a center site and two concentric rings, and has an aperture of approximately 1 km. All sites are equipped with a short-period vertical seismometer of type Geotech S-500, and the site at the center of the array has in addition two horizontal seismometers of the same type. Data are transmitted to Apatity by radio link. A dedicated full duplex 64 Kbps satellite link, based on Norwegian Telecom's NORSAT B system, has been installed between NORSAR and the Kola Regional Seismology Centre in Apatity. A computer-to-computer Ethernet link connects the two data centers.

During late October/early November 1992 a small-aperture array very similar to the Apatity array was installed on the island of Spitsbergen, east of Longyearbyen. Data from this array are transmitted by radio and terrestrial link to Norwegian Telecom's satellite hub station at Isfjord Radio, from where a dedicated simplex 64 Kbps satellite link is used for transmission of the continuous data to Norway. The Spitsbergen array deployment is supported financially by Norwegian oil companies, and the integration of this array into the IMS (Intelligent Monitoring System) is sponsored by DARPA.

Section 7.2 presents initial processing results from the Apatity array. The noise level is found to be similar to that of ARCESS at frequencies below 2 Hz, and slightly higher than ARCESS at higher frequencies. This is consistent with the expectations. Diurnal noise variation at Apatity is similar to that seen at NORESS. The Apatity array appears to provide excellent noise suppression ($\sqrt{N}$ or better) at frequencies above 2.5 Hz. Initial event processing shows that frequency-wavenumber processing gives well-defined peaks in the F-K diagram both for P and S type phases. A particularly noteworthy feature is the excellent stability in azimuth determination of local events using the low-frequency Rg phases. It is emphasized that these results are preliminary and that more definite conclusions must await analysis of more extensive data sets.

Section 7.3 discusses the use of regionalized wave propagation characteristics in automatic global phase association. This is basically an attempt to establish a strategy for retrieving and organizing regionally dependent propagation parameters that are useful for generalized beamforming of global network data. Examples from the GSETT-2 data base are used to illustrate features such as the distance-dependent occurrence of seismic phases, the reliability of phase labels reported by NDCs and the accuracy of one-station event locations.

Section 7.4 presents and compares two techiques for construction of a uniform grid system covering the earth's surface. The first technique deploys equidistant grid points along equidistant latitude circles. The second method uses triangulation of icosaeders. The second technique is recommended for application in the generalized beamforming process because it gives more effective coverage and provides a well-defined pointer structure from each point to its neighbors. The latter property is important for beampacking, since it enables us to refine a given grid in a straightforward manner.

Section 7.5 outlines some of the fundamental concepts for using the generalized beamforming (GBF) method to conduct phase association and event location on a global scale. Using the icosaeder-based method described in Section 7.4, a global grid of beam-steering points is defined. Formulas for time tolerances and slowness vector tolerances are developed, taking into account both the tolerance required to compensate for the grid spacing and the tolerances due to effects of sampling rates, earth inhomogeneities, estimation uncertainties and other random errors. A step-by-step description for a global GBF algorithm is outlined. An example of processing a 1-hour time interval of GSETT-2 detection data is presented. This interval includes a small earthquake in Tadjikistan, and this earthquake is correctly processed by the GBF method using either 162, 642 or 2562 global grid steering points. The precision is illustrated by color contour mapos, and is naturally highest for the highest point density. However, it is noteworthy that an acceptable solution is found even with only 162 steering points. This indicates that the method is very robust as long as parameter tolerances are adjusted to reflect the density of the beam deployment.

Section 7.6 reviews available NORSAR detection data for an event in Ukraine on 16 Sep 1979, which was recently reported in Izvestiya to have been a nuclear explosion of 1/3 kt yield, detonated next to a Ukrainian coal mine. Using the location of the mining town as an assumed epicenter, we found an entry in the NORSAR automatic detection list that is consistent with an origin time exactly at noon (Moscow time) and a location approximately as given in the press report. The automatically calculated magnitude was $m_b = 3.3$. Some implications of this case study for seismic monitoring are discussed.

Section 7.7 is a review of induced seismicity caused by mining activities in the Khibiny Massif, Kola Peninsula. It is demonstrated that the extraction of large volumes of rock mass has led to a significant increase in earthquakes and rockbursts in recent years. Although earthquakes have been found to be triggered by explosions in many cases, it is too early to give a definite conclusion abut the triggering mechanism. The array recently installed near Apatity is located close to the Khibiny Massif, and will provide useful data for further investigation of the source characteristics of earthquakes and mining explosions in this area.

2   NORSAR Operation

2.1   Detection Processor (DP) operation

There have been 88 breaks in the otherwise continuous operation of the NORSAR online system within the 6-month reporting interval. The uptime percentage for the period is 96.7% as compared to 99.6% for the previous period.

Fig. 2.1.1 and the accompanying Table 2.1.1 both show the daily DP downtime for the days between 1 April and 30 September 1992. The monthly recording times and percentages are given in Table 2.1.2.

The breaks can be grouped as follows:

a)	Hardware failure	43
b)	Stops related to program work or error	0
c)	Hardware maintenance stops	8
d)	Power jumps and breaks	3
e)	TOD error correction	0
f)	Communication lines	34

The total downtime for the period was 142 hours and 14 minutes. The mean-time-between-failures (MTBF) was 2.0 days, as compared to 4.6 for the previous period.

J. Torstveit
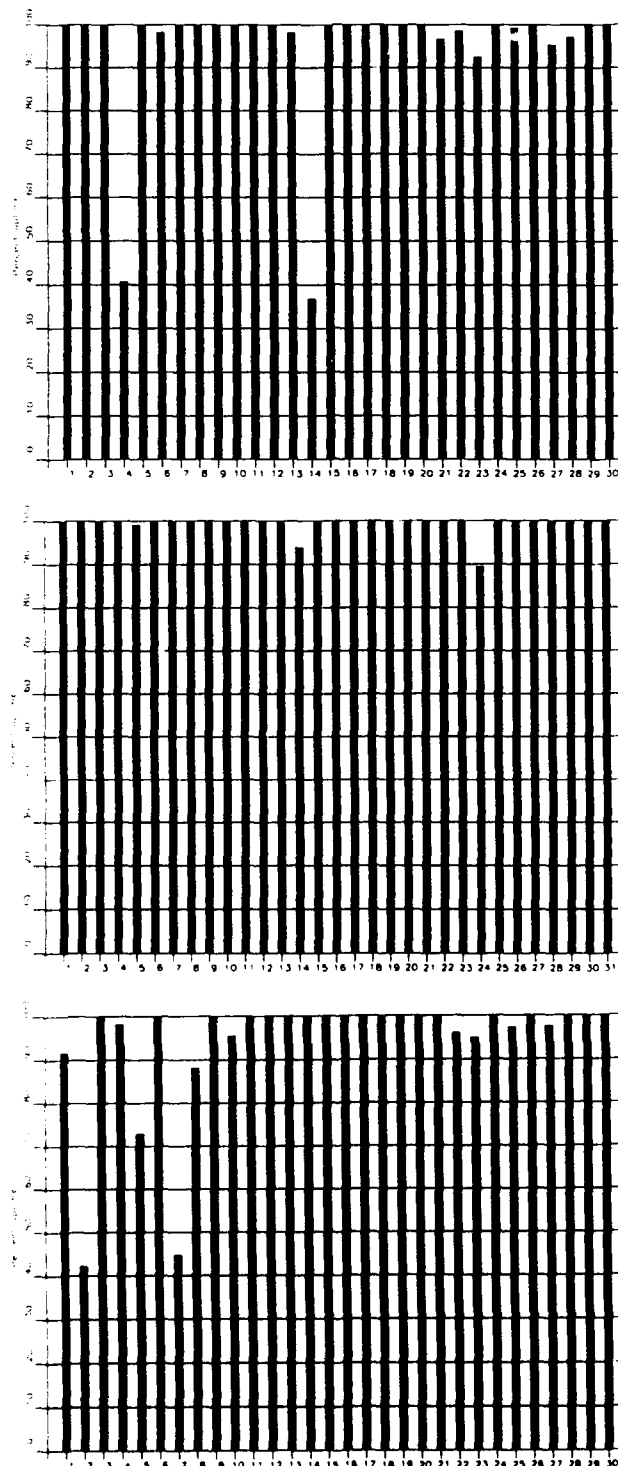
Fig. 2.1.1. Detection Processor uptime for April (top), May (middle) and June (bottom) 1992.
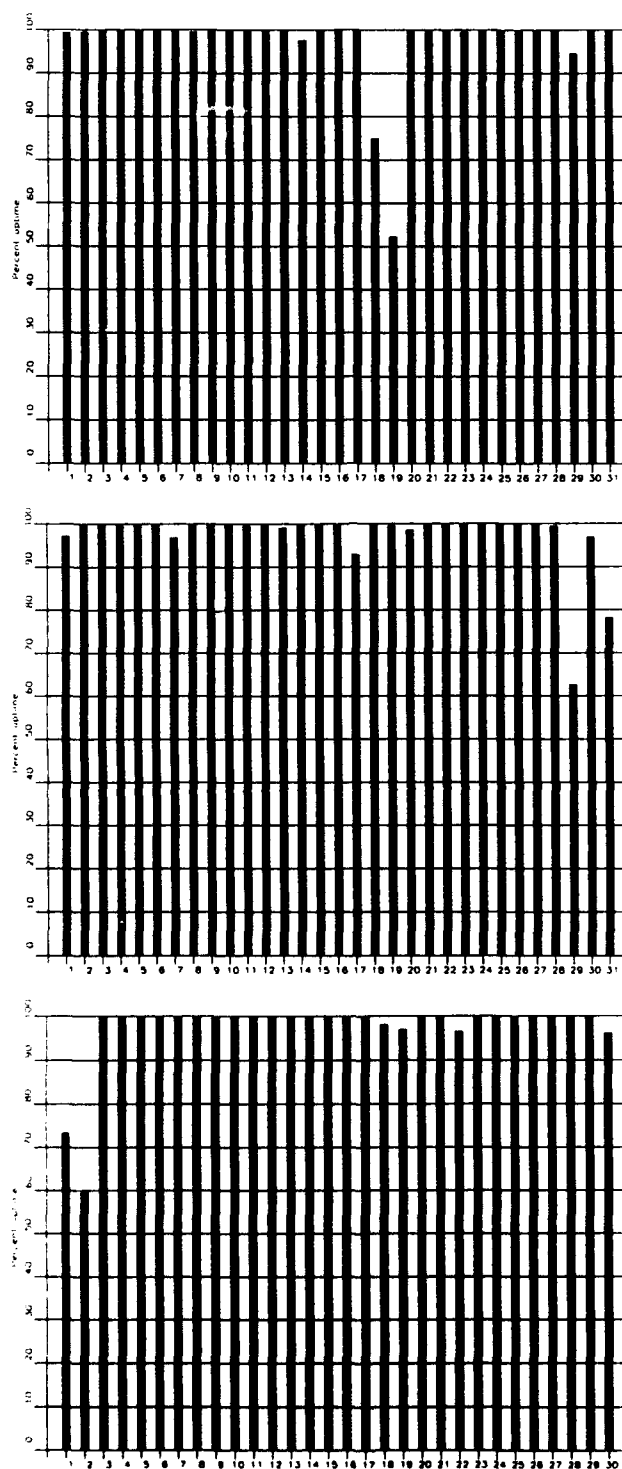
Fig. 2.1.1. Detection Processor uptime for July (top), August (middle) and September (bottom) 1992.

Date	Time	Cause
04 Apr	0057 - 1512	Hardware failure
06 Apr	0930 - 0956	Hardware maintenance
13 Apr	2333 -	Hardware failure
14 Apr	- 1511	Hardware failure
21 Apr	2052 - 2140	Hardware failure
23 Apr	0653 - 0841	Hardware maintenance
27 Apr	0540 - 0648	Line failure
28 Apr	1826 - 1907	Hardware failure
14 May	0905 - 1034	Line failure
24 May	1125 - 1358	Aircondition failure
01 Jun	2200 -	Hardware failure after power break
02 Jun	- 1352	Hardware failure after power break
05 Jun	0223 - 0854	Hardware failure
07 Jun	0003 - 1319	Power break
08 Jun	1153 - 1445	Hardware failure due to thunderstorm
10 Jun	2059 - 2158	Hardware failure
22 Jun	0712 - 0810	Hardware maintenance
23 Jun	0200 - 0311	Hardware failure
27 Jun	0636 - 0711	Hardware maintenance
14 Jul	1123 - 1158	Hardware failure
18 Jul	1800 -	Hardware failure
19 Jul	- 1128	Hardware failure
29 Jul	1423 - 1514	Hardware failure
01 Aug	0120 - 0200	Hardware failure
07 Aug	1914 - 2000	Hardware failure
17 Aug	1602 - 1741	Hardware failure
28 Aug	2352 -	Aircondition failure
29 Aug	- 0816	Aircondition failure
29 Aug	2024 - 2107	Hardware failure
30 Aug	1643 - 1728	Hardware failure
31 Aug	0257 - 0341	Hardware failure
31 Aug	1434 - 1738	Hardware failure
31 Aug	2212 - 2332	Hardware failure
01 Sep	0005 - 0440	Hardware failure
01 Sep	0715 - 0755	Hardware maintenance
01 Sep	1136 - 1240	Hardware maintenance
02 Sep	0233 - 1215	Hardware failure
19 Sep	0119 - 0203	Hardware failure
22 Sep	0359 - 0451	Hardware failure
30 Sep	1747 - 1841	Hardware failure

Table 2.1.1. The major downtimes in the period 1 April - 30 September 1992.

Month	DP Uptime Hours	DP Uptime %	No. of DP Breaks	No. of Days with Breaks	DP MTBF* (days)
Apr 92	684.38	95.09	16	11	1.7
May 92	739.33	99.40	6	6	4.4
Jun 92	676.02	93.89	22	16	1.2
Jul 92	723.57	97.31	13	10	2.2
Aug 92	724.51	97.31	20	13	1.4
Sep 92	700.45	97.34	11	7	2.4
		96.74	88	63	2.0

*Mean-time-between-failures = total uptime/no. of up intervals.

Table 2.1.2. Online system performance, 1 April - 30 September 1992.

2.2   Array communications

General

Table 2.2.1 reflects the performance of the communications system throughout the reporting period. Also this period single, groups and all systems (simultaneously) have been affected. Types of events have varied, as:

- Bad communications cable
- Reduced line level
- SLEM (stuck)
- SLEM (power)
- Power (SA)
- Power (NDPC)
- Sync problems
- Modems (CTV)
- Modem (Avanti 230 Kbit NDPC) caused bad communications between Modcomp and 2701 communications adapter
- NTA carrier
- Lightning
- IBM disk storage
- Defective UPS batteries (NDPC)

Detailed Summary

April (weeks 14-18), 30.3-3.5.92

Reliable performance for all systems weeks 14 and 15, except for 06C, which was affected 3 and 4 April. Besides reliable operation 01B, 02B, 02C and 06C week 17. All systems were affected weeks 16 and 18. 01A, 03C and 04C were affected week 17. An IBM disc storage device, the NTA carrier system and the Modcomp have caused most of the problems. Average outage in April, individual weeks (5):

Week 14 (-06C)	: 0.0005%	0.115% (all)
Week 15 (all)	: 0.0006%	
Week 16 (all)	: 9.821%	
Week 17 (-01A,03C,04C)	: 0.001%	16.96% (all)
Week 18 (all)	: 15.17%	

May (weeks 19-22), 4-31.5.92

The NTA carrier frequency system failed again between 3 and 4 May, week 21. All systems were affected. A line test was carried out between NDPC and 03C 14 May in cooperation with NMC/Hamar. No errors were observed in C-loop (digital loop). 02B was down between 20 and 26 May due to a power outage. 02C was affected between 22 and 24 May, probably caused by the line. 01B was down between 26 May and 1 June. Average outage in May, individual weeks:

Week 19 (all)	:	4.169%
Week 20 (all)	:	0.0008%
Week 21 (-02C)	:	0.002%
Week 22 (-01B,02B)	:	0.0005%

June (weeks 23-26), 1-28.6.92

Without warning the local power company disconnected the power 1 June at 2200 hrs. The UPS (Uninterrupted Power Supply) failed and therefore all systems lost power immediately. The alarm system did not warn the person on duty, and as a result of this the systems were not restarted until the next day at 1355 hrs.

01B went down 4 June due to a faulty SLEM power unit (which also supplies the modem), caused excessive amounts of communications errors. 12 June the power unit was replaced.

5 June NORSAR was down approximately 6 hrs 30 min in connection with replacing a power supply in a disc controller.

7 June a short power outage caused vital equipment, such as the 2701 adapter and a disc controller to drop power. In this connection the communications systems was down for about 13 hrs.

9 June 02C went down 20.38 hrs. A Modcomp restart the next day restored the subarray operation.

11 June a 01B communications test revealed bad C-loop (digital loop). 12 June 01B SLEM power unit was replaced and normal operation was restored.

16 June A comtest on the 01A B/C-loop revealed a bad communications cable. NTA/ Hamar tried to improve the conditions by using two other pairs in the cable but without success. A new communications test 22 June only confirmed the degraded quality. According to NTA/Hamar the cable repair had to be postponed because the damage was located to that part of the cable crossing a corn field.

24 June at 2226 hrs spikes and "time mismatch" was observed on the NORSAR system. 25 June the Modcomp was restarted and normal operation restored.

Average outage in June, individual weeks:

Week 23 (-01B)	:	0.003%
Week 24 (-01B,02C)	:	0.021%
Week 25 (all)	:	0.035%
Week 26 (-01A)	:	0.004%

July (weeks 27-31), 29.6-2.8.92

Also in July the NORSAR communications systems were affected either individually or all simultaneously. The individually affected systems were caused by bad communications cables, short outages, lightning in the subarray area, sync problems, etc. Simultaneously

affected systems were probably caused by short interruptions in the NTA group transmission equipment. Also the NDPC communications-related equipment has been considered as a possible source.

01A was inoperative also throughout July. 02C and 04C were down between 1 and 2 July. 02C was affected again 6 and 7 July. All systems were affected between 18 and 19 July. The Modcomp was restarted and the systems resumed operation (-01A,01B,02B). 04C and 06C were affected 14 July. 19 July 02C, 03C, 04C and 06C were affected for approximately 1 hour. 20 July 01B resumed operation; 02B on 21 July (both had been down since 19 July). 02B was affected again 27-28 July caused by lightning. 02C indicated sync problems 29 July between 0000 and 0300 hrs.

In the period the Modcomp was restarted 16 times in order to restore the operation of one or several subarrays, but also in order to align TOD band NORSAR data.

Average outages in July, individual weeks:

Week 27 (-01A)	:	0.007%
Week 28 (-01A,02C)	:	0.009%
Week 29 (N/A)	:	--
Week 30 (-01A,01B,02B)	:	0.009%
Week 31 (-01A)	:	0.043%

August (weeks 32-35), 3-30.8.92

01A was also out of operation also in August. 01B, 02B, 04C and 06C have been affected this period.

01B performance was reduced 9-10 August, but the SLEM unit was replaced and operation established again 20 August.

02B was affected 5-7 and 11-13 August in connection with lightning in the 02B area. 04C was affected by a thunderstorm 12-13 August, and 06C was down between 10 and 11 August, probably due to short line outages.

All system (-02C) dropped out 10 August between 20 and 23 hrs. After a Modcomp restart 0453 hrs 11 August the systems resumed operation.

Average outages in August, individual weeks (4):

Week 32 (-01A,02B)	:	0.016%
Week 33 (N/A)	:	--
Week 34 (-01A,01B)	:	0.002%
Week 35 (-01A)	:	0.009%

September (weeks 36-39), 31.8-27.9.92

1 September between 1136 and 1240 hrs the communication between the IBM 2701 and the Modcomp was broken, caused by a faulty Avanti 230 Kbit modem. After repair, the data exchange started again.

2 September a disc failed which again caused loss of NORSAR data from 0233 hrs until the disc was replaced 1215 hrs.

06C was affected 2 September between 10 and 13 hrs. A Modcomp restart reinitiated the system. 01B was affected 22-23 September caused by a broken communications cable between Kjeller and Lillestrøm. Power at 02B was broken a few hours 23 September, but did not affect the subarray operation due to satisfactory operation of the backup batteries.

Average outages in September, individual weeks (4):

Week 36 (-01A)	:	0.028%
Week 37 (-01A)	:	0.0008%
Week 38 (-01A)	:	0.012%
Week 39 (-01A)	:	0.298%
(-01A, 01B)		0.0007%

O.A. Hansen

Sub-Arrays	Apr (5) 30.3-3.5.92	May (4) 4-31.5.92	Jun (4) 1-28.6.92	Jul (5) 29.6-28.7.92	Aug (4) 3.8-30.8.92	Sep (4) 31.8-27.9.F92	Average 1/2 year
01A	0.0006[1]	1.043	0.112[11]	100.0	100.0	100.0	0.514[28]
01B	0.0004[2]	1.390[8]	0.0007[12]	0.020[14]	0.057[20]	0.001[24]	0.245
02B	0.0003[3]	1.389[9]	0.001	0.075[15]	0.003[21]	0.0003	0.245
02C	0.0007[4]	1.390[10]	0.002[13]	0.011[16]	0.001	0.016	0.237
03C	0.0005[5]	1.043	0.004	0.003[17]	0.004	0.002	0.176
04C	0.0008[6]	1.044	0.005	0.002[18]	0.002[22]	0.001[1]	0.176
06C	0.268[7]	1.043	0.002	0.009[19]	0.003[23]	0.042	0.228
Aver	0.039	1.192	0.018	0.020[25]	0.012[26]	0.010[27]	0.260

Figures representing error rate (in per cent) followed by number 1), 2), etc., are related to legend below.,

Table 2.2.1. Communications performance. The numbers represent error rates in per cent based on total transmitted frames/week (1 April - 30 September 1992).

1),5),6)	Average 2 weeks	(14,15)	14),15)	Average 3 weeks	(27,28,31)
12)	"	(25,26)	16)	"	(27,30,31)
20)	"	(32,35)	22),23)	"	(32,34,35)
21)	"	(34,35)	24)	"	(36,37,38)
2),3),4),7)	Average 3 weeks	(14,15,17)	17),18),19)	Average 4 weeks	(27,28,30,31)
8),9)	"	(19,20,21)	25),26),27)	6 subarrays	(01B-06C)
10)	"	(19,20,22)			
11)	"	(23,24,25)	28)	Average 3 months	(Apr, May, Jun)
13)	"	(23,25,26)			

2.3   NORSAR Event Detection operation

In Table 2.3.1 some monthly statistics of the Detection and Event Processor operation are given. The table lists the total number of detections (DPX) triggered by the on-line detector, the total number of detections processed by the automatic event processor (EPX) and the total number of events accepted after analyst review (teleseismic phases, core phases and total).

| | Total DPX | Total EPX | Accepted Phases | | | |
			P-phases	Core Phases	Sum	Daily
Apr 92	10400	1308	245	64	309	10.3
May 92	6100	1301	384	104	488	15.7
Jun 92	7600	1301	296	87	383	12.8
Jul 92	9825	1505	359	69	428	13.8
Aug 92	9225	1402	383	62	445	14.4
Sep 92	9000	1188	269	53	322	10.7
			1936	439	2375	13.0

Table 2.3.1. Detection and Event Processor statistics, 1 April - 30 September 1992.

NORSAR Detections

The number of detections (phases) reported by the NORSAR detector during day 092, through day 274, 1992, was 52,129, giving an average of 285 detections per processed day (183 days processed). Table 2.3.2 shows daily and hourly distribution of detections for NORSAR.

B. Paulsen Gammelby
T. Schøyen

NAO .DPX Hourly distribution of detections

Day	00	01	02	03	04	05	06	07	08	09	10	11	12	13	14	15	16	17	18	19	20	21	22	23	Sum	Date		
92	22	26	20	11	19	15	8	5	5	20	6	32	21	21	11	14	26	16	18	15	18	27	16	31	423	Apr 01	Wednesday	
93	25	26	20	24	17	8	16	5	4	18	18	16	17	20	22	19	24	19	22	15	21	23	17	14	436	Apr 02	Thursday	
94	13	19	21	22	11	13	11	13	15	33	17	22	22	44	51	37	26	19	11	18	15	19	13	22	502	Apr 03	Friday	
95	23	0	0	0	0	0	1	0	4	10	0	24	15	0	0	14	13	19	6	10	21	17	23	10	183	Apr 04	Saturday	
96	15	16	14	15	13	13	14	18	1	6	13	6	18	15	11	14	16	9	10	10	16	17	6	13	291	Apr 05	Sunday	
97	20	18	14	19	6	7	3	14	1	7	24	5	11	25	26	16	18	8	5	19	16	25	12	22	346	Apr 06	Monday	
98	18	29	16	26	19	10	9	8	10	11	14	4	9	21	17	2	0	3	9	14	2	17	11	10	276	Apr 07	Tuesday	
99	16	10	17	16	5	7	2	11	4	11	28	18	11	25	3	6	1	12	6	2	8	8	9	4	242	Apr 08	Wednesday	
100	13	10	9	4	5	10	9	4	11	4	14	27	28	20	10	12	7	10	13	13	15	17	11	16	255	Apr 09	Thursday	
101	24	23	23	30	16	9	2	11	13	7	12	16	5	10	24	18	23	16	16	10	14	14	8	9	373	Apr 10	Friday	
102	10	9	21	19	12	6	13	13	13	13	13	27	11	15	14	10	8	16	12	10	10	15	10	17	297	Apr 11	Saturday	
103	14	16	14	14	12	11	9	12	11	10	3	3	5	5	7	10	0	6	16	10	22	13	7	12	241	Apr 12	Sunday	
104	14	34	10	13	11	0	17	5	28	0	34	0	11	13	22	21	10	17	19	21	22	27	19	15	406	Apr 13	Monday	
105	0	0	0	0	0	0	0	0	0	0	6	9	10	13	9	16	17	17	23	21	22	21	21	24	166	Apr 14	Tuesday	
106	26	20	27	20	16	13	11	16	19	0	6	39	24	29	9	16	17	17	23	33	17	10	15	12	464	Apr 15	Wednesday	
107	15	31	17	14	14	16	10	16	19	15	25	16	17	23	14	9	23	19	11	15	17	11	13	16	405	Apr 16	Thursday	Skj(rt
108	26	17	18	19	41	26	10	20	33	27	28	16	15	18	17	14	35	12	17	13	12	24	15	24	457	Apr 17	Friday	Langfr
109	19	22	24	27	22	22	18	24	10	36	20	14	15	28	22	27	22	25	23	13	17	5	13	13	480	Apr 18	Saturday	
110	14	16	17	17	41	23	31	21	15	16	16	17	30	20	18	21	28	18	22	25	30	20	25	19	493	Apr 19	Sunday	Frste
111	18	29	11	19	28	26	30	26	17	24	13	29	30	20	17	19	23	16	24	23	25	20	16	13	504	Apr 20	Monday	Annen
112	19	11	11	12	6	4	4	0	9	11	14	8	17	12	6	12	10	16	14	17	12	6	7	20	254	Apr 21	Tuesday	
113	15	12	22	33	22	31	1	3	0	18	11	26	6	11	12	11	16	8	12	9	13	10	14	18	333	Apr 22	Wednesday	
114	12	11	19	12	11	2	8	0	3	11	13	16	17	13	9	5	6	16	9	16	9	12	9	16	253	Apr 23	Thursday	
115	16	20	12	13	5	0	12	26	0	15	11	21	12	13	17	21	8	16	16	11	31	26	24	84	405	Apr 24	Friday	
116	10	0	0	0	0	6	30	16	3	13	11	6	16	26	7	11	13	19	17	20	25	20	30	19	294	Apr 25	Saturday	
117	18	21	0	24	0	15	21	21	12	21	19	21	26	26	16	22	12	34	21	23	30	20	22	20	544	Apr 26	Sunday	
118	29	17	24	17	14	16	17	26	17	12	19	19	5	6	16	8	24	14	7	17	9	19	7	8	346	Apr 27	Monday	
119	9	19	29	17	17	9	4	28	23	11	8	26	12	17	6	14	4	5	3	17	6	5	4	6	288	Apr 28	Tuesday	
120	17	7	11	2	1	6	2	6	24	24	5	24	18	18	7	8	21	16	18	9	9	15	5	0	188	Apr 29	Wednesday	
121	6	10	0	6	0	3	5	8	23	12	15	11	11	11	8	11	11	8	7	8	8	10	7	5	253	Apr 30	Thursday	
122	10	10	0	0	0	0	0	0	5	12	0	6	6	10	10	11	8	9	20	13	0	15	5	6	126	May 01	Friday	Frste
123	2	3	0	13	12	4	3	0	4	12	7	5	3	3	7	14	8	6	6	10	13	10	3	0	170	May 02	Saturday	
124	10	18	19	19	19	17	12	6	13	4	7	10	9	8	4	4	2	5	6	6	0	0	0	5	207	May 03	Sunday	
125	0	0	0	0	0	0	3	12	6	25	13	17	14	14	7	18	21	10	6	12	8	14	3	0	214	May 04	Monday	
126	26	21	11	0	25	1	1	2	22	16	7	17	13	18	17	16	6	12	6	7	9	16	11	17	312	May 05	Tuesday	
127	14	16	18	14	16	7	22	21	7	10	11	17	11	10	17	6	13	11	11	12	10	10	14	16	274	May 06	Wednesday	
128	13	9	10	13	8	9	10	13	10	10	23	17	8	10	4	8	13	10	11	8	7	9	8	8	240	May 07	Thursday	
129	7	11	13	14	0	10	15	3	16	9	13	16	8	11	2	4	10	10	12	12	10	7	4	14	226	May 08	Friday	
130	15	8	13	14	12	10	15	12	6	5	6	6	14	3	18	0	0	10	15	8	13	11	7	9	242	May 09	Saturday	
131	12	14	13	14	25	18	10	2	5	1	11	5	14	11	11	10	2	12	6	4	11	8	8	6	251	May 10	Sunday	
132	6	6	12	10	9	4	8	3	2	8	26	7	13	7	7	1	9	0	6	3	7	0	5	14	154	May 11	Monday	
133	19	19	16	27	8	3	2	3	10	4	15	16	9	18	8	16	3	8	5	12	17	21	11	20	313	May 12	Tuesday	
134	21	17	18	24	16	11	6	12	8	5	12	15	21	21	18	1	6	6	11	7	3	16	16	13	254	May 13	Wednesday	
135	15	13	11	13	8	6	4	2	10	12	14	17	18	10	18	8	13	11	12	13	4	9	8	14	233	May 14	Thursday	
136	15	12	17	14	14	21	3	20	16	16	16	25	14	11	12	10	11	10	15	8	3	7	14	9	234	May 15	Friday	
137	5	6	15	14	9	5	11	5	2	4	8	6	4	9	4	3	0	4	6	4	5	13	8	6	182	May 16	Saturday	
138	13	12	16	10	22	16	8	8	7	11	16	16	3	20	18	9	9	0	4	13	1	0	5	11	209	May 17	Sunday	Syten
139	4	6	9	11	8	6	8	0	5	4	26	8	0	9	7	10	5	7	7	12	3	2	3	0	177	May 18	Monday	
140	3	4	5	7	7	16	2	2	10	4	10	40	27	18	20	1	3	2	0	4	3	4	2	5	190	May 19	Tuesday	
141	4	1	3	1	1	0	10	3	0	5	15	26	18	20	29	8	0	5	4	0	1	1	1	0	146	May 20	Wednesday	
142	3	7	7	7	7	11	3	0	18	12	9	21	24	6	28	1	1	8	5	8	28	4	12	17	207	May 21	Thursday	
143	12	0	0	0	0	4	1	10	8	16	14	15	20	3	27	0	9	5	4	4	5	5	15	6	219	May 22	Friday	
144	0	7	3	3	2	4	3	4	2	0	1	0	8	0	0	0	0	0	5	4	7	0	7	20	112	May 23	Saturday	
145	6	4	1	0	2	2	1	2	0	0	3	0	6	6	4	1	0	1	1	4	8	4	0	0	79	May 24	Sunday	
146	0	10	0	8	8	8	2	0	3	1	1	9	0	0	6	0	4	15	2	18	5	6	6	4	134	May 25	Monday	
147	3	3	5	5	7	7	5	4	9	12	17	13	13	9	20	2	7	0	6	3	13	3	3	2	164	May 26	Tuesday	

Table 2.3.2 (Page 1 of 4)

NAO .DPX Hourly distribution of detections

Day	00	01	02	03	04	05	06	07	08	09	10	11	12	13	14	15	16	17	18	19	20	21	22	23	Sum	Date		
148	2	4	7	0	1	22	4	6	11	3	10	23	13	13	8	7	5	8	5	4	11	9	14	6	196	May 27	Wednesday	
149	2	6	1	2	7	4	6	4	10	15	14	10	11	11	8	4	1	2	5	0	8	12	8	13	162	May 28	Thursday	Kristi
150	6	1	0	4	2	4	2	4	14	7	15	15	19	11	0	9	6	7	5	0	0	6	20	15	196	May 29	Friday	
151	12	4	1	1	4	13	5	2	14	13	15	12	38	6	2	1	16	11	3	12	10	6	3	5	176	May 30	Saturday	
152	0	1	4	8	3	2	7	3	2	1	2	7	17	2	0	4	7	9	3	8	2	4	6	2	106	May 31	Sunday	
153	5	7	0	3	3	4	3	0	1	2	6	17	4	6	13	10	11	5	17	8	8	3	0	0	150	Jun 01	Monday	
154	0	0	0	0	0	0	0	4	0	11	0	18	0	9	10	6	1	9	4	4	0	4	0	9	95	Jun 02	Tuesday	
155	4	7	7	7	5	0	11	14	2	2	11	14	13	3	9	5	6	8	11	5	7	2	9	4	178	Jun 03	Wednesday	
156	3	3	2	0	4	0	0	0	7	7	1	4	0	12	7	9	10	4	4	7	3	9	2	9	135	Jun 04	Thursday	
157	2	1	3	7	0	4	3	0	8	15	5	9	13	10	9	1	2	8	11	8	6	2	4	7	137	Jun 05	Friday	
158	11	5	1	2	0	0	1	0	4	5	7	4	16	31	2	9	4	11	5	3	3	4	3	10	164	Jun 06	Saturday	
159	8	3	5	3	0	4	0	0	0	10	0	0	0	16	52	16	11	5	6	8	7	1	17	2	124	Jun 07	Sunday	Frste
160	0	7	2	9	3	0	3	1	4	7	4	9	0	3	5	8	2	6	1	3	0	3	7	7	129	Jun 08	Monday	Annen
161	16	3	8	6	1	5	2	6	6	1	5	5	11	11	5	5	14	7	1	7	1	5	6	8	139	Jun 09	Tuesday	
162	6	11	11	2	9	2	2	1	59	5	8	25	1	15	5	2	7	4	7	3	4	7	1	3	189	Jun 10	Wednesday	
163	7	1	7	13	2	2	2	5	0	8	14	20	3	15	8	1	20	16	5	6	5	5	1	2	168	Jun 11	Thursday	
164	5	6	8	8	0	7	9	10	15	3	14	18	13	12	5	10	11	13	14	13	5	4	6	5	206	Jun 12	Friday	
165	7	6	0	3	3	2	9	7	14	2	14	4	3	4	8	7	15	9	16	10	9	6	5	16	181	Jun 13	Saturday	
166	11	6	6	8	27	16	5	13	14	1	11	3	10	12	18	18	8	1	9	10	13	12	12	14	285	Jun 14	Sunday	
167	21	14	8	21	8	3	2	2	0	3	13	22	5	11	8	10	7	16	11	11	26	12	16	13	223	Jun 15	Monday	
168	22	21	16	20	10	9	2	22	0	13	3	29	12	12	19	11	13	17	7	12	16	14	14	8	291	Jun 16	Tuesday	
169	17	15	20	13	13	2	2	12	6	26	3	24	5	19	15	3	13	10	16	2	15	18	19	17	288	Jun 17	Wednesday	
170	16	12	14	12	13	5	5	11	11	14	8	31	4	12	12	8	12	17	13	15	21	23	15	11	330	Jun 18	Thursday	
171	13	19	12	14	6	2	9	8	13	13	17	22	13	17	10	9	17	24	22	18	21	13	6	1	324	Jun 19	Friday	
172	21	22	26	21	2	9	11	17	10	24	23	16	20	20	26	23	21	22	17	22	33	20	12	5	505	Jun 20	Saturday	
173	15	18	20	24	16	17	26	10	16	21	17	34	16	17	21	16	24	18	19	28	13	13	13	16	450	Jun 21	Sunday	
174	14	24	14	14	16	6	8	4	16	11	11	7	52	14	15	6	14	11	10	5	10	13	12	10	289	Jun 22	Monday	
175	11	16	0	11	14	9	3	9	3	18	13	5	25	19	11	7	11	20	9	0	9	16	14	13	292	Jun 23	Tuesday	
176	6	13	14	0	17	12	12	12	5	16	22	17	22	14	7	19	19	10	0	8	12	10	16	21	281	Jun 24	Wednesday	
177	56	27	4	11	12	9	2	7	13	15	16	23	36	13	12	12	10	10	15	7	26	18	14	11	369	Jun 25	Thursday	
178	0	9	17	17	9	11	22	27	12	15	22	26	20	13	10	20	16	17	22	15	27	20	20	16	356	Jun 26	Friday	
179	16	22	15	18	16	8	1	9	7	3	23	20	24	17	18	4	21	10	13	23	17	13	18	16	341	Jun 27	Saturday	
180	21	24	20	17	20	21	11	7	16	6	24	10	36	10	19	21	15	18	11	17	27	16	16	27	474	Jun 28	Sunday	
181	24	15	15	15	18	3	12	12	16	15	27	3	15	10	16	6	6	9	7	6	6	12	16	13	287	Jun 29	Monday	
182	7	9	6	12	9	5	0	1	1	15	14	10	4	12	16	11	4	6	8	11	15	5	12	13	215	Jun 30	Tuesday	
183	10	14	20	16	8	8	18	18	6	16	9	5	11	10	18	14	30	10	9	23	31	14	12	10	308	Jul 01	Wednesday	
184	14	21	21	11	26	9	3	3	7	14	4	12	4	16	16	8	16	13	22	19	12	14	16	26	309	Jul 02	Thursday	
185	13	16	12	10	13	2	1	18	4	8	9	28	5	11	18	7	13	15	10	16	11	17	19	17	291	Jul 03	Friday	
186	15	15	18	10	17	6	0	4	17	23	13	27	11	4	9	15	21	10	7	20	15	16	13	13	325	Jul 04	Saturday	
187	21	11	19	33	24	12	14	17	18	23	17	17	21	8	13	13	21	14	17	10	33	18	13	20	424	Jul 05	Sunday	
188	14	23	18	24	7	5	4	2	8	12	17	17	6	8	9	12	9	7	9	20	18	6	13	7	261	Jul 06	Monday	
189	24	5	4	16	16	6	5	6	14	14	29	36	22	8	9	20	11	19	26	15	15	7	7	7	250	Jul 07	Tuesday	
190	9	14	14	8	12	8	11	10	14	8	18	13	24	22	18	33	10	9	23	23	33	11	15	17	333	Jul 08	Wednesday	
191	16	15	13	6	12	8	11	4	9	8	10	13	11	24	16	16	10	22	19	41	21	11	13	13	356	Jul 09	Thursday	
192	8	10	15	19	19	9	6	30	4	14	16	21	18	11	13	3	13	17	6	15	27	16	13	20	283	Jul 10	Friday	
193	22	9	18	12	12	11	8	7	17	10	15	17	19	29	17	8	14	9	15	33	25	18	19	13	369	Jul 11	Saturday	
194	12	12	12	10	18	8	12	16	9	10	21	13	34	6	26	11	18	14	14	41	21	18	15	20	344	Jul 12	Sunday	
195	16	17	10	13	13	3	4	11	11	10	13	7	13	26	9	22	16	21	9	17	27	25	15	13	334	Jul 13	Monday	
196	22	13	11	15	15	14	10	25	7	17	45	17	12	13	26	19	22	19	26	15	21	9	15	12	409	Jul 14	Tuesday	
197	17	19	13	24	24	9	10	19	11	20	21	12	10	22	36	21	11	41	21	15	20	2	18	18	384	Jul 15	Wednesday	
198	12	33	19	27	19	30	14	17	7	15	18	15	22	13	17	8	25	21	4	11	10	0	9	17	354	Jul 16	Thursday	
199	6	32	12	13	20	14	12	17	11	13	16	12	16	22	17	22	17	16	0	20	10	16	15	13	345	Jul 17	Friday	
200	16	22	22	26	25	15	15	12	46	0	10	54	10	36	16	25	29	0	0	16	0	0	0	0	481	Jul 18	Saturday	
201	0	0	0	0	10	2	0	7	0	2	5	9	4	8	5	10	11	15	9	14	0	0	8	0	166	Jul 19	Sunday	
202	3	10	15	14	0	7	8	8	26	25	7	4	5	10	5	9	17	9	23	14	23	9	15	8	243	Jul 20	Monday	
203	13	12	11	9	1	2	21	9	6	3	6	17	5	3	4	9	22	13	14	1	11	11	9	4	216	Jul 21	Tuesday	

Table 2.3.2. (Page 2 of 4)

NAO .DPX Hourly distribution of detections

Day	00	01	02	03	04	05	06	07	08	09	10	11	12	13	14	15	16	17	18	19	20	21	22	23	Sum	Date	
204	6	12	7	9	9	3	5	6	4	11	3	17	17	10	13	6	13	14	17	19	16	19	16	17	269	Jul 22	Wednesday
205	14	11	14	14	17	3	5	6	3	11	2	11	2	11	8	10	10	8	12	19	18	21	14	18	267	Jul 23	Thursday
206	11	12	25	21	16	24	9	9	10	15	11	13	22	18	22	12	16	13	20	19	20	10	12	9	376	Jul 24	Friday
207	9	11	7	14	11	2	19	45	35	6	4	4	5	10	6	7	34	12	7	6	6	5	4	9	165	Jul 25	Saturday
208	4	11	3	9	9	6	2	47	12	7	9	5	11	21	35	12	5	10	13	8	8	14	16	7	303	Jul 26	Sunday
209	9	13	13	9	10	7	12	6	7	7	14	8	21	11	12	7	12	11	11	12	17	15	11	9	282	Jul 27	Monday
210	16	11	6	16	10	10	5	6	16	16	14	16	12	28	17	23	12	16	5	8	11	11	20	20	302	Jul 28	Tuesday
211	19	10	35	22	22	10	1	4	14	7	9	20	12	11	14	14	21	10	14	29	21	9	10	17	361	Jul 29	Wednesday
212	8	9	14	13	9	15	5	9	8	13	13	30	9	19	10	28	16	15	5	18	10	15	17	16	337	Jul 30	Thursday
213	23	22	12	24	31	13	26	24	15	15	4	20	12	17	23	14	11	23	25	16	18	16	7	7	379	Jul 31	Friday
214	8	11	12	25	14	16	29	20	16	24	11	16	28	20	18	8	7	31	10	14	10	22	21	18	461	Aug 01	Saturday
215	22	17	19	14	14	11	7	20	12	8	13	20	12	19	11	4	11	5	25	12	13	8	18	19	339	Aug 02	Sunday
216	9	5	12	11	11	10	4	13	4	5	4	23	11	10	8	8	7	9	11	12	8	11	11	10	218	Aug 03	Monday
217	10	7	13	10	10	8	6	13	16	14	22	28	21	39	39	10	9	11	10	6	11	23	15	18	342	Aug 04	Tuesday
218	8	7	13	11	12	6	6	15	16	6	7	12	21	17	18	13	7	10	17	15	11	6	12	14	294	Aug 05	Wednesday
219	10	9	10	11	10	8	6	14	16	16	13	12	6	4	19	13	14	14	17	15	14	18	19	15	269	Aug 06	Thursday
220	16	15	21	19	19	8	6	14	16	14	10	16	21	11	7	10	11	16	22	11	15	15	18	13	353	Aug 07	Friday
221	13	15	21	21	18	27	11	12	15	14	13	8	5	16	16	19	14	13	13	14	15	10	11	19	329	Aug 08	Saturday
222	16	13	13	15	18	5	11	11	11	12	8	15	19	30	7	15	12	5	13	23	23	24	30	19	337	Aug 09	Sunday
223	13	16	13	15	18	11	14	17	12	6	17	13	10	17	16	10	8	12	5	107	14	10	6	11	374	Aug 10	Monday
224	22	13	6	8	14	8	9	4	13	7	6	10	14	22	7	10	9	6	22	22	14	24	6	14	266	Aug 11	Tuesday
225	12	15	13	13	15	5	9	4	6	55	3	23	13	21	13	10	13	14	10	4	15	10	13	11	342	Aug 12	Wednesday
226	11	14	10	6	17	4	7	15	8	6	20	19	12	10	17	13	7	16	17	5	4	14	9	17	316	Aug 13	Thursday
227	16	18	15	9	16	18	6	16	11	8	4	16	21	11	18	9	9	7	16	12	10	9	10	11	272	Aug 14	Friday
228	7	13	8	13	27	6	16	13	11	5	9	9	5	10	10	9	8	4	9	3	40	13	8	20	239	Aug 15	Saturday
229	8	11	11	11	15	7	16	11	11	3	24	4	19	6	7	12	3	3	4	1	13	9	7	9	195	Aug 16	Sunday
230	20	7	6	1	12	4	8	6	0	10	11	14	14	6	10	6	1	3	12	0	3	4	13	8	138	Aug 17	Monday
231	10	9	11	11	37	7	14	6	13	17	11	5	21	16	8	15	16	14	12	5	11	11	3	6	202	Aug 18	Tuesday
232	10	52	39	15	30	8	6	24	14	17	13	16	23	21	8	21	16	18	18	3	14	17	8	13	407	Aug 19	Wednesday
233	2	16	13	17	37	15	4	7	4	14	13	10	19	16	16	4	22	26	26	14	3	12	6	5	277	Aug 20	Thursday
234	5	7	2	6	9	4	2	3	1	13	4	14	8	23	5	12	5	16	16	16	3	17	15	9	220	Aug 21	Friday
235	10	3	10	6	7	14	14	2	20	6	16	11	8	21	14	10	10	9	12	16	18	18	11	11	215	Aug 22	Saturday
236	15	13	25	15	13	16	13	16	14	14	17	20	19	18	13	2	10	14	16	16	19	17	9	9	359	Aug 23	Sunday
237	13	19	9	20	6	5	10	15	9	6	10	25	8	18	4	6	10	3	4	10	5	13	3	11	213	Aug 24	Monday
238	5	11	1	4	18	3	7	2	9	14	6	9	11	10	1	2	2	7	14	12	11	13	9	1	190	Aug 25	Tuesday
239	14	23	10	16	16	10	2	7	6	16	30	12	8	26	21	9	3	11	3	12	11	13	12	3	252	Aug 26	Wednesday
240	7	4	16	13	8	9	8	6	29	7	5	14	12	16	23	19	24	18	18	16	8	17	11	24	247	Aug 27	Thursday
241	22	12	21	10	10	8	7	4	15	8	7	14	10	6	10	10	9	10	25	13	8	17	15	15	310	Aug 28	Friday
242	0	0	10	20	2	0	5	0	10	37	16	17	15	19	10	16	5	14	14	7	21	15	10	23	237	Aug 29	Saturday
243	9	6	8	6	14	4	4	13	13	13	3	11	11	9	8	9	9	7	23	13	23	0	0	10	258	Aug 30	Sunday
244	26	0	20	0	11	7	16	16	13	37	31	13	7	7	7	0	5	0	21	10	12	20	10	10	271	Aug 31	Monday
245	1	0	0	0	7	11	6	0	5	6	8	9	13	21	10	7	15	7	8	10	12	12	19	10	196	Sep 01	Tuesday
246	10	5	5	4	4	4	7	2	0	5	11	14	24	24	16	13	21	13	9	2	6	18	19	12	220	Sep 02	Wednesday
247	15	17	12	16	14	3	14	11	2	11	13	13	16	11	11	25	18	20	21	19	18	14	17	21	271	Sep 03	Thursday
248	20	30	24	20	14	8	4	23	10	13	14	10	22	24	16	21	13	20	19	19	19	26	21	26	436	Sep 04	Friday
249	16	14	19	21	12	15	15	19	13	16	16	17	12	14	14	4	13	16	23	18	40	13	20	32	419	Sep 05	Saturday
250	15	19	13	18	13	9	15	13	25	12	12	11	9	14	25	27	15	18	18	17	23	27	20	10	388	Sep 06	Sunday
251	26	24	23	18	16	7	7	17	12	10	10	17	9	13	11	14	8	21	24	14	18	24	19	21	362	Sep 07	Monday
252	16	24	19	32	16	10	16	17	16	10	12	14	21	11	12	16	18	11	11	14	24	14	14	25	391	Sep 08	Tuesday
253	19	22	22	17	25	25	14	17	17	19	19	15	24	29	11	13	20	23	12	14	10	24	26	15	429	Sep 09	Wednesday
254	23	16	13	18	16	16	11	11	16	10	9	21	8	8	20	11	12	19	11	16	17	15	27	20	370	Sep 10	Thursday
255	17	24	28	18	20	5	5	4	11	15	25	16	14	14	12	25	16	10	23	23	24	21	26	20	377	Sep 11	Friday
256	31	25	19	14	23	23	18	23	22	10	23	23	25	25	17	13	16	22	18	24	13	22	18	18	507	Sep 12	Saturday
257	25	27	17	14	11	24	22	7	15	22	24	22	22	22	9	14	26	34	19	7	23	24	20	17	527	Sep 13	Sunday
258	17	25	23	19	8	10	3	1	13	19	12	12	11	11	15	13	7	13	13	8	13	13	9	9	299	Sep 14	Monday
259	15	11	25	18	19	14	1	1	12	15	10	10	15	15	15	14	16	15	9	8	17	25	8	18	322	Sep 15	Tuesday

Table 2.3.2. (Page 3 of 4)

NAO .DPX Hourly distribution of detections

Day	00	01	02	03	04	05	06	07	08	09	10	11	12	13	14	15	16	17	18	19	20	21	22	23	Sum	Date
260	11	17	20	18	17	15	11	10	3	11	13	10	6	22	18	15	14	22	18	9	11	14	19	9	333	Sep 16 Wednesday
261	30	22	20	11	9	6	12	11	6	10	1	35	19	29	6	9	6	28	9	8	11	11	10	12	324	Sep 17 Thursday
262	7	9	14	13	9	12	3	2	2	3	1	13	11	6	8	4	7	14	12	2	11	8	8	13	192	Sep 18 Friday
263	16	5	13	4	17	20	7	10	14	9	2	13	10	14	9	7	13	11	8	13	13	11	20	19	277	Sep 19 Saturday
264	22	21	27	20	19	17	13	5	8	7	11	4	6	4	14	6	12	8	7	9	12	13	13	11	293	Sep 20 Sunday
265	25	14	19	16	8	1	2	8	1	13	13	10	10	19	9	6	6	12	8	5	12	5	10	10	243	Sep 21 Monday
266	10	10	10	14	6	4	4	6	4	6	6	4	4	19	34	14	6	11	12	13	11	9	9	11	253	Sep 22 Tuesday
267	20	9	12	17	18	9	12	7	5	22	6	8	17	16	14	16	8	13	2	11	4	14	14	8	268	Sep 23 Wednesday
268	10	17	6	11	11	11	5	2	4	8	11	8	11	11	11	6	6	11	7	8	4	11	11	3	201	Sep 24 Thursday
269	3	12	12	7	11	4	2	4	16	3	6	10	6	19	6	6	5	9	6	9	9	6	4		192	Sep 25 Friday
270	7	2	7	11	13	15	4	5	8	3	6	7	11	3	5	8	8	5	11	5	8	6	23	6	177	Sep 26 Saturday
271	11	6	4	14	6	14	5	13	2	18	8	7	11	13	10	9	4	12	11	9	6	8	16	9	228	Sep 27 Sunday
272	6	14	8	5	11	10	7	8	6	2	6	11	28	16	8	4	3	5	6	4	7	5	5	7	204	Sep 28 Monday
273	28	9	9	6	14	6	8	9	4	4	5	5	23	19	22	15	7	4	9	5	9	9	9	9	257	Sep 29 Tuesday
274	14	6	8	19	9	14	13	13	9	13	29	14	22	18	12	3	9	2	1	6	3	2	15	8	265	Sep 30 Wednesday

NAO	00	01	02	03	04	05	06	07	08	09	10	11	12	13	14	15	16	17	18	19	20	21	22	23		
Sum	2319	2286	2309	2156	1712	1484	1731	1724	2092	2180	2794	2242	2504	2346	2012	2056	2177	2228	2078	2356	2337	2246	2381		52129	Total sum
183	13	13	12	13	12	9	9	9	11	12	15	12	14	13	11	11	12	12	11	13	13	12	13		285	Total average
125	13	13	13	13	11	8	6	8	9	11	12	16	12	14	13	10	11	12	12	11	13	12	13		277	Average workdays
58	12	12	12	13	14	12	11	12	11	12	12	13	13	12	12	12	13	12	14	12	13	13	13		297	Average weekends

Table 2.3.2. Daily and hourly distribution of NORSAR detections. For each day is shown number of detections within each hour of the day and number of detections for that day. The end statistics give total number of detections distributed for each hour and the total sum of detections during the period. The averages show number of processed days, hourly distribution and average per processed day.

3   Operation of regional arrays

3.1   Recording of NORESS data at NDPC, Kjeller

Table 3.1.1 lists the main outage times and reasons.

The average recording time was 98.55% as compared to 99.78% during the previous reporting period.

Date	Time		Cause
09 Apr	0127	- 0225	Transmission line failure
09 Apr	1007	- 1426	Transmission line failure
05 May	2342	-	Transmission line failure
06 May		- 0008	Transmission line failure
01 Jun	2200	-	Power break at NDPC
02 Jun		- 0454	Power break at NDPC
02 Jun	0454	-	Reduced data quality (HUB problems)
03 Jun		- 0130	Reduced data quality (HUB problems)
03 Jun	1207	-	Reduced data quality (HUB problems)
04 Jun		- 0100	Reduced data quality (HUB problems)
04 Jun	1130	- 2200	Reduced data quality (HUB problems)
11 Aug	1607	- 1723	Transmission line maintenance
11 Aug	1731	- 1923	Transmission line maintenance
11 Aug	1927	- 2323	Transmission line maintenance
11 Aug	2329	-	Transmission line maintenance
12 Aug		- 0123	Transmission line maintenance
12 Aug	0145	- 0324	Transmission line maintenance
12 Aug	1108	- 1124	Transmission line maintenance
12 Aug	1151	- 1324	Transmission line maintenance
27 Sep	0059	- 0200	Transmission line failure

Table 3.1.1. Interruptions in recording of NORESS data at NDPC, 1 April - 30 September 1992.

Monthly uptimes for the NORESS on-line data recording task, taking into account all factors (field installations, transmissions line, data center operation) affecting this task were as follows:

April	:	99.20
May	:	99.88
June	:	96.23
July	:	99.95
August	:	96.17
September	:	99.86

Fig. 3.1.1 shows the uptime for the data recording task, or equivalently, the availability of NORESS data in our tape archive, on a day-by-day basis, for the reporting period.

J. Torstveit
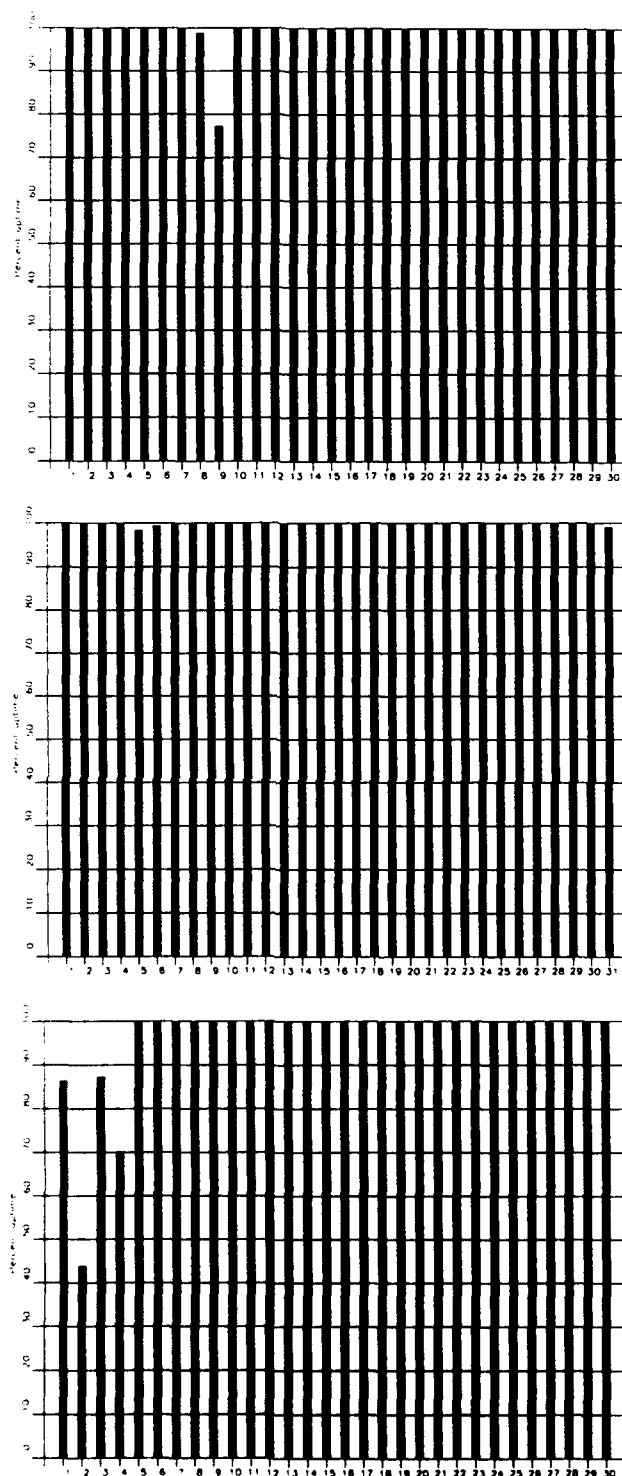
Fig. 3.1.1. NORESS data recording uptime for April (top), May (middle) and June (bottom) 1992.

Fig. 3.1.1. (cont.) NORESS data recording uptime for July (top), August (middle) and September (bottom) 1992.

3.2   Recording of ARCESS data at NDPC, Kjeller

Table 3.2.1 lists the main outage times and reasons.

The average recording time was 99.25 % as compared to 97.28% for the previous reporting period..

Date	Time	Cause
01 Apr	1104 - 1130	Service on the satellite modem
26 Apr	1718 - 2005	Power break HUB
28 Apr	1245 - 2106	Hardware failure NDPC
11 May	0926 - 0936	Service on the satellite modem
01 Jun	2200 -	Power break NDPC
02 Jun	- 0457	Power break NDPC
06 Jun	2040 - 2130	Hardware failure NDPC
21 Jun	1826 - 2031	Service HUB
22 Jun	1744 - 1754	Service HUB
14 Jul	2049 - 2137	Unknown
17 Aug	1658 - 1710	Satellite link failure
17 Aug	1733 - 1748	Satellite link failure
17 Aug	1902 - 1917	Satellite link failure
07 Sep	0646 - 0656	Hardware service NDPC
07 Sep	2310 -	Satellite link failure
08 Sep	- 0052	Satellite link failure

**Table 3.2.1.** The main interruptions in recording of ARCESS data at NDPC, 1 April - 30 September 1992.

Monthly uptimes for the ARCESS on-line data recording task, taking into account all factors (field installations, transmissions line, data center operation) affecting this task were as follows:

April	:	97.74%
May	:	99.97%
June	:	98.37%
July	:	99.86%
August	:	99.84%
September	:	99.71%

Fig. 3.2.1. shows the uptime for the data recording task, or equivalently, the availability of ARCESS data in our tape archive, on a day-by-day basis, for the reporting period.

J. Torstveit

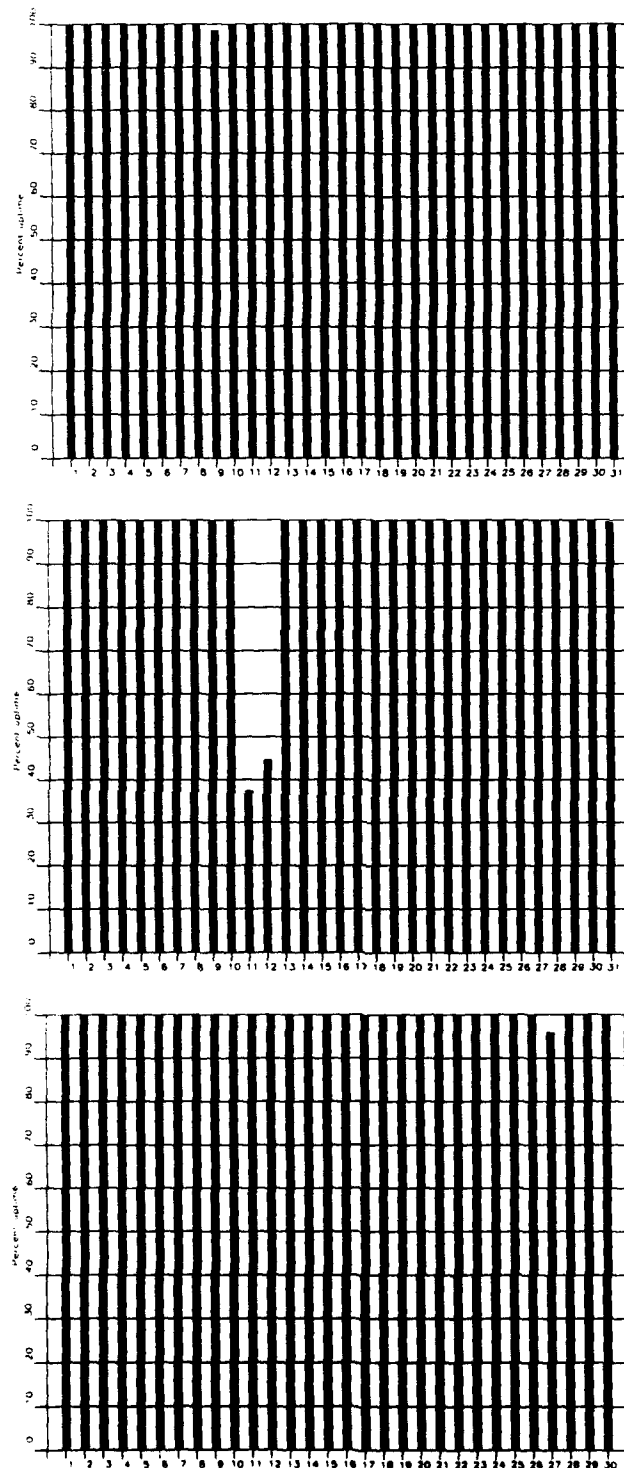**Fig. 3.2.1.** ARCESS data recording uptime for April (top), May (middle) and June(bottom) 1992.

Fig. 3.2.1. ARCESS data recording uptime for July (top), August (middle) and September (bottom) 1992.

3.3   Recording of FINESA data at NDPC, Kjeller

The average recording time was 93.75% as compared to 95.5% for the previous period. As can be seen from Table 3.3.1 below, the main reason for the downtime is transmission line failure and Hub failure.

Date	Time			Cause
23 Apr	2328	-		Transmission line failure
24 Apr		-	0518	Transmission line failure
09 May	1042	-		Transmission line failure
11 May		-	0917	Transmission line failure
22 May	1000	-	1021	Transmission line failure
01 Jun	2200	-		Power failure NDPC
02 Jun		-	0458	Power failure NDPC
18 Jun	1833	-	2140	Transmission line failure
20 Jun	0853	-		Transmission line failure
22 Jun		-	1310	Transmission line failure
05 Jul	0309	-		Transmission line failure
06 Jul		-	0727	Transmission line failure
13 Jul	1359	-		Transmission line failure
14 Jul		-	0815	Transmission line failure
27 Jul	1116	-	1143	Transmission line failure
31 Jul	1240	-		Hardware failure HUB
03 Aug		-	1218	Hardware failure HUB
06 Aug	1137	-	1149	Transmission line failure
10 Aug	2038	-	2109	Transmission line failure
10 Aug	2119	-		Transmission line failure
11 Aug		-	0808	Transmission line failure
17 Aug	1229	-	1327	Transmission line failure
01 Sep	0335	-		Transmission line failure
02 Sep		-	0638	Transmission line failure

Table 3.3.1. The main interruptions in recording of FINESA data at NDPC, 1 April - 30 September 1992.

Monthly uptimes for the FINESA on-line data recording task, taking into account all factors (field installations, transmission lines, data center operation) affecting this task were as follows:

April   : 99.13%
May   : 93.65%
June   : 91.25%
July   : 92.09%
August   : 90.17%
September : 96.22%

Fig. 3.3.1 shows the uptime for the data recording task, or equivalently, the availability of FINESA data in our tape archive, on a day-by-day basis, for the reporting period.
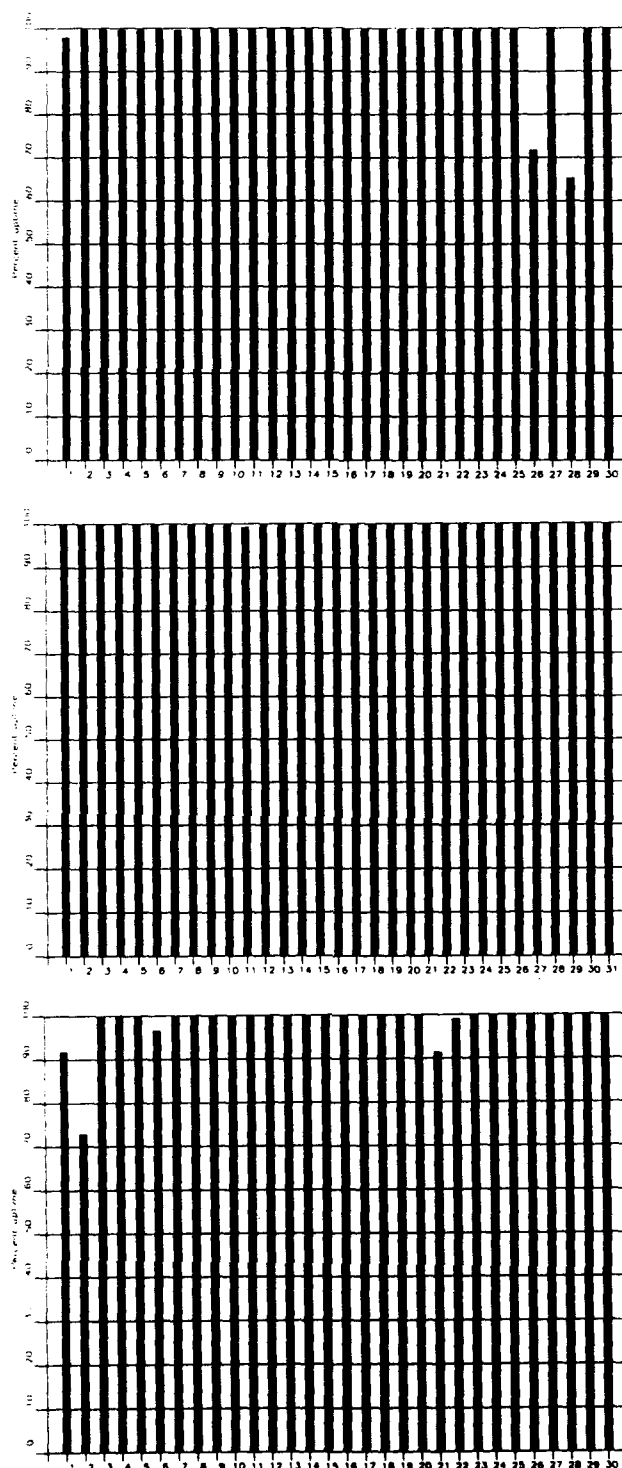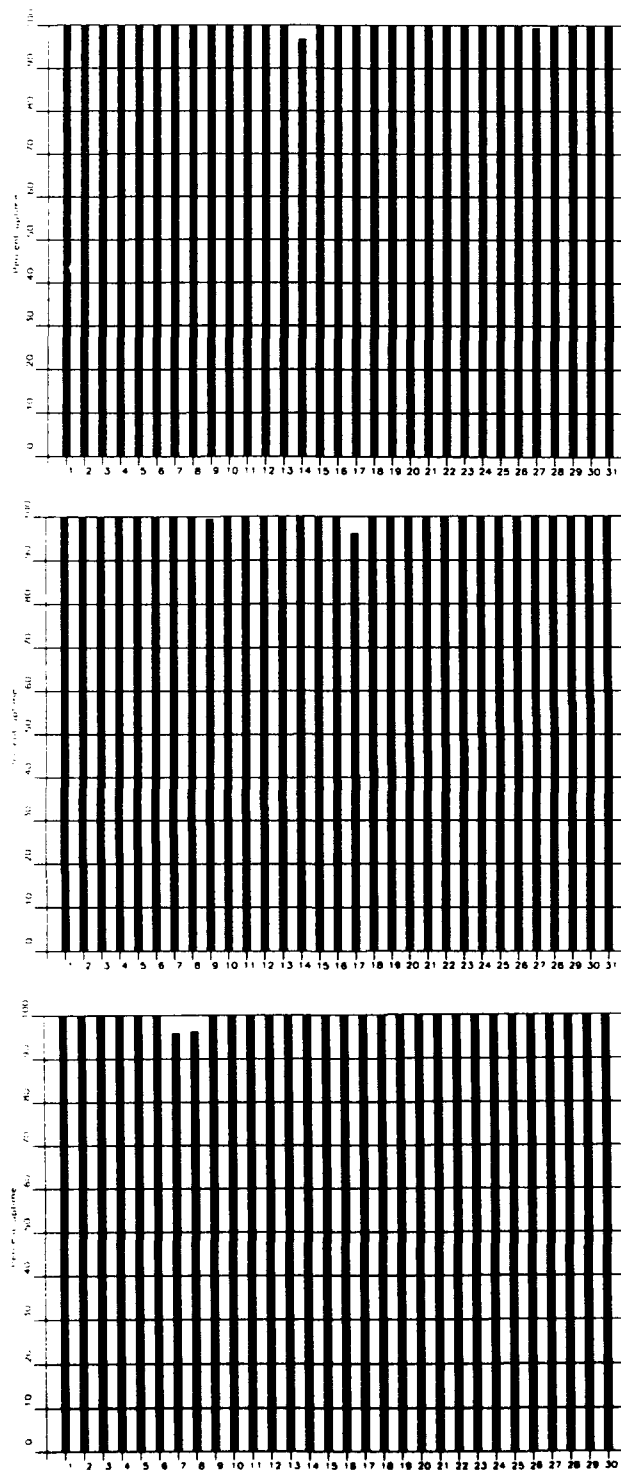
J. Torstveit
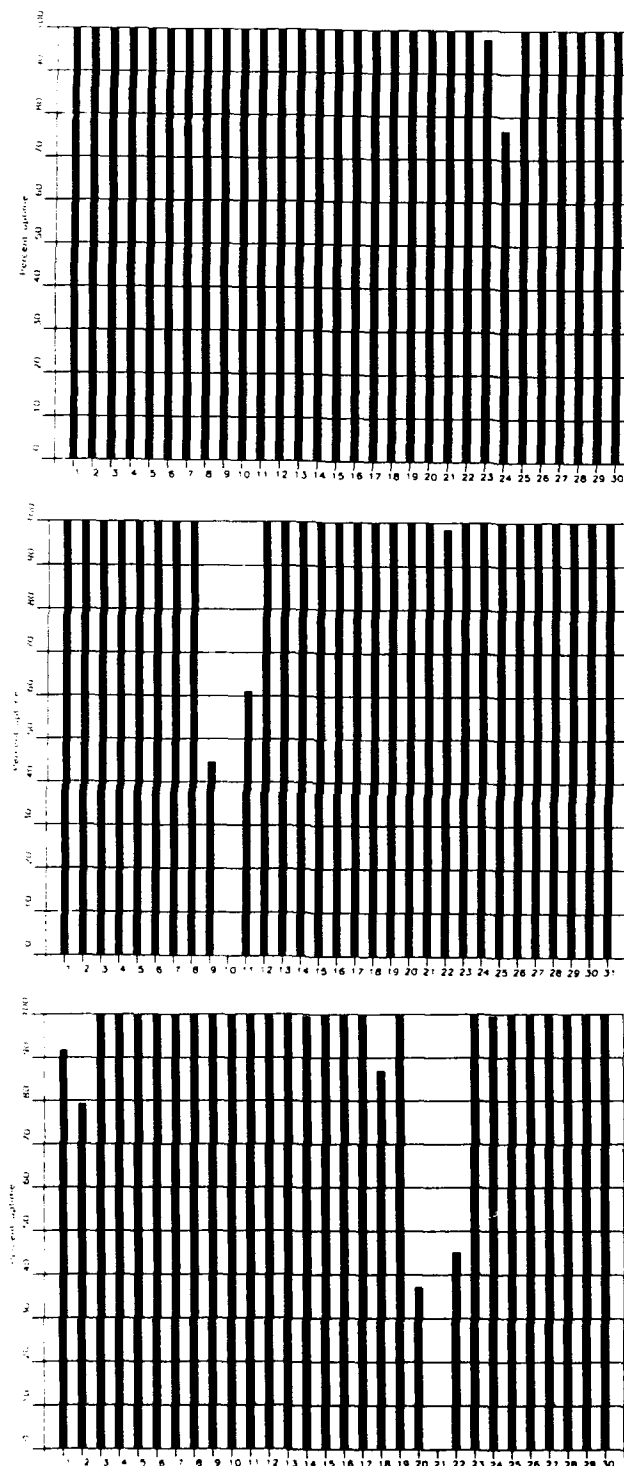
Fig. 3.3.1. FINESA data recording uptime for April (top), May (middle) and June (bottom) 1992.
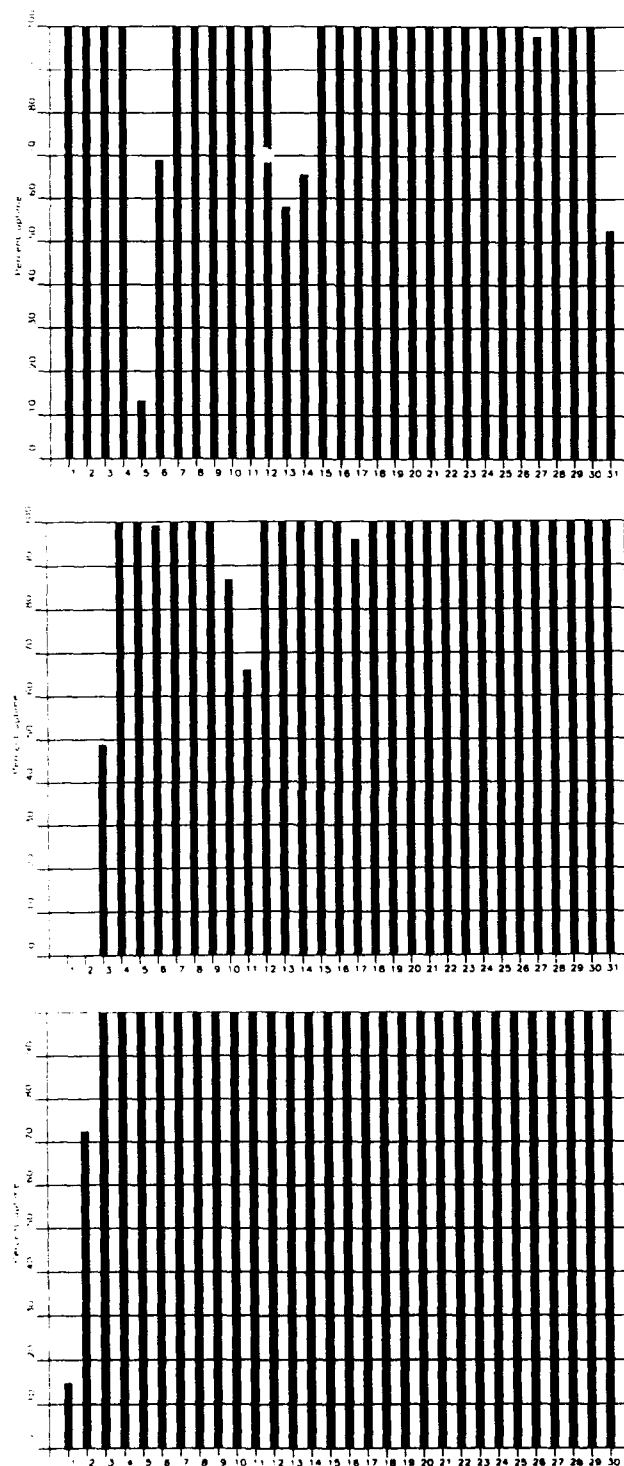
Fig. 3.3.1. FINESA data recording uptime for July (top), August (middle) and September (bottom) 1992.

3.4   Event detection operation

This section reports results from one-array automatic processing using signal processing recipes and "ronapp" recipes for the ep program (NORSAR Sci. Rep. No 2-88/89).

Three systems are in parallel operation to associate detected phases and locate events:

1.   The ep program with "ronapp" recipes is operated independently on each array to obtain simple one-array automatic solutions.

2.   The Generalized Beamforming method (GBF) (see F. Ringdal and T. Kværna (1989), A mulitchannel processing approach to real time network detection, phase association and threshold monitoring, BSSA Vol 79, no 6, 1927-1940) processes the four arrays jointly and presents locations of regional events.

3.   The IMS system is operated on the same set of arrivals as ep and GBF and reports also teleseismic events in addition to regional ones.

IMS results are reported in section 3.5 and GBF results in section 3.6.

In addition to these three event association processes, we are running test versions of the so-called Threshold Monitoring (TM) process. This is a process that monitors the seismic amplitude level at the four regional arrays continuously in time to estimate the upper magnitude limit of an event that might go undetected by the network. The current TM process is beamed to several sites of interest, including the Novaya Zemlya test site. Simple displays of so-called threshold curves reveal instants of particular interest; i.e., instants when events above a certain magnitude threshold may have occurred in the target region. Results from the three processes described above are used to help resolve what actually happened during these instances.

NORESS detections

The number of detections (phases) reported from day 092, 1992, through day 274, 1992, was 42,587, giving an average of 233 detections per processed day (183 days processed).

Table 3.4.1 shows daily and hourly distribution of detections for NORESS.

Events automatically located by NORESS

During days 092, 1992, through 274, 1992, 2556 local and regional events were located by NORESS, based on automatic association of P- and S-type arrivals. This gives an average of 14.0 events per processed day (183 days processed). 60% of these events are within 300 km, and 85% of these events are within 1000 km.

ARCESS detections

The number of detections (phases) reported during day 092, 1992, through day 274, 1992, was 92,044, giving an average of 503 detections per processed day (182 days processed).

ARCESS detections

The number of detections (phases) reported during day 092, 1992, through day 274, 1992, was 92,044, giving an average of 503 detections per processed day (182 days processed).

Table 3.4.2 shows daily and hourly distribution of detections for ARCESS.

Events automatically located by ARCESS

During days 092, 1992, through 274, 1992, 3875 local and regional events were located by ARCESS, based on automatic association of P- and S-type arrivals. This gives an average 21.3 events per processed day (182 days processed). 47% of these events are within 300 km, and 86% of these events are within 1000 km.

FINESA detections

The number of detections (phases) reported during day 092, 1992, through day 274, 1992, was 43,036, giving an average of 240 detections per processed day (179 days processed).

Table 3.4.3 shows daily and hourly distribution of detections for FINESA.

Events automatically located by FINESA

During days 092, 1992, through 274, 1992, 2973 local and regional events were located by FINESA, based on automatic association of P- and S-type arrivals. This gives an average of 16.6 events per processed day (179 days processed). 71% of these events are within 300 km, and 88% of these events are within 1000 km.

GERESS detections

The number of detections (phases) reported from day 092, 1992, through day 274, 1992, was 43,293, giving an average of 242 detections per processed day (178 days processed).

Table 3.4.4 shows daily and hourly distribution of detections for GERESS.

Events automatically located by GERESS

During days 092, 1992, through 274,1992, 3966 local and regional events were located by GERESS, based on automatic association of P- and S-type arrivals. This gives an average of 22.3 events per processed day (178 days processed). 66% of these events are within 300 km, and 85% of these events are within 1000 km.

J. Fyen

NRS .FKX Hourly distribution of detections

Day	00	01	02	03	04	05	06	07	08	09	10	11	12	13	14	15	16	17	18	19	20	21	22	23	Sum	Date		
92	4	0	6	9	0	1	4	1	2	2	3	24	22	9	11	8	1	1	11	12	6	11	5	11	195	Apr 01	Wednesday	
93	4	1	0	8	2	6	1	0	5	8	13	16	11	8	9	14	22	10	5	15	6	8	3	4	185	Apr 02	Thursday	
94	4	1	4	3	1	4	6	1	6	23	24	15	13	30	26	22	11	25	8	20	5	4	3	6	271	Apr 03	Friday	
95	3	10	5	7	9	6	5	6	4	7	8	9	13	5	15	9	3	10	8	1	3	4	5	6	225	Apr 04	Saturday	
96	3	3	1	3	5	10	0	5	4	2	2	7	8	8	5	9	3	8	0	1	1	4	5	6	107	Apr 05	Sunday	
97	3	3	5	7	1	1	5	8	13	7	24	6	17	20	26	16	20	11	11	19	3	3	3	9	243	Apr 06	Monday	
98	6	4	0	3	7	4	4	14	18	31	13	27	23	23	14	4	7	5	13	28	3	4	3	5	294	Apr 07	Tuesday	
99	2	6	6	7	0	24	24	12	29	34	43	44	15	22	10	16	0	11	11	20	3	6	3	1	346	Apr 08	Wednesday	
100	2	4	2	0	10	2	9	20	5	8	18	23	13	9	12	4	7	9	8	22	10	6	1	5	180	Apr 09	Thursday	
101	2	3	3	7	0	4	11	1	11	8	0	18	13	5	16	12	0	11	11	20	1	4	1	1	209	Apr 10	Friday	
102	2	2	2	16	10	2	1	1	4	8	8	23	8	3	1	5	7	9	8	10	7	6	4	2	90	Apr 11	Saturday	
103	2	4	3	1	7	2	7	4	6	1	8	0	4	5	5	17	0	30	2	2	3	1	5	0	79	Apr 12	Sunday	
104	0	2	2	0	1	2	11	5	2	5	18	1	18	3	17	5	9	2	6	6	5	4	0	3	188	Apr 13	Monday	
105	5	13	3	12	10	7	14	7	5	17	13	1	39	29	13	17	8	3	4	2	3	0	5	2	230	Apr 14	Tuesday	
106	2	10	2	7	1	9	15	13	10	6	10	13	16	11	6	8	2	6	2	3	6	2	0	7	180	Apr 15	Wednesday	Skj(rt
107	3	0	6	1	6	2	12	5	13	17	17	9	16	7	3	2	10	1	7	18	6	9	6	10	148	Apr 16	Thursday	Langfr
108	20	14	13	10	1	15	8	13	13	8	12	18	13	11	12	4	14	5	7	11	1	0	6	2	252	Apr 17	Friday	
109	7	5	6	0	9	3	9	7	7	9	7	6	8	8	8	1	4	1	3	3	6	4	0	3	110	Apr 18	Saturday	
110	0	1	7	5	1	4	1	0	2	3	1	3	3	11	12	2	10	4	12	1	1	1	4	3	96	Apr 19	Sunday	Frste
111	0	8	21	13	14	3	12	2	5	10	18	18	10	9	4	10	5	1	6	6	3	10	3	3	181	Apr 20	Monday	Annen
112	6	6	16	16	3	1	1	3	3	13	13	12	13	9	10	5	0	9	8	17	1	2	6	4	179	Apr 21	Tuesday	
113	1	1	6	12	14	11	7	0	8	12	13	19	11	5	14	6	7	11	11	10	3	3	3	5	199	Apr 22	Wednesday	
114	2	4	15	1	8	4	18	3	1	2	8	17	9	7	23	9	6	21	10	9	8	8	8	3	218	Apr 23	Thursday	
115	5	5	5	8	7	0	2	10	5	8	10	17	17	9	7	6	3	27	7	16	1	5	2	10	200	Apr 24	Friday	
116	1	1	5	5	6	1	5	5	4	0	7	13	13	13	4	4	2	5	14	6	8	2	2	1	121	Apr 25	Saturday	
117	1	10	8	9	1	0	4	4	7	9	2	1	8	2	3	11	10	8	4	3	0	4	4	7	111	Apr 26	Sunday	
118	0	2	6	7	8	0	8	8	0	1	5	13	8	9	6	2	5	22	6	14	2	2	2	1	153	Apr 27	Monday	
119	2	3	0	4	4	1	10	10	19	6	10	12	2	13	12	4	6	10	11	15	2	1	4	7	180	Apr 28	Tuesday	
120	0	0	1	0	8	5	10	8	9	11	6	14	8	11	11	11	3	7	9	16	2	2	2	1	170	Apr 29	Wednesday	
121	2	2	1	1	4	8	12	2	19	12	12	20	15	22	8	8	10	8	20	16	1	1	3	5	202	Apr 30	Thursday	
122	3	3	1	6	3	7	2	1	7	9	6	24	15	10	10	17	5	4	3	4	1	1	2	2	95	May 01	Friday	Frste
123	10	15	27	31	19	36	34	34	34	31	35	6	15	12	11	8	6	6	22	4	32	24	8	2	403	May 02	Saturday	
124	6	26	5	3	6	6	8	6	8	5	9	6	9	12	11	17	17	23	13	23	3	17	17	25	303	May 03	Sunday	
125	17	26	25	22	13	12	6	5	8	9	8	2	9	16	9	7	15	11	13	23	6	8	8	6	281	May 04	Monday	
126	8	11	12	13	5	12	14	11	15	15	19	22	14	10	18	18	17	10	5	16	5	5	6	8	306	May 05	Tuesday	
127	11	19	20	0	8	10	5	14	19	13	7	8	22	14	23	3	6	13	5	16	1	7	2	0	264	May 06	Wednesday	
128	4	0	7	7	2	3	14	2	16	10	11	11	4	13	9	17	9	16	11	5	0	0	6	4	167	May 07	Thursday	
129	5	2	9	1	2	3	6	6	9	4	14	4	7	3	4	7	1	9	5	3	7	2	3	0	139	May 08	Friday	
130	4	6	6	5	3	2	4	4	3	13	10	3	3	6	7	8	1	0	1	4	2	5	5	5	105	May 09	Saturday	
131	12	14	14	15	21	11	7	4	1	0	2	9	9	4	12	9	7	9	11	8	3	10	5	10	281	May 10	Sunday	
132	27	35	24	24	16	4	9	4	4	7	10	15	17	15	13	12	4	4	8	10	1	23	29	30	305	May 11	Monday	
133	29	13	14	22	1	12	6	4	9	16	11	12	10	10	5	17	15	10	10	14	5	15	25	11	287	May 12	Tuesday	
134	3	3	2	0	2	7	5	5	3	3	6	8	12	14	14	12	17	6	16	11	7	6	5	6	165	May 13	Wednesday	
135	3	8	4	19	10	11	3	9	11	7	11	22	8	19	12	1	15	7	8	24	0	7	3	1	248	May 14	Thursday	
136	6	0	3	12	2	5	15	5	7	10	6	14	10	17	7	7	20	16	14	13	2	5	5	1	235	May 15	Friday	
137	1	1	9	0	2	3	4	4	9	3	13	11	8	10	7	11	1	9	5	3	8	6	5	2	116	May 16	Saturday	
138	3	1	5	7	10	2	7	0	3	0	16	4	2	1	0	2	3	0	3	5	1	0	0	2	66	May 17	Sunday	Sytten
139	1	1	2	1	8	10	16	0	3	7	12	15	20	14	17	12	26	16	12	8	6	1	3	7	211	May 18	Monday	
140	2	1	5	4	2	6	16	6	16	12	8	12	41	19	32	25	7	7	18	15	0	9	0	2	290	May 19	Tuesday	
141	3	3	3	4	6	5	13	5	33	16	13	10	18	20	30	15	6	11	10	11	9	9	5	8	248	May 20	Wednesday	
142	4	4	1	6	10	8	13	13	16	14	19	19	20	17	17	20	1	2	2	18	2	5	3	4	288	May 21	Thursday	
143	3	5	4	3	0	13	16	6	14	16	30	25	10	7	7	5	1	12	11	11	8	6	5	10	251	May 22	Friday	
144	1	1	3	9	9	3	1	1	2	3	6	2	3	0	0	2	3	4	3	2	4	1	5	0	75	May 23	Saturday	
145	5	9	5	5	1	0	5	2	7	0	4	21	3	5	4	1	6	0	1	2	4	8	2	1	74	May 24	Sunday	
146	2	4	3	2	3	8	16	9	12	10	8	2	17	12	22	14	13	10	7	22	12	6	5	8	235	May 25	Monday	
147	2	3	3	8	3	15	15	15	14	12	24	20	22	17	25	8	8	6	11	23	5	4	4	7	281	May 26	Tuesday	

Table 3.4.1. (Page 1 of 4)

NRS .FKX Hourly distribution of detections

Day	00	01	02	03	04	05	06	07	08	09	10	11	12	13	14	15	16	17	18	19	20	21	22	23	Sum	Date		
148	8	8	9	6	9	9	20	7	12	12	15	20	18	28	18	12	11	7	7	24	5	6	6	2	279	May 27	Wednesday	
149	1	3	4	2	2	0	4	6	1	9	14	6	20	5	5	2	0	0	7	4	6	9	5	9	121	May 28	Thursday	Kristi
150	4	2	2	2	4	10	15	26	11	11	23	7	15	15	4	7	10	18	8	11	4	3	2	0	237	May 29	Friday	
151	7	2	3	0	2	10	7	6	9	3	5	7	11	3	1	2	10	5	6	15	10	3	4	5	134	May 30	Saturday	
152	2	1	2	6	2	1	6	2	5	5	17	1	5	4	1	2	10	7	5	12	3	2	0	0	87	May 31	Sunday	
153	2	2	5	6	0	11	13	9	15	17	4	25	18	16	47	51	27	17	11	19	40	3	0	0	394	Jun 01	Monday	
154	7	9	0	6	1	8	23	21	8	15	18	19	37	22	2	20	17	0	0	0	0	3	27	52	223	Jun 02	Tuesday	
155	0	10	7	0	1	7	20	10	19	15	18	16	27	32	31	0	4	0	8	47	10	1	18	31	397	Jun 03	Wednesday	
156	18	10	6	5	0	2	0	21	6	19	18	8	59	19	4	20	0	0	0	0	1	4	2	12	228	Jun 04	Thursday	
157	25	14	9	8	6	6	11	10	5	4	21	11	18	14	15	9	16	9	9	19	0	3	6	5	303	Jun 05	Friday	
158	23	13	11	6	8	8	9	5	10	7	12	18	3	14	9	21	13	0	11	2	5	21	8	1	205	Jun 06	Saturday	
159	6	4	6	5	6	3	8	5	4	17	7	29	7	8	2	6	6	0	7	1	0	6	2	5	173	Jun 07	Sunday	Frste
160	6	8	2	11	2	3	1	10	4	18	27	4	10	15	12	6	0	8	5	2	5	4	3	1	124	Jun 08	Monday	Annen
161	10	1	0	11	0	13	12	5	14	14	17	11	34	15	17	18	32	16	11	4	1	2	4	5	255	Jun 09	Tuesday	
162	3	2	2	2	3	11	8	19	51	21	18	13	11	12	4	7	6	19	6	12	6	3	2	1	237	Jun 10	Wednesday	
163	2	3	1	13	3	5	9	6	14	14	16	10	17	12	17	12	14	13	13	15	9	3	1	0	222	Jun 11	Thursday	
164	3	1	3	14	5	5	12	13	13	18	18	13	21	9	17	8	12	8	23	28	2	1	1	0	222	Jun 12	Friday	
165	3	0	0	4	0	1	2	4	2	0	5	1	2	2	11	10	3	6	4	3	4	3	0	1	78	Jun 13	Saturday	
166	6	8	1	9	1	4	4	3	2	7	7	17	3	5	15	4	0	6	2	6	3	1	1	0	90	Jun 14	Sunday	
167	1	4	1	2	12	2	2	13	4	2	11	17	12	0	8	11	10	5	5	2	1	1	1	4	157	Jun 15	Monday	
168	2	6	9	16	1	4	6	15	10	10	11	15	10	21	27	12	12	2	3	6	11	9	5	5	206	Jun 16	Tuesday	
169	12	0	3	1	2	15	30	18	24	21	11	18	25	14	17	13	11	2	7	14	10	5	8	11	336	Jun 17	Wednesday	
170	4	5	2	6	4	17	15	7	10	10	12	20	27	13	15	11	16	4	5	17	30	21	6	7	251	Jun 18	Thursday	
171	35	25	10	4	5	8	11	11	16	6	15	8	22	16	12	7	3	3	4	8	11	17	1	12	281	Jun 19	Friday	
172	3	1	1	3	1	5	6	9	4	3	5	5	2	6	5	15	16	16	8	6	8	1	3	4	180	Jun 20	Saturday	
173	1	2	3	5	5	3	3	9	15	11	9	14	4	4	3	7	5	8	10	15	9	1	5	14	89	Jun 21	Sunday	
174	3	1	2	1	5	3	16	11	21	18	31	15	11	20	25	25	8	13	7	22	8	4	6	2	244	Jun 22	Monday	
175	1	2	1	11	2	11	17	10	10	22	11	15	46	20	20	10	13	5	13	19	9	9	3	14	325	Jun 23	Tuesday	
176	4	7	1	1	5	6	18	10	10	17	20	20	23	8	10	10	32	4	20	19	2	2	6	1	223	Jun 24	Wednesday	
177	2	0	5	7	2	13	20	19	17	15	25	25	47	5	5	19	23	15	8	23	10	7	3	2	279	Jun 25	Thursday	
178	5	4	8	9	1	7	5	19	12	17	5	7	9	14	13	4	10	0	6	17	5	3	9	2	274	Jun 26	Friday	
179	3	1	3	0	0	5	8	1	2	5	3	6	16	6	12	5	2	4	7	2	4	3	4	2	119	Jun 27	Saturday	
180	9	3	5	1	3	5	16	5	7	6	13	9	24	21	18	12	5	15	10	6	8	3	5	10	163	Jun 28	Sunday	
181	13	0	11	11	1	19	16	15	8	16	17	18	17	60	85	16	5	9	12	19	1	4	5	9	254	Jun 29	Monday	
182	2	3	1	12	4	14	10	12	17	16	23	31	29	18	21	23	9	6	7	21	0	6	3	11	381	Jun 30	Tuesday	
183	2	1	4	16	1	44	71	16	25	36	23	57	18	49	18	17	17	11	1	21	7	4	4	7	431	Jul 01	Wednesday	
184	4	2	5	0	5	8	44	10	21	39	43	19	57	30	43	10	10	10	5	18	18	3	1	11	421	Jul 02	Thursday	
185	3	1	3	4	2	7	71	52	28	72	43	7	19	25	46	10	14	14	5	28	12	6	4	1	487	Jul 03	Friday	
186	6	2	8	6	3	9	4	6	7	5	10	9	4	0	57	11	9	9	2	3	5	3	1	11	177	Jul 04	Saturday	
187	0	2	5	1	2	3	5	6	8	11	13	4	4	1	1	2	4	9	3	9	4	10	8	3	119	Jul 05	Sunday	
188	10	7	2	8	6	22	19	12	16	15	23	23	23	39	29	72	92	63	44	24	4	4	1	13	564	Jul 06	Monday	
189	8	10	10	5	7	19	17	16	19	11	26	27	24	47	57	67	27	0	8	20	4	7	6	3	429	Jul 07	Tuesday	
190	7	8	1	8	7	7	25	17	29	21	21	23	48	32	32	6	3	36	20	32	20	4	8	1	318	Jul 08	Wednesday	
191	1	2	1	10	0	12	3	20	21	11	24	11	22	47	20	5	9	1	13	10	4	6	10	6	351	Jul 09	Thursday	
192	5	11	0	7	6	25	22	27	27	78	36	68	60	45	31	10	5	36	13	32	10	4	3	0	477	Jul 10	Friday	
193	7	7	6	1	6	18	44	88	49	17	35	4	4	18	7	8	3	21	10	7	8	6	10	10	394	Jul 11	Saturday	
194	8	5	1	6	6	16	6	3	3	2	5	5	5	29	18	3	8	4	4	8	2	6	3	6	232	Jul 12	Sunday	
195	10	11	9	1	13	13	16	21	11	36	75	67	47	43	85	67	21	7	22	4	17	4	2	5	636	Jul 13	Monday	
196	8	4	1	8	5	23	84	35	23	35	35	80	91	60	101	30	59	22	56	1	10	3	4	4	755	Jul 14	Tuesday	
197	6	0	0	7	4	10	115	13	17	78	56	91	12	18	83	11	116	56	15	2	5	4	6	3	865	Jul 15	Wednesday	
198	7	1	19	7	4	22	134	5	24	63	41	39	72	34	48	6	12	7	10	5	11	1	1	6	549	Jul 16	Thursday	
199	0	1	1	5	9	5	1	11	29	101	33	17	34	10	35	5	40	3	1	7	1	6	6	6	261	Jul 17	Friday	
200	2	3	0	10	1	4	1	8	27	21	13	32	13	13	13	10	6	24	24	10	5	5	5	7	263	Jul 18	Saturday	
201	4	7	10	2	7	8	2	7	2	3	10	11	2	3	7	15	15	9	9	1	0	27	4	8	155	Jul 19	Sunday	
202	4	12	12	10	9	1	1	27	29	29	32	30	35	2	28	11	17	11	7	17	5	5	4	7	378	Jul 20	Monday	
203	9	6	3	6	6	1	1	11	5	13	25	27	10	10	4	10	29	14	8	2	5	12	3	2	222	Jul 21	Tuesday	

Table 3.4.1. (Page 2 of 4)

NRS .FKX Hourly distribution of detections

Day	00	01	02	03	04	05	06	07	08	09	10	11	12	13	14	15	16	17	18	19	20	21	22	23	Sum	Date	
204	2	2	3	2	2	7	2	7	9	9	5	11	15	8	8	9	6	1	7	6	3	7	3	5	139	Jul 22	Wednesday
205	1	1	0	3	6	3	1	7	9	4	17	7	6	20	8	10	5	5	9	6	3	3	1	9	135	Jul 23	Thursday
206	6	6	7	9	8	6	4	4	6	13	19	13	15	20	8	9	6	1	8	16	6	1	1	4	176	Jul 24	Friday
207	1	8	9	9	2	2	15	1	4	12	3	15	10	10	3	4	4	4	2	2	5	1	1	2	105	Jul 25	Saturday
208	2	3	0	0	2	3	0	21	4	17	4	8	2	2	3	10	4	3	3	2	5	6	4	5	116	Jul 26	Sunday
209	1	3	6	6	5	6	5	7	7	7	6	5	12	12	8	6	8	10	8	1	2	0	9	6	161	Jul 27	Monday
210	5	4	1	1	3	3	6	8	12	9	17	16	11	12	10	13	4	22	6	3	9	1	8	3	148	Jul 28	Tuesday
211	5	3	2	2	14	11	3	2	9	9	17	18	20	20	11	11	6	10	10	3	1	8	4	3	185	Jul 29	Wednesday
212	3	4	4	8	4	4	4	8	4	7	20	16	13	20	14	3	9	6	2	1	8	3	4	3	185	Jul 30	Thursday
213	7	3	8	9	7	5	5	6	12	8	5	3	8	13	14	3	13	9	10	3	2	6	4	3	158	Jul 31	Friday
214	5	0	9	9	5	7	12	6	4	7	11	3	24	10	5	9	14	10	10	1	4	1	1	0	157	Aug 01	Saturday
215	3	0	7	4	10	5	5	4	1	8	4	13	17	10	7	3	6	13	2	13	9	3	6	2	114	Aug 02	Sunday
216	7	1	4	9	2	7	2	11	3	2	13	3	10	10	15	9	3	10	10	4	4	1	1	1	195	Aug 03	Monday
217	0	1	1	9	12	6	6	13	9	12	13	13	17	16	11	12	13	15	10	20	9	3	5	2	251	Aug 04	Tuesday
218	1	1	7	5	14	5	3	13	9	15	17	12	13	22	22	38	8	22	24	19	5	10	1	1	194	Aug 05	Wednesday
219	3	2	2	1	7	1	6	15	17	17	11	17	23	20	20	9	7	5	8	16	3	6	1	6	172	Aug 06	Thursday
220	0	2	3	2	8	7	9	9	9	3	14	10	11	2	8	12	4	10	6	6	1	1	1	5	144	Aug 07	Friday
221	1	5	1	7	4	3	4	5	11	1	9	4	5	9	5	5	4	12	12	3	5	1	5	6	110	Aug 08	Saturday
222	2	1	5	2	7	3	11	5	39	3	2	2	5	12	7	6	9	9	8	1	12	7	6	5	206	Aug 09	Sunday
223	2	4	2	7	2	3	3	2	3	2	7	0	5	2	15	5	1	5	12	18	56	67	20	6	292	Aug 10	Monday
224	11	0	11	12	8	3	0	1	69	22	0	0	0	21	0	0	6	13	0	1	0	0	3	5	130	Aug 11	Tuesday
225	0	0	6	0	0	3	6	0	0	0	0	0	0	0	0	0	0	0	5	18	8	6	0	0	52	Aug 12	Wednesday
226	1	0	2	0	1	0	0	1	10	4	10	11	18	21	12	3	10	7	8	9	8	6	3	1	170	Aug 13	Thursday
227	1	4	4	6	9	5	1	5	26	23	31	35	42	6	12	14	2	12	27	7	27	23	36	52	310	Aug 14	Friday
228	40	47	41	37	41	41	42	30	30	38	33	23	38	30	33	39	39	46	52	19	54	45	34	44	931	Aug 15	Saturday
229	41	38	42	44	39	44	34	42	27	11	33	23	20	20	26	22	31	33	21	28	29	20	26	34	776	Aug 16	Sunday
230	29	32	22	18	23	9	6	10	30	9	7	11	15	14	16	10	21	18	14	12	20	23	15	22	373	Aug 17	Monday
231	22	29	21	21	16	9	1	7	15	9	6	11	18	7	14	12	9	11	13	15	9	24	12	24	380	Aug 18	Tuesday
232	19	14	42	32	24	4	2	2	8	18	15	17	12	26	12	13	30	14	17	13	13	16	13	11	340	Aug 19	Wednesday
233	10	10	21	12	11	12	7	7	3	5	10	15	25	26	16	27	11	5	24	24	19	11	13	11	286	Aug 20	Thursday
234	5	4	12	12	3	1	2	2	3	18	15	17	18	15	25	17	28	30	17	24	44	46	42	45	487	Aug 21	Friday
235	27	43	28	22	11	36	17	14	7	9	15	14	8	15	10	1	2	5	9	5	15	4	7	3	313	Aug 22	Saturday
236	2	7	3	10	4	4	6	4	7	8	3	17	5	5	7	13	14	4	24	4	28	36	0	3	122	Aug 23	Sunday
237	36	6	1	10	20	0	12	2	2	8	28	11	13	12	12	6	15	5	9	22	15	36	46	37	331	Aug 24	Monday
238	9	43	35	30	18	18	16	5	5	6	5	5	21	21	25	8	21	21	12	8	7	9	8	5	374	Aug 25	Tuesday
239	7	10	12	11	6	10	2	3	16	7	17	4	18	12	22	10	11	11	14	7	3	7	10	5	195	Aug 26	Wednesday
240	7	2	2	3	8	3	1	0	8	6	5	10	12	2	9	9	36	5	10	2	2	1	1	7	189	Aug 27	Thursday
241	2	6	6	3	9	3	2	4	11	11	17	4	18	12	22	8	10	17	2	16	4	4	2	1	216	Aug 28	Friday
242	4	2	0	6	3	7	5	8	8	6	5	6	12	4	4	10	5	2	10	6	8	0	4	4	122	Aug 29	Saturday
243	3	5	8	4	0	5	2	4	11	13	7	6	8	6	6	9	2	5	11	3	0	3	2	2	122	Aug 30	Sunday
244	5	2	4	6	6	1	5	4	8	13	9	14	26	22	5	5	12	12	6	9	10	2	2	3	141	Aug 31	Monday
245	25	14	10	6	3	3	5	5	4	7	13	9	9	22	7	5	7	11	6	6	9	6	2	2	167	Sep 01	Tuesday
246	4	2	6	6	3	6	14	17	13	8	16	11	12	22	11	5	11	7	4	7	7	0	1	0	203	Sep 02	Wednesday
247	4	2	3	6	3	4	7	17	13	11	14	14	16	11	10	6	18	11	1	6	5	3	0	3	189	Sep 03	Thursday
248	1	2	0	3	2	1	2	3	10	13	10	14	19	9	8	4	4	4	3	1	4	9	3	2	180	Sep 04	Friday
249	3	3	3	0	1	1	1	0	1	4	4	3	6	6	8	11	14	5	8	3	9	0	6	6	93	Sep 05	Saturday
250	2	7	2	3	8	12	1	3	11	7	3	7	7	13	11	13	1	7	5	0	2	4	2	6	115	Sep 06	Sunday
251	3	1	4	2	4	4	11	18	25	9	10	14	12	10	10	7	25	11	11	10	4	4	6	2	148	Sep 07	Monday
252	7	2	7	5	4	7	11	11	19	14	16	11	16	22	12	19	17	14	6	19	4	11	6	2	269	Sep 08	Tuesday
253	2	2	1	2	1	16	10	11	19	11	19	16	16	17	25	16	13	14	11	8	11	8	7	13	276	Sep 09	Wednesday
254	1	1	3	5	18	8	9	7	10	11	12	14	14	14	20	13	14	26	23	20	8	7	8	6	227	Sep 10	Thursday
255	3	3	10	4	3	3	9	11	6	11	12	16	16	11	17	8	13	11	14	11	7	8	7	13	226	Sep 11	Friday
256	7	10	9	3	11	18	18	4	8	20	90	42	42	55	60	37	38	30	6	9	4	1	3	6	500	Sep 12	Saturday
257	4	5	9	6	2	7	11	12	12	11	8	6	8	22	12	10	3	4	3	6	2	7	3	5	142	Sep 13	Sunday
258	6	4	4	5	2	16	7	7	12	9	8	16	25	17	10	6	18	5	9	3	4	8	5	5	224	Sep 14	Monday
259	3	3	6	6	8	8	10	5	12	8	8	12	15	14	1	6	15	8	10	7	13	3	3	3	185	Sep 15	Tuesday

Table 3.4.1. (Page 3 of 4)

NRS .FKX Hourly distribution of detections

Day	00	01	02	03	04	05	06	07	08	09	10	11	12	13	14	15	16	17	18	19	20	21	22	23	Sum	Date	
260	9	4	7	3	7	5	16	9	6	8	8	10	25	18	14	7	5	11	6	8	4	3	5	3	201	Sep 16	Wednesday
261	11	3	5	6	3	4	5	11	7	7	10	27	22	28	10	6	2	15	2	6	1	0	7	2	200	Sep 17	Thursday
262	1	7	0	2	0	3	12	11	0	0	0	14	5	8	2	3	3	4	4	7	2	2	0	0	89	Sep 18	Friday
263	5	0	1	10	3	5	9	5	14	3	3	13	4	4	3	6	2	6	6	9	7	23	0	15	176	Sep 19	Saturday
264	4	2	8	4	8	6	2	2	5	1	8	2	5	4	3	5	5	2	3	10	9	0	0	0	110	Sep 20	Sunday
265	1	1	3	10	3	12	18	11	13	11	16	8	22	17	7	7	8	6	1	4	2	2	3	6	212	Sep 21	Monday
266	3	1	4	4	3	4	9	10	8	8	8	8	13	25	6	5	10	13	6	8	8	3	3	2	171	Sep 22	Tuesday
267	4	3	1	5	6	2	4	5	10	3	7	11	6	18	15	7	9	9	1	4	5	5	4	1	149	Sep 23	Wednesday
268	0	2	1	1	4	1	1	3	8	7	14	11	10	18	11	6	3	0	7	5	1	3	5	1	114	Sep 24	Thursday
269	1	1	2	0	6	2	3	3	6	8	6	4	9	12	5	7	6	7	6	1	0	5	4	1	116	Sep 25	Friday
270	9	2	3	1	5	6	4	5	5	6	10	4	5	7	10	2	0	4	16	6	3	4	13	1	105	Sep 26	Saturday
271	3	0	0	1	6	4	7	3	3	4	4	4	12	6	6	6	4	0	9	2	2	1	0	2	92	Sep 27	Sunday
272	4	3	1	1	5	2	7	7	3	7	5	4	28	18	10	2	3	9	3	1	1	0	7	1	132	Sep 28	Monday
273	17	1	0	1	4	7	6	6	5	11	8	7	16	20	15	14	7	1	1	1	0	1	2	0	165	Sep 29	Tuesday
274	3	2	2	12	2	6	13	5	9	17	19	11	16	18	10	17	4	4	3	4	1	3	5	2	192	Sep 30	Wednesday
NRS	00	01	02	03	04	05	06	07	08	09	10	11	12	13	14	15	16	17	18	19	20	21	22	23	Sum		
Sum	1047	1361	1050	1378	1872	1926	2126	1996	2676	2523	2723	2649	2646	2194	2083	1953	1583	2012	1265	1158	1016	1154			42587	Total sum	
	1079	1117			1050		1872																				
183	6	6	6	7	6	8	11	10	11	12	14	15	15	14	14	12	11	11	9	11	7	6	6	6	233	Total average	
125	6	5	6	8	5	8	11	11	12	14	16	17	18	18	17	13	13	12	9	13	7	6	5	6	257	Average workdays	
58	6	6	6	7	6	8	9	9	8	7	10	10	8	8	9	9	8	7	7	7	7	6	6	6	180	Average weekends	

Table 3.4.1. Daily and hourly distribution of NORESS detections. For each day is shown number of detections within each hour of the day and number of detections for that day. The end statistics give total number of detections distributed for each hour and the total sum of detections during the period. The averages show number of processed days, hourly distribution and average per processed day.

FRS .FKX Hourly distribution of detections

Day	00	01	02	03	04	05	06	07	08	09	10	11	12	13	14	15	16	17	18	19	20	21	22	23	Sum	Date		
92	11	10	7	14	11	10	14	24	13	17	15	18	43	29	25	10	16	7	15	6	6	25	16	17	379	Apr 01	Wednesday	
93	11	5	7	8	13	15	13	19	21	22	35	29	24	28	23	25	14	21	15	8	8	11	15	23	406	Apr 02	Thursday	
94	7	6	8	26	15	18	18	15	33	33	35	23	23	21	21	6	8	21	16	14	12	16	23	8	460	Apr 03	Friday	
95	20	20	22	12	13	14	15	15	11	25	33	23	18	13	6	6	20	10	9	10	24	21	27	7	374	Apr 04	Saturday	
96	12	4	7	11	13	17	6	16	13	9	14	19	17	19	9	16	7	8	8	22	24	9	6	9	278	Apr 05	Sunday	
97	12	7	11	9	12	19	26	26	28	27	37	28	28	19	9	20	20	10	21	16	18	14	6	6	409	Apr 06	Monday	
98	4	12	9	19	5	11	9	12	8	25	28	26	8	12	23	15	5	18	20	12	18	10	14	12	323	Apr 07	Tuesday	
99	8	4	10	12	16	6	11	19	19	19	27	32	24	16	20	24	8	10	21	11	22	11	10	16	359	Apr 08	Wednesday	
100	6	6	4	7	16	10	18	12	23	22	34	41	24	22	21	16	5	18	7	31	14	26	22	14	412	Apr 09	Thursday	
101	9	14	7	8	7	14	16	26	19	34	35	22	12	9	24	12	30	6	9	14	14	23	11	4	421	Apr 10	Friday	
102	5	21	15	6	22	22	18	12	11	23	24	12	12	16	6	6	6	5	7	12	17	7	15	4	256	Apr 11	Saturday	
103	3	3	8	3	9	20	16	5	11	4	13	14	12	13	17	11	18	22	15	6	10	19	11	8	236	Apr 12	Sunday	
104	4	15	5	17	17	15	7	5	21	23	20	13	15	23	14	9	9	8	16	14	8	15	21	6	321	Apr 13	Monday	
105	5	5	11	9	12	7	18	12	23	16	16	19	14	18	17	8	14	8	16	4	11	21	9	5	298	Apr 14	Tuesday	
106	7	22	7	35	30	30	24	23	26	26	34	14	20	19	14	14	8	9	7	13	2	10	9	6	414	Apr 15	Wednesday	Skjrt
107	9	13	11	18	12	15	12	30	21	21	27	34	5	7	1	5	10	4	9	7	12	14	7	4	297	Apr 16	Thursday	Langfr
108	8	1	3	9	16	12	8	14	17	16	31	21	18	7	11	14	11	12	2	17	2	10	5	5	246	Apr 17	Friday	
109	3	5	11	6	10	9	3	23	13	29	14	20	5	7	17	5	4	18	8	18	4	4	6	6	244	Apr 18	Saturday	
110	5	3	7	6	3	12	7	2	5	4	4	5	5	0	5	10	4	6	11	4	9	4	3	6	132	Apr 19	Sunday	Frste
111	11	3	7	8	5	12	6	9	13	8	13	34	13	26	12	6	11	1	12	13	14	4	9	13	259	Apr 20	Monday	Annen
112	8	4	4	4	13	16	24	11	16	19	19	21	20	20	12	6	6	16	7	9	9	11	9	7	318	Apr 21	Tuesday	
113	2	8	4	3	5	21	20	20	16	31	16	29	11	21	17	19	18	9	13	10	11	4	15	3	291	Apr 22	Wednesday	
114	1	14	3	10	10	34	12	15	10	6	6	21	20	13	17	8	9	18	13	13	8	17	17	8	311	Apr 23	Thursday	
115	14	14	9	10	33	42	30	14	26	23	27	52	9	19	13	5	18	4	14	10	24	24	15	4	484	Apr 24	Friday	
116	16	21	12	17	11	16	8	14	18	10	18	24	19	23	17	15	19	7	22	13	16	19	20	8	344	Apr 25	Saturday	
117	6	8	10	10	17	8	4	7	11	6	3	20	8	0	0	11	2	2	6	0	5	25	25	10	212	Apr 26	Sunday	
118	18	4	8	1	17	6	12	2	20	22	17	9	8	26	13	13	16	16	14	0	8	17	15	12	277	Apr 27	Monday	
119	8	8	17	6	10	8	10	29	18	22	15	40	46	33	16	0	0	13	22	11	0	20	25	16	222	Apr 28	Tuesday	
120	4	9	4	19	7	17	11	23	21	31	15	40	18	18	26	14	26	15	15	11	16	14	17	7	420	Apr 29	Wednesday	
121	5	9	1	17	16	10	20	23	21	32	15	42	24	27	14	16	11	7	12	15	16	14	14	5	450	Apr 30	Thursday	
122	5	7	6	11	8	2	16	17	9	10	7	25	15	15	3	16	21	20	15	15	13	17	13	4	253	May 01	Friday	Frste
123	4	6	6	7	15	18	8	8	20	12	16	5	15	11	13	15	10	10	10	16	6	6	8	9	254	May 02	Saturday	
124	2	8	2	10	16	14	14	4	16	16	14	26	17	21	18	20	10	12	16	11	4	7	22	4	224	May 03	Sunday	
125	2	11	5	6	19	16	5	17	20	25	14	19	19	22	26	15	12	18	10	16	21	28	23	20	357	May 04	Monday	
126	35	24	12	11	13	13	15	23	11	16	23	35	28	28	16	8	13	18	14	10	3	25	23	14	451	May 05	Tuesday	
127	5	24	12	3	18	20	18	16	11	33	33	32	24	28	6	30	16	16	10	22	14	31	31	18	404	May 06	Wednesday	
128	3	11	14	6	20	20	16	14	26	23	24	32	24	14	7	24	9	17	22	22	5	23	15	22	391	May 07	Thursday	
129	9	6	20	15	14	14	13	21	27	6	16	57	52	28	24	21	21	16	11	11	17	20	20	22	474	May 08	Friday	
130	10	3	3	2	13	22	22	13	8	20	13	16	16	16	6	4	16	6	6	5	7	19	13	13	253	May 09	Saturday	
131	6	12	7	2	12	10	4	12	3	26	12	15	15	10	20	18	20	9	12	4	10	10	13	12	292	May 10	Sunday	
132	10	5	9	12	10	15	13	19	17	19	30	21	21	21	9	19	14	12	18	13	33	30	21	30	424	May 11	Monday	
133	15	13	14	13	12	12	15	12	28	18	28	13	11	11	13	15	18	24	24	23	23	21	39	15	366	May 12	Tuesday	
134	11	22	14	17	5	21	15	20	18	10	29	32	22	30	20	40	27	18	17	12	15	6	24	20	444	May 13	Wednesday	
135	13	7	8	8	8	21	10	18	33	35	34	32	30	39	38	22	25	17	9	17	15	15	22	36	482	May 14	Thursday	
136	17	19	16	16	13	21	8	27	18	25	16	20	20	22	20	4	11	21	16	7	15	9	36	20	379	May 15	Friday	
137	10	7	11	16	8	14	7	10	6	19	23	16	18	10	7	17	15	21	13	18	10	15	11	9	312	May 16	Saturday	
138	7	12	3	9	13	16	8	8	11	11	31	17	17	28	15	15	14	15	16	9	13	8	11	9	274	May 17	Sunday	Sytten
139	6	11	13	13	17	5	8	6	17	11	11	35	20	12	15	18	18	19	9	13	13	13	13	12	357	May 18	Monday	
140	6	7	6	6	10	9	8	13	22	5	17	17	22	14	13	5	5	14	14	14	5	11	11	4	264	May 19	Tuesday	
141	2	4	13	20	10	15	16	13	16	25	42	36	36	14	15	12	12	24	5	6	24	1	20	11	326	May 20	Wednesday	
142	4	6	5	12	12	25	13	16	32	22	25	48	48	24	17	4	14	15	13	13	10	7	11	21	393	May 21	Thursday	
143	10	24	5	13	6	15	14	29	32	37	40	21	13	24	27	43	15	12	25	27	9	21	21	21	470	May 22	Friday	
144	8	4	18	6	18	18	14	11	17	16	21	18	20	20	4	14	20	6	6	13	10	5	18	13	341	May 23	Saturday	
145	7	7	5	22	22	10	13	5	8	8	17	11	8	20	19	14	24	15	33	27	16	15	18	13	308	May 24	Sunday	
146	9	15	14	24	10	19	13	12	20	29	14	17	13	13	21	12	26	24	31	13	11	21	15	13	416	May 25	Monday	
147	10	10	10	10	10	26	9	14	23	20	16	21	23	18	28	18	19	8	18	28	11	18	15	17	396	May 26	Tuesday	

Table 3.4.2 (Page 1 of 4)

FRS .FKX Hourly distribution of detections

Day	00	01	02	03	04	05	06	07	08	09	10	11	12	13	14	15	16	17	18	19	20	21	22	23	Sum	Date		
148	2	15	16	8	8	47	18	8	20	23	18	44	20	17	10	10	16	15	17	12	6	8	31	3	390	May 27	Wednesday	
149	2	16	7	8	7	18	18	8	20	23	18	20	17	10	11	10	14	17	17	12	6	31	8	7	280	May 28	Thursday	
150	6	7	5	14	12	0	10	24	18	16	27	36	19	9	11	5	10	7	15	16	18	19	28	24	432	May 29	Friday	
151	14	6	11	5	7	7	0	12	29	30	23	11	17	27	7	12	8	6	12	7	10	8	8	2	314	May 30	Saturday	
152	5	11	10	8	8	25	6	12	18	16	11	11	17	24	5	17	17	12	10	10	3	0	23	0	215	May 31	Sunday	
153	14	6	12	5	7	9	7	7	13	23	6	14	19	25	7	21	16	13	6	10	10	23	0	7	333	Jun 01	Monday	Kristl
154	14	17	10	17	7	7	9	34	11	8	17	22	34	24	26	17	13	10	10	15	5	8	0	0	243	Jun 02	Tuesday	
155	0	0	0	0	2	14	7	11	11	11	25	25	4	6	8	16	13	14	6	14	14	11	19	0	410	Jun 03	Wednesday	
156	8	4	8	7	7	21	18	10	31	28	21	24	19	18	18	21	13	11	19	14	17	0	19	0	322	Jun 04	Thursday	
157	5	5	3	0	17	24	25	10	19	15	24	17	24	42	33	9	9	11	0	5	0	11	0	4	244	Jun 05	Friday	
158	17	14	0	2	0	3	9	15	15	17	20	17	20	20	6	11	11	6	8	3	12	0	24	9	285	Jun 06	Saturday	
159	9	22	17	10	6	5	5	15	18	27	36	32	15	16	33	18	6	8	17	4	8	24	6	4	339	Jun 07	Sunday	Frste
160	16	18	11	8	17	7	7	15	11	19	21	10	12	15	16	5	16	12	16	5	5	13	13	7	263	Jun 08	Monday	Annen
161	22	18	10	9	6	16	20	15	23	21	21	15	15	22	18	11	16	16	8	10	6	18	21	7	374	Jun 09	Tuesday	
162	14	15	11	16	5	7	20	8	16	31	30	17	17	18	14	20	11	8	8	6	8	17	22	12	351	Jun 10	Wednesday	
163	8	11	11	8	7	13	8	8	16	31	32	53	56	26	39	64	31	21	40	95	99	73	56	35	864	Jun 11	Thursday	
164	50	29	26	65	40	40	13	77	88	85	90	48	16	36	36	53	31	40	19	37	37	18	27	11	1009	Jun 12	Friday	
165	6	2	1	5	8	31	10	3	3	8	8	47	10	17	16	3	4	4	14	7	14	21	14	1	228	Jun 13	Saturday	
166	8	10	7	15	15	5	4	17	18	12	19	14	10	17	43	12	11	15	42	16	11	15	16	3	339	Jun 14	Sunday	
167	6	8	10	17	8	14	14	15	20	20	12	20	27	24	24	16	6	6	6	6	14	16	16	14	336	Jun 15	Monday	
168	4	4	5	15	5	14	18	10	9	11	18	15	8	11	17	20	6	7	6	16	13	20	20	18	293	Jun 16	Tuesday	
169	11	4	14	14	22	20	20	22	32	18	22	40	27	27	20	22	20	21	18	18	11	27	36	16	493	Jun 17	Wednesday	
170	4	11	10	14	22	6	24	6	26	18	32	58	18	18	9	16	10	13	13	18	8	17	16	2	389	Jun 18	Thursday	
171	10	7	7	7	3	5	5	9	23	12	35	39	20	17	8	8	9	14	21	21	17	17	10	4	400	Jun 19	Friday	
172	3	5	2	10	11	13	13	16	14	28	25	28	25	21	33	17	18	12	13	13	6	15	5	11	353	Jun 20	Saturday	
173	4	6	12	12	20	1	7	20	10	12	8	27	8	17	11	9	11	13	13	13	7	10	5	23	244	Jun 21	Sunday	
174	5	12	7	18	10	13	18	20	16	16	12	27	40	39	21	28	17	16	21	13	7	26	23	6	407	Jun 22	Monday	
175	13	13	18	24	13	8	23	9	20	23	28	28	22	22	46	31	15	32	8	16	16	27	19	6	486	Jun 23	Tuesday	
176	13	6	11	18	13	11	39	67	55	39	58	58	39	51	24	36	21	9	18	16	16	13	13	17	583	Jun 24	Wednesday	
177	16	22	11	42	28	28	16	22	63	26	41	39	18	30	49	18	26	3	28	38	21	20	15	17	574	Jun 25	Thursday	
178	4	8	8	34	24	19	31	31	40	43	75	53	53	90	45	26	21	28	10	10	21	25	21	5	729	Jun 26	Friday	
179	4	13	6	12	15	28	19	19	67	50	50	26	20	61	28	19	26	21	14	6	16	25	16	17	498	Jun 27	Saturday	
180	2	5	8	17	13	18	18	27	40	38	24	24	20	30	16	4	19	5	14	4	25	16	12	5	427	Jun 28	Sunday	
181	14	8	17	23	38	68	68	68	43	59	90	37	76	27	27	8	7	12	4	6	21	13	4	17	787	Jun 29	Monday	
182	6	0	12	11	22	46	19	43	22	43	46	37	33	33	27	25	14	5	16	4	4	24	20	9	592	Jun 30	Tuesday	
183	3	3	14	44	34	18	43	48	36	52	43	56	48	46	53	40	33	6	18	27	21	25	7	13	737	Jul 01	Wednesday	
184	15	3	20	20	22	46	26	51	30	59	58	28	26	33	48	28	20	34	16	16	34	10	10	18	622	Jul 02	Thursday	
185	31	11	14	11	11	37	10	23	30	37	58	57	56	26	24	50	21	17	14	9	7	2	13	10	481	Jul 03	Friday	
186	8	13	11	27	18	10	32	19	20	22	19	18	18	18	8	12	12	10	8	8	8	10	10	6	351	Jul 04	Saturday	
187	8	12	12	21	20	12	12	20	35	23	40	40	27	40	20	16	18	16	11	19	15	15	13	31	513	Jul 05	Sunday	
188	1	9	11	11	20	26	11	44	52	36	52	51	27	51	20	30	16	53	19	28	28	18	18	10	638	Jul 06	Monday	
189	5	8	6	21	29	29	44	60	61	49	56	61	45	45	32	26	23	27	36	17	17	16	29	17	767	Jul 07	Tuesday	
190	6	9	19	19	53	52	68	70	48	54	71	80	29	29	49	36	13	20	19	36	28	51	11	11	879	Jul 08	Wednesday	
191	18	9	18	28	25	42	22	42	66	76	57	56	58	58	51	40	42	22	28	28	17	49	22	22	920	Jul 09	Thursday	
192	25	42	25	8	15	26	26	23	42	73	60	60	47	47	24	20	37	26	15	6	2	16	7	6	726	Jul 10	Friday	
193	14	15	15	22	22	1	19	29	33	53	34	50	30	30	27	28	15	23	14	14	11	7	19	3	521	Jul 11	Saturday	
194	13	13	10	28	11	31	17	17	21	27	27	51	44	44	23	38	17	24	35	35	18	19	22	28	516	Jul 12	Sunday	
195	12	12	14	16	20	22	30	10	20	16	34	65	33	30	30	25	15	11	27	27	21	23	23	6	514	Jul 13	Monday	
196	2	4	4	19	14	37	23	41	32	24	40	48	40	52	24	28	13	17	14	14	17	17	17	12	652	Jul 14	Tuesday	
197	5	9	5	28	19	37	17	48	48	32	66	51	37	37	37	30	12	20	18	35	20	22	19	10	742	Jul 15	Wednesday	
198	13	3	16	28	20	16	30	17	26	41	34	46	35	25	23	25	22	37	27	15	21	23	22	12	637	Jul 16	Thursday	
199	5	14	20	14	14	50	23	30	43	32	53	53	35	57	57	8	37	31	17	17	20	17	23	10	543	Jul 17	Friday	
200	5	4	36	19	14	22	16	23	69	54	48	56	26	47	47	15	15	15	16	22	41	20	10	7	669	Jul 18	Saturday	
201	5	5	10	21	10	13	13	16	26	41	53	44	52	37	37	12	12	18	16	9	47	42	10	10	459	Jul 19	Sunday	
202	7	6	30	30	20	11	11	26	43	50	40	40	40	52	52	23	50	16	24	7	30	22	33	36	723	Jul 20	Monday	
203	44	21	47	47	12	26	26	42	43	36	47	43	43	43	39	31	37	50	43	29	22	30	30	19	849	Jul 21	Tuesday	
204	7	24	4	27	16	30	36	36	42	48	54	59	45	48	35	37	21	15	19	16	6	24	10	23	677	Jul 22	Wednesday	

Table 3.4.2. (Page 2 of 4)

FRS .FKX Hourly distribution of detections

Day	00	01	02	03	04	05	06	07	08	09	10	11	12	13	14	15	16	17	18	19	20	21	22	23	Sum	Date	
205	3	10	4	23	25	21	16	21	15	28	27	21	21	23	33	21	16	12	18	19	24	14	22	23	470	Jul 23	Thursday
206	6	2	12	15	5	18	28	51	46	50	48	55	26	53	32	19	35	24	23	17	24	15	22	5	647	Jul 24	Friday
207	26	5	4	41	5	28	11	33	42	48	14	35	50	38	30	16	25	17	34	11	7	34	13	14	570	Jul 25	Saturday
208	8	5	3	4	21	24	33	31	46	33	34	40	39	33	38	15	5	17	20	34	9	7	18	15	478	Jul 26	Sunday
209	3	11	5	7	23	51	33	28	32	52	33	42	39	51	47	24	22	25	16	25	13	15	23	6	647	Jul 27	Monday
210	11	3	7	13	13	33	27	39	27	47	46	30	36	41	21	25	30	17	10	13	35	12	16	2	591	Jul 28	Tuesday
211	16	7	15	17	18	34	27	54	58	40	42	52	22	40	27	20	24	21	20	11	30	30	24	6	581	Jul 29	Wednesday
212	11	18	5	26	28	32	33	40	58	46	52	43	43	38	95	68	28	8	33	19	35	20	29	15	771	Jul 30	Thursday
213	17	7	24	16	17	20	20	44	53	48	46	57	22	48	20	35	24	26	23	11	30	15	23	24	770	Jul 31	Friday
214	6	18	4	20	10	13	17	4	30	28	36	16	16	20	35	16	28	21	18	46	6	5	4	3	383	Aug 01	Saturday
215	5	5	28	19	14	17	21	20	24	36	32	15	25	50	20	37	41	47	39	32	41	19	4	21	562	Aug 02	Sunday
216	15	7	1	26	10	24	78	90	82	90	67	67	58	92	91	86	90	37	39	46	47	22	22	12	1214	Aug 03	Monday
217	39	3	6	24	74	78	84	92	73	75	97	89	98	29	54	97	97	70	22	32	18	34	34	6	1390	Aug 04	Tuesday
218	20	1	20	18	37	43	108	68	41	48	57	71	57	54	48	46	30	37	33	26	41	28	28	12	1029	Aug 05	Wednesday
219	15	17	29	49	78	89	78	71	54	87	45	78	125	86	28	19	10	17	22	33	47	46	29	12	1031	Aug 06	Thursday
220	15	15	24	29	62	62	68	11	54	30	45	66	62	94	78	30	27	7	19	24	24	9	18	8	882	Aug 07	Friday
221	4	24	5	2	2	16	7	13	42	49	29	35	29	21	48	7	10	11	16	4	6	12	12	2	440	Aug 08	Saturday
222	8	3	3	18	7	9	13	10	7	16	20	12	16	16	14	8	7	11	5	16	2	8	8	13	290	Aug 09	Sunday
223	13	13	15	15	27	13	48	49	52	57	59	31	22	16	30	15	16	35	9	20	19	19	16	7	774	Aug 10	Monday
224	26	20	13	12	52	67	61	60	72	75	68	39	91	52	30	55	27	53	35	7	20	15	28	10	966	Aug 11	Tuesday
225	1	11	3	16	70	61	59	23	61	70	39	37	39	30	30	19	45	34	15	52	25	32	16	26	654	Aug 12	Wednesday
226	6	6	16	16	88	43	43	20	18	45	35	53	53	91	91	52	26	13	28	15	34	11	16	13	792	Aug 13	Thursday
227	9	13	7	3	26	43	73	37	51	60	54	62	46	34	30	20	10	14	15	28	25	21	21	13	694	Aug 14	Friday
228	13	9	15	10	43	76	46	51	29	32	35	18	24	33	27	24	14	13	12	28	15	19	7	13	490	Aug 15	Saturday
229	9	5	7	18	16	21	15	32	19	32	18	21	11	11	40	20	14	13	13	16	12	29	23	5	371	Aug 16	Sunday
230	13	12	23	21	90	84	93	76	28	45	59	51	55	68	109	78	72	31	28	8	31	18	28	21	1113	Aug 17	Monday
231	12	8	12	12	40	13	47	28	36	59	49	57	52	42	33	24	23	8	36	20	28	22	22	7	836	Aug 18	Tuesday
232	18	23	41	41	40	38	57	94	56	48	41	52	36	36	34	39	18	33	17	19	20	10	20	7	873	Aug 19	Wednesday
233	10	20	14	15	32	24	23	36	24	24	41	51	54	31	36	25	25	27	15	17	10	8	10	7	598	Aug 20	Thursday
234	7	14	12	16	18	18	33	41	44	28	35	48	54	21	21	34	39	24	29	15	23	13	37	4	652	Aug 21	Friday
235	7	12	7	2	18	18	11	1	28	35	59	59	27	33	21	21	19	17	27	6	11	27	30	12	445	Aug 22	Saturday
236	7	13	3	12	18	11	17	26	14	14	39	24	29	52	50	21	9	16	34	6	11	22	23	18	346	Aug 23	Sunday
237	5	15	14	14	27	39	39	52	33	33	52	39	36	29	41	16	44	35	21	22	21	21	37	12	700	Aug 24	Monday
238	28	9	17	11	12	37	80	57	38	38	80	51	51	50	29	40	35	35	23	30	24	24	22	18	753	Aug 25	Tuesday
239	14	14	11	15	14	37	23	46	52	39	39	46	41	37	29	33	26	20	15	26	38	15	22	14	650	Aug 26	Wednesday
240	17	10	15	10	15	21	21	33	43	25	46	45	33	23	36	19	23	24	15	18	30	17	17	10	599	Aug 27	Thursday
241	17	26	17	26	25	25	69	54	54	53	49	45	41	36	40	60	43	56	30	19	17	14	14	10	802	Aug 28	Friday
242	3	2	2	6	16	12	23	13	13	49	12	23	4	33	42	28	32	11	24	16	14	6	12	5	420	Aug 29	Saturday
243	4	7	10	2	7	15	16	16	35	18	16	26	4	40	40	23	11	16	18	24	19	19	33	10	419	Aug 30	Sunday
244	10	11	8	40	40	41	35	28	79	52	52	54	17	40	12	21	21	18	35	27	24	24	16	34	695	Aug 31	Monday
245	4	20	13	5	7	25	37	31	24	48	74	38	38	28	21	21	11	26	23	24	11	13	16	10	560	Sep 01	Tuesday
246	20	26	19	19	32	39	46	46	74	50	43	27	38	53	27	13	29	17	21	11	20	24	45	5	790	Sep 02	Wednesday
247	5	16	15	10	15	24	25	21	30	35	46	46	38	22	17	29	21	25	25	20	22	18	18	6	545	Sep 03	Thursday
248	6	12	6	6	6	15	12	14	13	24	20	38	28	19	24	13	31	21	13	12	6	9	14	9	373	Sep 04	Friday
249	7	5	12	3	8	11	16	10	19	16	24	13	23	18	15	23	24	14	20	4	9	13	17	4	262	Sep 05	Saturday
250	1	3	3	12	21	11	19	19	16	14	13	17	11	29	19	26	17	18	35	35	29	16	33	1	400	Sep 06	Sunday
251	13	20	7	7	19	28	26	30	27	37	37	24	17	16	24	24	18	26	17	16	14	13	16	13	504	Sep 07	Monday
252	2	1	5	19	12	18	17	24	16	27	24	24	24	28	18	15	12	20	33	17	25	18	35	22	376	Sep 08	Tuesday
253	21	7	13	12	12	24	16	18	27	50	42	65	65	53	35	25	29	22	40	30	35	18	44	11	689	Sep 09	Wednesday
254	4	6	21	9	27	16	27	27	31	70	64	34	21	68	25	25	21	21	14	18	24	24	28	22	585	Sep 10	Thursday
255	8	18	5	18	14	25	39	30	41	24	40	53	34	40	40	25	25	21	24	9	36	9	11	14	634	Sep 11	Friday
256	8	20	2	20	26	12	30	47	26	25	21	12	28	40	44	44	4	21	16	26	18	18	11	14	303	Sep 12	Saturday
257	18	7	9	14	1	16	16	18	20	26	13	15	10	16	7	16	4	9	30	7	26	9	24	5	336	Sep 13	Sunday
258	5	19	6	11	6	6	16	22	30	30	14	13	13	26	35	12	12	18	18	29	29	6	18	14	511	Sep 14	Monday
259	19	10	11	9	29	13	16	30	41	41	38	23	34	36	35	39	30	10	41	19	6	23	23	15	705	Sep 15	Tuesday
260	7	103	6	29	29	48	34	35	31	38	30	35	34	32	18	20	34	38	13	65	12	33	31	24	753	Sep 16	Wednesday
261	13	13	11	20	15	20	43	34	17	29	39	55	36	18	33	17	23	14	5	7	15	14	25	5	564	Sep 17	Thursday

Table 3.4.2 (Page 3 of 4)

FRS .FKX Hourly distribution of detections

Day	00	01	02	03	04	05	06	07	08	09	10	11	12	13	14	15	16	17	18	19	20	21	22	23	Sum	Date	
262	23	15	5	9	15	27	60	44	6	0	4	50	51	29	29	26	27	23	17	6	22	26	36	2	555	Sep 18	Friday
263	9	11	6	3	10	13	1	12	20	32	27	14	24	19	20	9	13	16	17	6	12	10	30	7	341	Sep 19	Saturday
264	10	8	21	4	3	13	14	6	10	6	8	11	22	32	11	11	26	31	13	24	10	4	18	6	322	Sep 20	Sunday
265	34	8	3	7	13	32	29	28	75	46	51	46	61	70	56	39	27	40	18	11	8	24	40	10	748	Sep 21	Monday
266	11	1	9	17	11	51	52	52	68	40	53	45	48	60	48	30	20	19	11	19	9	9	40	12	740	Sep 22	Tuesday
267	5	9	5	18	16	50	59	57	94	36	82	63	69	71	89	30	27	20	19	13	8	8	26	6	881	Sep 23	Wednesday
268	11	13	5	13	13	52	73	56	49	53	66	48	64	21	10	27	9	8	22	13	9	8	29	10	704	Sep 24	Thursday
269	28	18	4	12	13	21	26	39	80	45	48	41	34	20	26	18	10	12	15	23	8	18	27	4	588	Sep 25	Friday
270	6	10	20	10	19	15	21	13	34	46	31	26	12	12	34	8	23	15	9	6	22	21	29	3	445	Sep 26	Saturday
271	12	9	6	4	10	10	9	11	8	10	23	9	17	18	26	11	13	11	19	9	11	3	15	22	306	Sep 27	Sunday
272	11	11	16	3	21	20	32	79	91	64	58	66	68	76	42	40	30	23	15	19	11	24	5	13	895	Sep 28	Monday
273	28	13	8	3	6	10	32	28	28	9	26	24	17	27	19	9	22	11	6	19	6	23	15	20	412	Sep 29	Tuesday
274	5	9	6	11	8	20	33	18	23	17	28	21	32	23	51	72	13	14	11	12	15	4	6	23	475	Sep 30	Wednesday

FRS	00	01	02	03	04	05	06	07	08	09	10	11	12	13	14	15	16	17	18	19	20	21	22	23			
Sum	1930	2651	4429	4839	5571	6443	5413	5443	4899	3945	3475	3040	3424	2764	3600												
	1890	1862	2532	4417	5604	6287					2744	2854	1988												92044	Total sum	
183	10	11	10	14	14	24	24	26	31	30	34	35	30	30	27	22	19	17	19	15	15	16	20	11	503	Total average	
125	11	12	11	15	15	29	29	33	36	34	39	42	35	34	30	25	22	18	20	16	17	22	12		573	Average workdays	
58	8	8	9	12	10	13	13	13	19	22	25	21	17	20	19	13	12	12	17	13	13	15	8		347	Average weekends	

Table 3.4.2. Daily and hourly distribution of ARCESS detections. For each day is shown number of detections within each hour of the day and number of detections for that day. The end statistics give total number of detections distributed for each hour and the total sum of detections during the period. The averages show number of processed days, hourly distribution and average per processed day.

FIN .FKX Hourly distribution of detections

Day	00	01	02	03	04	05	06	07	08	09	10	11	12	13	14	15	16	17	18	19	20	21	22	23	Sum	Date		
92	12	9	6	4	1	0	4	12	10	20	17	24	23	31	3	10	4	4	4	6	13	15	7	16	255	Apr 01	Wednesday	
93	13	8	14	7	7	4	7	12	16	16	30	26	19	18	10	6	6	3	7	12	4	8	4	3	260	Apr 02	Thursday	
94	7	9	7	16	5	2	9	8	17	21	16	20	10	10	18	13	6	4	5	5	1	3	5	8	225	Apr 03	Friday	
95	1	12	8	5	8	7	2	3	5	4	4	4	10	1	1	13	3	7	1	1	3	1	12	1	113	Apr 04	Saturday	
96	5	4	7	8	2	9	7	9	11	11	8	6	7	2	8	6	10	10	8	13	9	9	6	6	170	Apr 05	Sunday	
97	13	13	10	9	9	6	4	13	9	10	22	19	20	16	13	12	12	5	7	9	11	6	8	11	252	Apr 06	Monday	
98	11	12	6	8	2	6	8	4	15	19	18	24	7	15	12	11	6	5	11	5	11	13	7	7	248	Apr 07	Tuesday	
99	6	9	12	11	2	10	6	11	11	19	25	17	21	17	10	10	9	7	17	9	16	18	10	10	263	Apr 08	Wednesday	
100	16	17	9	8	2	3	6	12	16	25	27	32	16	14	15	10	2	7	17	16	17	7	7	26	343	Apr 09	Thursday	
101	25	29	20	11	9	12	5	5	20	21	20	17	16	7	8	4	12	4	3	3	4	18	22	0	285	Apr 10	Friday	
102	6	9	20	6	4	3	7	12	4	6	3	3	2	4	2	2	4	1	4	5	7	7	0	10	139	Apr 11	Saturday	
103	1	4	4	9	13	4	4	5	5	10	20	32	16	7	5	5	2	5	1	3	6	5	2	2	132	Apr 12	Sunday	
104	3	14	5	13	4	3	7	3	19	9	20	3	3	6	3	2	2	5	5	6	11	5	12	9	214	Apr 13	Monday	
105	3	4	9	14	8	1	1	6	6	10	20	20	6	13	7	7	5	14	6	4	3	8	10	8	226	Apr 14	Tuesday	
106	8	10	11	11	0	11	11	7	18	12	8	21	17	9	17	10	8	8	5	10	6	8	6	11	245	Apr 15	Wednesday	Skj[rt
107	7	18	23	13	6	10	0	11	22	18	34	16	17	5	2	7	9	3	6	14	10	8	6	5	274	Apr 16	Thursday	Langfr
108	14	3	8	8	6	10	1	9	11	17	17	10	16	12	11	13	14	9	6	11	11	7	6	5	232	Apr 17	Friday	
109	7	8	21	7	8	5	7	6	18	13	20	20	16	11	15	2	8	6	10	10	15	9	6	5	226	Apr 18	Saturday	
110	8	8	15	7	11	10	6	6	11	11	12	13	10	13	10	9	6	11	15	14	11	7	8	18	237	Apr 19	Sunday	Frste
111	22	12	29	7	11	0	13	7	11	16	15	27	22	10	14	6	12	10	4	11	12	12	8	10	278	Apr 20	Monday	Annen
112	8	7	11	5	9	5	3	14	19	16	18	11	5	21	16	9	9	10	11	7	12	13	9	7	250	Apr 21	Tuesday	
113	9	9	13	6	9	3	5	12	12	19	30	18	16	10	16	6	6	10	7	5	9	13	10	12	273	Apr 22	Wednesday	
114	7	9	8	2	13	8	7	14	11	15	16	29	11	15	10	13	15	3	6	7	5	7	9	5	223	Apr 23	Thursday	
115	0	0	0	0	1	2	5	9	23	14	6	27	9	8	14	9	4	4	5	5	7	3	2	11	167	Apr 24	Friday	
116	6	6	11	11	0	13	2	9	3	5	12	3	9	10	4	15	5	10	6	10	5	4	12	15	180	Apr 25	Saturday	
117	10	20	15	10	6	7	11	11	5	10	18	22	13	17	16	10	10	4	17	16	9	17	21	5	260	Apr 26	Sunday	
118	13	13	16	9	6	4	15	12	15	17	16	34	29	14	16	13	6	4	8	12	7	12	7	8	257	Apr 27	Monday	
119	13	18	12	12	2	2	6	16	17	17	16	36	16	17	14	13	7	5	20	22	15	13	13	13	288	Apr 28	Tuesday	
120	6	10	10	9	7	11	12	11	13	17	23	32	16	7	7	13	6	8	14	12	6	6	5	9	285	Apr 29	Wednesday	
121	10	9	2	12	2	12	6	16	12	18	12	10	8	4	6	11	8	3	4	22	8	18	9	13	247	Apr 30	Thursday	
122	9	3	9	9	7	11	4	11	7	4	7	4	2	17	2	5	14	3	7	8	6	15	2	2	186	May 01	Friday	Frste
123	1	13	5	4	14	8	15	12	16	23	10	10	10	4	9	17	12	15	10	10	6	18	11	1	257	May 02	Saturday	
124	22	15	13	6	6	0	4	7	19	17	7	27	15	5	11	17	4	5	10	11	11	11	9	9	251	May 03	Sunday	
125	11	15	15	3	2	0	2	8	18	23	24	11	16	13	21	13	4	8	10	13	13	11	9	6	264	May 04	Monday	
126	14	4	14	6	2	4	8	13	13	16	24	18	11	10	15	5	10	4	10	6	9	11	6	10	239	May 05	Tuesday	
127	12	7	19	6	4	5	8	9	11	17	27	14	8	14	5	9	3	9	6	9	17	7	7	5	212	May 06	Wednesday	
128	8	12	6	8	3	10	4	8	22	24	16	23	12	4	11	12	9	10	9	11	6	11	9	9	249	May 07	Thursday	
129	13	8	15	6	5	18	7	12	19	17	34	41	20	17	8	7	7	14	22	8	21	11	5	5	318	May 08	Friday	
130	6	3	0	9	8	3	1	4	6	7	5	0	0	4	4	0	11	0	0	15	2	0	0	0	78	May 09	Saturday	
131	0	0	0	0	0	0	0	0	0	0	0	0	0	0	0	0	0	0	0	0	0	0	0	0	0	May 10	Sunday	
132	0	13	16	5	5	0	2	11	8	6	13	20	10	6	3	15	7	3	6	9	7	13	13	13	144	May 11	Monday	
133	14	18	14	16	5	1	7	8	19	7	24	16	15	15	9	7	5	5	17	11	11	10	13	15	274	May 12	Tuesday	
134	12	8	18	14	3	10	8	12	23	15	24	23	8	13	13	11	10	14	10	17	11	12	20	11	292	May 13	Wednesday	
135	8	12	20	8	12	18	6	8	13	16	18	18	12	10	12	12	15	22	22	8	21	12	20	20	330	May 14	Thursday	
136	6	3	8	6	10	3	12	13	19	17	14	22	12	4	4	7	17	5	4	14	6	6	9	7	241	May 15	Friday	
137	4	19	19	10	5	29	1	31	4	13	15	16	10	11	21	24	10	18	15	32	24	19	7	23	353	May 16	Saturday	
138	30	41	24	28	25	17	29	7	15	22	23	16	14	17	4	8	4	11	9	14	23	32	16	16	402	May 17	Sunday	Sytten
139	8	11	14	8	17	7	7	7	13	9	10	19	17	13	13	12	8	9	15	12	13	10	17	14	271	May 18	Monday	
140	10	22	13	11	6	6	7	7	7	22	17	19	19	15	13	13	11	1	9	13	3	13	16	12	264	May 19	Tuesday	
141	8	9	10	5	11	7	11	11	18	20	24	24	14	18	9	6	11	2	1	17	14	7	16	13	321	May 20	Wednesday	
142	9	10	13	7	4	7	5	9	18	18	8	51	14	9	18	9	6	7	4	9	5	6	24	20	255	May 21	Thursday	
143	25	11	15	5	2	4	3	7	18	12	11	31	8	17	9	7	24	6	7	15	17	14	9	18	257	May 22	Friday	
144	7	16	16	4	4	6	6	6	0	4	7	7	7	11	4	3	2	7	4	5	6	2	10	8	121	May 23	Saturday	
145	5	9	11	4	12	14	1	1	3	9	2	2	2	13	2	9	2	4	4	2	15	16	13	10	162	May 24	Sunday	
146	9	15	6	7	2	4	5	4	15	15	8	15	2	6	5	6	3	7	4	5	5	12	13	10	190	May 25	Monday	
147	9	14	15	12	1	5	3	2	15	15	21	21	12	14	16	7	5	1	6	8	11	10	8	11	238	May 26	Tuesday	

Table 3.4.3 (Page 1 of 4)

FIN .FKX Hourly distribution of detections

Day	00	01	02	03	04	05	06	07	08	09	10	11	12	13	14	15	16	17	18	19	20	21	22	23	Sum	Date		
148	8	10	10	1	4	5	2	9	13	19	28	21	13	3	6	2	6	4	4	4	10	6	6	0	194	May 27	Wednesday	
149	3	10	14	10	12	5	2	4	6	13	11	16	11	2	8	4	5	12	12	4	7	17	9	10	201	May 28	Thursday	Krist1
150	13	3	3	9	4	6	1	4	12	17	14	27	18	12	4	4	10	5	5	7	10	12	10	2	220	May 29	Friday	
151	8	1	12	5	6	13	3	2	5	7	16	12	15	13	4	17	39	14	8	9	15	5	5	0	151	May 30	Saturday	
152	3	0	1	8	3	10	5	5	12	16	7	10	8	9	24	17	39	7	11	13	10	5	5	8	236	May 31	Sunday	
153	9	10	16	13	3	1	2	8	13	13	12	33	16	14	14	7	6	5	7	12	8	11	11	0	207	Jun 01	Monday	
154	0	9	0	0	0	5	8	5	8	17	13	21	11	5	5	10	10	3	5	11	8	12	5	16	202	Jun 02	Tuesday	
155	11	6	6	7	9	1	0	14	18	13	17	33	15	15	4	7	8	8	7	7	0	3	8	14	216	Jun 03	Wednesday	
156	5	3	6	6	5	6	0	2	14	15	19	21	9	9	5	5	3	3	5	2	3	10	10	8	209	Jun 04	Thursday	
157	14	10	16	5	5	9	7	14	20	18	18	19	15	15	4	5	10	7	12	7	3	3	10	0	235	Jun 05	Friday	
158	5	7	6	6	4	10	4	2	8	24	10	6	4	15	20	4	11	5	13	10	11	1	4	9	142	Jun 06	Saturday	
159	15	9	8	4	4	2	3	6	5	15	25	24	21	12	6	6	6	13	13	5	2	9	9	3	275	Jun 07	Sunday	Frste
160	15	12	21	10	4	5	3	1	15	10	10	8	9	15	17	6	6	11	7	7	11	8	8	7	187	Jun 08	Monday	Anr en
161	10	13	16	6	3	4	0	15	15	23	23	10	8	7	6	6	5	5	11	10	26	7	3	8	240	Jun 09	Tuesday	
162	8	8	19	10	5	5	2	11	15	24	14	11	11	15	6	4	2	2	5	5	9	9	13	9	223	Jun 10	Wednesday	
163	8	4	23	10	9	3	1	11	11	18	19	40	13	9	8	9	6	10	10	7	8	13	13	8	264	Jun 11	Thursday	
164	14	6	6	8	8	9	11	8	17	11	12	24	8	9	16	5	5	6	21	27	18	7	3	9	250	Jun 12	Friday	
165	7	7	10	4	9	3	5	11	7	17	6	8	7	16	1	9	5	5	9	27	7	9	12	14	168	Jun 13	Saturday	
166	9	9	23	6	13	20	7	10	10	19	19	47	64	49	27	43	22	28	18	14	26	11	5	14	492	Jun 14	Sunday	
167	2	9	15	3	3	1	1	5	10	10	19	22	15	18	4	6	10	18	18	18	5	8	8	12	212	Jun 15	Monday	
168	18	7	10	8	3	3	1	6	11	23	23	16	18	17	18	21	18	3	3	14	18	14	11	18	330	Jun 16	Tuesday	
169	9	6	9	6	8	5	6	7	10	16	20	31	10	23	7	0	6	10	7	34	14	4	13	18	273	Jun 17	Wednesday	
170	5	20	9	6	5	2	1	6	10	24	16	29	20	25	25	20	4	4	31	17	7	4	4	16	283	Jun 18	Thursday	
171	10	5	13	15	14	1	2	10	11	18	14	18	20	19	19	20	10	30	20	0	16	4	6	9	308	Jun 19	Friday	
172	14	6	3	15	27	7	14	8	7	0	0	0	0	0	0	0	0	0	0	0	0	0	3	0	145	Jun 20	Saturday	
173	0	0	0	0	0	0	0	0	0	0	0	0	0	0	0	0	0	0	0	0	0	0	0	0	0	Jun 21	Sunday	
174	0	0	0	15	0	0	0	15	0	10	21	0	0	9	14	18	21	6	6	2	7	3	8	11	114	Jun 22	Monday	
175	13	11	10	13	0	9	16	0	28	21	21	46	22	22	23	23	11	15	10	10	6	26	8	6	408	Jun 23	Tuesday	
176	7	7	3	4	2	6	6	15	9	7	8	16	12	6	5	9	9	19	10	3	12	32	18	11	184	Jun 24	Wednesday	
177	7	8	12	8	15	2	2	11	7	15	13	8	13	5	5	1	1	17	14	6	6	5	4	5	208	Jun 25	Thursday	
178	8	18	8	2	6	0	7	11	16	11	17	26	13	8	16	22	22	4	2	11	6	6	5	6	254	Jun 26	Friday	
179	5	2	6	6	6	6	0	4	7	7	7	14	4	16	22	17	7	7	11	16	3	6	14	10	150	Jun 27	Saturday	
180	11	7	2	2	4	6	3	6	2	12	16	56	56	11	11	6	11	11	7	10	1	1	1	9	258	Jun 28	Sunday	
181	11	7	2	10	4	6	3	8	6	12	16	11	13	1	11	5	11	7	7	9	9	9	7	21	179	Jun 29	Monday	
182	8	13	5	5	2	2	4	8	14	14	20	16	20	3	5	11	5	5	4	8	14	2	9	15	219	Jun 30	Tuesday	
183	8	11	11	9	4	4	3	12	14	15	17	18	16	6	2	3	9	10	10	4	13	9	11	13	230	Jul 01	Wednesday	
184	12	6	16	8	1	3	3	12	15	10	12	20	15	9	7	7	3	3	10	3	6	7	5	13	216	Jul 02	Thursday	
185	3	2	16	6	2	9	6	6	18	19	15	27	21	10	8	5	5	4	4	6	1	8	5	8	197	Jul 03	Friday	
186	2	3	13	7	5	0	9	27	26	11	11	14	13	10	9	9	14	5	9	5	6	0	2	0	219	Jul 04	Saturday	
187	8	3	0	1	0	0	0	0	0	0	0	0	0	0	0	0	0	0	0	0	0	0	0	7	20	Jul 05	Sunday	
188	0	0	0	3	3	0	9	6	15	16	18	19	23	6	16	19	6	9	2	4	6	11	11	8	157	Jul 06	Monday	
189	12	3	12	7	3	1	0	3	6	17	10	24	5	5	6	13	3	3	7	3	1	13	11	15	212	Jul 07	Tuesday	
190	7	6	6	6	9	3	3	6	10	17	13	4	15	7	2	2	7	6	4	7	6	7	7	13	171	Jul 08	Wednesday	
191	9	9	14	9	3	11	6	14	14	22	16	18	18	10	9	9	4	8	9	9	15	7	8	13	214	Jul 09	Thursday	
192	12	10	6	1	2	6	2	12	15	21	12	11	15	5	9	7	8	10	10	3	7	7	4	10	213	Jul 10	Friday	
193	5	5	13	6	8	14	10	7	7	10	5	20	17	18	18	27	5	5	2	4	5	5	5	7	214	Jul 11	Saturday	
194	5	19	10	13	14	7	9	0	15	19	9	11	11	5	16	16	9	9	10	0	16	19	20	20	260	Jul 12	Sunday	
195	12	14	42	13	14	4	0	11	18	13	18	12	32	14	0	0	0	0	0	0	0	8	21	0	229	Jul 13	Monday	
196	0	0	0	0	0	0	0	0	0	13	25	8	8	5	50	19	6	17	17	10	6	11	11	17	193	Jul 14	Tuesday	
197	14	10	20	13	10	11	12	12	11	17	24	14	14	13	6	23	12	12	12	5	19	8	19	13	318	Jul 15	Wednesday	
198	22	10	7	10	7	3	5	4	13	26	20	8	8	4	13	17	10	4	4	11	14	14	12	16	222	Jul 16	Thursday	
199	3	10	10	7	8	2	1	3	8	21	26	20	7	6	5	2	9	5	2	7	7	16	6	3	207	Jul 17	Friday	
200	4	0	0	10	4	9	5	4	11	10	10	29	14	14	28	15	0	0	15	5	13	26	13	12	346	Jul 18	Saturday	
201	14	7	14	13	6	7	1	3	5	2	3	8	6	6	5	2	12	2	12	11	8	5	12	12	166	Jul 19	Sunday	
202	6	6	10	8	10	4	10	10	11	22	20	13	13	14	8	11	10	10	11	14	14	14	13	12	249	Jul 20	Monday	
203	22	8	25	0	8	3	5	14	8	27	20	11	11	5	7	16	15	9	14	7	16	12	16	9	303	Jul 21	Tuesday	

Table 3.4.3 (Page 2 of 4)

FIN .FKX Hourly distribution of detections

Day	00	01	02	03	04	05	06	07	08	09	10	11	12	13	14	15	16	17	18	19	20	21	22	23	Sum	Date	
204	11	7	11	3	6	0	3	6	11	16	12	16	19	6	10	6	8	2	6	11	7	14	9	12	215	Jul 22	Wednesday
205	10	8	13	6	4	4	7	10	14	10	18	15	19	17	18	11	6	13	1	13	17	15	10	20	275	Jul 23	Thursday
206	8	14	0	1	6	5	5	9	20	17	15	16	13	14	4	12	12	10	5	13	7	7	8	6	236	Jul 24	Friday
207	6	8	7	6	1	4	7	3	10	15	7	9	13	16	10	12	10	8	5	2	7	5	5	7	178	Jul 25	Saturday
208	3	12	10	9	14	11	4	4	7	6	10	14	4	7	11	9	4	10	11	11	10	18	16	11	250	Jul 26	Sunday
209	16	12	9	6	2	2	8	3	8	10	14	11	16	11	20	12	6	11	9	11	12	12	14	15	228	Jul 27	Monday
210	16	11	10	8	5	5	5	9	16	22	19	22	11	16	25	21	7	13	12	14	15	25	19	28	339	Jul 28	Tuesday
211	14	17	19	8	12	7	7	17	17	23	28	27	15	30	10	26	15	8	13	8	10	11	4	11	330	Jul 29	Wednesday
212	7	10	8	9	3	4	6	6	9	23	16	17	21	15	5	15	36	31	10	19	11	11	18	8	320	Jul 30	Thursday
213	15	8	20	5	7	12	9	12	12	22	33	29	11	15	10	0	0	0	0	0	0	0	0	0	197	Jul 31	Friday
214	0	0	0	0	0	0	0	0	0	0	0	0	0	0	0	0	0	0	0	0	0	0	0	0	0	Aug 01	Saturday
215	0	0	0	0	0	0	0	0	0	0	0	0	2	0	0	0	4	5	6	7	8	9	12	8	89	Aug 02	Sunday
216	3	13	0	4	8	8	0	19	12	13	29	6	10	7	13	11	4	5	6	7	13	18	15	7	249	Aug 03	Monday
217	0	11	19	6	2	5	5	13	20	18	18	22	14	13	13	9	9	7	8	15	13	9	8	11	235	Aug 04	Tuesday
218	16	12	15	8	5	7	13	24	12	13	25	14	10	13	13	14	16	11	8	6	11	11	7	11	258	Aug 05	Wednesday
219	25	10	16	7	10	10	24	19	10	17	25	18	10	10	6	6	7	4	15	6	9	11	7	11	285	Aug 06	Thursday
220	8	4	1	7	10	50	33	24	2	10	17	9	7	11	11	21	14	13	8	14	10	4	7	8	318	Aug 07	Friday
221	9	1	8	2	4	4	4	12	7	13	17	7	9	9	5	6	2	4	7	14	5	4	7	0	159	Aug 08	Saturday
222	15	17	10	12	2	4	3	9	2	19	22	8	8	14	9	5	3	15	20	16	10	10	0	10	291	Aug 09	Sunday
223	0	0	12	0	4	4	4	7	15	22	17	8	14	9	17	10	32	20	30	31	52	24	9	7	248	Aug 10	Monday
224	7	0	4	2	4	4	3	12	6	13	12	14	9	10	9	12	9	8	20	16	11	7	0	6	231	Aug 11	Tuesday
225	5	3	7	4	4	8	12	10	15	22	12	10	7	18	10	7	32	22	30	31	1	9	9	4	310	Aug 12	Wednesday
226	12	8	7	10	16	4	6	6	19	20	12	38	6	17	7	8	5	8	20	35	16	12	12	8	236	Aug 13	Thursday
227	8	14	4	7	16	2	4	5	14	13	17	22	24	34	48	27	8	22	23	16	3	27	14	9	422	Aug 14	Friday
228	17	5	9	9	2	3	7	12	11	6	15	18	19	56	4	3	11	5	25	18	9	21	14	13	250	Aug 15	Saturday
229	12	14	21	10	12	12	7	1	19	18	14	24	19	9	11	19	11	1	8	2	7	9	16	34	283	Aug 16	Sunday
230	17	17	20	10	14	12	1	14	16	15	22	26	19	11	13	13	5	4	12	7	4	28	38	47	329	Aug 17	Monday
231	12	27	69	28	22	14	4	16	15	19	34	22	25	11	11	15	11	5	19	9	9	15	38	13	431	Aug 18	Wednesday
232	17	17	24	7	14	2	14	14	16	15	34	17	13	14	8	12	5	4	10	7	12	15	10	11	273	Aug 19	Wednesday
233	10	11	7	0	7	1	3	4	13	24	23	26	17	17	8	11	11	12	6	7	12	10	10	11	236	Aug 20	Thursday
234	7	11	7	4	6	1	4	7	5	19	7	17	17	11	6	5	4	9	14	7	9	10	10	6	143	Aug 21	Friday
235	3	3	13	9	6	3	7	13	6	24	26	9	9	6	10	5	9	8	14	10	6	11	15	5	226	Aug 22	Saturday
236	13	9	6	6	4	7	17	16	9	23	26	12	16	16	6	7	18	16	14	14	21	7	7	17	447	Aug 23	Sunday
237	8	10	9	6	4	8	4	16	11	15	24	26	12	6	9	9	31	62	28	14	13	42	6	4	272	Aug 24	Monday
238	13	10	11	8	5	6	12	12	19	17	41	55	20	11	11	50	25	7	28	28	11	6	5	8	495	Aug 25	Tuesday
239	13	15	5	5	5	6	6	12	17	17	30	33	51	36	42	2	10	10	28	5	13	11	6	4	196	Aug 26	Wednesday
240	8	7	11	4	5	10	13	16	11	14	17	25	21	9	2	3	15	7	9	6	2	8	9	10	214	Aug 27	Thursday
241	9	6	8	5	2	5	1	3	11	8	14	17	5	5	3	6	5	3	5	5	4	8	11	5	177	Aug 28	Friday
242	23	12	14	4	5	5	4	5	7	11	17	10	7	8	10	11	4	9	13	12	5	11	13	10	294	Aug 29	Saturday
243	10	29	20	18	8	8	5	17	3	13	13	6	5	11	11	10	15	7	17	18	18	10	10	5	217	Aug 30	Sunday
244	11	10	30	3	0	8	1	18	13	17	11	7	11	11	11	11	10	0	0	13	8	0	0	18	79	Aug 31	Monday
245	11	30	24	14	0	0	0	4	8	10	13	17	0	0	0	11	7	0	4	2	0	10	10	0	169	Sep 01	Tuesday
246	10	9	21	9	0	5	6	6	12	17	14	15	15	18	5	7	9	14	14	4	5	6	6	5	167	Sep 02	Wednesday
247	10	0	9	2	1	3	13	13	12	7	11	16	11	11	11	9	2	2	4	4	4	7	6	2	233	Sep 03	Thursday
248	9	9	8	5	4	0	2	4	19	16	30	26	24	17	7	9	7	1	7	5	6	7	6	1	170	Sep 04	Friday
249	6	8	6	4	2	6	6	13	7	11	1	33	18	3	1	7	4	8	7	4	7	6	6	6	93	Sep 05	Saturday
250	3	0	8	0	1	1	1	1	12	11	23	25	7	3	12	2	10	3	7	1	1	1	4	7	178	Sep 06	Sunday
251	9	8	11	13	2	2	2	13	11	11	23	22	7	15	8	4	7	5	6	11	8	3	4	10	212	Sep 07	Monday
252	14	5	13	7	0	5	2	4	2	9	17	18	8	10	10	13	15	3	8	0	5	14	14	6	213	Sep 08	Tuesday
253	8	14	7	10	0	2	4	12	16	17	18	24	15	16	17	2	4	1	7	7	17	12	13	9	291	Sep 09	Wednesday
254	16	3	9	7	1	6	14	13	14	19	19	18	12	10	3	12	13	8	8	12	10	21	12	6	302	Sep 10	Thursday
255	20	8	12	12	0	6	7	6	7	26	15	13	5	6	4	2	2	7	11	10	12	10	15	10	236	Sep 11	Friday
256	25	2	2	21	6	15	18	9	7	3	14	25	3	9	17	4	7	5	14	14	14	22	21	16	433	Sep 12	Saturday
257	22	33	25	20	15	6	8	8	51	9	15	5	30	6	15	17	9	25	14	11	7	10	36	10	283	Sep 13	Sunday
258	17	18	7	7	2	2	8	11	16	18	20	14	12	23	13	2	7	2	6	4	14	14	15	6	225	Sep 14	Monday
259	15	10	16	7	9																					Sep 15	Tuesday

Table 3.4.3 (Page 3 of 4)

FIN .FKX Hourly distribution of detections

Day	00	01	02	03	04	05	06	07	08	09	10	11	12	13	14	15	16	17	18	19	20	21	22	23	Sum	Date		
260	8	9	6	5	2	1	1	6	8	9	9	13	12	9	9	4	8	7	12	7	7	9	7	12	180	Sep	16	Wednesday
261	11	10	12	5	7	3	6	15	9	12	12	21	19	14	8	9	9	12	9	9	8	4	9	12	234	Sep	17	Thursday
262	9	13	9	12	8	5	10	10	13	11	17	16	21	15	6	6	8	5	6	9	3	11	11	18	254	Sep	18	Friday
263	20	32	3	3	5	16	31	14	15	7	2	5	4	5	5	13	7	3	17	10	6	7	12	14	285	Sep	19	Saturday
264	16	19	10	8	13	13	4	10	15	10	10	4	9	7	5	4	4	6	7	5	4	7	7	8	220	Sep	20	Sunday
265	9	8	10	2	6	1	1	7	8	7	15	9	8	12	9	6	9	13	12	12	6	11	7	8	207	Sep	21	Monday
266	13	14	14	3	3	4	1	8	18	19	14	16	16	13	17	8	7	6	6	15	9	6	11	15	263	Sep	22	Tuesday
267	10	5	16	8	4	6	6	6	12	12	19	21	12	18	11	11	8	7	6	10	9	9	12	17	225	Sep	23	Wednesday
268	7	10	13	8	6	9	13	13	20	9	28	22	10	7	5	7	3	15	15	10	4	4	7	8	237	Sep	24	Thursday
269	8	8	17	2	2	4	10	10	13	17	22	8	18	3	4	5	5	3	3	8	8	3	5	4	190	Sep	25	Friday
270	3	5	7	9	5	9	8	6	5	5	5	1	7	7	4	6	3	1	1	1	6	4	8	10	118	Sep	26	Saturday
271	6	5	0	6	5	2	3	3	5	9	8	5	9	2	7	6	6	7	6	5	4	4	6	9	133	Sep	27	Sunday
272	15	9	9	8	8	3	2	4	8	8	5	16	19	16	19	12	3	2	10	5	5	7	6	4	209	Sep	28	Monday
273	9	6	17	6	4	6	8	8	9	9	6	14	14	17	14	11	11	4	8	6	5	7	10	10	218	Sep	29	Tuesday
274	12	7	4	16	11	12	10	10	16	23	12	19	30	20	9	7	7	4	9	7	8	8	10	6	284	Sep	30	Wednesday

FIN	00	01	02	03	04	05	06	07	08	09	10	11	12	13	14	15	16	17	18	19	20	21	22	23				
Sum	1736	1376	1040	1461	2465	3106	2023	1695	1422	1627	1744	1796																
	1751	2116	1043	1060	2131	2798	2382	1822	1571	1540	1620	1711													43036	Total sum		
179	10	10	12	8	6	6	6	8	12	14	16	17	13	11	10	9	9	8	9	9	9	10	10	10	240	Total average		
125	10	10	12	7	5	4	5	8	13	15	18	20	14	12	10	9	9	8	9	9	9	10	10	11	246	Average workdays		
54	9	10	12	9	9	9	7	8	9	9	11	10	9	9	9	9	8	8	9	9	9	9	9	8	218	Average weekends		

Table 3.4.3. Daily and hourly distribution of FINESA detections. For each day is shown number of detections within each hour of the day and number of detections for that day. The end statistics give total number of detections distributed for each hour and the total sum of detections during the period. The averages show number of processed days, hourly distribution and average per processed day.

GER .FKX Hourly distribution of detections

Day	00	01	02	03	04	05	06	07	08	09	10	11	12	13	14	15	16	17	18	19	20	21	22	23	Sum	Date		
92	8	1	4	10	5	7	8	13	8	16	19	22	13	9	8	4	4	2	3	3	0	0	2	11	192	Apr 01	Wednesday	
93	6	5	7	7	7	1	7	10	1	10	15	7	23	19	11	14	4	6	6	4	4	12	3	4	183	Apr 02	Thursday	
94	2	6	5	8	9	1	7	16	25	17	25	30	1	13	11	1	8	8	6	9	3	6	6	8	227	Apr 03	Friday	
95	2	0	0	0	0	0	0	0	0	0	0	0	0	0	0	0	0	0	0	0	0	0	0	0	11	Apr 04	Saturday	
96	0	2	0	0	0	0	0	0	0	0	0	0	0	0	0	1	0	0	0	0	0	0	3	0	8	Apr 05	Sunday	
97	16	6	1	7	2	0	8	8	15	13	14	10	25	15	19	11	13	3	5	8	4	0	0	2	201	Apr 06	Monday	
98	9	5	3	14	4	5	8	16	14	18	18	25	18	8	10	10	9	5	7	1	5	3	5	4	186	Apr 07	Tuesday	
99	5	5	7	7	1	1	8	7	11	10	24	25	6	13	7	14	8	7	7	2	2	1	2	13	192	Apr 08	Wednesday	
100	7	3	3	7	0	20	1	11	11	10	13	22	10	6	10	8	6	6	7	19	7	4	5	7	222	Apr 09	Thursday	
101	8	16	5	14	7	4	8	7	12	13	18	25	0	7	5	8	15	5	4	6	10	15	4	16	241	Apr 10	Friday	
102	8	4	8	6	2	14	3	11	2	6	13	22	7	7	11	2	7	6	2	6	6	4	6	6	146	Apr 11	Saturday	
103	4	1	8	3	6	2	7	2	7	20	4	7	7	4	3	4	5	5	4	6	3	6	3	10	109	Apr 12	Sunday	
104	4	11	8	10	6	14	13	12	12	32	7	13	20	9	9	8	7	6	6	8	15	0	3	7	215	Apr 13	Monday	
105	6	15	25	15	16	5	28	32	45	11	25	40	23	17	18	14	14	2	4	4	4	0	9	4	378	Apr 14	Tuesday	
106	6	5	5	6	3	8	5	12	17	11	29	34	17	18	18	19	12	13	2	16	17	10	3	4	280	Apr 15	Wednesday	
107	3	8	5	3	0	0	12	5	11	10	22	33	30	12	13	15	11	12	10	5	4	3	9	4	249	Apr 16	Thursday	Skj(rt Langfr
108	9	2	2	0	2	2	0	2	1	0	7	8	2	8	4	3	2	3	4	5	4	1	5	4	80	Apr 17	Friday	
109	8	0	1	10	0	3	1	5	5	4	7	5	0	6	5	2	1	2	4	0	6	2	6	0	93	Apr 18	Saturday	
110	3	1	2	0	2	0	2	1	1	9	13	10	11	6	5	3	8	4	7	5	8	2	3	1	139	Apr 19	Sunday	Frste
111	2	7	6	8	25	3	2	9	12	10	13	10	11	8	20	14	3	3	6	15	13	5	1	11	160	Apr 20	Monday	Annen
112	13	7	10	4	2	10	1	7	2	31	12	19	10	17	7	10	8	7	6	2	8	5	3	10	187	Apr 21	Tuesday	
113	7	6	6	5	1	0	13	9	31	17	12	36	22	18	16	10	10	3	9	16	13	6	1	7	236	Apr 22	Wednesday	
114	12	6	6	1	0	8	3	2	6	10	17	18	13	28	16	18	8	3	6	5	4	3	9	10	221	Apr 23	Thursday	
115	5	10	2	5	2	5	12	11	18	2	27	7	10	7	13	7	2	11	6	5	1	4	4	3	177	Apr 24	Friday	
116	2	2	3	0	0	4	2	5	4	16	5	8	8	10	5	3	5	5	5	1	0	2	5	13	115	Apr 25	Saturday	
117	1	18	6	0	5	4	7	3	6	10	16	24	11	12	2	2	4	1	4	4	10	4	1	5	178	Apr 26	Sunday	
118	5	11	6	11	4	4	3	12	16	36	18	13	19	17	2	36	11	3	6	7	1	10	6	5	243	Apr 27	Monday	
119	10	3	9	9	5	4	17	17	20	26	22	21	17	15	6	4	4	2	4	21	6	5	6	3	241	Apr 28	Tuesday	
120	10	0	6	0	3	4	12	12	21	21	21	10	21	6	16	11	3	2	8	5	2	2	2	1	177	Apr 29	Wednesday	
121	3	1	0	1	7	0	9	12	21	13	18	14	11	23	10	10	12	4	6	1	4	8	2	0	202	Apr 30	Thursday	
122	5	1	1	2	0	2	6	4	5	10	11	5	3	6	2	5	6	4	10	5	3	2	1	2	109	May 01	Friday	Frste
123	2	2	2	8	2	1	0	6	1	7	22	8	9	4	6	6	7	11	8	3	2	1	2	9	121	May 02	Saturday	
124	10	4	6	13	7	0	2	1	5	10	10	10	6	13	9	2	6	2	6	7	5	6	1	6	138	May 03	Sunday	
125	5	3	9	3	6	6	13	14	11	28	22	8	11	12	9	7	5	3	5	4	3	2	1	7	202	May 04	Monday	
126	9	9	5	7	7	13	3	12	16	22	16	33	8	19	7	6	1	7	5	4	5	6	2	6	228	May 05	Tuesday	
127	10	3	3	1	2	3	7	11	14	32	23	26	3	10	8	7	8	3	7	3	7	1	1	7	214	May 06	Wednesday	
128	8	2	9	10	10	4	8	7	14	25	16	24	18	6	9	9	9	10	10	2	0	0	8	6	193	May 07	Thursday	
129	8	2	1	3	3	14	14	27	17	25	21	18	10	15	23	9	9	4	11	17	4	4	4	10	278	May 08	Friday	
130	26	6	12	24	10	29	7	2	2	10	7	10	10	21	5	5	9	7	10	4	4	2	3	9	202	May 09	Saturday	
131	12	15	5	21	3	16	11	11	10	32	26	21	20	10	15	1	9	9	9	3	13	9	2	6	267	May 10	Sunday	
132	7	9	9	4	2	7	12	9	5	2	12	8	18	8	12	2	5	3	13	6	6	3	3	12	277	May 11	Monday	
133	10	3	6	14	5	5	3	12	2	26	22	24	1	10	21	12	13	15	19	7	3	2	2	12	182	May 12	Tuesday	
134	7	4	2	14	9	8	13	21	31	22	22	8	12	10	8	8	8	7	20	1	6	13	2	7	227	May 13	Wednesday	
135	11	1	3	5	4	21	21	27	13	13	31	24	13	19	7	16	5	10	6	14	3	8	13	7	247	May 14	Thursday	
136	4	2	1	11	4	8	5	13	18	15	20	14	13	6	9	12	15	13	6	9	3	3	4	2	275	May 15	Friday	
137	6	3	4	7	11	13	21	8	10	28	17	15	15	5	1	16	4	10	49	4	10	6	4	11	184	May 16	Saturday	
138	4	6	3	5	7	2	2	21	21	24	29	22	11	7	14	12	3	2	4	5	9	11	6	12	181	May 17	Sunday	Sytten
139	5	4	9	10	11	13	13	2	16	30	23	24	22	16	12	14	2	9	5	0	7	3	8	14	234	May 18	Monday	
140	9	9	5	11	7	6	11	11	22	27	16	25	25	14	11	12	3	2	9	6	5	2	2	8	158	May 19	Tuesday	
141	12	18	8	17	0	8	8	17	16	16	25	62	37	37	10	7	42	11	28	10	6	4	8	4	320	May 20	Wednesday	
142	19	6	1	3	4	1	11	9	13	14	16	21	21	2	2	14	7	11	5	4	0	2	4	8	345	May 21	Thursday	
143	1	7	3	8	13	9	9	17	13	10	25	18	12	20	10	8	7	2	9	8	5	4	4	3	239	May 22	Friday	
144	6	4	2	3	5	4	7	7	4	5	14	7	10	2	2	0	2	7	4	7	0	4	5	10	172	May 23	Saturday	
145	6	14	9	10	9	4	1	6	15	36	22	12	12	10	10	8	4	4	9	9	5	5	11	6	178	May 24	Sunday	
146	8	16	8	9	5	7	4	1	13	16	14	13	13	9	11	8	0	2	9	7	13	6	6	5	233	May 25	Monday	
147	9	2	5	5	8	8	4	8	13	24	16	21	9	8	11	11	7	4	9	14	10	2	5	2	232	May 26	Tuesday	

Table 3.4.4 (Page 1 of 4)

GER .FKX Hourly distribution of detections

Day	00	01	02	03	04	05	06	07	08	09	10	11	12	13	14	15	16	17	18	19	20	21	22	23	Sum	Date		
148	5	9	2	6	5	11	9	13	15	20	18	17	17	17	9	8	10	9	31	5	8	7	4	8	263	May 27	Wednesday	Kristi
149	3	3	9	4	4	6	10	6	11	23	14	18	25	11	14	9	5	4	6	5	5	7	4	10	216	May 28	Thursday	
150	9	5	5	7	9	5	13	20	15	20	15	8	14	13	8	9	10	5	11	5	8	7	6	8	225	May 29	Friday	
151	6	5	10	3	2	6	9	8	10	6	9	11	8	5	8	4	8	7	20	7	5	8	2	2	187	May 30	Saturday	
152	3	2	3	8	2	4	7	7	19	7	12	20	5	5	8	4	6	5	6	5	8	3	5	9	156	May 31	Sunday	
153	10	12	9	0	0	9	0	18	11	21	26	20	13	5	21	44	35	7	8	9	6	3	2	0	299	Jun 01	Monday	
154	0	5	5	5	0	4	14	13	14	26	34	13	13	11	14	6	4	5	8	9	2	8	4	14	211	Jun 02	Tuesday	
155	14	17	0	20	12	20	18	12	10	21	22	78	132	11	21	4	10	11	7	9	9	7	11	9	555	Jun 03	Wednesday	
156	18	21	5	17	2	16	8	14	14	41	83	29	29	69	26	6	7	9	8	10	5	4	3	3	382	Jun 04	Thursday	
157	16	9	7	20	12	18	9	12	10	21	13	13	17	3	8	6	5	3	7	4	12	2	1	0	302	Jun 05	Friday	
158	2	4	9	5	4	3	8	14	9	5	6	4	7	2	4	6	4	8	5	6	5	6	3	4	117	Jun 06	Saturday	Frste
159	3	4	4	5	5	2	0	0	6	5	19	11	6	3	1	4	7	3	8	4	1	6	2	0	100	Jun 07	Sunday	Annen
160	4	1	0	7	2	0	10	5	7	10	12	12	14	16	8	6	7	6	5	4	15	6	5	11	182	Jun 08	Monday	
161	29	10	6	10	2	10	11	13	20	20	17	21	14	16	17	6	9	3	6	3	3	5	5	5	214	Jun 09	Tuesday	
162	9	0	10	6	1	5	11	14	20	18	25	99	43	11	24	7	8	5	7	3	5	5	6	8	369	Jun 10	Wednesday	
163	10	2	6	5	1	6	11	12	17	17	28	21	11	8	7	9	9	5	8	7	1	6	6	9	239	Jun 11	Thursday	
164	9	3	1	9	2	2	8	16	7	25	13	21	13	13	7	5	3	5	7	7	6	7	5	0	188	Jun 12	Friday	
165	6	1	3	9	4	7	6	16	19	30	19	12	7	1	10	6	3	4	9	2	2	4	5	1	201	Jun 13	Saturday	
166	6	3	9	5	4	13	10	10	12	13	11	8	8	12	14	14	9	7	6	5	2	4	5	1	155	Jun 14	Sunday	
167	8	9	5	5	7	1	17	16	26	29	29	11	16	7	4	5	7	2	9	3	5	2	1	7	175	Jun 15	Monday	
168	7	4	9	13	4	0	15	13	26	24	22	22	16	13	22	14	4	4	9	2	3	5	4	8	257	Jun 16	Tuesday	
169	8	4	9	9	3	9	13	13	29	26	26	18	11	11	7	5	4	6	10	9	2	0	5	8	242	Jun 17	Wednesday	
170	5	1	1	9	7	1	9	11	9	19	19	17	13	12	7	5	9	3	0	3	0	2	6	9	189	Jun 18	Thursday	
171	11	3	3	13	3	11	0	11	12	20	28	16	16	16	7	17	5	9	3	7	4	2	1	3	281	Jun 19	Friday	
172	2	5	4	1	1	0	7	7	20	14	23	14	47	87	15	15	15	54	10	3	4	0	2	2	294	Jun 20	Saturday	
173	9	2	2	6	3	0	0	10	6	9	10	12	30	9	8	10	3	11	3	7	3	3	1	10	162	Jun 21	Sunday	
174	7	9	5	3	1	4	7	7	26	23	12	14	11	13	7	12	6	13	8	8	1	7	6	7	221	Jun 22	Monday	
175	6	1	10	8	5	6	24	15	19	22	22	17	11	22	13	15	11	10	6	5	1	3	4	11	274	Jun 23	Tuesday	
176	8	20	9	9	2	3	7	11	7	19	18	40	13	16	14	8	17	16	6	5	3	8	7	5	284	Jun 24	Wednesday	
177	7	11	2	4	11	6	4	5	14	37	50	58	47	43	8	28	9	14	14	8	6	4	6	2	432	Jun 25	Thursday	
178	10	12	4	4	6	8	15	11	11	25	27	0	0	0	4	1	18	4	4	6	0	17	17	0	198	Jun 26	Friday	
179	4	11	11	13	8	5	4	7	14	4	4	21	8	0	4	9	5	3	5	3	6	8	6	16	127	Jun 27	Saturday	
180	6	3	2	9	5	10	9	5	18	23	4	2	35	8	4	1	18	8	4	3	0	4	17	12	192	Jun 28	Sunday	
181	21	4	4	4	3	8	11	15	16	22	22	16	10	16	22	13	11	3	2	9	3	3	4	11	258	Jun 29	Monday	
182	4	4	7	7	4	3	11	14	18	23	18	18	15	12	17	8	5	5	9	3	6	7	3	5	235	Jun 30	Tuesday	
183	5	2	1	14	1	10	13	22	16	23	18	18	12	15	15	12	11	8	11	4	6	6	3	18	189	Jul 01	Wednesday	
184	2	10	0	14	2	13	11	17	11	14	18	18	16	12	30	11	12	6	7	9	4	3	13	0	276	Jul 02	Thursday	
185	3	0	3	1	7	6	10	13	16	29	54	45	21	16	14	10	10	8	6	2	2	2	2	1	258	Jul 03	Friday	
186	3	1	0	4	2	4	6	2	6	6	17	20	16	5	38	4	5	6	4	1	3	0	1	7	159	Jul 04	Saturday	
187	8	0	3	8	1	4	4	4	14	8	7	4	3	14	2	6	0	3	9	6	1	1	4	4	121	Jul 05	Sunday	
188	8	14	0	4	1	1	5	5	15	33	21	15	9	7	7	7	8	2	2	2	2	0	9	6	192	Jul 06	Monday	
189	9	1	7	6	4	4	9	6	13	18	16	30	16	9	9	10	5	3	16	2	7	2	5	1	188	Jul 07	Tuesday	
190	1	6	9	3	1	1	9	15	10	24	21	35	12	29	12	12	3	6	11	16	6	0	2	5	219	Jul 08	Wednesday	
191	10	9	7	3	15	5	13	14	13	14	13	18	16	18	15	9	7	4	8	11	8	2	5	4	236	Jul 09	Thursday	
192	4	2	3	10	13	9	4	14	10	36	34	27	21	9	18	8	1	6	0	17	1	3	9	6	210	Jul 10	Friday	
193	6	2	10	0	17	9	6	13	16	34	42	42	16	12	22	13	4	7	5	5	3	2	3	1	259	Jul 11	Saturday	
194	1	2	4	4	5	2	1	0	4	7	17	6	3	14	5	12	3	5	2	2	1	0	2	0	107	Jul 12	Sunday	
195	10	7	5	5	1	7	14	19	15	24	15	15	9	17	17	9	6	6	15	5	4	2	5	15	215	Jul 13	Monday	
196	7	1	3	13	7	14	0	6	13	16	30	35	13	4	18	10	3	11	8	2	7	5	4	0	218	Jul 14	Tuesday	
197	5	4	9	5	13	9	2	8	15	25	16	13	12	13	12	13	7	3	13	1	1	9	5	5	218	Jul 15	Wednesday	
198	7	3	1	13	17	10	8	18	10	37	19	17	16	5	8	9	10	5	16	3	2	0	4	4	224	Jul 16	Thursday	
199	3	4	7	15	17	5	3	19	22	21	33	7	13	5	5	8	6	7	10	8	0	2	11	11	233	Jul 17	Friday	
200	5	3	5	13	7	2	2	2	15	11	15	5	5	11	13	6	2	5	8	5	1	1	7	13	138	Jul 18	Saturday	
201	3	6	13	7	3	0	3	0	6	5	11	1	10	13	4	6	7	4	8	9	5	17	12	6	138	Jul 19	Sunday	
202	9	7	10	5	5	2	3	14	12	17	16	16	10	13	12	12	1	2	8	15	5	7	6	3	209	Jul 20	Monday	

Table 3.4.4 (Page 2 of 4)

GER .FKX Hourly distribution of detections

Day	00	01	02	03	04	05	06	07	08	09	10	11	12	13	14	15	16	17	18	19	20	21	22	23	Sum	Date	
203	9	4	3	4	4	0	8	20	7	28	21	15	18	8	5	9	9	2	2	5	5	10	10	21	227	Jul 21	Tuesday
204	15	12	5	5	6	2	16	19	16	6	10	22	18	20	10	11	2	6	6	47	52	10	4	8	320	Jul 22	Wednesday
205	11	1	6	13	4	2	2	10	12	24	21	18	10	17	12	1	5	9	8	16	8	8	3	15	245	Jul 23	Thursday
206	7	3	9	9	6	2	15	13	15	16	17	17	20	10	10	7	3	4	10	12	5	4	1	9	233	Jul 24	Friday
207	1	4	2	23	12	1	3	0	8	14	15	7	5	9	6	1	1	3	4	6	6	1	3	1	142	Jul 25	Saturday
208	6	5	0	2	1	3	21	14	11	7	4	8	9	3	3	5	5	5	3	3	1	2	8	10	126	Jul 26	Sunday
209	12	11	4	3	11	13	14	14	10	42	15	12	0	9	15	13	14	6	8	7	10	0	1	6	249	Jul 27	Monday
210	5	3	4	0	8	4	2	6	14	21	22	22	4	13	11	3	4	0	6	3	4	5	7	4	221	Jul 28	Tuesday
211	3	3	12	2	6	7	6	10	18	14	15	29	9	16	16	9	8	4	6	6	0	1	7	9	218	Jul 29	Wednesday
212	5	2	4	9	0	7	10	15	14	4	15	25	11	11	11	14	5	4	4	13	3	1	1	11	210	Jul 30	Thursday
213	12	2	0	3	11	1	11	11	14	26	27	8	17	13	18	4	1	10	14	9	9	1	8	13	199	Jul 31	Friday
214	2	0	13	6	7	24	4	11	5	5	13	23	15	11	11	4	4	5	6	9	5	1	6	3	174	Aug 01	Saturday
215	7	1	1	11	1	7	7	1	10	1	9	4	17	11	16	10	8	0	10	1	36	2	3	0	156	Aug 02	Sunday
216	11	4	3	8	4	2	1	15	17	48	21	17	15	13	9	5	2	5	9	6	6	7	4	8	187	Aug 03	Monday
217	2	11	8	3	4	6	9	5	15	13	18	23	13	7	17	13	8	11	10	5	5	2	2	3	230	Aug 04	Tuesday
218	10	2	7	4	3	1	6	8	12	18	17	21	12	11	20	14	1	1	14	8	0	1	5	5	198	Aug 05	Wednesday
219	3	5	11	8	7	9	10	0	15	15	19	12	8	15	9	5	4	4	10	4	3	2	7	6	189	Aug 06	Thursday
220	4	1	3	6	0	2	18	18	10	22	26	18	5	11	9	10	4	4	2	6	8	4	6	5	219	Aug 07	Friday
221	4	4	6	10	6	6	10	5	13	5	6	9	14	0	7	4	0	8	17	10	3	2	8	10	140	Aug 08	Saturday
222	8	1	10	3	7	1	4	4	10	18	8	11	8	10	9	5	7	6	6	8	0	7	13	6	138	Aug 09	Sunday
223	6	8	6	17	0	3	14	9	18	18	18	24	8	7	11	8	2	0	10	10	3	0	9	7	275	Aug 10	Monday
224	10	6	7	13	6	6	16	15	15	25	14	19	11	11	15	11	5	4	4	6	6	6	16	6	226	Aug 11	Tuesday
225	8	6	13	5	10	1	7	15	18	31	13	26	11	17	11	10	3	7	5	2	5	3	7	1	243	Aug 12	Wednesday
226	8	3	7	10	13	7	12	10	13	24	38	42	20	8	14	4	0	6	4	6	0	1	4	3	268	Aug 13	Thursday
227	4	6	3	7	16	11	12	20	26	24	11	11	15	12	17	2	7	8	4	1	3	4	3	5	261	Aug 14	Friday
228	1	1	5	3	5	3	2	2	4	12	4	16	15	9	7	7	2	3	4	11	1	2	1	8	101	Aug 15	Saturday
229	1	7	14	7	7	8	2	12	6	27	36	10	6	9	18	8	3	2	1	2	4	0	3	7	151	Aug 16	Sunday
230	6	0	3	26	34	12	12	12	18	27	36	27	18	25	28	24	22	10	28	10	3	3	7	0	367	Aug 17	Monday
231	2	7	26	20	100	28	28	10	18	22	18	18	18	10	14	1	1	4	3	4	11	3	8	0	366	Aug 18	Tuesday
232	7	14	34	23	11	9	10	15	16	19	25	24	20	15	21	20	9	4	7	9	1	9	8	1	338	Aug 19	Wednesday
233	3	7	11	12	10	9	13	12	22	24	15	14	13	18	24	11	3	5	5	2	8	8	1	26	270	Aug 20	Thursday
234	5	7	0	7	20	5	6	8	30	56	20	26	15	15	6	7	7	5	3	2	18	82	66	27	392	Aug 21	Friday
235	22	8	17	24	16	5	6	9	12	14	21	4	26	15	24	5	3	4	23	4	4	3	13	0	348	Aug 22	Saturday
236	4	4	14	14	8	4	6	7	14	21	35	16	16	22	16	5	6	2	19	7	7	3	7	1	214	Aug 23	Sunday
237	6	7	8	19	13	17	6	11	15	24	21	30	8	12	16	15	5	6	14	7	2	5	6	2	290	Aug 24	Monday
238	7	2	7	9	10	0	7	11	14	14	15	28	13	10	19	14	14	6	2	7	2	5	0	24	248	Aug 25	Tuesday
239	2	2	9	12	18	4	24	24	16	14	15	22	11	14	14	20	4	7	45	28	37	5	23	4	369	Aug 26	Wednesday
240	25	22	11	13	7	11	7	10	12	22	24	26	17	15	12	12	10	14	19	0	6	4	4	3	276	Aug 27	Thursday
241	2	2	2	2	18	7	7	6	28	17	18	7	13	11	11	6	0	11	7	7	3	3	20	2	252	Aug 28	Friday
242	1	1	6	3	13	2	2	8	17	11	8	11	11	7	11	5	5	2	4	2	6	4	0	6	199	Aug 29	Saturday
243	4	3	3	10	0	3	1	13	9	11	4	5	8	12	9	9	7	4	6	13	1	0	2	4	146	Aug 30	Sunday
244	3	2	6	5	7	7	16	14	13	23	9	23	6	9	13	3	9	8	8	2	7	4	3	6	198	Aug 31	Monday
245	9	9	12	10	10	16	16	11	4	18	25	23	17	17	6	8	6	5	4	1	1	4	3	0	253	Sep 01	Tuesday
246	12	17	0	0	21	15	16	14	13	18	21	19	15	12	13	11	7	10	8	8	7	3	3	3	248	Sep 02	Wednesday
247	4	1	1	15	6	10	6	12	14	21	26	21	2	23	23	11	6	3	4	13	4	3	1	8	255	Sep 03	Thursday
248	2	0	5	9	12	14	9	7	16	31	26	4	20	4	10	5	9	6	5	8	0	6	7	14	232	Sep 04	Friday
249	11	5	11	1	7	6	6	10	8	14	15	8	4	10	14	6	9	0	4	11	1	2	6	3	193	Sep 05	Saturday
250	4	3	7	2	12	4	5	7	11	14	11	5	5	5	8	8	7	7	2	2	8	6	3	6	150	Sep 06	Sunday
251	6	8	6	6	7	4	6	0	4	23	18	26	17	9	10	10	6	10	17	3	15	6	3	5	175	Sep 07	Monday
252	5	5	4	5	15	6	13	13	14	19	21	23	12	9	9	9	15	6	0	1	2	9	3	0	178	Sep 08	Tuesday
253	1	3	2	9	1	6	11	14	23	11	26	33	28	22	9	9	0	9	2	17	0	6	1	8	203	Sep 09	Wednesday
254	3	4	1	7	12	15	9	11	10	31	21	26	20	27	14	2	8	6	4	8	17	2	8	14	248	Sep 10	Thursday
255	2	1	11	12	7	4	6	0	8	14	15	24	6	5	8	10	6	0	5	11	8	6	6	3	214	Sep 11	Friday
256	8	5	3	5	3	2	2	6	12	11	7	7	7	5	5	4	4	9	1	3	15	2	5	6	137	Sep 12	Saturday
257	5	0	1	1	14	7	7	6	4	3	13	9	3	8	2	0	0	3	8	2	9	8	8	6	125	Sep 13	Sunday

Table 3.4.4 (Page 3 of 4)

GER .FKX Hourly distribution of detections

Day	00	01	02	03	04	05	06	07	08	09	10	11	12	13	14	15	16	17	18	19	20	21	22	23	Sum	Date	
258	6	6	6	3	4	10	6	12	9	30	16	24	19	12	29	14	5	6	6	2	11	6	0	7	248	Sep 14	Monday
259	7	5	15	5	10	6	13	10	11	37	21	33	13	14	9	6	6	8	3	3	2	9	5	6	258	Sep 15	Tuesday
260	7	1	14	9	7	7	18	16	33	34	38	13	17	9	4	6	7	2	5	4	5	8	8	9	281	Sep 16	Wednesday
261	8	8	4	16	7	8	8	15	22	11	19	24	20	12	8	11	7	3	5	5	7	4	0	0	269	Sep 17	Thursday
262	3	10	4	4	5	6	17	15	22	27	20	24	10	10	7	14	5	5	6	4	1	3	3	3	236	Sep 18	Friday
263	6	3	7	1	6	3	4	4	12	5	5	12	6	3	2	0	2	6	4	9	2	10	2	5	127	Sep 19	Saturday
264	6	7	5	9	7	6	5	11	11	7	7	15	21	6	0	6	2	5	5	5	10	5	3	4	159	Sep 20	Sunday
265	4	5	5	7	5	2	5	11	3	40	35	34	39	8	27	6	27	7	11	10	31	8	8	14	418	Sep 21	Monday
266	16	8	14	19	58	166	43	26	31	40	50	65	21	21	21	8	15	12	24	59	12	7	7	16	756	Sep 22	Tuesday
267	26	11	11	22	133	29	33	24	32	69	85	72	54	51	31	42	20	13	8	20	12	10	22	13	1020	Sep 23	Wednesday
268	21	46	12	18	48	43	32	69	41	18	51	26	52	57	25	25	8	34	28	8	8	12	9	19	1263	Sep 24	Thursday
269	22	9	160	433	449	440	63	26	19	62	33	36	29	19	23	17	24	8	12	11	21	19	18	0	1935	Sep 25	Friday
270	0	0	0	0	0	0	0	0	0	22	27	0	0	0	0	0	0	0	0	0	0	0	0	0	49	Sep 26	Saturday
271	0	0	0	0	0	0	0	0	0	0	0	0	0	0	0	0	0	0	0	0	0	0	0	0	0	Sep 27	Sunday
272	0	0	0	0	0	0	0	0	0	0	0	0	0	0	0	0	0	0	0	0	0	0	0	0	0	Sep 28	Monday
273	0	0	0	0	0	0	0	0	0	0	0	0	0	0	0	0	0	0	0	0	0	0	0	0	0	Sep 29	Tuesday
274	0	0	0	0	0	0	0	0	0	0	0	0	0	0	0	0	0	0	0	0	0	0	0	0	0	Sep 30	Wednesday

GER	00	01	02	03	04	05	06	07	08	09	10	11	12	13	14	15	16	17	18	19	20	21	22	23			
Sum	1263	999	1206	1830	1619	2348	1750	1901	2185	3361	3422	3579	2607	2252	2134	1644	1262	1139	1449	1180	1072	975	967	1149	43293	Total sum	
179	7	6	7	10	9	13	10	11	12	19	19	20	15	13	12	9	7	6	8	7	6	5	5	6	242	Total average	
122	8	7	8	11	11	17	12	13	14	23	22	24	16	14	14	11	8	7	8	7	6	6	5	7	280	Average workdays	
57	5	3	4	8	5	4	5	5	8	9	12	12	11	9	8	5	4	4	7	5	5	5	5	6	157	Average weekends	

Table 3.4.4. Daily and hourly distribution of GERESS detections. For each day is shown number of detections within each hour of the day and number of detections for that day. The end statistics give total number of detections distributed for each hour and the total sum of detections during the period. The averages show number of processed days, hourly distribution and average per processed day.

3.5   IMS operation

The Intelligent Monitoring System (IMS) was installed at NORSAR in December 1989 and was operated at NORSAR from 1 January 1990 for automatic processing of data from ARCESS and NORESS. A new version of IMS that accepts data from an arbitrary number of arrays and single 3-component stations was installed at NORSAR in October 1991, and regular operation of the system comprising analysis of data from the 4 arrays ARCESS, NORESS, FINESA and GERESS started on 15 October 1991. As opposed to the first version of IMS, the one in current operation also locates events at teleseismic distance.

The operational stability of IMS has been very good during the reporting period. In fact the IMS event processor (pipeline) has had no downtime of its own; i.e., all data available to IMS have been processed by IMS.

Events automatically located by IMS

During days 092, 1992, through 274, 1992, 15,158 events (local, regional, teleseismic) were automatically located by IMS. This gives an average of 82.8 events per processed day (183 days processed). 56% of these events are within 300 km of nearest station, and 69% of these events are within 1000 km of nearest station.

45.8% of these events were defined by 2 regional phases and 8.9% were defined by 2 teleseismic phases. 84.8% of all events had 3 defining phases or less. 18.4% of the available detections (phases) were automatically associated to events.

Events located by analyst review of IMS results

During days 092, 1992, through 274, 1992, 11,770 events (local, regional and teleseismic) were defined following analyst review of IMS results. This gives an average of 64 events per processed day (184 days processed). 67% of these events are within 300 km of nearest station, and 77% of these events are within 1000 km of nearest station.

47.2% of these events were defined by 2 regional phases and 4.6% were defined by 2 teleseismic phases. 77.7% of all events had 3 defining phases or less.

81.4% of the events had regional phases only. 15.9% of the events had teleseismic phases only.

Phase and event statistics

Table 3.5.1 gives a sumary of phase detections and events declared by IMS. From top to bottom the table gives the total number of detections by the IMS, the number of detections that are associated with events automatically declared by the IMS, the number of detections that are not associated with any events, the number of events automatically declared by the IMS, the total number of events defined by the analyst, and finally the number of

events accepted by the analyst without any changes (i.e., from the set of events automatically declared by the IMS).

	Apr 92	May 92	Jun 92	Jul 92	Aug 92	Sep92	Total
Phase detections	27729	31278	34017	43251	43331	37724	217330
- Associated phases	8324	8225	7702	8603	7543	8673	49070
- Unassociated phases	19405	23053	26315	34648	35788	29051	168260
Events automatically declared by IMS	2530	2493	2344	2600	2346	2665	14978
No. of events defined by the analyst	2078	2032	1802	2040	1856	1854	11662
No. of events accepted without modifications	1463	1717	1580	1841	1532	1503	9636

Table 3.5.1. IMS phase detections and event summary.

U. Baadshaug
B. Ferstad
B. Paulsen Gammelby
B.Kr. Hokland
L.B. Loughran

3.6   GBF operation

Events automatically located by GBF

During days 092, 1992, through 274, 1992, 11,354 local and regional events were located by GBF. This gives an average of 62.0 events per processed day (183 days processed). 68% of these events are within 300 km of nearest station, and 89% of these events are within 1000 km of the nearest station.

75.9% of these events were defined by 2 regional phases. Teleseismic phases are currently not used by GBF. 91.1% of all events had 3 defining phases or less.

16.4% of the available detections (phases, including teleseismic) were associated to regional events.

T. Kværna

4   Improvements and Modifications

4.1   NORSAR

NORSAR data acquisition

No modification has been made to the NORSAR data acquisition system.

The data are recorded on a 30-hour circular disk buffer on the IBM system, and archived onto 1/2 inch magnetic tapes. In addition to this, the data are now regularly transmitted to a SUN system for recording on a 48-hour circular disk buffer.

NORSAR detection processing

The NORSAR detection processor has been running satisfactorily on the IBM 4381 computer during this reporting period.

Detection statistics are given in section 2. In addition to the detection processing done on IBM, the dp program is doing regular detection processing on a SUN system, using the unix-based circular disk buffer (see below). A detection SNR threshold of 20.0 triggers automatic saving of waveforms into CSS 3.0 data files.

NORSAR event processing

There have been no changes in the routine processing of NORSAR events, using the IBM system.

Routine event processing is done on a SUN computer using the "old" IBM time delay correction data base that has been converted to SUN/UNIX. The automatic solutions produced are equal to or "better" than the old system with a lower false alarm rate. Alert messages are sent USGS for events above magnitude 5.5.

NORSAR refurbishment

As reported earlier, the main problem in this refurbishment is to find 24-bit A/D converters with small power consumption. Manufacturers have so far not been able to present production units for evaluation. One exception has been Refraction Technology, which has allowed us to evaluate two prototype units. Testing is still going on, but the units do seem to perform within specifications. By the writing of this report, a new digitizer from Teledyne Geotech and one from Science Horizons have been received for evaluation. All three units will now be put out in the field for power evaluation and comparison with the NORESS system.

4.2   Regional Arrays

Detection processing

The routine detection processing of the arrays is running satisfactorily on each of the array's SUN-3/280 acquisition systems. The same program is used for NORSAR, NOR-ESS, ARCESS, FINESA, GERESS, but with different "recipes". The beam table for NORESS and ARCESS is found in NORSAR Sci. Rep. No. 1-89/90. The beam table for FINESA and GERESS is found in NORSAR Sci. Rep. No. 1-90/91.

Detection statistics are given in section 3.

Signal processing. Phase estimation

This process performs f-k and polarization analysis for each detection to determine phase velocity, azimuth and type of phase, and the results are put into the ORACLE detection data base for use by the IMS.

Event Processing. Plot and epicenter determination

A description of single-array event processing is found in NORSAR Sci. Rep. No. 2-88/89, and NORSAR Sci. Rep. No. 2-89/90.

New processes

The data from the Apatity array are acquired on a SUN-IPC system. Detection and signal and event processing are all performed on the same computer. The new array requires some tuning of the recipes before data will be routinely put into IMS.

J. Fyen

5   Maintenance Activities

5.1   Activities in the field and at the Maintenance Center

This section summarizes the activities at the Maintenance Center (NMC) Hamar, and NDPC activities related to monitoring and control of NORSAR, including monitoring of NORESS, ARCESS, FINESA, GERESS and Poland (KSP) partly.

Activities involve preventive and corrective maintenance, modification of equipment, installation planning (Apatity, Spitsbergen), and finally installation (Apatity).

NORSAR

- Visit to subarray in connection with power outage
- Locating cables
- Replacement of SLEM power supply
- Communication check in connection with a bad communications cable
- Cable repair/splicing
- Replacement of SLEM
- Replacement of modem

NMC

- Preparing the Apatity and Spitsbergen installations
- NORSAR upgrading activities
- Other tasks related to repair of equipment

NORESS

- Cable location in connection with road work
- Replacement of Hub card

ARCESS

- Replacement of clock, antenna and amplifier
- Replacement of fiber optics
- Replacement of preamplifier A2 outdoors and D2 indoors
- Fiber optic adjustment

Apatity

- Representatives from NTI (Norwegian Telecom International) and NORSAR installed NORSAT B earth station and SUN workstation (May)
- Representatives from NTI and NORSAR installed array equipment in the field and on the premises of the Kola Science Centre in Apatity (Sept)

Subarray/ Area	Task	Date
NORSAR	No visits to the subarrays	April
NMC	NORSAR upgrading and preparatory work related to Apatity and Spitsbergen installations	April
ARCESS	UPS restart	April
NDPC	Daily check of all arrays has been done, i.e., NORSAR NORESS, ARCESS, FINESA, GERESS and Poland (KSP,SFP). SP/LP instruments have been calibrated. FP and MP were measured and adjusted (when feasible from NDPC) when outside specifications.	April

NORSAR

03C	Cable pointed out for the landowner. Loop test in connection with verification of the communication performance.	May
02B	Visit in connection with a power outage	25 May
03C	Adjustment of V, NS LP-seismometer	1 May
06C	Adjustment of channel gain SP 1,2,3 and 5 Replacement of LTA card ch 1,2	18 May
Apatity	Representatives from NORSAR and NTA installed NORSAT B earth station and a SUN workstation	May
NMC	NORSAR upgrading Preparing the Apatity and Spitsbergen installations	May "
NDPC	Daily check of all arrays, i.e., NORSAR, NORESS, ARCESS, FINESA, GERESS and Poland (KSP). NORSAR SP/LP instruments calibrated every week. Free Period (FP) and Mass Position (MP) have been measured and adjusted when outside tolerances (when feasible from NDPC)	May

Table 5.1. Activities in the field and the NORSAR Maintenance Center, including NDPC activities related to the NORSAR, NORESS, ARCESS, FINESA and GERESS arrays and the two 3-component stations in Poland (KSP, SFP), 1 April - 30 September 1992.

Subarray/ Area	Task	Date
NORSAR		
01B	Replaced SLEM power supply	10,11 June
	Adjusted SP channel (gain) 2,3,6	
02B	Replaced FP motor	15 June
	Adjusted channel gain SP ch 5,6	
01A	Communication check in connection with a bad cable	16 June
01B	Cable SP04 damaged and temporarily repaired	16 June
02B	Adjustment of MP/FP V, NS, EW LP seismometer	19 June
	Also observed that "TEST ON" indicator went on	
	in connection with supposed spurious commands	
	in the ICW flow from NDPC, cauing misadjustment	
	of the 6 FP/MP motors	
ARCESS	Replaced clock, antenna and amplifier. Also replaced	17,18 June
	fiber optics B4 A2 outdoors and D2 indoors. Replaced	
	DHL70 preamp. D6 outdoors. Adjusted transmit fiber	
	optics Hub.	
NMC	Preparatory work in connection with the Apatity and	June
	Spitsbergen installations	
NDPC	Daily check of all arrays, i.e., NORSAR, NORESS,	June
	ARCESS, FINESA, GERESS and Poland (KSP,SFP when	
	when running).	
	SP/LP instruments calibrated. FP and MP were	
	measured and adjusted, and those outside specifications	
	were adjusted (when feasible from NDPC).	
NORSAR		
02B	Adjustment of channel gain SP 1,2,3,4,5,6	13 July
	Adjustment of channel gain LP V, NS, EW	
	Adjustment of MP/FP V, NS, EW seismometers	
04C	Adjustment of channel gain SP 1,2,3,4,5,6	14 July
	Adjustment of channel gain LP V, NS, EW	
	Adjustment of MP/FP V, NS, EW seismometers	
02B	Adjustment of channel gain SP 1,2,3,4,6	17 July
	Adjustment of channel gain LP V, NS, EW	
	Adjustment of MP/FP V, NS, EW seismometers	

Table 5.1 (cont.)

Subarray/ Area	Task	Date
02C	Adjustment of channel gain SP 1,2,3,4,6 Adjustment of channel gain LP V, NS, EW Adjustment of MP/FP V, NS, EW seismometers	20 July
02B	Visits in connection with power outage after lightning	21,28 July
03C	Adjustment of channel gain SP1,2,3,4,5,6 Adjustment of channel gain LP V, NS, EW Adjustment of MP/FP V, NS, EW seismometers	21 July
NORESS	Pointed out cables for the landowner in connection with road work	7,8,9,10 July
NMC	Preparatory work in connection with the Apatity and Spitsbergen installations	July
NDPC	Daily check of all arrays, i.e., NORSAR, NORESS, ARCESS, FINESA, GERESS and Poland (KSP). Weeks 27, 28 and 29 SP/LP instruments have been calibrated. Free Period (FP) and Mass Position (MP) were measured and adjusted when outside tolerances (when possible from NORSAR, Kjeller).	July

NORSAR

Subarray/ Area	Task	Date
02B	Adjustment of MP/FP V, NS, EW seismometers	13 Aug
01B	Replaced SLEM and modem	20 Aug
NORESS	Replaced Hub interface card	12 Aug
NMC	Continued installation planning in connection with Apatity and Spitsbergen installations	Aug
NDPC	Daily check of all arrays has been carried out, i.e., NORSAR, NORESS, ARCESS, FINESA, GERESS and Poland (KSP) and Apatity (partly). NORSAR SP/LP instruments calibrated weeks 27, 28 and 29. Free Period (FP) and Mass Position (MP) have been measured and adjusted when outside tolerances (when possible from NORSAR, Kjeller).	Aug

Table 5.1 (cont.)

Subarray/ Area	Task	Date
NORSAR	No visits to the subarrays	Sept
NMC	Preparations for the installations in Apatity and Spitsbergen continued	part of Sept
Apatity	Representatives from NORSAR and NTA satellite office arrived in Apatity 22 September, and started the installation the following day. The work continued through 30 September	Sept
NDPC	Daily check of all arrays has been carried out, i.e., NORSAR, NORESS,ARCESS, FINESA, GERESS and Apatity. NORSAR SP/LP instruments calibrated every week. Free Period (FP) and Mass Position (MP) have been measured and adjusted when outside tolerances (when possible from NORSAR, Kjeller).	

Table 5.1 (cont.)

5.2   Array status

As of 30 September 1992 the following NORSAR channels deviated from tolerances:

    01A 01   8 Hz filter
        02   8 Hz filter
        04   30 dB attenuation
    02B 09
    03C 04
    06C04

O.A. Hansen

6   Documentation Developed

Fyen, J. (1992): Processing techniques for regional array data, in: Proceedings of the GERESS-Symposium, Waldkirchen, Germany, June 22-24, 1992.

Kværna, T., S. Mykkeltveit, F. Ringdal and J. Fyen (1992): Concepts for processing of data from a network of regional arrays, in: Papers presented at 14th Annual PL/ DARPA Seismic Research Symposium, September 16-18, 1992, Phillips Laboratory, Hanscom AFB, MA, and Defense Advanced Research Projects Agency, Arlington, VA.

Ringdal, F. and T. Kværna (1992): Continuous seismic threshold monitoring, Geophys. J. Int., 111, 505-514.

Ringdal, F. and T. Kværna (1992): Processing of regional seismic array data using the continuous threshold monitoring technique, in: Proceedings of the GERESS-Symposium, Waldkirchen, Germany, June 22-24, 1992.

Ringdal, F., P.D. Marshall and R.W. Alewine (1992): Seismic yield determination of Soviet underground nuclear explosions at the Shagan River test site, Geophys. J. Int., 109, 65-77.

Ruud, B.O., E.S. Husebye and S.O. Hestholm (1993): Rg observations from four continents: inverse and forward modelling experiments, Geophys. J. Int., in press.

Semiannual Tech. Summary, 1 Oct 91 - 31 Mar 92, NORSAR Sci. Rep. 2-91/92, NORSAR, Kjeller, Norway

Tsvang, S.L., V.I. Pinsky and E.S. Husebye (1993): Enhanced seismic source discrimination using NORESS recordings from Eurasian events, Geophys. J. Int., 112, 1-14.

7   Summary of Technical Reports / Papers Published

7.1   Extensions of the Northern Europe Regional Array Network -- New small-aperture arrays at Apatity, Russia, and on the Arctic island of Spitsbergen

As of the summer of 1992, the Northern Europe Regional Array Network contributing real-time data to the NORSAR Data Processing Center comprised the high-frequency arrays NORESS and ARCESS in Norway, FINESA in Finland and GERESS in Germany, as well as the two three-component stations KSP and SFP in Poland. In addition, data were available in an off-line mode from a three-component station installed in Apatity on the Kola Peninsula of Russia in June 1991 (see Mykkeltveit et al, 1991). The transmission of continuous data to NORSAR via satellite from the two stations in Poland was discontinued on September 30, 1992.

In September and October 1992, two new small-aperture arrays were added to the network. These are located near Apatity, Russia, and on the Arctic island of Spitsbergen. This contribution offers technical descriptions of these two new arrays and their integration into the network. Fig. 7.1.1 shows the network as of 1 November 1992. From approximately 1 January 1993, all data from the six arrays of this network will be processed jointly in the Intelligent Monitoring System (IMS).

A new small-aperture array near Apatity, Russia

As described in Mykkeltveit et al. (1991), a digital, high-quality three-component station was installed in Apatity on the Kola Peninsula of Russia in June 1991, as part of an agreement of scientific cooperation between NORSAR and the Kola Science Centre of the Russian Academy of Sciences. During June 1991 - June 1992 data from this station were recorded locally in Apatity and copied to cartridge tapes that were sent to NORSAR.

During the summer and autumn of 1992, several significant extensions and changes were made to the installations in Apatity. In June, a dedicated satellite link, based on Norwegian Telecom's NORSAT B system, was installed between NORSAR and the Kola Regional Seismological Centre (KRSC) in Apatity. A computer-to-computer Ethernet connection was established over this link. This enables NORSAR to retrieve continuous data from the system in Apatity. At the same time, several SUN workstations for data analysis were installed, and a NORAC array controller (Paulsen, 1992) replaced the PC system installed in June 1991 with respect to the data acquisition function. The configuration of the three-component station was otherwise unchanged. From June 1992, continuous data from the Apatity three-component station are thus stored on Exabyte cassettes at NORSAR.

In late September, a small-aperture array was installed approximately 17 km to the west of KRSC in Apatity, at the location indicated in Fig. 7.1.2. The geometry of the array is shown in Fig. 7.1.3. The instruments are placed on two concentric rings plus one in the center, and the aperture is approximately 1 km. All sites are equipped by a short period

vertical seismometer of type Geotech S-500, and the site at the center of the array has in addition two horizontal seismometers of the same type.

The field work in preparation for the array installation work was organized and conducted by the KRSC and sponsored by the Kola Nuclear Power Plant (Kola NPP). The Kola NPP is located approximately 30 km southwest of the array (see Fig. 7.1.2). An assessment of the local seismicity is a topic of interest to the Kola NPP.

At each of the seismometer sites on the A- and B-rings, the soil overburden was removed, and an iron tube with a bottom plate was placed in wet concrete on top of competent rock. Iron rods attached to the underside of the bottom plate ensure the coupling of the tube to the concrete and underlying bedrock. The vertical seismometers were then placed inside the tube, resting on the bottom iron plate. Power (commercial power is available at the central housing of the array) is provided to the seismometers via trenched cables, and the same cables are used to transmit analog signals from each seismometer to a centrally located housing in the array. The three-component station at the central site A0 is placed in a shallow vault.

Fig. 7.1.4 shows in detail how the data from the new array are acquired at the seismometer sites, digitized at the central array site and then transmitted via three radio channels to Apatity where the NORAC array controller collects and timetags the data. The digitizers used are of types Nanometrics three-channel RD-3 and six-channel RD-6, which are both 16-bit converters with gain ranging. Short-period data from the nine vertical sensors of the array are sampled at 40 Hz. The amplitude (displacement) response function of the short-period channels is given in Fig. 7.1.5. Data from the three seismometers at site A0 are sampled at 80 Hz, thus providing a high-frequency three-component station integrated with the array. The seismic data from the vertical sensor at site A0 are thus sampled both at 40 Hz (and used in the processing together with the vertical sensors of the A- and B-rings) and at 80 Hz (and used as part of the high-frequency three-component station). As shown in Fig. 7.1.4, there is a certain redundancy in the data acquisition, with data from sensors B2 and B3 being represented twice in the data stream. This ensures that data from a useful array geometry are received even in case of failure of one of the digitizers or one of the radio channels. Also note that timing signals in the form of second marks are recorded as a separate time series, using one of the available channels. Fig. 7.1.4 also shows the three-component broad-band seismometer installed on the pier of the basement of the building of the KRSC in Apatity. The seismometer is of type Guralp CMG-3T, and the data are digitized using a Nanometrics RD-3 digitizer. Timing is provided throughout the system on the basis of reception of GPS signals, as shown in the figure.

Fig. 7.1.6 shows the current configuration of the data acquisition and analysis system at the KRSC. The figure shows the local Ethernet established, the NORAC array controller that receives data from the four digitizers, three SUN Sparcstations (kan, imandra and umb) and a SUN X-terminal, and the Cisco router that provides the gateway connection to NORSAR via the dedicated satellite link. Also shown schematically is the multiplexing equipment used for a phone/fax connection via the same satellite channel. IDU is the satellite indoor unit containing the modem and other communications equipment. The system described in Fig. 7.1.6 allows the staff at the KRSC to perform on-line processing as well

as interactive analysis of the data recorded at Apatity. Using the satellite link, all data recorded at NORSAR from the other arrays of the network can also be retrieved by the KRSC personnel.

The overall picture related to the Apatity developments is given in Fig. 7.1.7. It shows that the data acquired in Apatity and retrieved via the NORSAT B satellite link are made available to the IMS at NORSAR.

A new small-aperture array on the Arctic island of Spitsbergen

A small-aperture array very similar to the Apatity array described above was installed on the island of Spitsbergen (see Fig. 7.1.1) during late October/early November 1992. The implementation of this array was supported financially by Oljeindustriens Landsforening (OLF), which is an association of oil companies taking part in oil exploration and production on the Norwegian Continental Shelf. The establishment and operation of the communications channels needed in order to integrate the Spitsbergen array data into IMS is being supported by DARPA in the follow-on contract to the one reported on here.

A suitable location for the Spitsbergen array was found during a site-selection survey in August 1991. The site is located on Janssonhaugen in Adventdalen approximately 15 km east-southeast of Longyearbyen (see Fig. 7.1.8), which is the largest Norwegian settlement and also administrative center on the island. Longyearbyen has direct airline connections to mainland Norway. Janssonhaugen is a hill in the middle of a valley (Adventdalen), and the array is deployed on the plateau of this hill. The rocks at the site are of Cretaceous age, covered by thin moraine of variable depth. The sensors are placed at the bottom of 6 m deep cased boreholes. The bottom of the boreholes are either in Cretaceous rock or in moraine material in stable permafrost conditions (temperature approximately -5°C all year round at a depth of 6 m), such that there is no melting/freezing taking place at this depth.

Fig. 7.1.9 shows the geometry of the Spitsbergen array. All nine seismometer sites are equipped with short-period vertical seismometers of type Geotech S-500. Cables on the ground connect each of the sites with a housing located approximately 40 m south of site B4. The entire system with seismometers, digitizers, radio links and array controller is shown schematically in Fig. 7.1.10. The system design is very similar to that of the Apatity array described above. Power at the Spitsbergen array site is provided through the use of a windmill which delivers 12V DC through a battery bank. Data from the two Nanometrics RD-6 digitizers located at the housing close to site B4 are transmitted over two radio links to Longyearbyen, where the data are entered into a NORAC array controller located at a Norwegian Telecom facility. As can be seen from the figure, there is a certain data redundancy, as data from channels B2 and B3 are transmitted on both radio links. As of November 1992, the seismometers at sites A1, A2 and B3 are not yet connected. They will be connected in the spring of 1993, as soon as permitted by the prevailing Arctic conditions.

From Longyearbyen, the Spitsbergen array data are transmitted via a terrestrial link to Norwegian Telecom's satellite hub station at Isfjord Radio, from where a simplex 64 kbits/s satellite link (Norwegian Telecom's NORSAT B system) is used for transmission

of the continuous data to Norway. The NORAC array controller in Longyearbyen is also connected to NORSAR via a dial-up line, thus providing a back-link for control and command purposes.

The data from the new Spitsbergen array provides another data source for the IMS. As this array is located in an area of much younger geology than the other five arrays, its integration into IMS is expected to present interesting seismological challenges.

S. Mykkeltveit   A. Dahle   J. Fyen   T. Kværna
P.W. Larsen   F. Paulsen   F. Ringdal
I. Kuzmin, Kola Science Centre

References

Kremenetskaya, E.O. (1991): Contemporary seismicity of the NW part of the USSR, Semiann. Tech. Summ. 1 April - 30 September 1991, NORSAR Sci. Rep. No. 1-91/92, Kjeller, Norway

Mykkeltveit, S., A. Dahle, J. Fyen, T. Kværna, P.W. Larsen, R. Paulsen, F. Ringdal and E.O. Kremenetskaya (1991): Extensions of the Northern Europe Regional Array Network -- a new three-component station at Apatity, USSR, and a planned array at Spitsbergen, Semiann. Tech. Summ. 1 April - 30 September 1991, NORSAR Sci. Rep. No. 1-91/92, Kjeller, Norway

Paulsen, R. (1992): NORAC: A new array controller, Semiann. Tech. Summ. 1 October 1991 - 31 March 1992, NORSAR Sci. Rep. No. 2-91/92, Kjeller, Norway
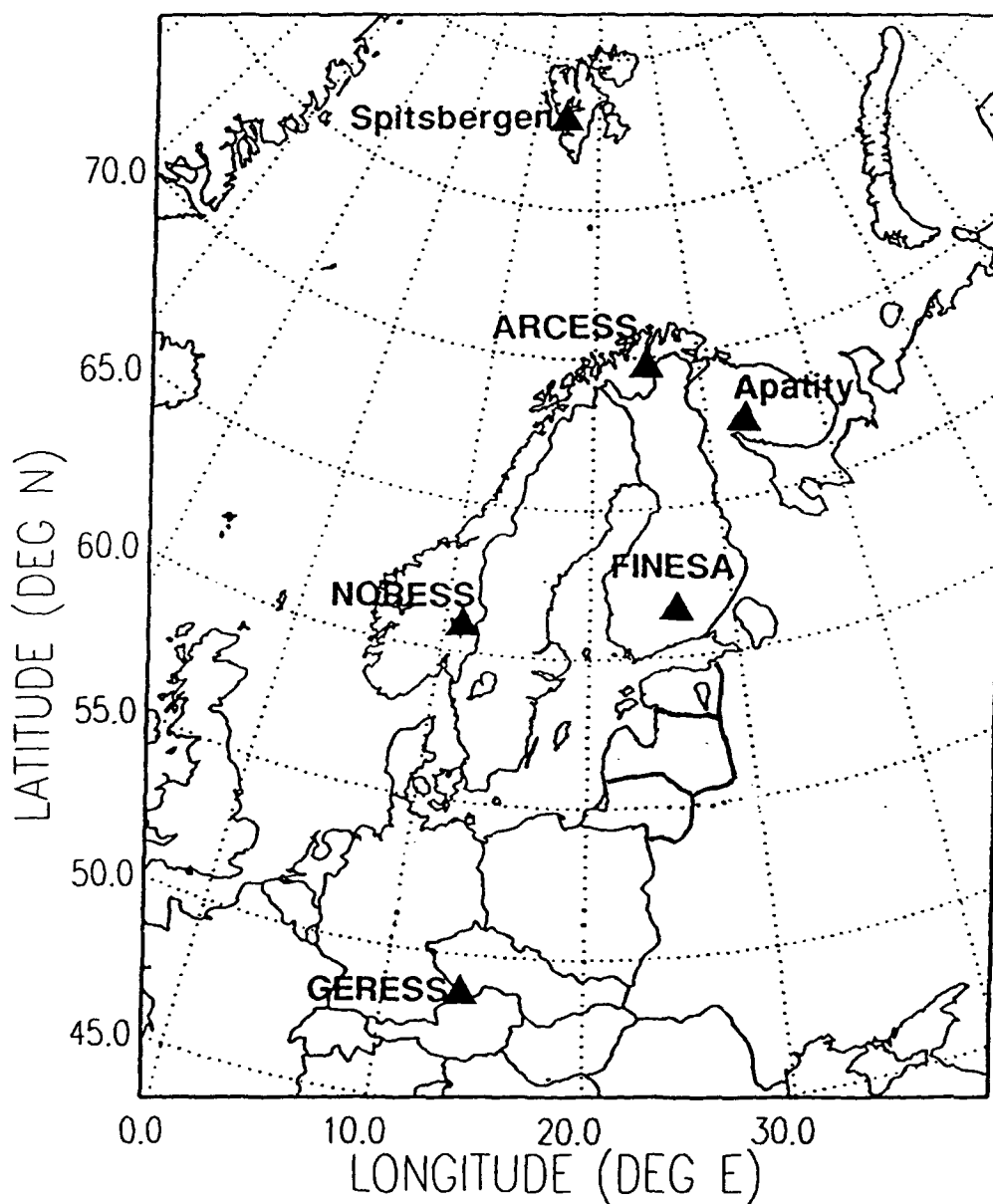
Fig. 7.1.1. The figure shows the stations of the Northern Europe Regional Array Network as of November 1992. All stations of the network are small-aperture arrays.
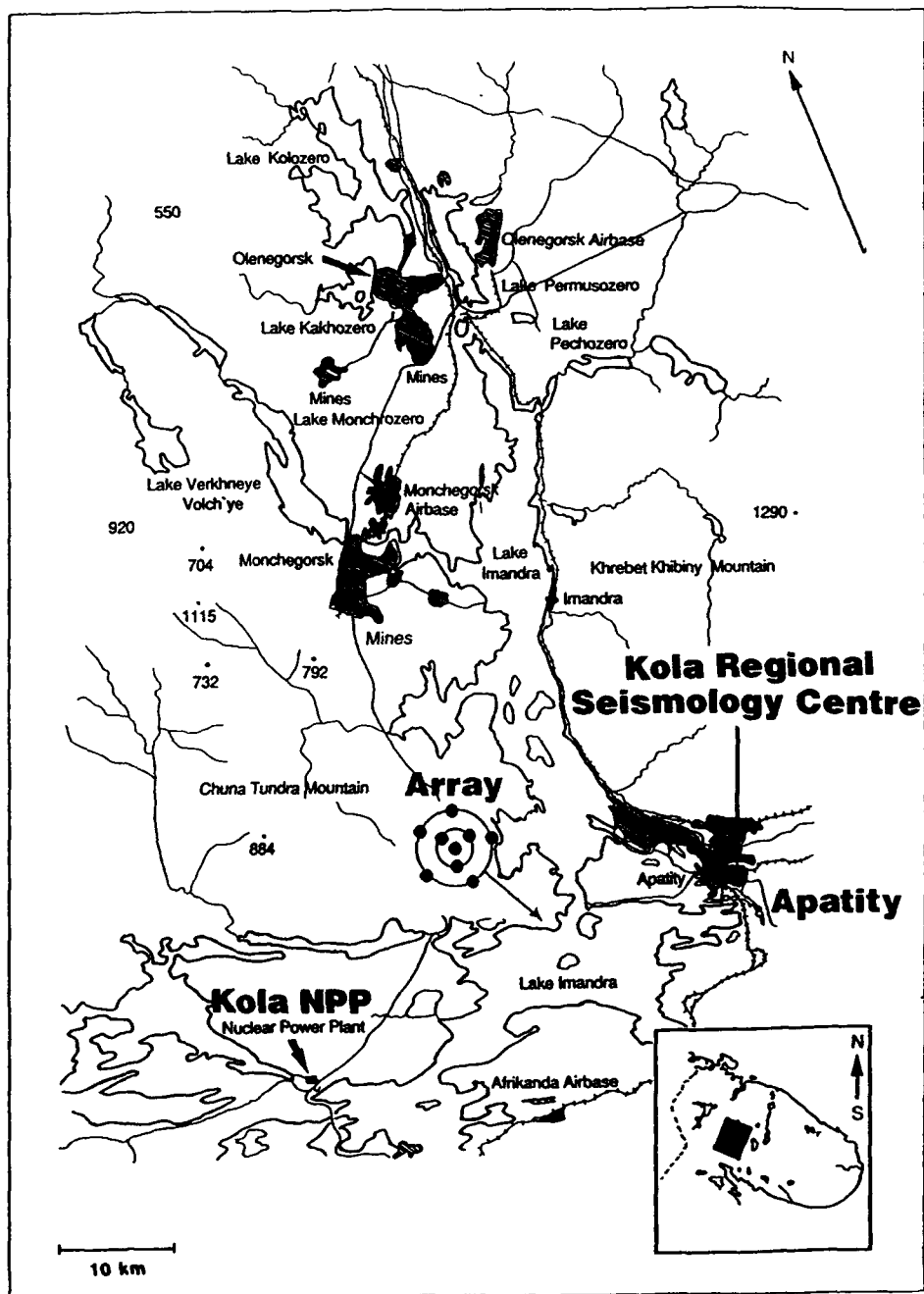
Fig. 7.1.2. Map of the Apatity region on the Kola Peninsula of Russia, showing the location of the Kola Regional Seismology Centre and the location of the new small-aperture array (not drawn to scale; the array aperture is 1 km). Also shown are the mining areas in Monchegorsk and Olenegorsk to the north of the array. The seismicity in the area, and in particular the seismicity associated with the mining activity in the Khibiny Mountain area to the northeast of Apatity, is described in Kremenetskaya (1991).
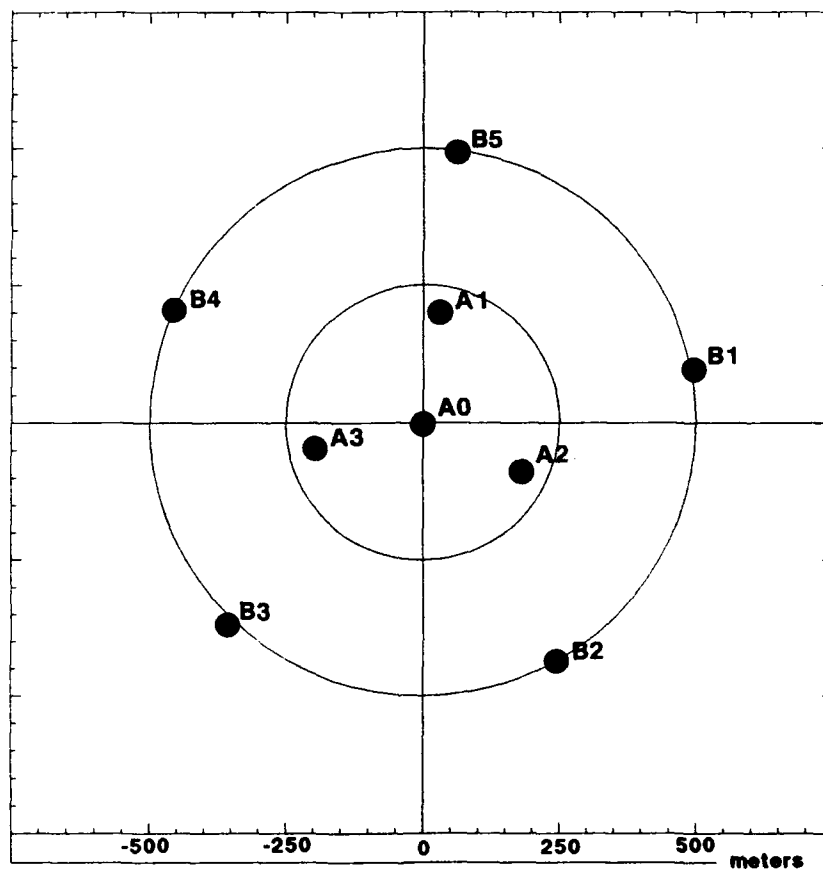
Fig. 7.1.3. Configuration of the new Apatity small-aperture array.
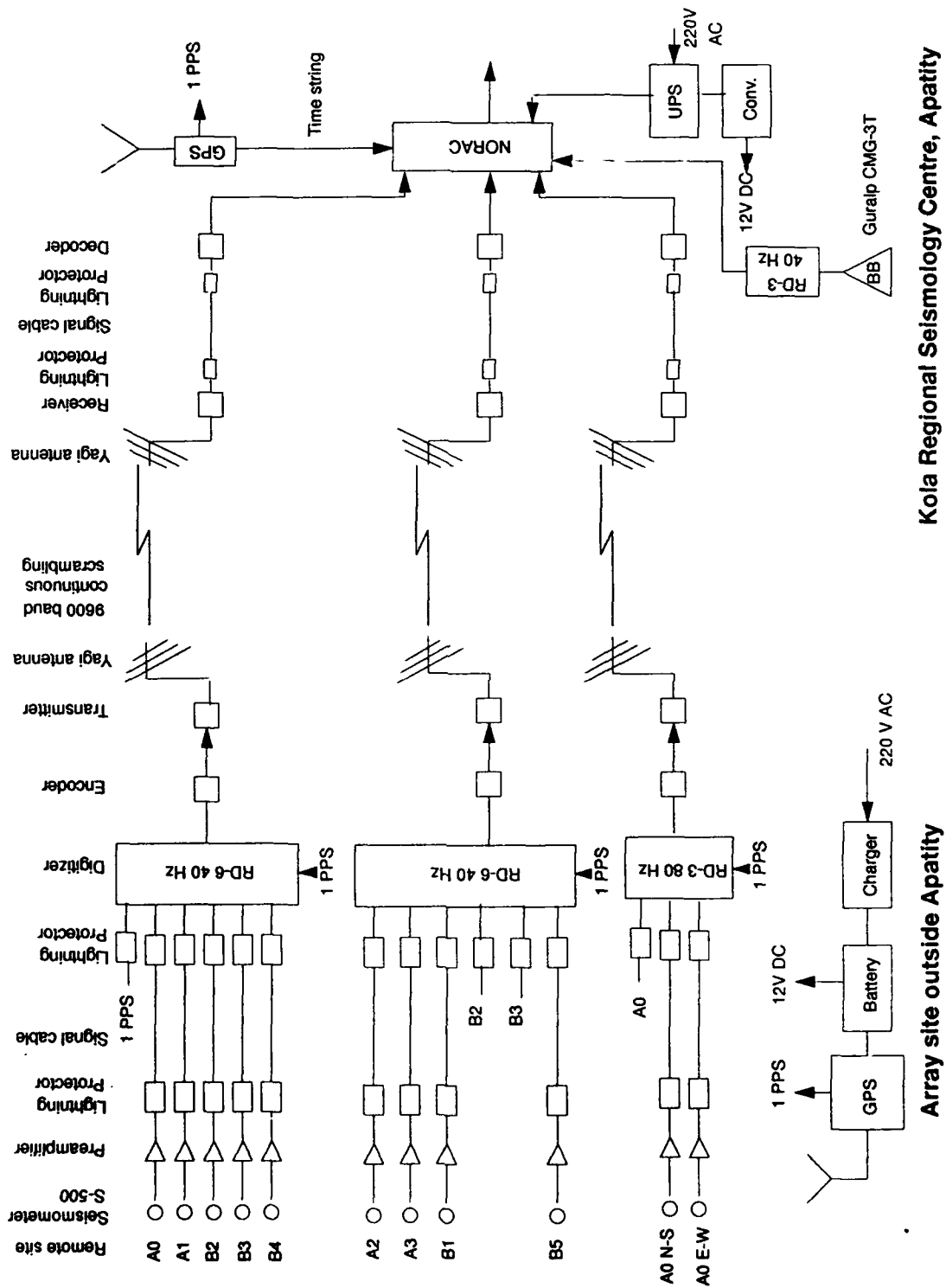
Fig. 7.1.4. Data flow chart for the array and the broadband station in Apatity. 1 PPS ("one pulse per second") denotes timing signals.
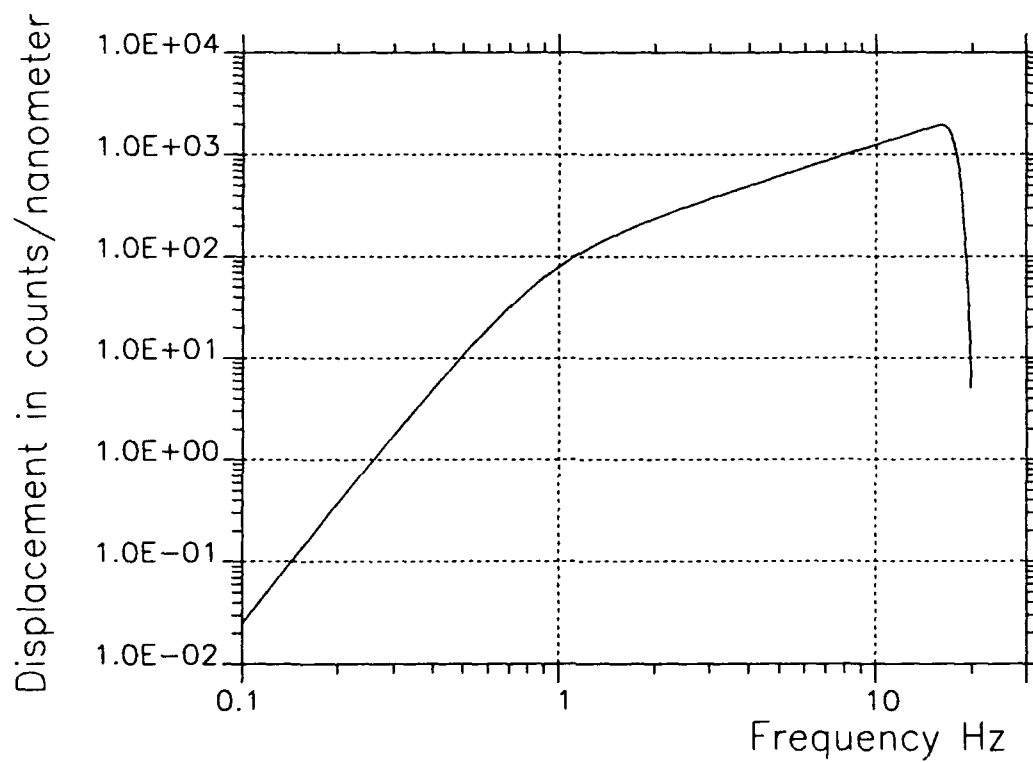
Fig. 7.1.5. Amplitude (displacement) response function for the nine short-period channels of the small-aperture array installed in Apatity in September 1992.
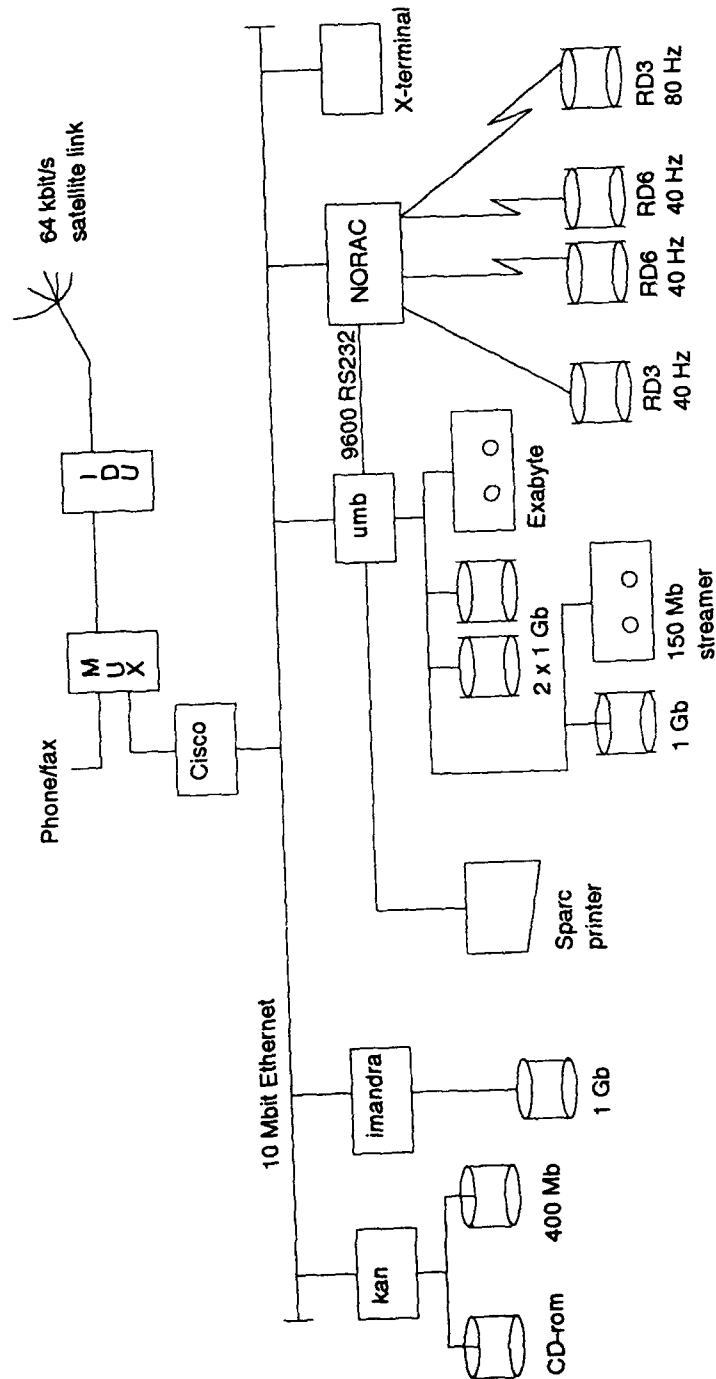
Fig 7.1.6. The figure shows the configuration of the computer system installed at the Kola Regional Seismology Centre in Apatity. Also shown is the network connection to NORSAR via the dedicated 64 kbits/s satellite link.
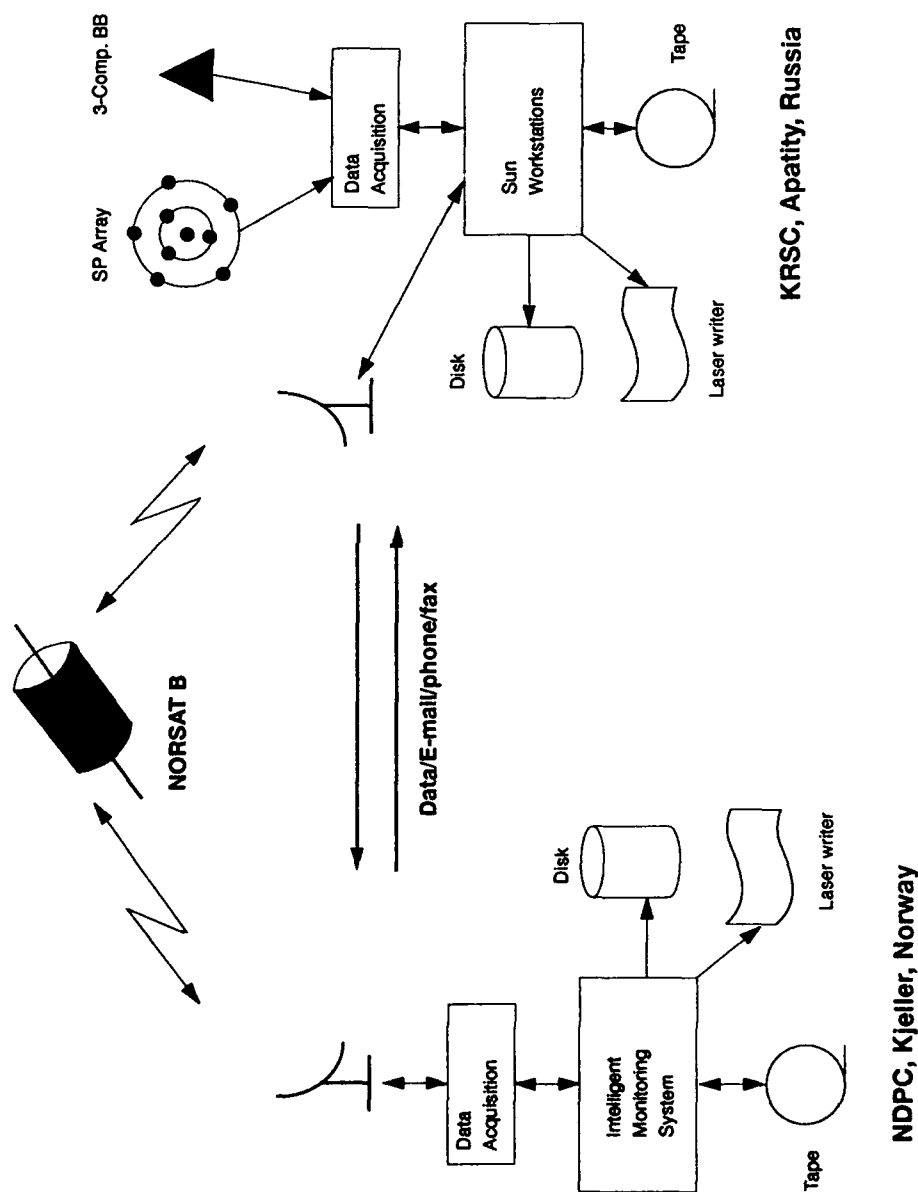
Fig. 7.1.7. Schematic overview of the field installations and computer system in Apatity and the interfacing with the NORSAR Data Processing Center (NDPC) in Norway via the NORSAT B satellite link.
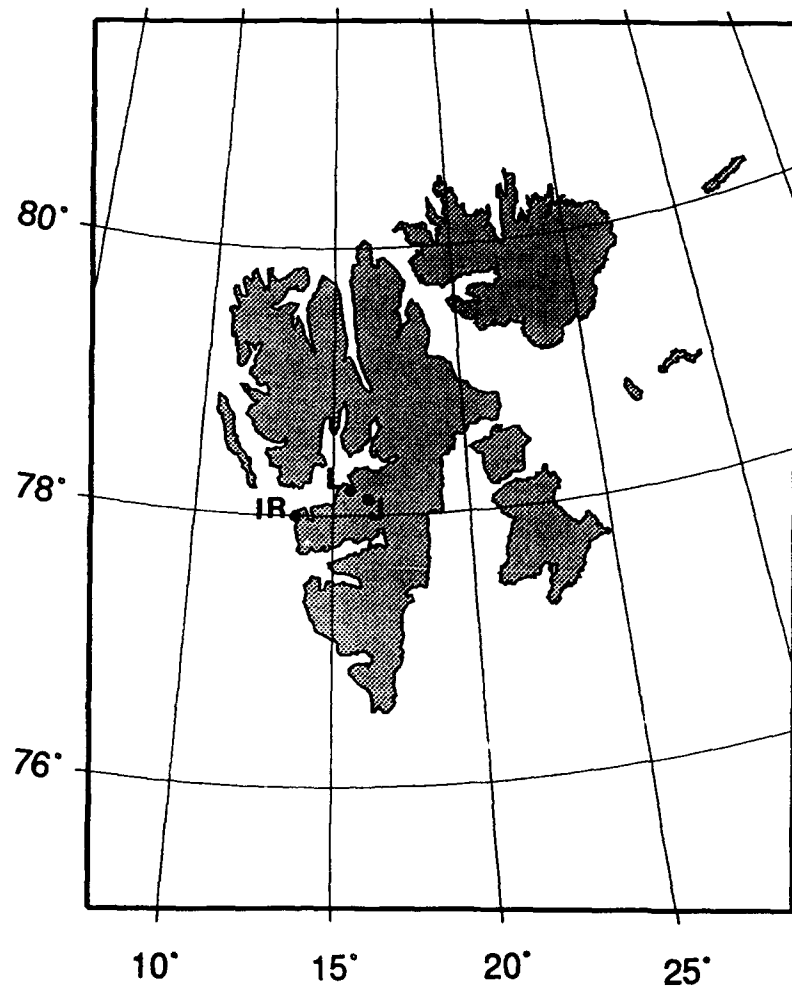
Fig. 7.1.8. This map of the Svalbard archipelago with its main island Spitsbergen shows the location of the array site at Janssonhaugen (J), the location of the array controller at Norwegian Telecom's facility at Longyearbyen (L), and the location of the NOR-SAT B earth station at Isfjord Radio (IR).
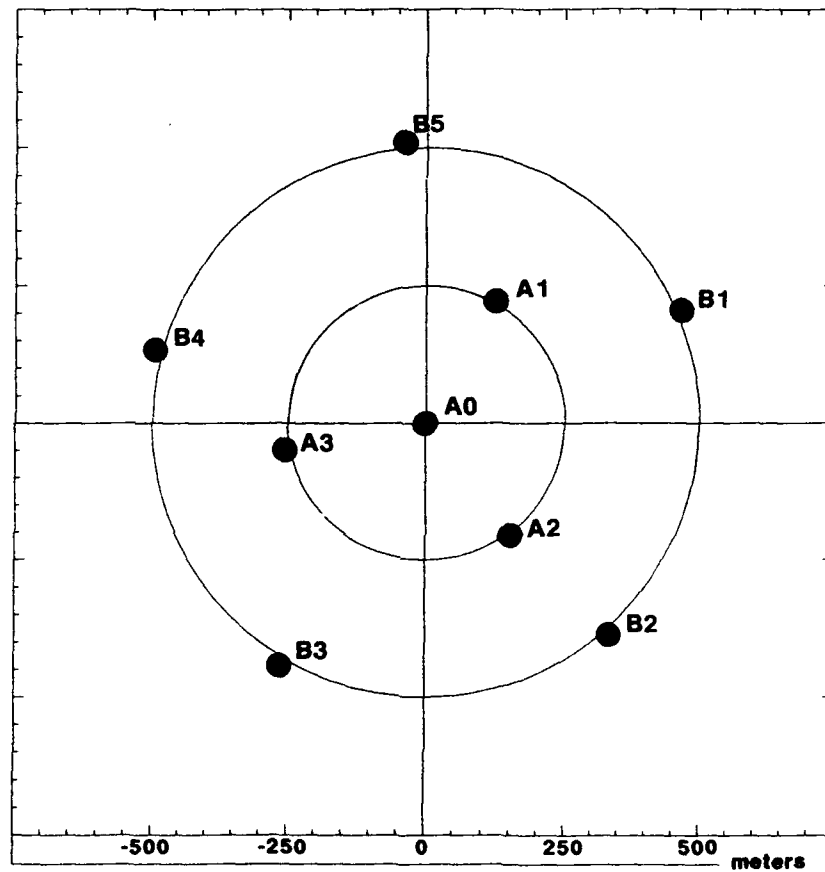
Fig. 7.1.9. Configuration of the new Spitsbergen small-aperture array.
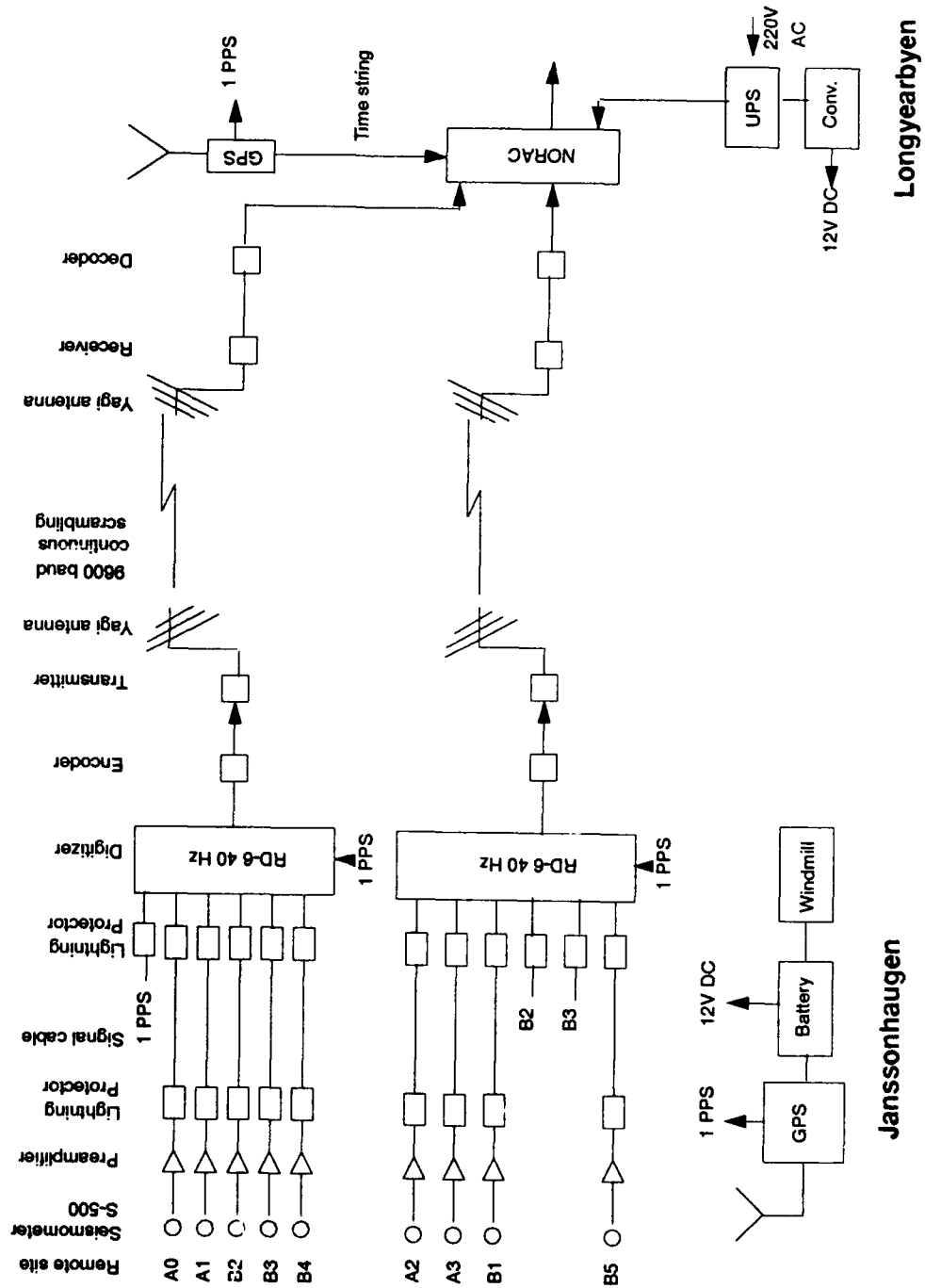
Fig. 7.1.10. Data flow chart for the Spitsbergen array. 1 PPS ("one pulse per second") denotes timing signals.

7.2   Initial processing results from the Apatity small-aperture array

During the fall of 1992, a new regional array was installed near the town of Apatity on the Kola Peninsula (see Section 7.1). Figs. 7.1.1 and 7.1.2 show the location of this array and Fig. 7.1.3 shows the array geometry.

In the following we report on some initial results from analyzing data from the new array. It is emphasized that these results are preliminary, since the available data cover only a few weeks. Thus a more comprehensive assessment must await the collection of data over a longer time span.

Noise spectra

Fig. 7.2.1a shows an example of corrected noise spectra for the 9 vertical elements of the Apatity array, taken at 00.00 hours (GMT) on day 345, 1992. For comparison, the ARCESS spectra for the same number of channels and taken at the same time are shown in Fig. 7.2.1b. From these figures, it is seen that the Apatity array has a higher noise level than ARCESS at frequencies above 2 Hz, whereas the noise levels are similar at lower frequencies.

The higher noise level at Apatity above 2 Hz is not unexpected, taking into account the higher level of industrial activity in this region. On the other hand, the noise level at the Apatity array site is considerably lower than that of the APA station situated in the town of Apatity (see NORSAR Sci. Rep. 1-91/92).

Fig. 7.2.2a shows 24 uncorrected noise spectra, taken hourly between 00.00 GMT and 23.00 GMT on day 344 for the Apatity array (instrument A0Z). For comparison, a similar set of NORESS spectra is shown in Fig. 7.2.2b. The range of variability is similar for the two sites, with the highest noise levels corresponding to local daytime.

Noise suppression

Previous studies have shown that regional arrays are very effective in suppressing seismic noise, thus providing gains that are often of the order of $\sqrt{N}$, or sometimes even in excess of this value (N being the number of sensors). Such better than $\sqrt{N}$ suppression occurs when particular subgeometries are chosen, enhancing the suppression of noise at certain frequencies. As a first check on the capabilities of the Apatity array in this regard, we have computed noise suppression curves and compared with corresponding results from NORESS.

We calculate an uncorrected power density spectrum first by prewhitening 60 seconds of data. Then we estimate the autocorrelation for 6 partially overlapping windows (window length 12 seconds), and compute power density spectra from the average autocorrelation, with compensation for the prewhitening filter.

An average spectrum is obtained by averaging the 9 individual channel spectra for the array. The averaging is done after a logarithmic transform of the spectra, and the standard

deviation for each frequency point is calculated. Each spectrum is pointwise compared to the average spectrum. If a value is outside 1.5 standard deviation from the mean value, the point is considered an outlier. If a single channel spectrum has more than 60% outliers, the spectrum is excluded and a new average spectrum is estimated. A beam is calculated using only those channels for which the spectrum was accepted. The suppression is then the beam spectrum divided by the average spectrum.

It should be noted that calculating suppression using a beam with all 9 elements compared to using only "accepted" channels makes little difference in practice. When calculating noise suppression the most stable results are obtained by dividing the beam spectrum with the average spectrum.

Fig. 7.2.3a shows noise suppression in the frequency range 0-20 Hz for an infinite-velocity beam (no time delays) for the Apatity array. There are 24 samples, taken hourly on day 344, 1992. For comparison, a corresponding plot for the 9-element NORESS B-ring array (A0Z, A1-3, B1-5) is shown in Fig. 7.2.3b. The $\sqrt{N}$ level is about -9.5 dB, and the general impression is that the Apatity array is at least as efficient in suppressing noise as the corresponding NORESS subgeometry. Between 1 and 5 Hz, the Apatity array has higher noise suppression than the NORESS B-ring geometry, and we attribute this to the slightly larger Apatity array aperture. Above 5 Hz, the two configurations are similar. At a frequency near 4 Hz, there is significantly better than $\sqrt{N}$ noise suppression for the Apatity array. In summary, it appears that the spatial noise characteristics at Apatity are similar to those found in other areas of Fennoscandia and the Baltic Shield.

Detection processing

Since the array was installed, the Apatity data have been subjected to continuous on-line detection processing (DP) at NORSAR using the detection algorithm described by Mykkeltveit and Bungum (1984). The initial beam deployment is shown in Table 7.2.1. At an early stage, the Apatity detection lists were incorporated into the Generalized Beam-forming (GBF) process (Ringdal and Kværna, 1989), which has been in automatic operation at NORSAR for nearly 3 years. It is noteworthy that both the DP and GBF could be implemented for the new array with success even without any special tailoring of parameter values and algorithms.

As an example of a regional seismic event recorded and processed using Apatity data, we show here results for a presumed mining explosion in the Kola Peninsula west of the array. This event is from an area different than the Khibiny Massif where most such explosions take place.

Fig. 7.2.4 shows B-ring seismograms for this event. Note the very clear Rg phase, which indicates a shallow source. The detector output, and the solution provided by the GBF algorithm, are shown in Table 7.2.2. A total of 10 phases from the four regional arrays in Fennoscandia have been associated with this event. The estimated magnitude (M_L) is 2.53.

Frequency-wavenumber analysis

Frequency-wavenumber solutions for the three phases Pg, Lg and Rg are shown in Fig. 7.2.5a-c. In spite of the small aperture of the array, the peaks in the F-K diagram are well-defined: typically the highest side lobe is at least 6 dB below the main peak in the F-K plot. Analysis of many events has shown that in particular the array gives a very stable determination of slowness and azimuth for the Rg phase in spite of the broad peak in the F-K diagram. It is remarkable how well an array of only 1 km diameter can resolve these low-frequency dispersive waves.

From Fig. 7.2.5 we note that the phase velocities of each of the three phases are consistent with the phase type; the Rg phase having the slowest velocity. The estimated azimuths are also consistent, with a few degrees' difference only.

Teleseismic events

An example of a small teleseismic recording is shown in Fig. 7.2.6. There is clearly a significant SNR gain on the array beam, and this supports the previous statements on noise suppression. Naturally, the gain at teleseismic signal frequencies for the Apatity array will be lower than for the full-scale NORESS, ARCESS and GERESS regional arrays. Nevertheless, for areas of favorable signal focusing effects, the small Apatity array may still show excellent teleseismic detection, and many examples of this have been observed.

In conclusion, our preliminary analysis indicates that the Apatity array will be an important supplement to the seismic array network in Northern Europe, both for regional and teleseismic event analysis. Its inclusion into the Intelligent Monitoring System (IMS) will in particular serve to improve the location precision and source characterization of the large number of seismic events in the Kola Peninsula and adjacent areas.

F. Ringdal

J. Fyen

References

Mykkeltveit, S. and H. Bungum (1984): Processing of regional events using data from small-aperture arrays, Bull. Seism. Soc. Am., 74, 2313-2333.

Ringdal, F. and T. Kværna (1989): A multi-channel processing approach to real-time network detection, phase association and threshold monitoring, Bull. Seism. Soc. Am., 79, 1927-1940.

BEAM	Velocity	Azim	Filter band		Thre	N	Configuration
A011	99999.9	0.0	0.5 –	1.5	4.40	6	AOB
A021	99999.9	0.0	1.0 –	3.0	4.40	6	AOB
A031	99999.9	0.0	1.5 –	3.5	4.40	6	AOB
A032	11.0	30.0	1.5 –	3.5	4.40	6	AOB
A033	11.0	90.0	1.5 –	3.5	4.40	6	AOB
A034	11.0	150.0	1.5 –	3.5	4.40	6	AOB
A035	11.0	210.0	1.5 –	3.5	4.40	6	AOB
A036	11.0	270.0	1.5 –	3.5	4.40	6	AOB
A037	11.0	330.0	1.5 –	3.5	4.40	6	AOB
A038	15.0	80.0	1.5 –	3.5	3.90	6	AOB
A039	10.0	20.0	1.5 –	3.5	3.90	6	AOB
A041	99999.9	0.0	2.0 –	4.0	4.40	9	AOAB
A042	10.2	30.0	2.0 –	4.0	4.40	9	AOAB
A043	10.2	90.0	2.0 –	4.0	4.40	9	AOAB
A044	10.2	150.0	2.0 –	4.0	4.40	9	AOAB
A045	10.2	210.0	2.0 –	4.0	4.40	9	AOAB
A046	10.2	270.0	2.0 –	4.0	4.40	9	AOAB
A047	10.2	330.0	2.0 –	4.0	4.40	9	AOAB
A048	15.0	80.0	2.0 –	4.0	3.90	9	AOAB
A049	10.0	20.0	2.0 –	4.0	3.90	9	AOAB
A051	99999.9	0.0	2.5 –	4.5	4.40	9	AOAB
A052	8.9	30.0	2.5 –	4.5	4.40	9	AOAB
A053	8.9	90.0	2.5 –	4.5	4.40	9	AOAB
A054	8.9	150.0	2.5 –	4.5	4.40	9	AOAB
A055	8.9	210.0	2.5 –	4.5	4.40	9	AOAB
A056	8.9	270.0	2.5 –	4.5	4.40	9	AOAB
A057	8.9	330.0	2.5 –	4.5	4.40	9	AOAB
A058	15.0	80.0	2.5 –	4.5	3.90	9	AOAB
A061	99999.9	0.0	3.0 –	5.0	4.40	9	AOAB
A062	10.5	30.0	3.0 –	5.0	4.40	9	AOAB
A063	10.5	90.0	3.0 –	5.0	4.40	9	AOAB
A064	10.5	150.0	3.0 –	5.0	4.40	9	AOAB
A065	10.5	210.0	3.0 –	5.0	4.40	9	AOAB
A066	10.5	270.0	3.0 –	5.0	4.40	9	AOAB
A067	10.5	330.0	3.0 –	5.0	4.40	9	AOAB
A068	15.0	80.0	3.0 –	5.0	3.90	9	AOAB
A071	99999.9	0.0	3.5 –	5.5	4.40	9	AOAB
A072	11.1	30.0	3.5 –	5.5	4.40	9	AOAB
A073	11.1	90.0	3.5 –	5.5	4.40	9	AOAB
A074	11.1	150.0	3.5 –	5.5	4.40	9	AOAB
A075	11.1	210.0	3.5 –	5.5	4.40	9	AOAB
A076	11.1	270.0	3.5 –	5.5	4.40	9	AOAB
A077	11.1	330.0	3.5 –	5.5	4.40	9	AOAB

Table 7.2.1. Apatity beam table, valid from 1992-274 (1 October 1992). The table shows the name of the beam, velocity (km/sec), azimuth (degrees), filter band (Hz), STA/ LTA threshold, and configuration. The configuration is described with number of sensors and a configuration code. Here, AOAB means center AO SPZ plus A-ring plus B-ring, and AOB means AO SPZ plus B-ring. The designator (alone) AO means three-component 80 Hz data from AO. AH01 - AH04 are three-component horizontal beams using the AO high-frequency system. AI01 - AI06 are incoherent beams using SPZ channels only. (Page 1 of 2)

BEAM	Velocity	Azim	Filter band	Thre	N	Configuration
A081	99999.9	0.0	4.0 — 8.0	4.40	9	AOAB
A082	9.5	30.0	4.0 — 8.0	4.40	9	AOAB
A083	9.5	90.0	4.0 — 8.0	4.40	9	AOAB
A084	9.5	150.0	4.0 — 8.0	4.40	9	AOAB
A085	9.5	210.0	4.0 — 8.0	4.40	9	AOAB
A086	9.5	270.0	4.0 — 8.0	4.40	9	AOAB
A087	9.5	330.0	4.0 — 8.0	4.40	9	AOAB
A091	99999.9	0.0	5.0 — 10.0	4.90	9	AOAB
A092	10.5	30.0	5.0 — 10.0	4.90	9	AOAB
A093	10.5	90.0	5.0 — 10.0	4.90	9	AOAB
A094	10.5	150.0	5.0 — 10.0	4.90	9	AOAB
A095	10.5	210.0	5.0 — 10.0	4.90	9	AOAB
A096	10.5	270.0	5.0 — 10.0	4.90	9	AOAB
A097	10.5	330.0	5.0 — 10.0	4.90	9	AOAB
A101	99999.9	0.0	8.0 — 16.0	4.90	9	AOAB
A102	9.9	30.0	8.0 — 16.0	4.90	9	AOAB
A103	9.9	90.0	8.0 — 16.0	4.90	9	AOAB
A104	9.9	150.0	8.0 — 16.0	4.90	9	AOAB
A105	9.9	210.0	8.0 — 16.0	4.90	9	AOAB
A106	9.9	270.0	8.0 — 16.0	4.90	9	AOAB
A107	9.9	330.0	8.0 — 16.0	4.90	9	AOAB
A201	99999.9	0.0	1.0 — 3.0	4.00	6	AOB
A207	99999.9	0.0	8.0 — 16.0	4.50	6	AOB
A254	99999.9	0.0	2.0 — 4.0	4.00	6	AOB
A282	99999.9	0.0	4.0 — 8.0	4.00	6	AOB
A310	99999.9	0.0	1.0 — 2.0	2.50	6	AOB
A312	99999.9	0.0	2.0 — 4.0	2.40	6	AOB
AH01	99999.9	0.0	2.0 — 4.0	2.80	3	AO
AH02	99999.9	0.0	3.5 — 5.5	2.80	3	AO
AH03	99999.9	0.0	5.0 — 10.0	2.80	3	AO
AH04	99999.9	0.0	8.0 — 16.0	2.80	3	AO
AI01	99999.9	0.0	0.5 — 1.5	2.90	6	AOB
AI02	99999.9	0.0	1.0 — 2.0	2.90	6	AOB
AI03	99999.9	0.0	1.5 — 2.5	2.90	6	AOB
AI04	99999.9	0.0	2.0 — 4.0	2.50	6	AOB
AI05	99999.9	0.0	3.5 — 5.5	2.50	6	AOB
AI06	99999.9	0.0	5.0 — 10.0	2.70	6	AOB

Table 7.2.1 (cont.) (Page 2 of 2)

Origin time   Lat   Lon   Azres   Timres   Wres   Nphase   Ntot   Nsta   Netmag
1992-298:11.18.12.0   67.45   30.50   6.13   1.87   3.40   10   22   4   2.53

Sta	Dist	Az	Ph	Time	Tres	Azim	Ares	Vel	Snr	Amp	Freq	Fkq	Pol	Arid	Mag
APA	107.7	262.2	Pg	11.18.29.1	-0.3	267.7	5.5	6.9	285.5	6816.3	6.10	2	1	15222	
APA	107.7	262.2	P	11.18.30.7		269.4	7.2	8.9	18.6	318.8	2.12	1	1	15223	
APA	107.7	262.2	P	11.18.36.7		254.2	-8.0	7.8	7.1	934.0	3.64	1		15224	
APA	107.7	262.2	P	11.18.40.1		276.7	14.5	4.3	3.0	4265.9	3.62	1		15225	
APA	107.7	262.2	*	11.18.41.3	-0.9	271.1	8.9	3.7	12.3	12857.0	4.96	2		15226	1.85
APA	107.7	262.2	Lg	11.18.43.0		275.3	13.1	4.0	5.5	1670.5	2.03	1	-2	15227	
APA	107.7	262.2	*	11.18.45.5		273.3	11.1	4.3	154.9	5927.3	1.54	1	-3	15228	
APA	107.7	262.2	*	11.18.47.8		282.6	2C.4	3.9	108.2	36857.6	1.09	1	-3	15229	2.80
APA	107.7	262.2	Rg	11.18.52.1	3.6	278.5	16.3	3.2	7.1	7395.9	2.04	1	1	15231	
ARC	309.6	136.3	Pn	11.18.55.6	-2.0	136.0	-0.3	7.3	576.2	8820.1	5.24	1		985943	
ARC	309.6	136.3	P	11.19.03.4		131.9	-4.4	7.0	7.6	2731.6	4.77	2		985945	
ARC	309.6	136.3	P	11.19.18.1		134.0	-2.3	6.8	2.8	1038.3	2.57	1	-1	985947	
ARC	309.6	136.3	Sn	11.19.27.2	-7.3	134.3	-2.0	5.1	3.5	2547.7	2.07	1		985948	1.67
ARC	309.6	136.3	*	11.19.32.0		130.3	-6.0	3.8	12.9	10251.3	2.08	1	-2	985950	2.27
ARC	309.6	136.3	Lg	11.19.37.6	-1.0	125.2	-11.1	3.1	4.0	7980.2	2.09	2		985952	2.16
ARC	309.6	136.3	*	11.19.41.4		136.4	0.1	4.8	4.3	10954.3	2.67	1		985953	
FIN	703.3	15.7	Pn	11.19.46.8	1.1	25.8	10.1	9.4	26.9	222.5	4.61	2	1	985942	
FIN	703.3	15.7	P	11.19.58.6		15.9	0.2	8.1	3.2	118.8	4.48	2	1	985944	
FIN	703.3	15.7	Lg	11.21.29.1	0.3	19.8	4.1	4.1	12.6	594.6	2.13	1		985957	2.49
FIN	703.3	15.7	*	11.21.35.3		21.7	6.0	4.6	5.8	720.1	2.58	1		985959	2.59
NRS	1182.9	42.7	Pn	11.20.42.7	-1.3	44.1	1.4	8.8	18.3	412.0	3.77	1	1	985949	
NRS	1182.9	42.7	Lg	11.23.43.9	1.0	41.1	-1.6	3.8	3.5	1141.4	1.36	1	-3	985958	2.45

Table 7.2.2. Automatic results from the on-line generalized beamforming process at NORSAR for the event described in the text. The upper two lines give estimated source parameters and residuals. The phase list shows the individual detections that have been associated with this event from the four arrays Apatity, ARCESS, FINESA and NORESS, and gives some detection parameters. Time residual (T_{res}) is only specified for the phases that have been used to define the event (10 out of 22 total associated phases).

APA Single channel corrected spectra.

60 sec start 1992-344.23.59.01.625 Wednesday 09 December
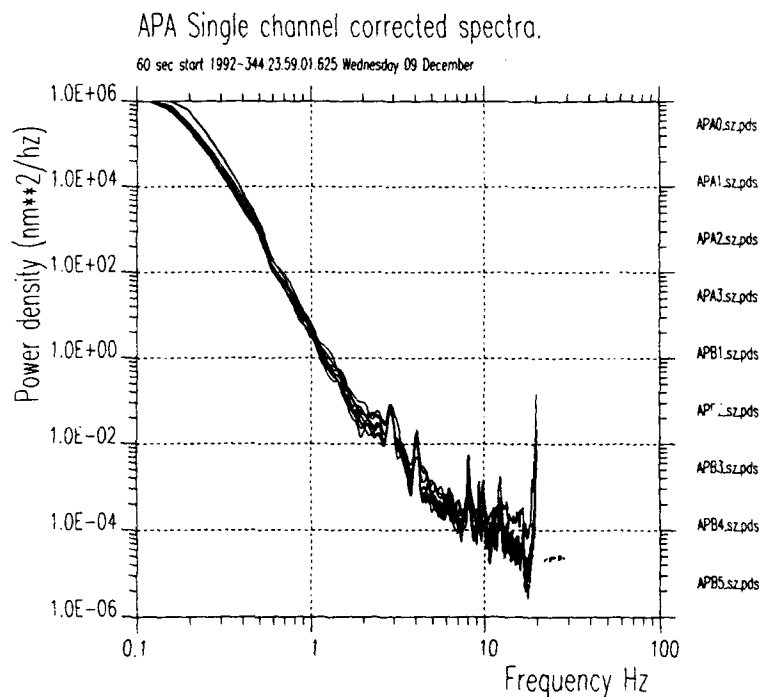
Fig. 7.2.1a. Noise spectra corrected for system response for the Apatity array for 9 vertical channels at A0, the A-ring and the B-ring. The spectra are based on one minute of data at 00.00 hours GMT on day 345, 1992. The power density is in nm^2/Hz.

ARC Single channel corrected spectra.

60 sec start 1992-345.00.01.16.556 Thursday 10 December
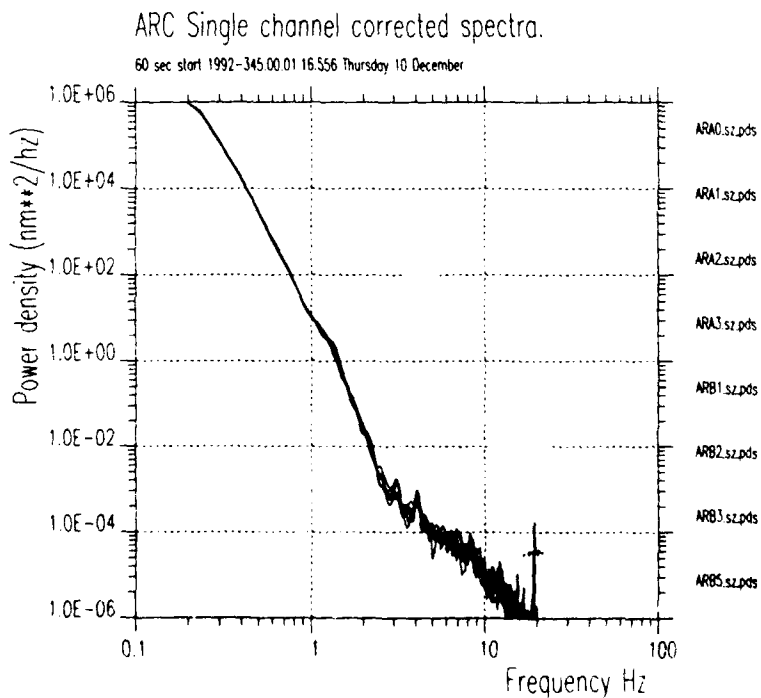
Fig. 7.2.1b. Same as Fig. 7.2.1a, but for ARCESS data (A0, A-ring, B-ring) taken at 00.00 hours GMT on day 345, 1992.

APA hourly channel spectra.
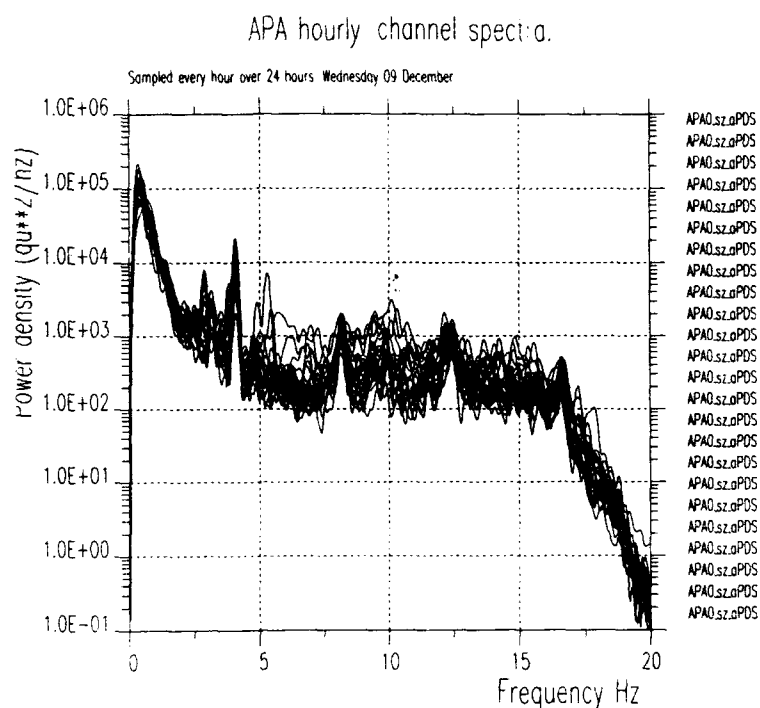
Fig. 7.2.2a. Uncorrected noise spectra for the Apatity array for 24 one-minute intervals taken hourly between 00.00 and 23.00 hours GMT on day 344, 1992. Each spectrum represents data from the A0 SPZ seismometer.

NRS hourly channel spectra.
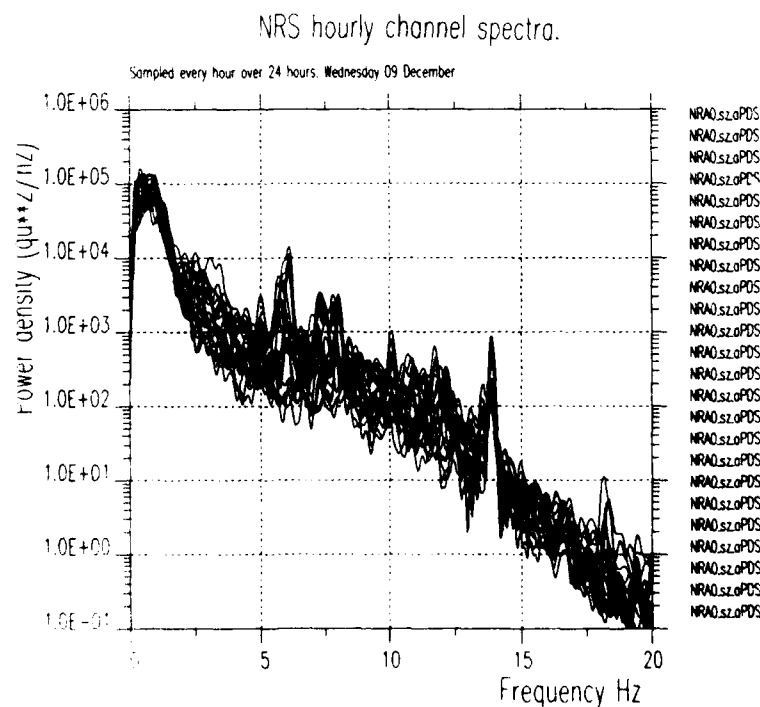
Fig. 7.2.2b. Same as Fig. 7.2.2a but for NORESS data (A0 SPZ seismometer) taken hourly between 00.00 and 23.00 hours GMT on day 344, 1992.

APA hourly noise suppression spectra.

Sampled every hour over 24 hours. Wednesday 09 December
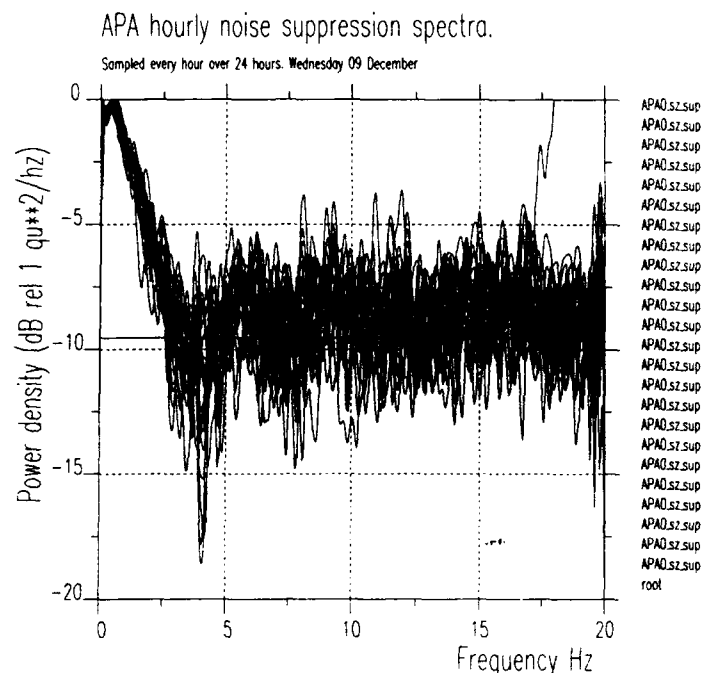
Fig. 7.2.3a. Apatity array noise suppression by beamforming for the geometry comprising A0, A- and B-ring SPZ sensors. To produce these curves, an infinite-velocity beam is formed and the spectrum for this beam is divided by the average of the single sensor spectra. The 24 curves result from one minute of data taken hourly between 00.00 and 23.00 hours GMT on day 344, 1992. The horizontal line at -9.5 dB represents $\sqrt{N}$ suppression for 9 sensors.

NRS hourly noise suppression spectra.

Sampled every hour over 24 hours. Wednesday 09 December
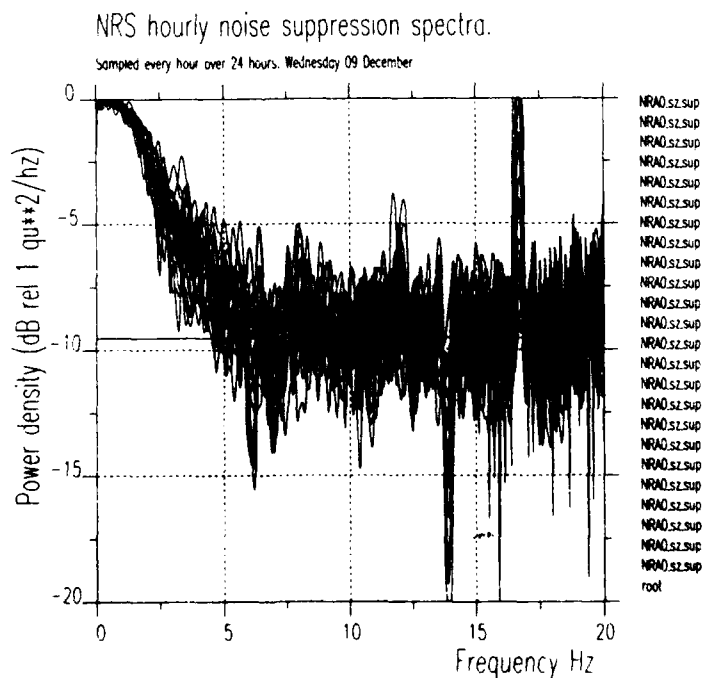
Fig. 7.2.3b. Same as Fig. 7.2.3a but for the 9-element sub-geometry of NORESS consisting of A0, the A- and B-rings.
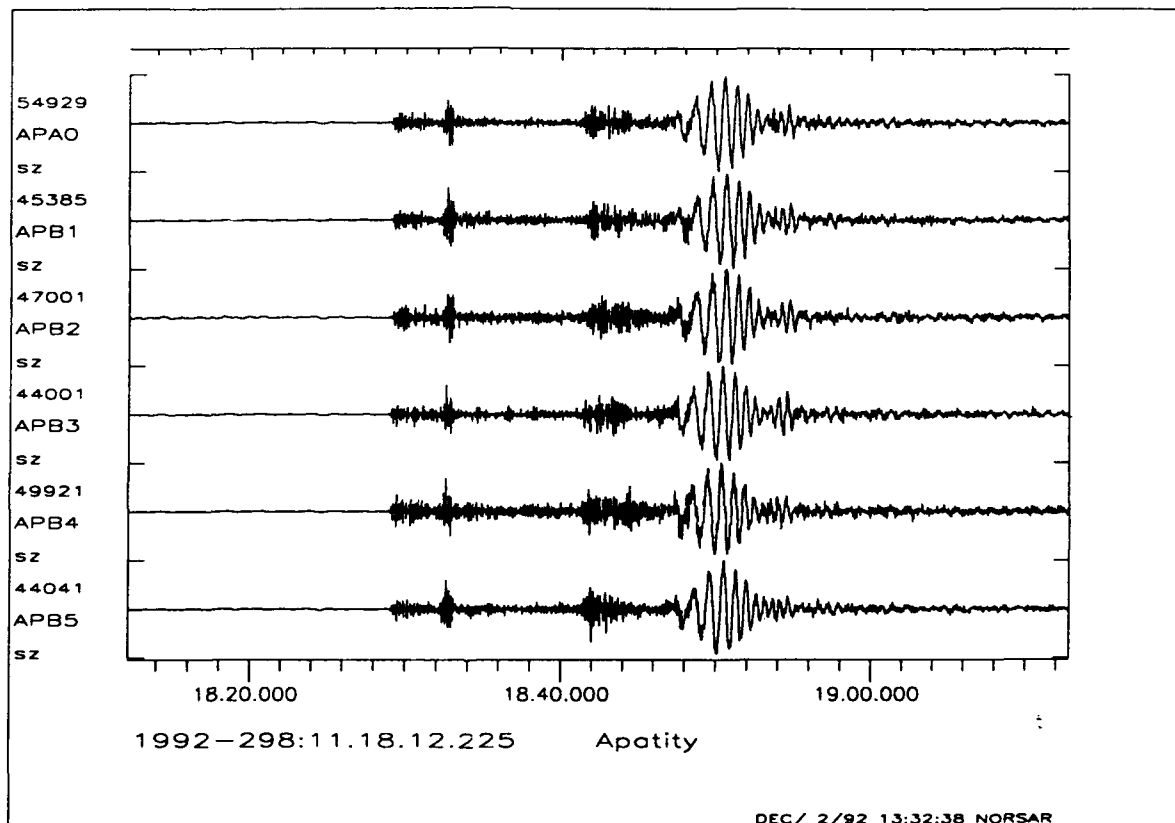
Fig. 7.2.4. Plot of individual APA SPZ channels for the presumed mining explosion discussed in the text (see Table 7.2.2). Note the very prominent Rg phase, indicating a shallow origin.

```
1992-298:11.18.29.000 +   1.00 SEC
WIDE-BAND SLOWNESS ANALYSIS                                    a)
CONTOURS IN DB BELOW MAXIMUM PEAK
```



```
VELOCITY CIRCLES (KM/SEC) AT
    8.00    6.00    3.00
CHANNELS:
APA_A0_SZ              APA_A1_SZ
APA_A2_SZ              APA_A3_SZ
APA_B1_SZ              APA_B2_SZ
APA_B3_SZ              APA_B4_SZ
APA_B5_SZ
```

```
BAND   3.8 -   7.5 HZ   REL.POWER   0.88
V,A    6.78 KM/S, 269.64 DEG    60.04 DB
```

NORSAR02/12/92 13:27:24
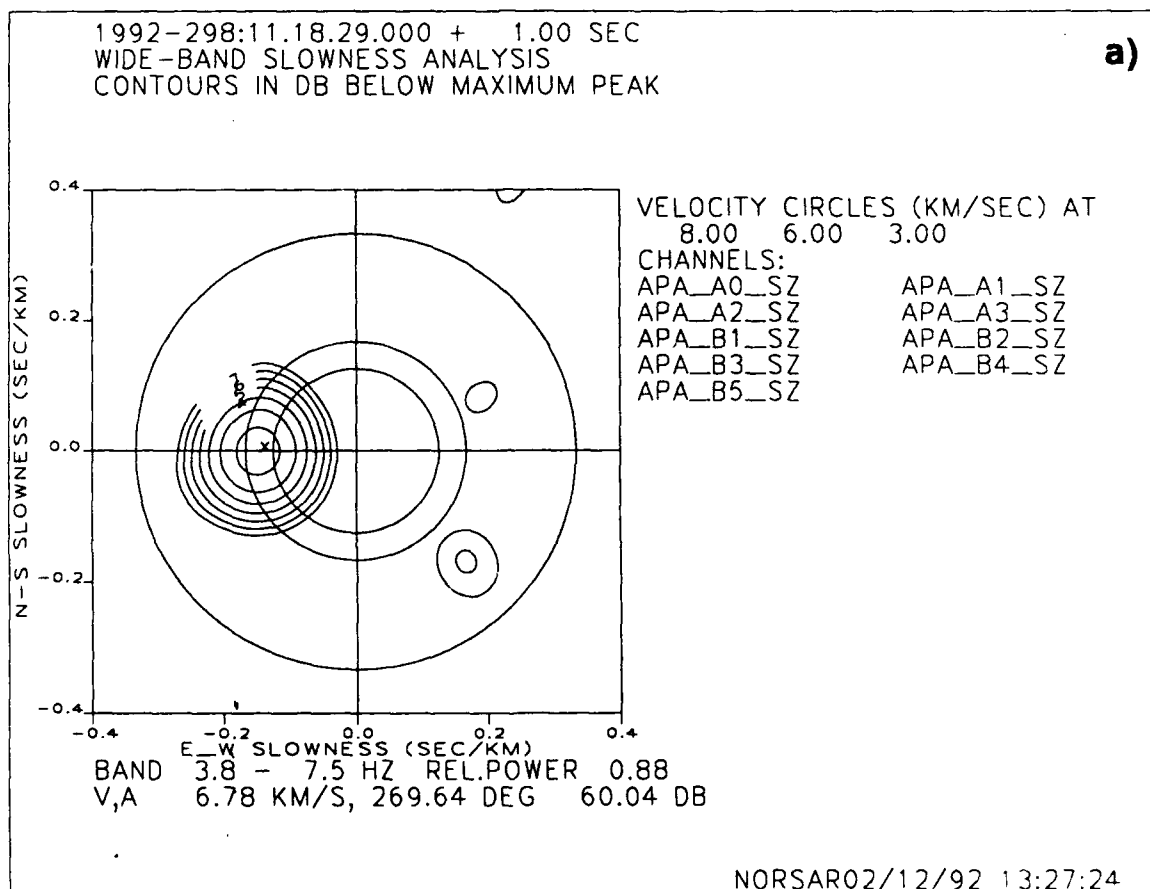
Fig. 7.2.5. Broadband F-K analysis results for the P, Lg and Rg phases of the event shown
in Fig. 7.2.4. The figure shows a) the Pg phase, b) the Lg phase and c) the Rg phase.
The three velocity circles correspond to 8, 6 and 3 km/s. (Page 1 of 3).

1992-298:11.18.41.000 +   1.50 SEC
WIDE-BAND SLOWNESS ANALYSIS   **b)**
CONTOURS IN DB BELOW MAXIMUM PEAK

VELOCITY CIRCLES (KM/SEC) AT
   8.00   6.00   3.00
CHANNELS:
APA_A0_SZ   APA_A1_SZ
APA_A2_SZ   APA_A3_SZ
APA_B1_SZ   APA_B2_SZ
APA_B3_SZ   APA_B4_SZ
APA_B5_SZ

BAND   2.5 - 5.0 HZ REL.POWER 0.86
V,A   3.82 KM/S, 273.68 DEG   65.64 DB

NORSAR02/12/9? 13:18:52

Fig. 7.2.5. (Page 2 of 3)

```
  1992-298:11.18.49.000 +   3.00 SEC
  WIDE-BAND SLOWNESS ANALYSIS                                    c)
  CONTOURS IN DB BELOW MAXIMUM PEAK
```

VELOCITY CIRCLES (KM/SEC) AT
    8.00   6.00   3.00
CHANNELS:
APA_A0_SZ   APA_A1_SZ
APA_A2_SZ   APA_A3_SZ
APA_B1_SZ   APA_B2_SZ
APA_B3_SZ   APA_B4_SZ
APA_B5_SZ

BAND 0.6 - 1.6 HZ REL.POWER 0.99
V,A   3.33 KM/S, 281.81 DEG   84.04 DB

NORSAR02/12/92 09:42:32

Fig 7.2.5. (Page 3 of 3)

Fig. 7.2.6. Example of teleseismic event processing for the Apatity array. The top six traces are individual seismometer recordings, filtered in the band 1.5-3.5 Hz. The two bottom traces are array beams, filtered and unfiltered. Note the significant SNR improvement for the filtered array beam.

7.3   On the use of regionalized wave propagation characteristics in automatic global phase association

The Generalized BeamForming (GBF) method for automatic phase association and event location (Ringdal and Kværna, 1989), uses the philosophy of matching the predicted phase arrivals from hypothetical events at a predefined set of target locations to the actual detections at each observing station. This approach gives us the opportunity of organizing and using knowledge on regionalized wave propagation characteristics in a simple and well-arranged way.

Examples of relevant questions are:

*   Which seismic phases are observable/detectable at the different stations from an event at a given target location.

*   What are the expected travel-times, slownesses, and azimuths of these phases, and the corresponding variability.

*   What are the amplitude versus magnitude relations for the different phases, and the corresponding variability.

The quality of the GBF results as well as the false alarm rate are dependent on how well our predictions match the actual observations. As illustrated in Fig. 7.3.1, the detectable seismic phases may vary strongly from one region to another, as do the corresponding travel-times. The obvious way to obtain good predictions at a given station is to collect and analyze events from a wide range of epicentral regions. For these calibration events, independent bulletin information on hypocenter location, origin time and magnitude should be available.

Detailed mapping of the wave propagation characteristics attributed to a given station do, however, require significant amount of data and a substantial amount of work (Kværna and Mykkeltveit, 1985; Mykkeltveit et al., 1990; Gestermann, 1992; Sereno et al., 1992). The Intelligent Monitoring System (IMS) (Bache et al., 1990), currently operating a net-work of arrays in northern Europe, has a design that facilitates retrieval of this kind of knowledge, using a database management system (DBMS). During its 2-3 years of opera-tion it has contributed significantly to improve the quality of the automatic processing results from this region of the world (Bratt et al., 1990).

The GSETT-2 database

Another interesting database is the waveforms and processing results from the GSETT-2 experiment conducted in 1991. During a period of six weeks (April 22 to June 2), 60 glo-bally distributed stations (including single-component stations, three-component stations and arrays) reported phase readings and waveforms to a common database, see Fig. 7.3.2. At four different data centers, automatic analysis as well as analyst review were conducted to obtain precise event locations and magnitude estimates.

In the instructions for the conduct of the GSETT-2 experiment (GSE/CRP/Rev. 4, 1991), there are detailed instructions on which parameters to use for the preparation of the event

bulletin. This includes the use of travel-times and slownesses derived from the Jeffreys-Bullen travel-time tables. There are also detailed instructions on which phases to consider, as well as their residual requirements on travel-time and slowness vector residuals for the different types of seismic stations.

A stepwise approach towards regionalization

When initiating phase association and event location with the GBF method on data from a new network like GSETT-2, the natural starting point is to use theoretically derived or globally averaged processing parameters like those described in the GSETT-2 instructions.

The GSETT-2 stations (see Fig. 7.3.2) are situated in very different geological provinces, and may experience systematic deviations from the globally averaged travel-times, slowness and azimuth estimates, especially for events within regional distances.

A first step towards regionalization would be to investigate if stations within the same geological province observe similar systematic anomalies with regard to, e.g., phase occurrence, travel-time, slowness or azimuth, and then accordingly introduce corrections to the parameters derived from the globally symmetric model.

Next, this can be refined by analyzing each station separately, and also, if possible, making corrections for source regions where the events exhibit anomalous behavior. For example, for seismic phases recorded at the GERESS array in Germany, both Gestermann (1992) and Sereno et al. (1992) have analyzed the characteristics of regional phases along different propagation paths.

Finally, for small areas with recurring events, such as mines, nuclear test sites and seismically very active regions, we can use the recorded events for calibration and obtain site-station specific processing parameters for use by the GBF method.

In the following, we will present samples from results we have obtained by searching the GSETT-2 database that are of relevance for improving the processing parameters for the GBF method. In this contribution we have used the event bulletin from the Washington Experimental International Data Center (EIDC) as the reference bulletin, also called WASCEL (WAShington Current Event List). This bulletin may not contain totally independent information because the phases we are to analyze have been used to produce the bulletin. However, for events with a sufficiently high number of associated phases, the bias due to this effect is considered negligible.

Phase occurrence

The optimum information on the occurrence of seismic phases at a given station would be to have a geographical map with indications on which phases may be observed from events in the different geographical areas. However, the derivation of such information requires a large number of recorded events, which can only be obtained for stations that have been operational over a long time period.

If we assume that the geology of the region surrounding a given station is rather uniform, the recording of seismic phases would primarily be distance- and magnitude- dependent (the effect of different source functions is ignored at this stage). The assumption of azimuthal symmetry will initially be made for the derivation of wave propagation characteristics from the GSETT-2 database. We will in the following use phase labels reported by the WASCEL as the reference.

As a first example we show a histogram of the occurrence of regional phases observed at the ARCESS array in Norway (ARA0) as reported in the WASCEL (Fig. 7.3.3.a). It is seen that certain distance ranges have more reported phases than others, corresponding to regions of high mining activity, like the Kola peninsula (3-4 degrees), the St. Petersburg region (8-9 degrees), and the Estonian region (10-11 degrees).

This data set indicates that beyond the critical distances, Pn and Sn can be expected to be seen for all regional distances, whereas Pg is not observed beyond 9 degrees. Lg is only observed within 12 degrees, and Rg only within 4 degrees.

It should be emphasized that this data set is sampled through a time period of only six weeks, and consequently only samples the lower part of the event magnitude distribution. It is therefore likely that phases from stronger events will be observable at larger distances than those found in this data. Such considerations have to be made when constraining the expected occurrence of seismic phases at a given station.

Fig. 7.3.4.a shows a histogram of the occurrence of teleseismic phases observed at ARCESS. The P and PKP phases generally follow the expected pattern of the global travel time curves. Some PcP phases are observed, probably corresponding to events in regions with favorable propagation paths and/or strong events.

In a similar way, such investigations can be conducted for each of the other GSETT-2 stations, but it should be noted that the GSETT-2 database probably contains too little data for a rigorous mapping of the occurrence of seismic phases.

Reported phase labels

Another interesting parameter that possibly can be utilized by the GBF algorithm is the phase labels given by the reporting stations. For direct comparison with the regional phase distribution of Fig. 7.3.3.a, we show in Fig. 7.3.3.b the same type of histogram, but based on phase labelling by the Norwegian National Data Center (NDC). From these figures it looks like there is good agreement with the final phase labels given in the WASCEL. On the other hand, from the histogram of NDC reported teleseismic phases of Fig. 7.3.4.b, we find that with very few exceptions, all phases were reported as P.

For the most frequently observed phases, the relation between the NDC reported phase labels and those reported in the WASCEL has been studied in more detail. The rows of Table 7.3.1 represent the ARCESS phase labels reported by the Norwegian NDC, and the columns represent the phase labels of the WASCEL. This matrix table thus gives an overview of the reliability of the NDC reported phase labels.

Phase labels reported in the WASCEL

	Pn	Pg	Sn	Sg	Lg	Rg	P	S	PP	PcP	PKP	pP	sP	UNK
Pn	186	4					4							1
Pg		17												1
Sn			119											2
Sg														
Lg		1	4		113									4
Rg						6								1
P	11	1					534		1	12	108	27	9	59
S														
PP									1					
PcP										3				
PKP							1				5			
pP												37		
sP													9	1
UNK													1	11

(NDC-reported phase labels, rows)

Table 7.3.1.

Let us consider phases reported as Pn by the Norwegian NDC:

186 of these phases were not renamed during global phase association, 4 were renamed to Pg,4 were renamed to P and 1 was renamed to be unknown. Similar statistics are seen for the other phase types. In the context of conducting event association by the GBF method, it is reasonable to introduce some general constraints on the use of NDC reported phases from the ARCESS array. For example, the following two constraints are quite apparent from the table:

- A phase reported to be of P-type (P, Pn, Pg, PKP,...) should not be associated with a hypothetical arrival of S-type. Out of 1032 P-type phases in this data set, none was renamed to an S-type phase.

- A phase reported to be of S-type (S, Sn, Lg, Rg) should not be associated with a hypothetical arrival of P-type. In this data set, out of 250 S-type reports (Sn, Lg, Rg), only one phase was changed to a P-type phase by WASCEL.

Many other constraints of more limited application can also be inferred from the table. For example, a phase reported as Pn should only be allowed to be renamed P or Pg (or retained as Pn). On the other hand, a phase reported as P could be renamed to either Pn, Pg, PP, PcP, PKP, pP, sP or, of course, retained as P. It is possible that some more refinements may

be made by taking into consideration the difference in the slowness estimates between core phases and P-phases, but this will be the topic of a separate investigation.

Without going into detail, it is clear that a database of the GSETT-2 type can provide a number of useful rules to constrain the reinterpretation of phases reported by an NDC. This in turn will reduce the probability of false associations in the global event definition process.

Reported event locations

During the GSETT-2 experiment, the National Data Centers (NDCs) were encouraged to provide information on location parameters of events detected at their participating stations.

These location parameters provide useful information to the automatic phase association procedure. Depending on the expected accuracy of the reported NDC location, a phase associated to an event by an NDC, can during the global phase association process be restricted to stem from events in target regions close to the NDC reported event location.

One-station event locations are usually found by associating a P- and an S-phase to a common event, getting a distance estimate from the S-P travel-time difference and source direction from the azimuth estimates of the phases. One-station event locations are thereby most commonly obtained for regional events, where clear P- and S-phases are frequently observed. Reliable azimuth estimates of both P- and S-phases are obtained by arrays, whereas three-component stations have the ability to estimate the azimuth of P-phases.

To investigate the reliability of the NDC locations provided by the regional arrays, ARCESS, FINESA, NORESS and GERESS, we have in Fig. 7.3.5 plotted the station-to-event distances of the NDC locations against the station-to-event distances of the corresponding locations of the WASCEL. As seen from the plots, there are, with few exceptions, good correspondence between these distance estimates.

A few phases associated to local or regional events by the NDC have, however, been associated to teleseismic events in the WASCEL. Incidentally, this is a violation of the rules outlined in GSE/CRP/Rev. 4 (1991) (Appendix B.3.2 (ii): "Observations of phases reported as originating from local or regional distances may be used only within local and/or regional distances").

Conclusions

We have in this paper outlined a strategy for retrieving and organizing information on regionalized wave propagation characteristics for use by the GBF method algorithm. Different types of relevant information derived from the GSETT-2 database have been shown in several examples. These examples illustrated features like the distance dependent occurrence of seismic phases, the reliability of reported phase labels and the accuracy of one-station event locations. In future work we plan to examine the GSETT-2 as well as

other data bases in more detail, in order to develop an optimum framework for application of the GBF method to a global network.

T. Kværna
U. Baadshaug

References

Bache, T.C., S.R. Bratt, J. Wang, R.M. Fung, C. Kobryn and J.W. Given (1990), The Intelligent Monitoring System, Bull. Seism. Soc. Am., 80, Part B, 1833-1851.

Bratt, S.R., H.J. Swanger, R.J. Stead, F. Ryall and T.C. Bache (1990), Initial results from the Intelligent Monitoring System, Bull. Seism. Soc. Am., 80, Part B, 1852-1873.

Gestermann, N. (1992), Interpretation of regional phases recorded at GERESS, in Proceedings from the GERESS symposium, June 22-24, 1992, Waldkirchen, Bavaria, Germany.

GSE/CRP190/Rev. 4 (1991), Instructions for the conduct of Phase 3 of GSETT-2, Group of Scientific Experts, U.N. Conference of Disarmament, Geneva, Switzerland.

Kværna, T. and S. Mykkeltveit (1985), Propagation characteristics of regional phases recorded at NORSAR, Semiann. Tech. Summary, 1 April-30 September 1985, NORSAR Sci. Rep. No. 1-85/86, Kjeller, Norway.

Kværna, T. (1990), Generalized beamforming using a network of four regional arrays, Semiann. Tech. Summary, 1 April-30 September 1990, NORSAR Sci. Rep. No. 1-90/91, Kjeller, Norway.

Mykkeltveit, S., F. Ringdal, T. Kværna and R.W. Alewine (1990), Bull. Seism. Soc. Am., 80, Part B, 1777-1800.

Ringdal, F. and T. Kværna (1989): A multi-channel processing approach to real-time network detection, phase association and threshold monitoring, Bull. Seism. Soc. Am., 79, 1927-1940.

Sereno, T.J., H.J. Swanger, R.D. Jenkins, W.C Nagy and D. Wahl (1992), Attenuation and travel-time characteristics of regional phases recorded at GERESS, in Proceedings from the GERESS symposium, June 22-24, 1992, Waldkirchen, Bavaria, Germany.
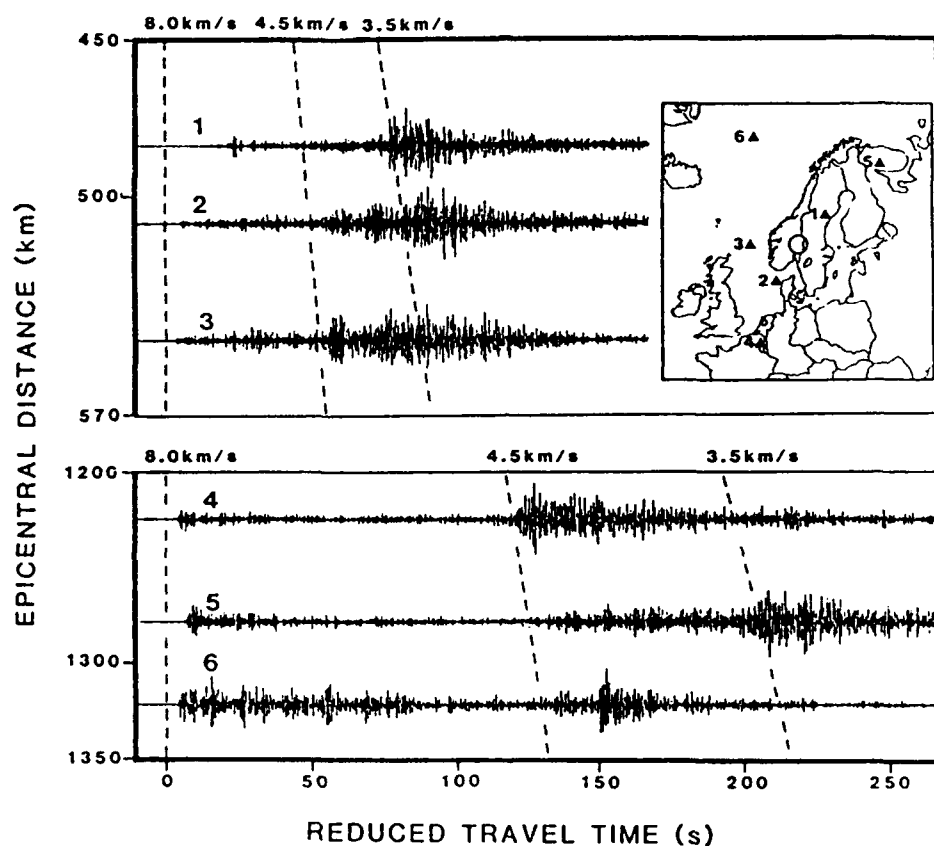
Fig. 7.3.1. Illustration of variation of relative importance of the phases Sn and Lg for six
events with locations as indicated in the map. The standard group velocities of 4.5
and 3.5 km/sec, commonly assigned to Sn and Lg, respectively, are marked by
dashed lines. The upper three traces cover the distance interval from 480 to 550 km,
while the lower three traces correspond to epicentral distances in the range from
1,225 to 1,320 km. The location of the NORSAR array is denoted by a ring on the
map, and the traces are from NORSAR seismometer 02B01. The data are bandpass-
filtered 1 to 5 Hz. The reduction velocity is 8.0 km/sec. From Mykkeltveit et al
(1990).

GSETT-2 stations
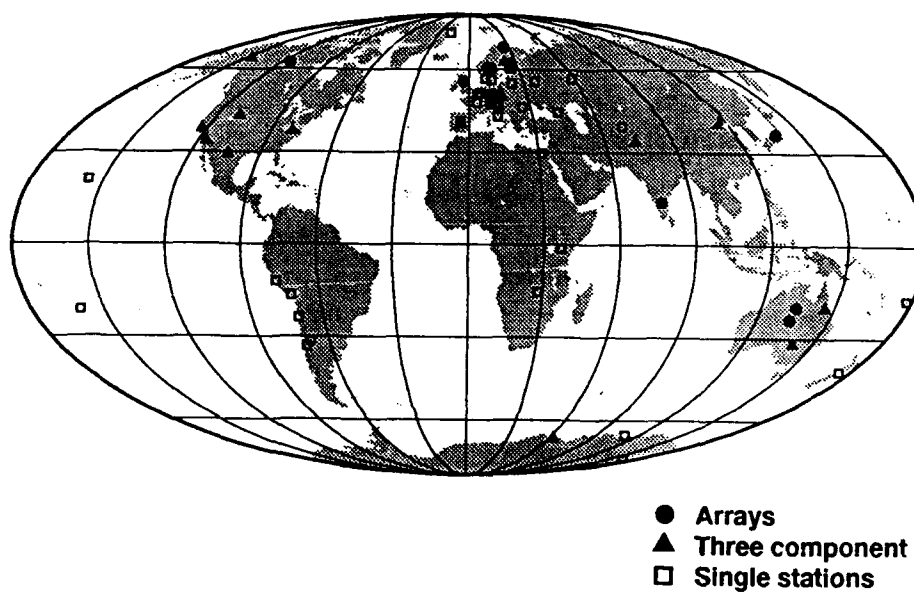
Fig. 7.3.2. Map showing the location of the stations participating in the GSETT-2 experiment.

ARA0 regional phase distribution
4 or more defining phases

Phase ids from WASCEL

a)

NDC reported phase ids

b)
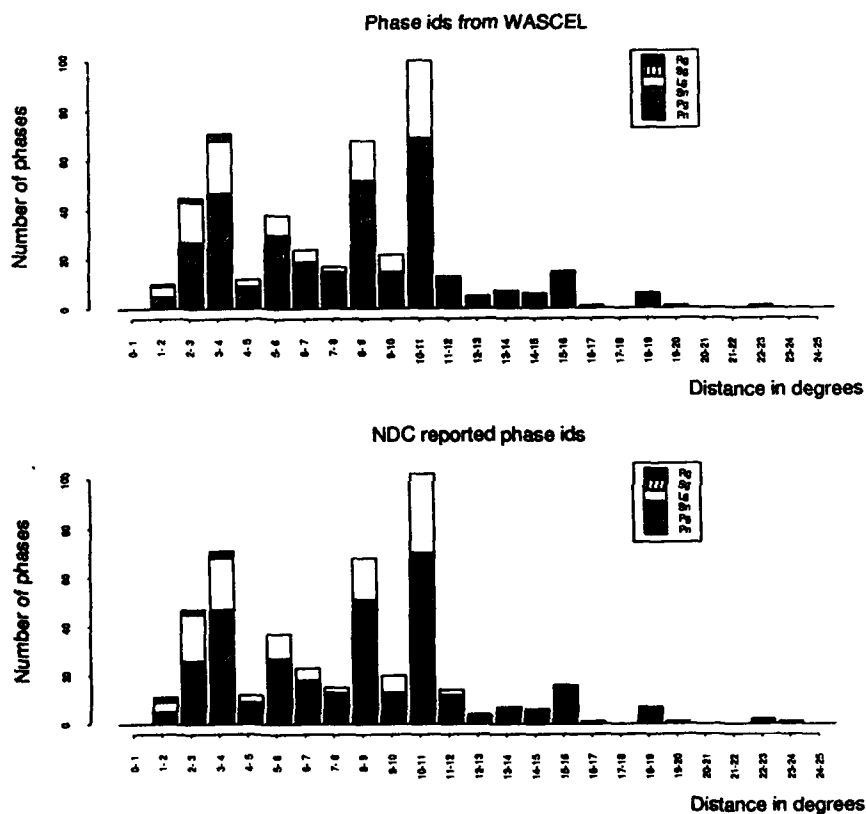
Fig. 7.3.3.

a)   Histogram showing the distance dependent occurrence of regional phases observed
     at the ARCESS array in Norway (ARA0). Event to station distances and phase
     labels are both taken from the WAShington Current Event List (WASCEL).

b)   Histogram showing the ARCESS regional phase labels reported by the Norwegian
     National Data Center (NDC). Event to station distances are taken from the WASh-
     ington Current Event List (WASCEL).

ARA0 teleseismic phase distribution
4 or more defining phases

Phase ids from WASCEL

a)

NDC reported phase ids

b)
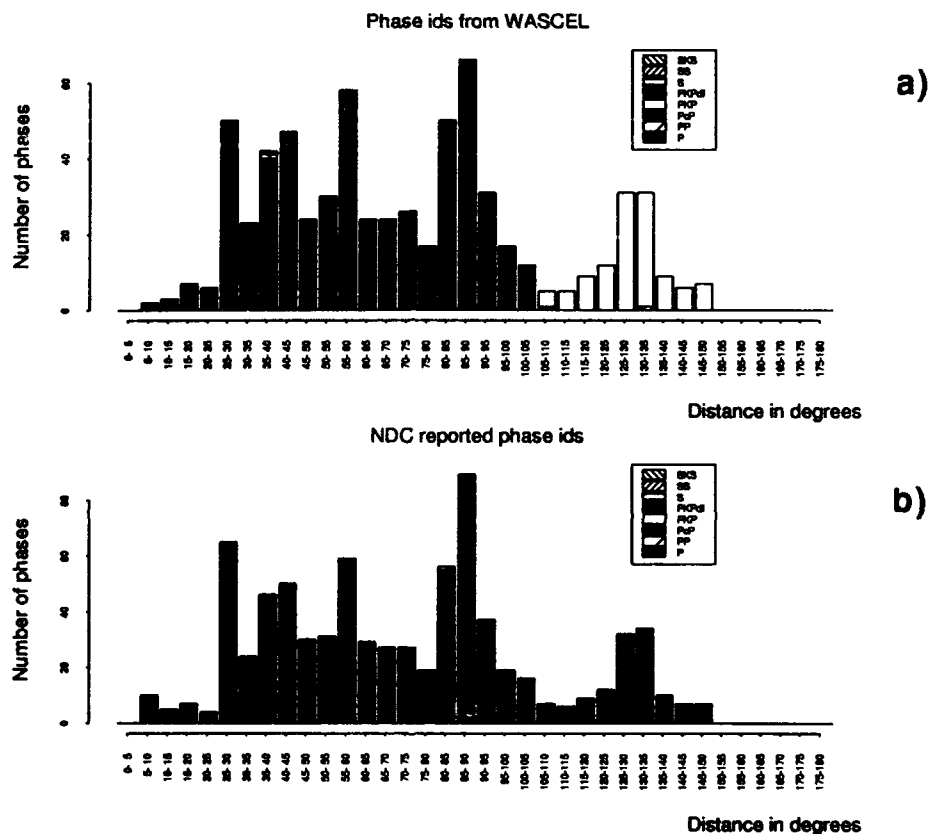
Fig. 7.3.4.

a)   Histogram showing the distance dependent occurrence of teleseismic phases
      observed at the ARCESS array in Norway (ARA0). Event to station distances and
      phase labels are both taken from the WAShington Current Event List (WASCEL).

b)   Histogram showing the ARCESS teleseismic phase labels reported by the Norwe-
      gian National Data Center (NDC). Event to station distances are taken from the
      WAShington Current Event List (WASCEL).
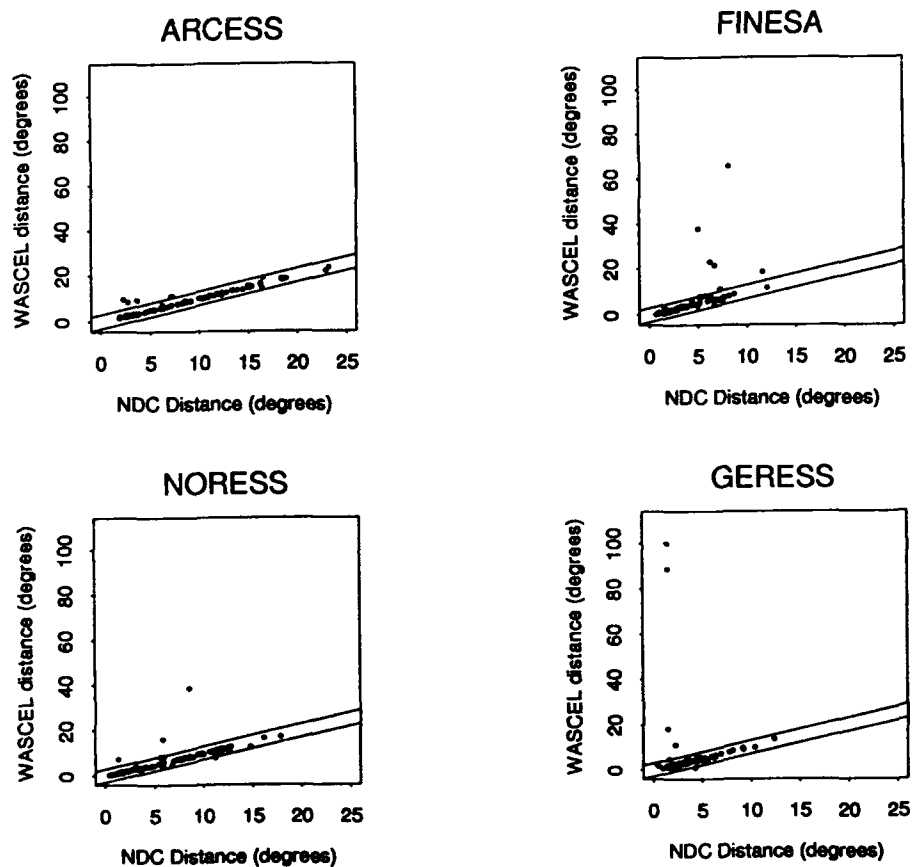
Fig. 7.3.5. Plots showing the relation between NDC reported event locations and those given in the WASCEL, obtained after global phase association, for the regional arrays ARCESS, FINESA, NORESS and GERESS. Two lines with deviations of ±3 degrees, respectively, are shown on each plot.

7.4   Two techniques for constructing a uniform grid system covering the Earth's surface

In many geophysical studies there is a need to divide the entire earth's surface into areas of equal size and shape. An example, discussed in subsection 7.5 is the application of the Generalized BeamForming technique for global seismic monitoring. According to Rottman (1960), there are only five polyeders that can be used for a such division, and among these, the icosaeder has the largest number of subareas (20 equilateral triangles). For further refinement, approximations have to be made.

We have investigated the characteristics of two different techniques for quasi-uniform gridding of the surface of the globe. The first method uses a reference meridian and a reference latitude as a starting point, and deploys equidistant grid points along equidistant latitude circles, see Fig. 7.4.1. To obtain complete and non-overlapping coverage, special care has to be taken in the polar regions and near the longitude opposite to the reference meridian.

The other method is adopted from seismic prospecting (Vinje et al., 1992), where triangulation of the icosaeder has been used to construct regularly sampled wavefronts, see Fig. 7.4.2. Unlike the first method, complete and non-overlapping coverage are directly obtained.

Properties of the gridding techniques

To visually compare the two methods, we have in Fig. 7.4.1 plotted a complete global grid system produced by the first technique, hereafter called the rectangular method. In Fig. 7.4.2 we have plotted a similar grid produced by triangulation of the icosaeder, hereafter called the triangular method. The number of points in these plots are nearly identical, i.e., 645 versus 642. We see that for the rectangular method the shape of the area spanned by each grid point and its eight neigbours becomes heavily distorted in certain regions. This is especially the case in the polar regions and for longitudes far away from the reference meridian. For the triangular method, the shape of the area spanned by each grid point and its six neighbours remains much more uniform. It should, however, be noticed that the 12 points constituting the original icosaeder only have five neighbors.

To obtain complete coverage of the earth, we define a circular region around each grid point. For the triangular grid, we have found that circles with radii as shown in Fig. 7.4.4 completely cover the earth surface. We could as well have chosen types of geometries different from the circle, like the pentagon or the hexagon where the degree of overlap is smaller, but for use in our subsequent analysis, the simplicity of the circle is preferable. For the rectangular grid, we have in Fig. 7.4.3 plotted circles with the same radii as in Fig. 7.4.4, and we find that there are certain areas that have not been spanned by any of the circular regions, and hence, circles with larger radii are required. The triangular method therefore gives more effective coverage.

Another appealing property of the triangular technique is that each grid point has a well-defined pointer structure to its neighbours. For a given sub-region, this enables us to construct a refined grid system in a straightforward manner.

In contrast to the rectangular method, where an arbitrary number of grid points can be specified, the number of grid points obtained by the triangular method can only take on certain discrete values. These values are given in Table 7.4.1, together with the radii of the corresponding circular regions.

Number of divisions of the icosaeder	Number of points	Circle radius (degrees)
0	12	43.8
1	42	21.9
2	162	11.0
3	642	5.5
4	2562	2.7
5	10242	1.4
6	40962	0.7

Table 7.4.1.

In conclusion, there are strong arguments for preferring the triangular method to the rectangular method. The only argument in favour of the rectangular method is the possibility of constructing a grid of arbitrary density.

T. Kværna

References

Rottman, K.: Mathematische Formelsammlung (1960): Bibliographisches Institut Mannheim/Wien/Zurich

Vinje, V., E. Iversen, H. Gjøystdal and K. Åstebøl (1992): Traveltime and amplitude estimation using wavefront construction. Abstract of papers presented at the 54th Meeting and Technical Exhibition of the European Association of Exploration Geophysicists, Paris, France, 1-5 June 1992.

645 grid points, rectangular
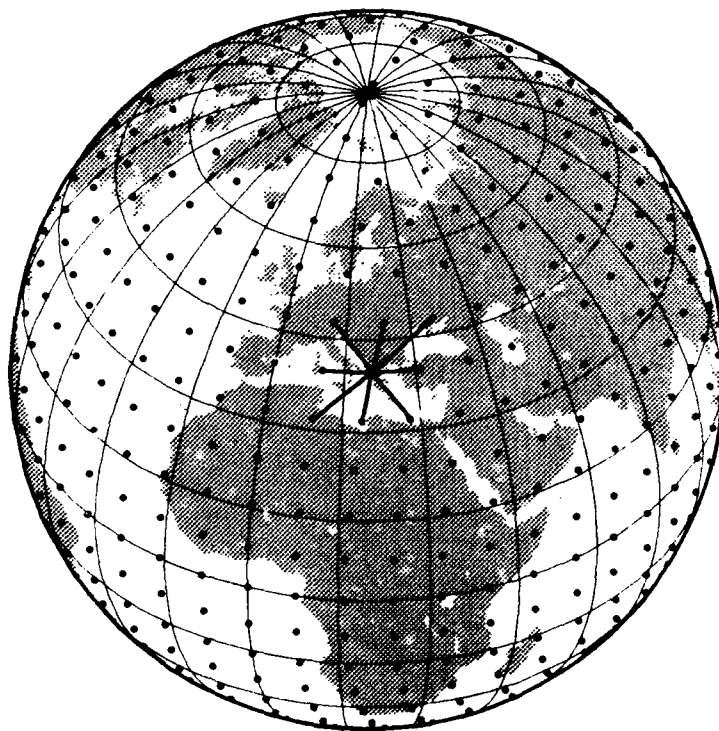
Fig. 7.4.1. Global grid constructed by the rectangular method. The latitude and longitude steps were chosen to be 7.95 deg. The connection lines between a grid point and its eight neighbours are also shown.

642 grid points, triangular
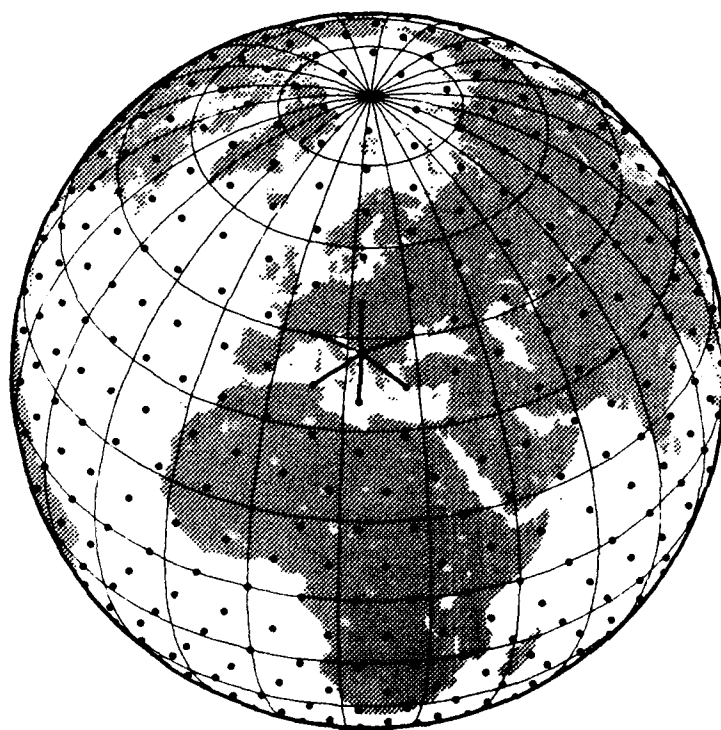
Fig. 7.4.2. Global grid constructed by the triangular method. The 642 points were
obtained by a tree-fold triangulation of the original icosaeder. The connection lines
between a grid point and its six neighbours are also shown.

645 grid points, rectangular
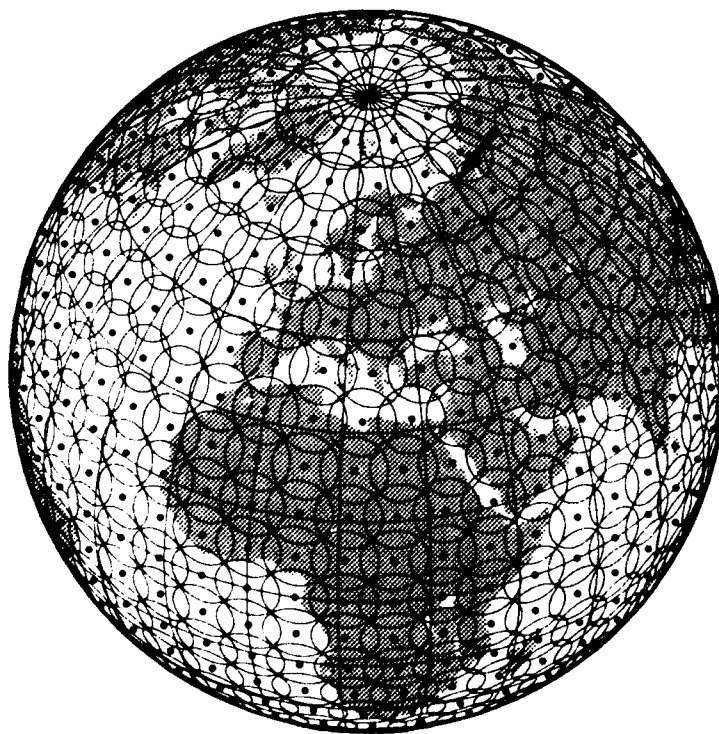
Fig. 7.4.3. Circular regions of radius 5.5 deg. encompassing each grid point constructed by the rectangular method. Note that for certain areas the coverage is not complete, e.g., around 70N, 60E (marked by an arrow).

642 grid points, triangular
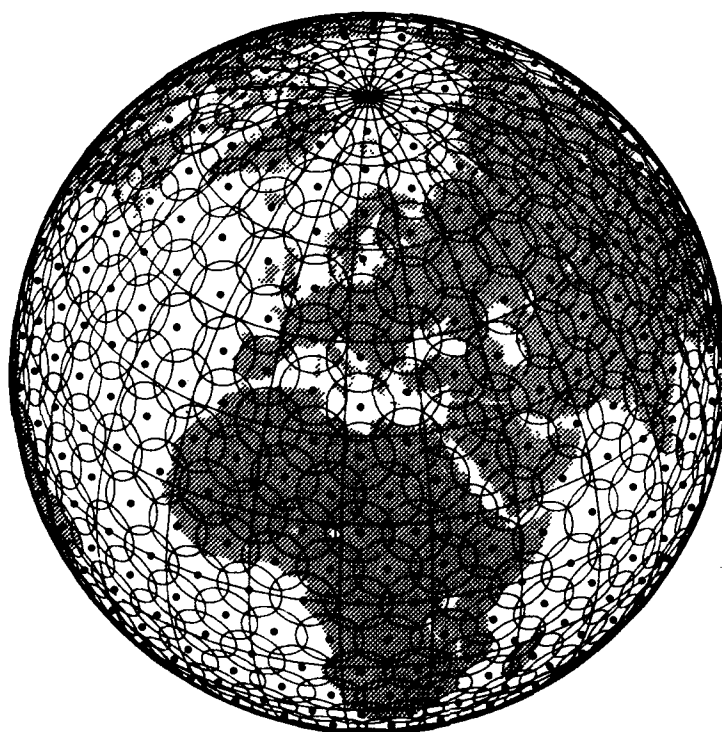
Fig. 7.4.4. Circular regions of radius 5.5 deg. encompassing each grid point constructed by the triangular method. Note that the coverage is complete.

7.5   Initial results from global Generalized Beamforming

We will in this paper outline some of the fundamental concepts for using the Generalized BeamForming method (GBF) to conduct phase association and event location on a global scale. Towards the end of the paper we will also present initial results from GBF processing of detection data from the GSETT-2 database. The GSETT-2 network consisted of about 60 globally distributed stations (including single-component, three-component and arrays), see Fig. 7.3.2., which reported phase readings and waveforms to a common database during a period of six weeks. Detailed instructions for the conduct of the GSETT-2 experiment are given in GSE/CRP190/Rev.4 (1991).

The Generalized Beamforming method for phase association and event location (Ringdal and Kværna, 1989), has been proven to work well on a regional scale (distances within approximately 2000 km) using continuous detection data from the four regional arrays ARCESS, FINESA, GERESS and NORESS (Kværna, 1990; Kværna, 1992). Taylor and Leonard (1992) are currently conducting research on applying this method to teleseismic data from a 17 station global network. Their results indicate that the GBF method can be effectively used as a means of conducting automatic global teleseismic phase association.

In order to extend the GBF method to work on both regional and teleseismic data from a large global network we have found it necessary to develop a framework that facilitates testing of the method with different parameter settings. We will in the following give a detailed description of this framework.

Division of the earth into regular target regions

The basic idea behind the GBF method is to match the predicted phase arrivals from hypothetical events in a predefined set of target regions to the actual detections at each observing station. We have chosen to define these target regions by their center coordinates and a circular area of a given radius. Initially we will deploy the center of the target regions at a common depth and ensure that the circular areas cover the entire surface of the earth. In practice, the target region will constitute a volume around the center grid point, and will thus also accommodate hypothetical events within a given depth range.

In section 7.4, we have described two techniques for constructing a uniform grid system covering the earth's surface. Results from this study indicate that the method based on triangulation of the icosaeder (the triangular method) is preferable. The density of the grid system is given by a single variable determining how many times the original icosaeder is divided by triangulation. Figs. 7.5.1 - 7.5.3 show global grid systems obtained by two-, three- and four-fold triangulation of the icosaeder. The number of global grid points in these figures are respectively 162, 642 and 2562, and the respective radii of the corresponding circular areas encompassing each grid point are 11.0, 5.5 and 2.7 degrees.

Parameter tolerances due to the areal extent of the target region

Time tolerances

On the global map of Fig. 7.5.4 we have plotted a 162-point global grid system with target regions of 11 degrees radii. Let us consider a P-phase at the NORESS array from a hypothetical event in the highlighted target region. As shown on Fig. 7.5.5, the P-phase travel-times from events within this target region can differ by almost 200 seconds. This has to be taken into account in the process of matching predicted and observed phase arrivals, and in practice, the following procedure is used:

Assume that we have a phase detection at the NORESS array with arrival time T_{arr}. The minimum and maximum predicted travel-times of P-phases from the highlighted target region are given by TT_{min} and TT_{max}. If the observed arrival at NORESS is to be a P-phase from an event in the target region, the origin time of the event would theoretically be bounded by OT_{min} and OT_{max} given by

$$OT_{min} = T_{arr} - TT_{max} \qquad (1)$$

$$OT_{max} = T_{arr} - TT_{min} \qquad (2)$$

Slowness vector tolerances

If the observing station is providing azimuth and/or slowness estimates of the detected phases, these estimates can constrain the use of the detections in the phase association process, and thus prevent false associations. Let us again consider a P-phase at the NORESS array from a hypothetical event in the highlighted target region shown on Fig. 7.5.4. To cover the entire target region, the P-phases will theoretically span an azimuth and slowness range falling within the solid curve of Fig. 7.5.6. In practice, we make an approximation to the area within the solid curve by specifying four parameters, i.e., the minimum and maximum values of slowness and azimuth. As seen on Fig. 7.5.6, this will constitute an area only marginally larger than the original. So in order to match the observed arrival at NORESS to a P-phase from a hypothetical event in the target region, the estimated azimuth and slowness would theoretically have to fall within these bounds.

Parameter tolerances due to deviations from the theoretical model

Time tolerances

In addition to the parameter tolerances compensating for the areal extent of the source region, we also have to take into account the effects of sampling rate, errors in the estimation of arrival-time and slowness vector, propagation path, source type and other types of random errors.

Let ΔT be the sampling rate in time of the generalized beam for the highlighted target region of Fig. 7.5.4, and let T_{dev-} (early arrival) and T_{dev+} (late arrival) be the maximum allowable deviations from the predicted P travel-time, taking into account path

effects, onset time estimation errors, source effects and other types of random errors. If we again consider the situation with a phase detection at the NORESS array with arrival time T_{arr}, hypothesized to be a P-phase from an event in the highlighted target region, we find that the origin time of the event has to be within the following bounds:

$$OT_{low} = T_{arr} - TT_{max} - \frac{\Delta T}{2} - T_{dev-} \qquad (3)$$

$$OT_{high} = T_{arr} - TT_{min} + \frac{\Delta T}{2} + T_{dev+} \qquad (4)$$

These are the bounds actually used in the GBF matching procedure. Initial residual requirements (T_{dev-} and T_{dev+}) for P-phases in the GSETT-2 experiment were 1.5 seconds, whereas for S-phases they were set to 7.5 seconds.

Slowness vector tolerances

One way of including the effects of random errors when matching the estimated and predicted slowness vectors, is to require the absolute value of the slowness vector residual to be less than a predefined value. In the GSETT-2 experiment different requirements were used for three-component stations, high-frequency arrays and short-period arrays, reflecting their different abilities to correctly estimate the slowness vector.

The procedure of comparing a slowness vector observation with the predicted slowness and azimuth range of a target region, including the residual requirement, can be described by the following example:

Let us again consider the situation of a P-phase at the NORESS array from a hypothetical event in the highlighted target region of Fig. 7.5.4. A phase detection at NORESS has a slowness and azimuth estimate given by the asterisk on Fig. 7.5.7, and according to the GSETT-2 instructions, the corresponding residual requirement is 3.0 sec/deg, indicated by the circular area encompassing the estimated slowness vector. If there is an overlap between this circular area and the sector segment corresponding to the expected range of slowness vectors from the target region (also see Fig. 7.5.6), the phase detection is said to match the P-phase of a hypothetical event in the actual target region. On the other hand, if there is no overlap, the observation is not matching this hypothesis.

Additional constraints on the use of a phase detection

When initiating the GBF procedure with a predefined set of target regions, we compute and store the minimum and maximum azimuths and distances to every station in the network. The availability of these parameters enables us to constrain the use of a phase detection in a simple and well-organized way.

As an example, assume that we have a phase detection with peak frequency well above 10 Hz, and that we are trying to match this detection to an Lg phase from a hypothetical event in a target region located 15-20 degrees away from the recording station. Accumulated statistics has shown that at this station, Lg with peak frequencies above 10 Hz are

never observed from events at distances greater than 5 degrees. As such information is easily included in the data structure of the GBF procedure, we can compare this information to the actual distance to the target region, and consequently find that this phase detection cannot be an Lg phase originating in this target region.

Another example: A P and an S-phase recorded at an array station have been associated and an initial event location has been provided. Accumulated event statistics at this station has given us an estimate of the uncertainty of such one-array event locations. If a target region is located too far away from the one-array event location, these two phases can be excluded as originating from an event in this target region.

A third example: Several successive phase detections at a given station have been associated with the same event, either by automatic processing or by an analyst. If we are matching these detections to an event in a target region from where Pn is expected to be the first-arriving phase, only the first of the consecutive detections can possibly be the Pn-phase (we ignore multiple events at this stage). Such context-dependent information is straight-forward to include in the GBF algorithm.

These three examples constitute samples from three different classes of constraints that can be imposed on the use of a phase detection.

- Constraints inferred from measurements on a single phase, e.g., slowness vector, dominant frequency, frequency spectrum, polarization attributes, signal-to-noise ratios, etc.

- Constraints inferred from a reported event location at a given station.

- Constraints inferred from the pattern of detections at a given station. The last two types of constraints are based on so-called context-dependent information.

Step-by-step description of the GBF method

Having defined some of the key elements of the GBF method for phase association and event location, we will continue with a step-by-step description of the algorithm.

- **Definition of the station network**: Determine which stations to process for phase association and event location.

- **Definition of initial phase type candidates**: Decide the phase types that may be considered in the phase matching process, e.g. P, PKP, Pn, Pg, S, Sn, Lg, Rg, etc.

- **Constraining the use of the phase detections**: From phase measurements (dominant frequency, slowness, azimuth, etc.), single station location reports and other single-station context information, we do, for every phase detection at every station, impose constraints on their use. For each initial phase type candidate, every detection is assigned a row in a database table. This row may contain information on the allowable distance range, depth range, and azimuth range of a hypothetical event creating this hypothetical phase type. If no constraints are imposed, the distance range is set to 0-180 degrees, the depth range to 0-1000 km and the azimuth range to

± 180 degrees. If it is determined that a detection does <u>not</u> correspond to one of the initial phase-type candidates, e.g. Rg, the distance range of the Rg-row is set to a negative value.

- **Construct a grid of target regions**: By using the triangular method, a global grid system of a predefined density is constructed, see section 7.4.

- **Determine which of the initial phase type candidates to consider**: For every station-target region combination, we decide which of the initial phase type candidates to consider for phase matching. E.g., if a target region is located 60-70 degrees away from a station, it makes no sense to use regional phases like Pn, Pg, Sn, Lg or Rg. On the other hand, if a target region is located at regional distances from a station, teleseismic phases for that station can be ignored. Along with the list of phases to consider from each target region, we store the expected travel-times, slownesses and azimuths, as well as the respective tolerance limits. The decision of which phases to consider and their corresponding travel-times and slowness vectors can be inferred from general travel-time tables and great-circle azimuths, or, if available, from regional knowledge on the wave propagation characteristics at a given station, see section 7.3.

- **Compute generalized beams for each target region**: For each target region, at regular origin time intervals, we match the observed phase detections in the network to the predicted phase arrivals from a hypothetical event in the region. The value of the generalized beam at a given origin time is the actual number of matching phase detections. To avoid a list of phase associations that may look unreasonable from a seismological point of view, we have imposed three constraints in the phase matching process. These are:

  i)   A phase detection can be associated with only one hypothetical phase arrival.

  ii) A hypothetical phase arrival can be associated with only one phase detection, preferably the one with the smallest time residual.

  iii) The chronological order of the associated phase detections have to match the chronological order of the predicted phase arrivals. This is to avoid inconsistencies like an S-phase associated to arrive before a P.

  Along with the identifications of the matching detections (arids), we also store the time residuals relative to the center location of the target region. For stations providing azimuth and slowness estimates, the corresponding residuals are also stored.

- **Finding the event location from the *best* generalized beam**: If our predictions of phase arrivals are reasonable, an event should be reflected by a peak in the generalized beam representing the event target region. However, like in conventional beamforming, we encounter the problem of sidelobes, and will therefore have to select one generalized beam peak as representing the origin time and location of the event. Initially, we will use the procedure of considering the peaks at all generalized beams within a predefined time interval and select the one with the highest number of matching phases, and if equality, select the one with the smallest absolute time residual.

- **Remove associated phases and look for next event**: Once an event is located and the associated phases identified, these phases have to be removed from further consideration. This is done by recreating the generalized beams without using the phases associated to the located event, and then look for new peaks and new events.

GBF processing on a global scale with a large number of target regions is a computer intensive task. One way of reducing the computational load is to start out with a coarse grid, and then reprocess a denser grid surrounding the initial event location for a time interval around the event origin time. In the next sub-section the effect of the grid density will be illustrated with examples from GBF processing of GSETT-2 data.

The influence of grid density; an example with an earthquake in Tadjikistan

As a first test of global Generalized BeamForming, we have processed a 1 hour time interval of GSETT-2 data that included an earthquake in Tadjikistan. The event location provided by the Washington Experimental International Data Center was:

Date	Origin time	Latitude	Longitude	Depth	m_b	M_S
91/05/14	00:28:45.4	37.63N	72.30E	7 km	4.3	4.2

The GSETT-2 database consisted of detections from 60 stations, and as initial phase type candidates we used the teleseismic phases P, S and PKP, and the regional phases Pn, Pg, Sn, Lg and Rg. This is in accordance with the GSETT-2 instructions on the procedures for preparing an initial event list. Jeffereys-Bullen travel-time tables were used to predict the travel-times and slownesses, and directions along the great-circles were used to predict azimuths. Regional phases were only considered for distances within 20 degrees, and Rg only within 4 degrees. The other instructions relevant to the GBF algorithm, like time and slowness vector residual requirements and restrictions on the use of reported phases were also followed in the processing.

To investigate the influence of grid spacing on the resolution and performance of the GBF method, we first deployed a 162-point grid system covering the earth's surface. The corresponding circular areas encompassing each grid point had a radius of 11.0 degrees. For the generalized beams representing each target region, we searched for the maxima in a time interval ± 20 minutes around the origin time of the event. These maxima were then interpolated and contoured onto the global map of Fig. 7.5.8, where the color scale represents the number of associated phases at the maxima of the generalized beams. A clear peak is found at target regions near the event location, and the overall maximum was 13 associated phases.

Fig. 7.5.9 and 7.5.10 represent the same type of data, but computed with denser grid spacing. It is clearly seen that the resolution is improved and the sidelobe effect is reduced with denser grid spacing. The overall maxima in these figures were only 12 associated phases,

indicating that with a coarse grid spacing, phases with large time and/or slowness vector residuals can be associated as defining phases. However, by looking at the results from processing the coarse 162 point grid system (Fig. 7.5.8), we find that it provides a good initial location of the event. This location can subsequently be improved by constructing and processing a denser grid around the initial location.

We have in this study outlined some of the fundamentals for global Generalized Beam-Forming. The procedures for processing target regions of different areal extent has been described, and a step-by-step description of the procedure has been given. To obtain automatic event locations from processing GSETT-2 detection data, more program coding is needed. However, we have developed the framework for GBF processing on a global scale that facilitate research and testing of the method. This will become very useful in the development of the complete system.

T. Kværna

References

GSE/CRP/190/Rev.4 (1991): Instructions for the conduct of Phase 3 of GSETT-2, Group of Scientific Experts, UN Conference of Disarmament, Geneva, Switzerland.

Kværna, T. (1990): Generalized beamforming using a network of four regional arrays, Semiann. Tech. Summary, 1 April - 30 September 1990, NORSAR Sci. Rep. No. 1-90/91, Kjeller, Norway.

Kværna, T. (1992): Automatic phase association and event location using data from a network of seismic microarrays, Semiann. Tech. Summary, 1 October 1991-31 March 1992, NORSAR Sci. Rep. No. 2-91/92, Kjeller, Norway.

Ringdal, F. and T. Kværna (1989): A multi-channel processing approach to real time network detection, phase association, and threshold monitoring, Bull. Seism. Soc. Am., 79, 1927-1940.

Taylor, D.W. A. and S.K. Leonard (1992): General beamforming for automatic association, in Papers presented at the 14th Annual PL/DARPA Seismic Research Symposium, 16-18 September 1992, Loews Ventana Canyon Resort, Tucson, AZ, USA.

162 grid points

Fig. 7.5.1. A 162-point global grid system projected onto an azimutal orthographic projection of the earth. This grid system was obtained by a two-fold triangulation of the icosaeder, and each grid point represents a target region of 11 degrees radius.

642 grid points
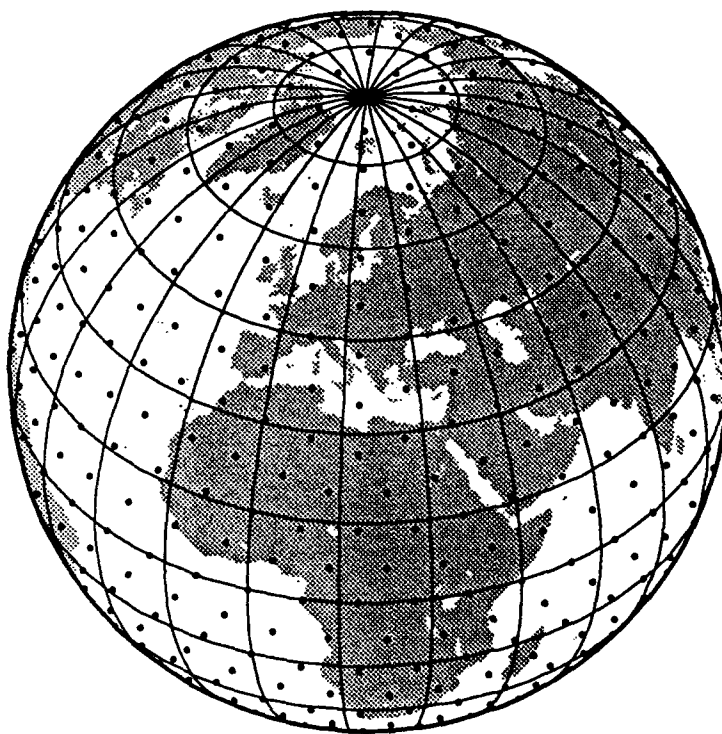
Fig. 7.5.2. A 642-point global grid system projected onto an azimutal orthographic projection of the earth. This grid system was obtained by a three-fold triangulation of the icosaeder, and each grid point represents a target region of 5.5 degrees radius.

2562 grid points
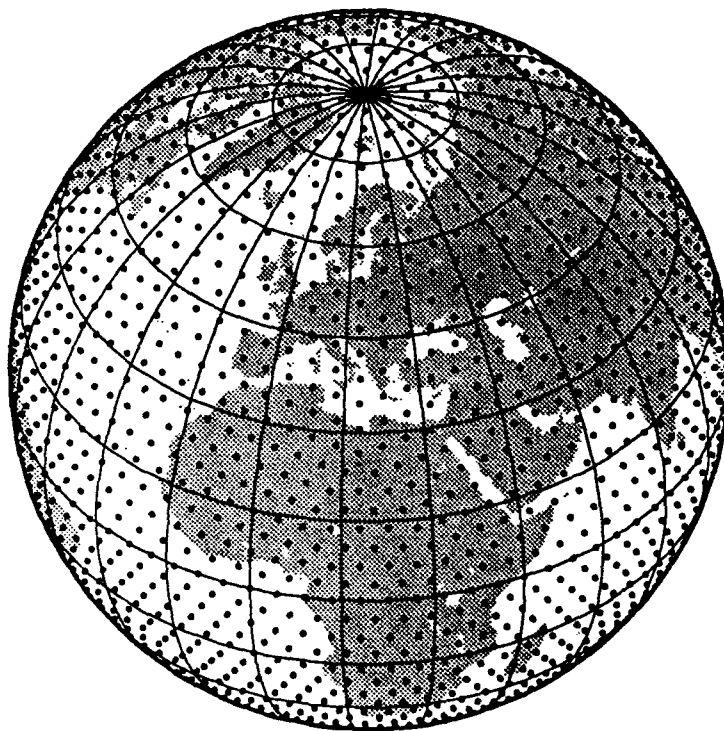
Fig. 7.5..3. A 2562-point global grid system projected onto an azimutal orthographic projection of the earth. This grid system was obtained by a four-fold triangulation of the icosaeder, and each grid point represents a target region of 2.7 degrees radius.

Distance 37.5 deg   Radius 11 deg
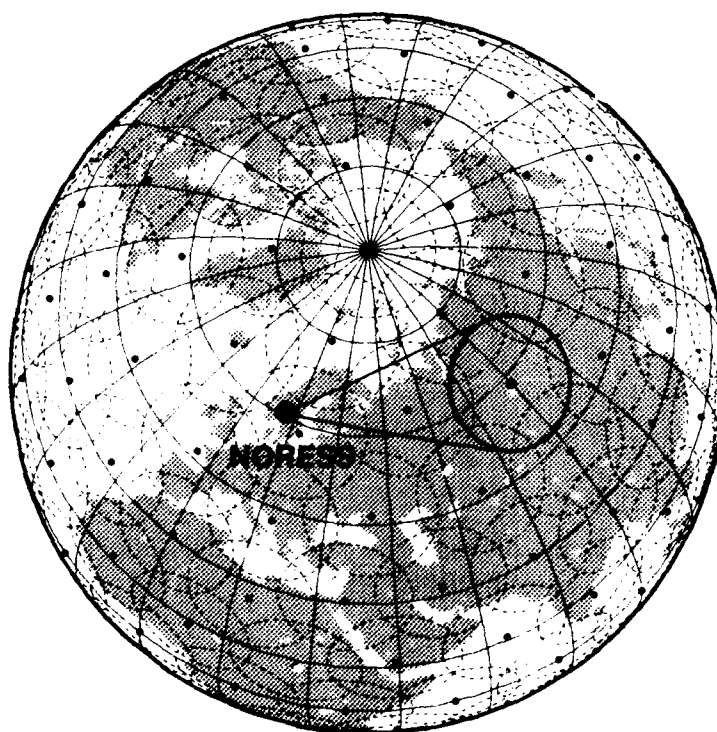
Fig. 7.5.4. A 162-point global grid system projected onto an azimutal orthographic projection of the earth. The circular target regions are shown by dashed circles, and the the highlighted target region is given special attention in this study. Its center point is located 37.5 degrees from the NORESS array. Minimum and maximum azimuthal lines from NORESS to the target region are also shown.

P-phase from 37.5 deg.
Region radius: 11 deg.

TT$_{min}$ TT$_{center}$ TT$_{max}$

300   350   400   450   500   550
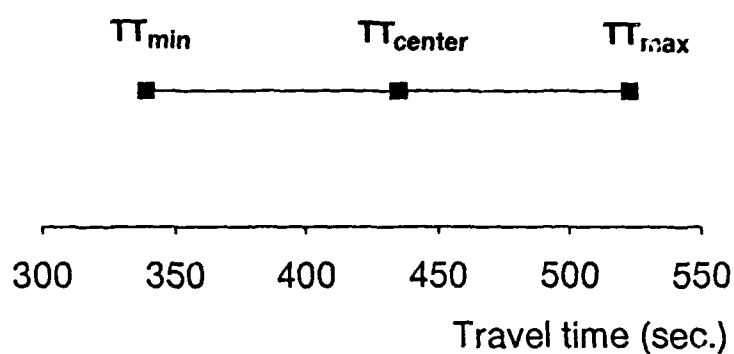
Travel time (sec.)

Fig. 7.5.5. Figure showing the range of predicted P-wave travel times from the highlighted
target region of Fig. 7.5.4 to the NORESS array.

P-phase from 37.5 deg.
Region radius: 11 deg.
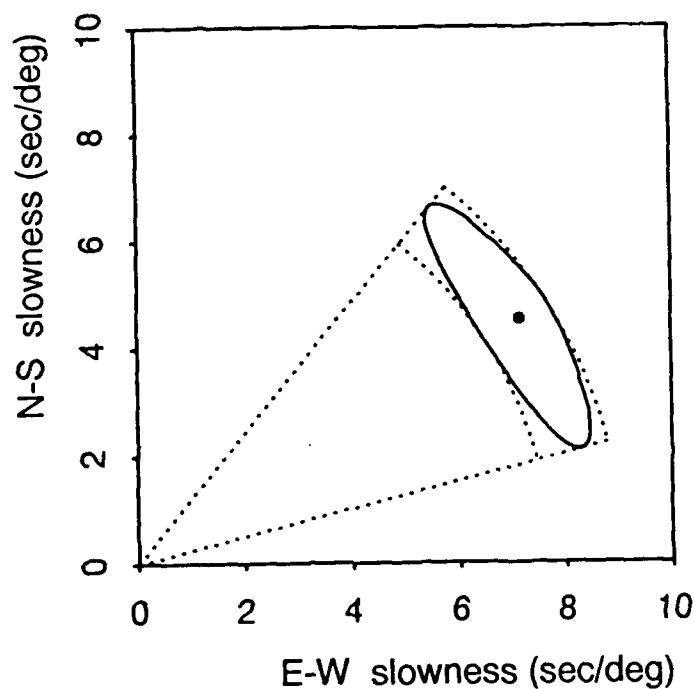
Fig. 7.5.6. Figure showing the range of predicted P-wave slowness vectors at NORESS for events in the highlighted target region of Fig. 7.5.4. The slowness vectors of the circular boundary of the target region are projeted onto the solid line of this figure. An approximation to the area inside this solid line is given by the dotted sector segment defined by the minimum and maximum azimuths and the minimum and maximum slownesses.

Matching slowness observation
Residual requirement: 3.0 sec/deg.
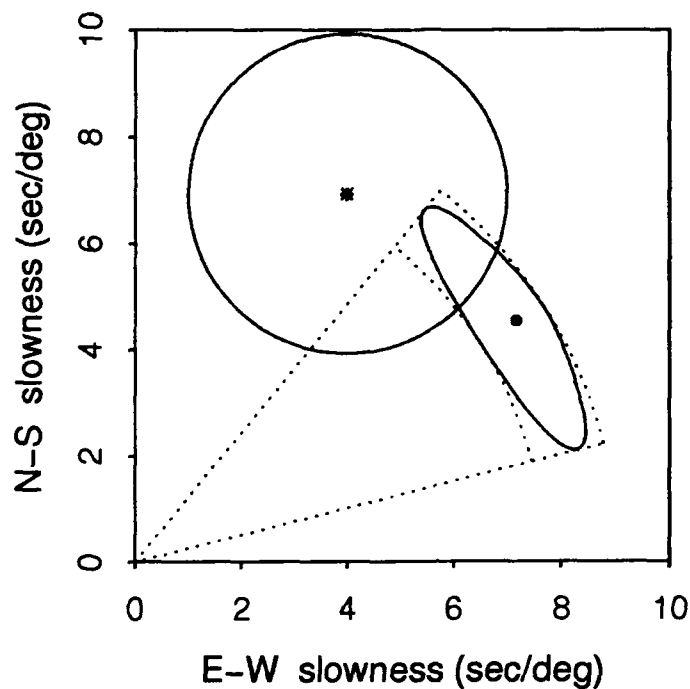
Fig.7.5.7. Figure illustrating the procedure used when matching observed and predicted slowness vectors. As explained in Fig. 7.5.6, the dotted sector segment approximate the expected range of P-wave slowness vectors for events in the target region. The slowness vector estimate of a detected phase is given by the asterisk, and the maximum allowable slowness vector residual (determined à priori) determines the surrounding circle. As seen on the figure, there is an overlap between this circular area and the sector segment corresponding to the expected range of slowness vectors for P-waves from the target region. Thereby, the phase detection is considered to match the slowness vector of the P-phase of a hypothetical event in the actual target region.

162 grid points
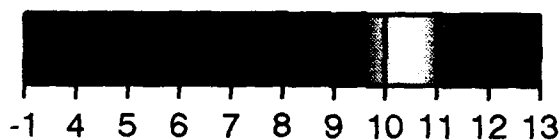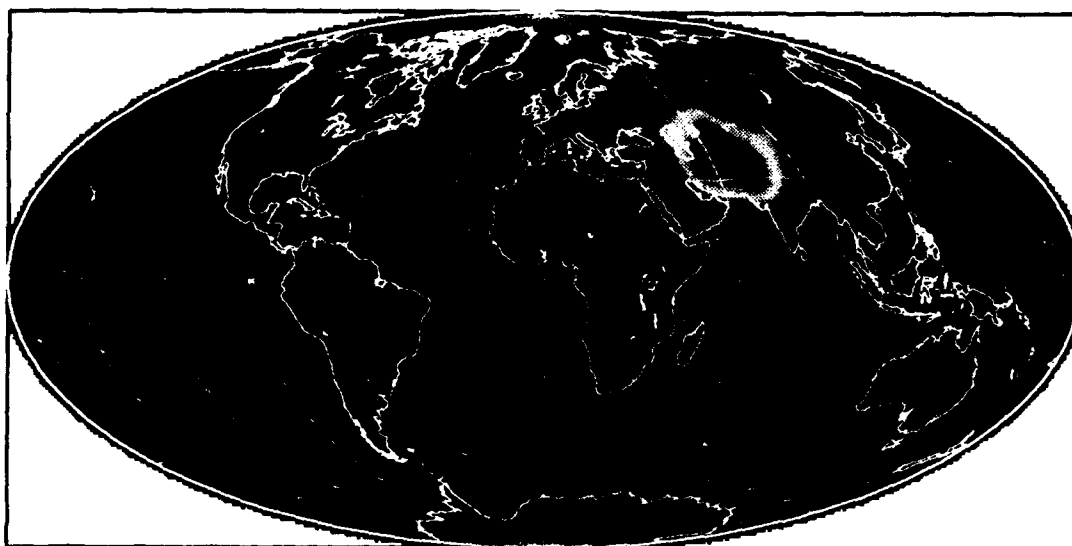
Tadjikistan

Fig. 7.5.8. Contoured maxima of generalized beams for a 162-point grid system. The maxima of each generalized beam were found by searching a time interval of ± 20 minutes around the origin time of an event in Tadjikistan. The colour scale represent the number of associated phases.

642 grid points
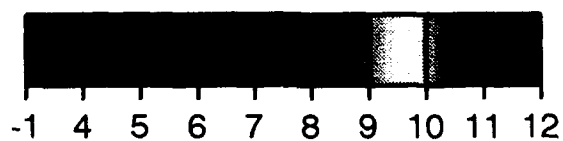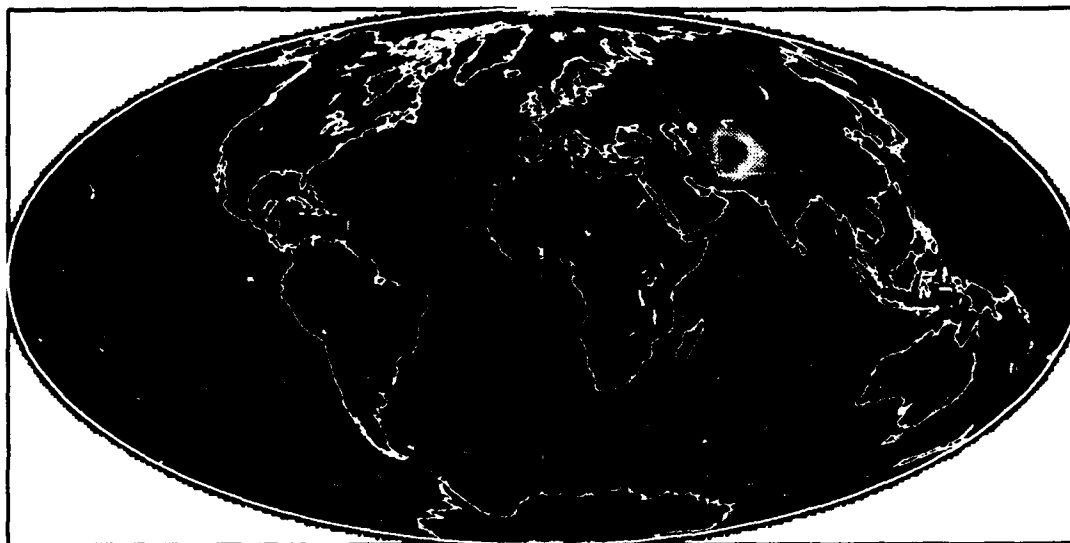
Tadjikistan

Fig. 7.5.9. Same as Fig. 7.5.8, but with a 642-point grid system.

2562 grid points
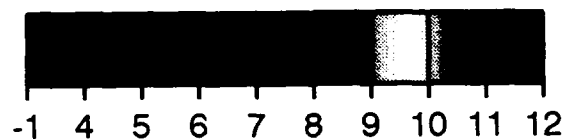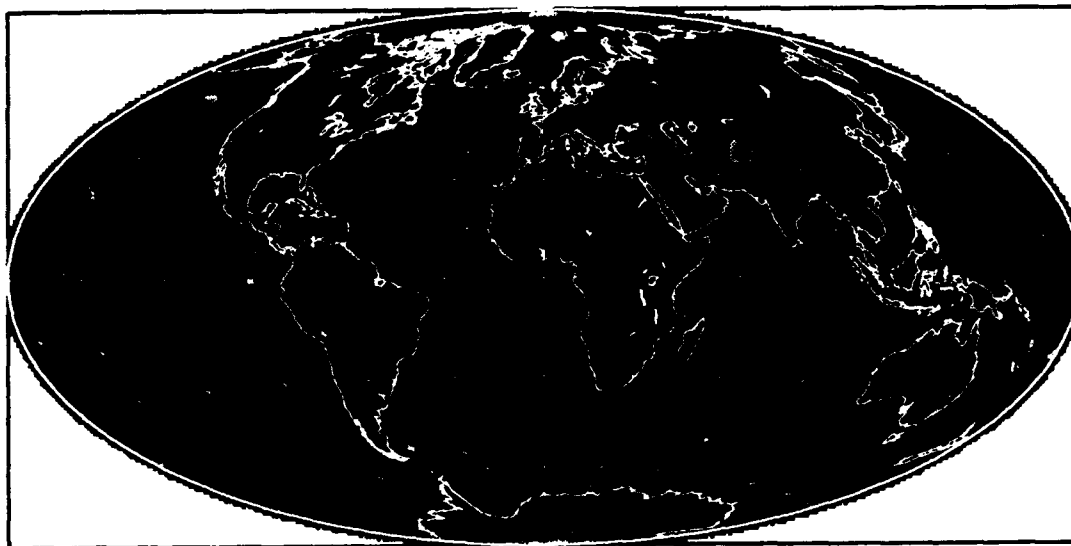
Tadjikistan

Fig. 7.5.10.. Same as Fig. 7.5.8, but with a 2562-point grid system.

7.6   The Ukrainian event of 16 September 1979

On 28 June 1992, an article appeared in the *New York Times* of considerable interest to scientists working in the field of seismic monitoring:

Excerpt from the New York Times, 28 June 1992

> "(headline) Izvestiya Reports '79 A-Test at Ukraine Mine
>
> MOSCOW, June 27 (AP) -- Soviet scientists set off a nuclear blast in 1979 next to a Ukrainian coal mine, then sent thousands of miners back to the shaft a day later without telling them, the newspaper Izvestiya reported.
>
> The article, published on Friday, may shed some light on long-standing assertions by miners that a nuclear blast caused unusually high levels of radiation around a town it identified as Yunokommunarsk.
>
> Izvestiya said officials have previously attributed the level of radiation in the area, which has registered three or four times normal, to industrial waste and to the 1986 nuclear disaster at Chernobyl, 625 miles to the northwest.
>
> Izvestiya did not report higher incidences of death, cancer or other diseases in the area near the mine, and officials could not be reached for comment today.
>
> The report said the bomb had been detonated to see if the explosion would clear the mine of dangerous methane gas. It added that officials had disguised the incident by staging a civil defense drill and evacuating the town's 8,000 residents, most of whom were miners."

It turned out that the original release from AP had more information than used by the *New York Times*. Thus AP stated that the detonation occurred at noon Sept 16, 1979 and that the yield was 1/3 kt. The location of the town, Yunokommunarsk, is approximately 48.22°N, 38.30°E.

Based on this information, we examined available seismic event lists in detail to see if this event could be confirmed. We searched for an event with origin time near 09.00.00 GMT, which corresponds to noon Moscow time. However, the event was not reported, neither by agencies using global network data (ISC, NEIC) nor by other available sources.

The Ukrainian event was not reported in the NORSAR monthly bulletin. However, the NORSAR automatic detector operates at a very low threshold, and many small events, especially at regional distances, are detected but not included in the monthly bulletins.

For this reason, we decided to check the original automatic detection lists in the NORSAR archive. It turned out that the automatic (unedited) NORSAR bulletin for 16 Sep 79 contains an event with the following parameters:

Origin time (GMT): 08.59.53
Location: 45N, 34E, Crimea region
Magnitude (m_b): 3.3

The automatic plot for this event has been saved (Fig. 7.6.1), and shows a high frequency signal, visible on at least 4 subarrays, but with poor signal coherency across the full NOR-SAR array. The analyst did not consider the event solution to be of high enough quality to include it in the final NORSAR bulletin, although there is no question that the event is real (and not a noise detection).

Unfortunately, at the time when this event occurred NORSAR could save only selected data intervals on tape. At the time, there seemed to be no reason to save this event, so the digital data is no longer available. Only the event plots and the detector listings have been retained.

The automatic location estimate (45N 34E) is somewhat different from the location of Yunokommunarsk, but well within the uncertainty for an event with such low signal coherency. The estimated origin time is 7 seconds before the hour. As is well known, the traditional Soviet PNE practice has been to detonate such explosions exactly on the hour.

Next, we tried to constrain the origin time of the event, under the assumption that its location was near Yunokommunarsk (see Fig. 7.6.2). Under the assumption that the event in question had an epicenter 48.22°N, 38.30°E, its origin time is estimated to be as follows:

08.59.59.6 (using the IASPEI 1991 travel-time tables)
08.59.56.7 (using the Jeffreys-Bullen tables).

In both cases, zero depth has been assumed. The signal arrival time was re-read visually from the plot (the correction was minor relative to the automatic arrival time estimate).

As is well known, the Jeffreys-Bullen tables tend to give 2-3 seconds too early origin time estimates for Eurasian explosions, so the data are consistent with an origin time exactly on the hour and a location approximately as given in the press report.

In terms of nuclear monitoring research, there are some important lessons to be learned from this case study. Most importantly, automatic detector information is valuable. It should not be discarded, even when the analyst determines that the signal is of poor quality, or the signal parameters are poorly defined. This is consistent with the conclusions reached by the Geneva Group of Scientific Experts, which has repeatedly stressed that all detected seismic signals should be reported by the participating stations in a future global seismic network.

This case study also highlights an important consideration for CTB verification: seismic methods will be only one of several monitoring tools. If an indication is obtained from some other source that a clandestine explosion might have taken place, it is important to be able to confirm it through seismic recordings. This requires that at least one station in a global network is sensitive enough to provide such confirmation.

Finally, it should be noted that at the time this event occurred there was no advanced regional array network in northern Europe. Today, the network of high-quality regional seismic arrays NORESS, ARCESS, FINESA, GERESS, as well as other contributing arrays, are in continuous operation. Their recordings are regularly analyzed using the advanced Intelligent Monitoring System (IMS). Had such an event occurred today, it would with high probability have been detected, accurately located and reported. However, an event this small would probably still be unidentified if the only data available were recorded at teleseismic distances. Even with regional data available, it can often be difficult to identify such low-magnitude events reliably using current methods. Event identification at low magnitudes remains one of the most important research topics in the field of seismic monitoring.

F. Ringdal, NORSAR
P.G. Richards, Columbia University

NORSAR BULLETIN   16 SEP 1979 (DOY 259)   EPX B4030   BPB 1.6-3.6 HZ
2 8 59 53 45.0N   34.0E   330 0 3.3 361 CRIMEA REGION
3 9 4 32.8 NB2 P   1.3   0.8   10.0 20.9   125.3
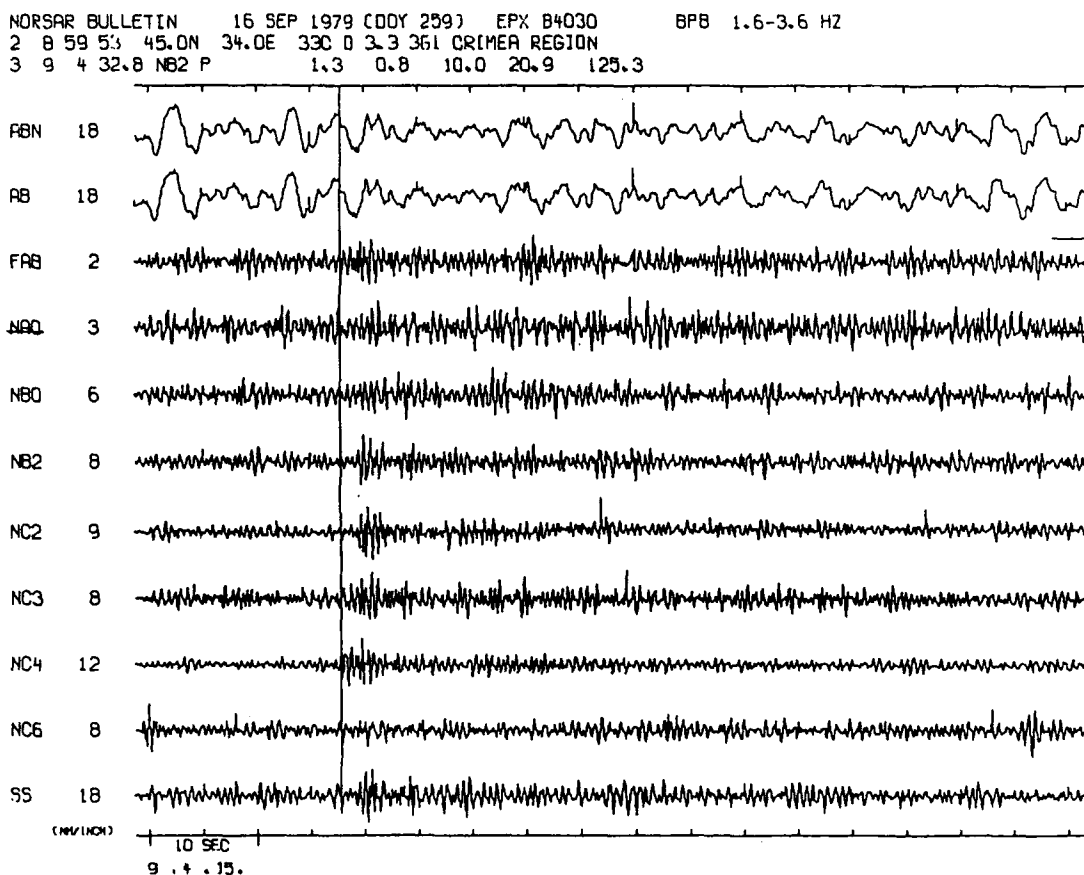
Fig. 7.6.1. NORSAR automatic event processing result for the event described in the text. The upper three traces are array beams, and the next 7 traces are subarray beams, filtered in the band 1.6-3.6 Hz. The vertical line marks the estimated arrival time. The three lines of text at the top summarize the automatically determined event parameters.
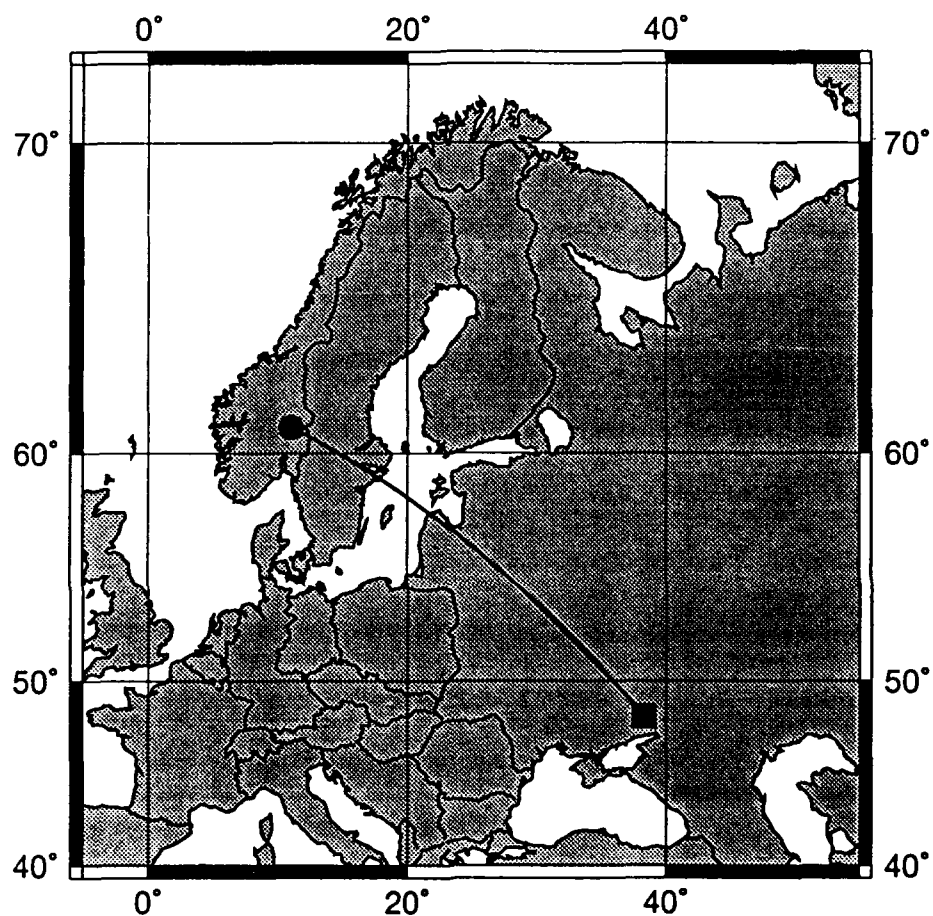
Fig. 7.6.2. Map showing the location of the town Yunokommunarsk in Ukraine (filled square) together with the great circle path to the NORSAR array (filled circle). The distance is approximately 2200 km.

7.7   Induced seismicity in the Khibiny Massif (Kola Peninsula)

The topic of this paper is to review recent processes of increasing seismic activity in the Khibiny Massif in the Kola Peninsula. It is a typical example of induced seismicity caused by rock deformation due to the extraction of more than $2 \cdot 10^{J}$ tons of rock mass since the mid-1960s. The dependence of seismic activity on the amount of extracted ore is demonstrated. Some, but not all, of the induced earthquakes coincide with large mining explosions, thus indicating a trigger mechanism. The largest earthquake, which occurred on 16 April 1989 ($M_L = 4.1$) could be traced along the surface for 1200 m and observed to a depth of at least 220 m. The maximum measured displacement was 20 cm.

Introduction

The Khibiny alkaline Massif (see Fig. 7.7.1) situated in the middle of the Kola Peninsula is tectonically unstable. Its seismic activity has been characterized by groups of a few earthquakes with typically 8-10 years between groups (Panasenko, 1969). The Massif consists of different blocks separated from each other by faults. The recent crustal movements are in the range from 2 to 4 mm/year (Yakovlev, 1982).

The exploitation of the Khibiny apatite ores started in 1929 and since then about $2.5 \cdot 10^{9}$ tons of rock have been mined from an area of about 10 km^2. This corresponds to a decrease of the gravitational component by typically 2.5-3.0 MPa, and for some parts of the Massif by as much as 9-12 MPa.

At the present time more than 10^8 tons of ore are extracted annually from three underground and three open-pit mines. The velocity of the uplift of the near-surface parts is of the order of 70 mm/year for some tunnels (Panasenko and Yakovlev, 1983).

Seismic activity of the Khibiny Massif

The extensive mining has disrupted the natural geodynamic process in the area, causing a redistribution of crustal stress, which in turn has led to increased seismic activity. Fig. 7.7.2 shows in this respect the cumulative seismic energy release and the amount of extracted ore for the mines in the Khibiny Massif. The seismic energy (E) released has been calculated from the formula (Meyer and Ahjos, 1985):

$$\log E = 12.30 + 1.27 M_L \tag{1}$$

where E is expressed in ergs. The similarity of the two curves strongly indicates a causal connection. It should be noted here that the earthquake catalogue is considered homogeneous back to 1978.

The dependence of seismic activity on the extracted deposit volume has long been known from observations (Glowacka and Kijko, 1989). In the Khibiny Massif a more intensive excavation began in the mid-1960s, while the first significant tremors occurred in 1981. During that year four felt earthquakes (intensity I = 3-4 on the MSK scale) occurred in the vicinity of the mines. Some of these earthquakes were accompanied by sonic effects.

Around the same time, many rockbursts occurred near mines I and II (see Fig. 7.7.1), each of them displacing tons of rocks (1-10 m^3). In fact, during five hours on 17 May 1981 more than 20 rockbursts occurred. And for the first time the occurrence of an earthquake at the time of an explosion was observed. Now this situation is typical for events in the Khibiny Massif.

The largest earthquakes

An earthquake with intensity more than 5 in the nearby town of Kirovsk occurred on 29 August 1982 immediately after an explosion of 106 tons in mine II and at the time of a smaller quarry explosion (4.6 tons) between mines I and II.

The next significant earthquake, felt with intensity I = 5 at Kirovsk, was on 19 June 1984. Less than one second before this earthquake there was a small explosion (40 kg, mine II). A large block of rock (65x70x70 m^3) was broken and one part of it was displaced relative to another by about 5 cm. After this earthquake there were so many rockbursts that it was impossible to carry out work in this mine for two weeks.

The strongest such earthquake (M_L = 4.1), on 16 April 1989, occurred almost simultaneously with a large explosion (240 tons) in mine I. This earthquake was felt with I = 8 in the upper levels of the mine and I = 5-6 at Kirovsk. The maximum measured displacement was 20 cm, and it occurred along a fault striking at 125-135° and dipping at 30-35° NE. The displacement was traced along the surface for 1200 m and observed to a depth of at least 220 m. This event was recorded by all seismic stations within a distance of 1000 km. Fig. 7.7.3 shows ARCESS recordings of this earthquake (distance 420 km).

The earthquake was accompanied by a great number of aftershocks attaining several hundred for the two subsequent months. On 24 July 1989 another earthquake occurred here. Its size was much less (see Table 7.7.1); however, remarkable destruction again took place in this mine.

Conclusions

This paper has discussed to principal topics: a) the question of induced seismicity caused by rock excavation and b) the question of mining explosions as a trigger for earthquakes and rockbursts.

At present it is too early to make a definite conclusion about the triggering mechanism between explosions and earthquakes. In some cases pairs of such events are separated by some milliseconds (for example, 16 April 1989, Fig. 7.7.3); in other cases they are separated by some seconds or more, sometimes they are not connected in time (for example, 2 June 1992, Fig. 7.7.4).

However, the increase of seismic activity in the Khibiny Massif caused by the rock deformation due to the extraction of large volumes of rock mass is clearly demonstrated.

E.O. Kremenetskaya and V.M. Trjapitsin
**Kola Regional Seismological Centre, Apatity, Russia**

References

Glowacka, E. and Kijko, A. (1989). Continuous evaluation of seismic hazard induced by the deposit extraction in selected mines in Poland. ESC Proceedings, 21st Gen. Ass. Sofia, Bulgaria, 23-27 August 1988, 444-451.

Meyer, K. and Ahjos, T. (1985). Temporal variations of energy release by earthquakes in the Baltic Shield. Geophysica, Vol. 21, 1, 51-64.

Panasenko, G.D. (1969). Seismic features of the northeast Baltic Shield. Leningrad: Nauka, 184 pp (in Russian).

Panasenko, G.D. and Yakovlev, V.M. (1983). About the nature of anomalous deformation of a transport tunnel in the mountain Yukspor. In: Geophysical Investigations in the Europe in North of the USSR, KB AS USSR, Apatity, 38-44 (in Russian).

Yakovlev, V.M. (1982). Recent crustal movement in the zone of the southern contact of the Khibiny Massif from data geometric levelling. In: Geophysic and geodynamic investigations of the North-East of the Baltic Shield, KB AS USSR, Apatity, 85-88 (in Russian).

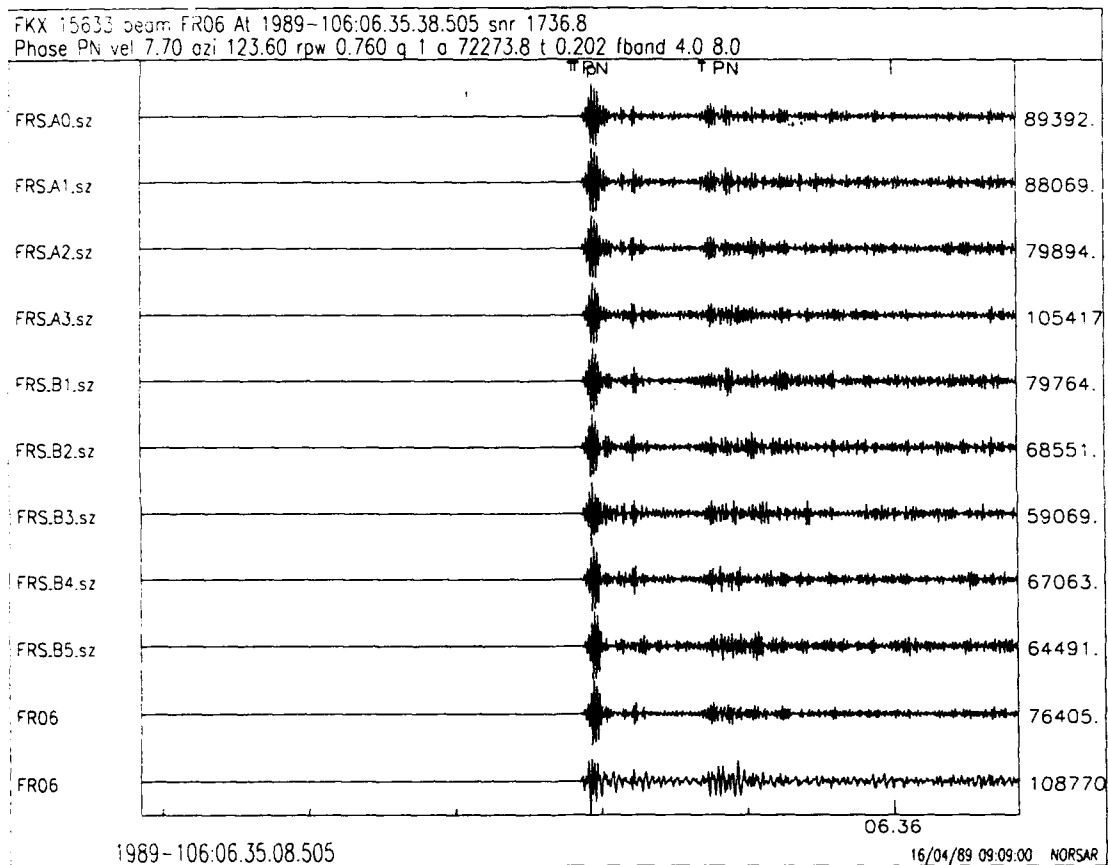| No.	Date	Origin time	Distance (km)	Coordinates		ML	Seismic energy (ergs)
1	1948	0923 0000	17.0	67.70 N	33.60 E	3.1	1.58E16
2	1955	0808 172059	17.0	67.70 N	33.60 E	3.2	2.24E16
3	1955	0831 2115	17.0	67.70 N	33.60 E	2.5	2.80E15
4	1960	0209 210731	10.0	67.60 N	33.60 E	2.0	7.08E14
5	1974	0930 091142	17.0	67.70 N	33.70 E	3.5	6.31E16
6	1979	1212 113452	13.0			2.1	9.27E14
7	1981	0416 205634	20.0			2.1	9.27E14
8	1981	0517 075528	17.0			2.3	1.30E15
9	1981	18 000747	19.2			2.5	2.98E15
10	1982	0422 110258	22.5			2.1	9.27E14
11	1982	0829 053335	17.0	67.70 N	33 70 E	3.3	3.10E16
12	1984	0619 054731	17.0	67.33 N	33.70 E	3.9	1.79E17
13	1984	1030 105158	35.0			2.2	1.24E15
14	1984	1030 142148	17.5	67.68 N	33.72 E	2.3	1.66E15
15	1987	0725 161339	22.5	67.66 N	33.90 E	2.9	9.60E15
16	1988	0113 025153	25.0	67.73 N	33.83 E	2.6	4.00E15
17	1988	0118 020948	24.0	67 65 N	33.96 E	2.6	4.00E15
18	1988	0120 121510	6.0	67.60 N	33.50 E	2.6	4.00E15
19	1988	0211 124113	27.0			2.2	1.20E15
20	1988	0304 231701	18.0	67.70 N	33.70 E	2.1	9.30E14
21	1988	0416 115725	18.0	67.66 N	33.75 E	2.1	9.30E14
22	1988	0622 013408	10.5	67.65 N	33.47 E	2.4	2.20E15
23	1988	1006 094741	32.0	67.61 N	34.19 E	3.3	3.10E16
24	1988	1123 211108	23.0	67.60 N	33.80 E	2.5	3.00E15
25	1989	0203 102741	33.7	67.80 N	33.90 E	2.2	1.20E15
26	1989	0416 063442	18.0	67.61 N	33.81 E	4.1	3.20E17
27	1989	0707 114924	26.5	67.71 N	33.93 E	3.4	4.10E16
28	1989	0724 223234	15.0	67.60 N	33.78 E	2.5	3.00E15
29	1989	0804 012618	21.0	67.60 N	33.90 E	2.1	9.30E14
30	1990	0210 163907	37.1	67.89 N	33.48 E	2.2	1.20E15
31	1990	0403 075417	26.5	67.60 N	33.90 E	2.1	9.30E14
32	1990	0612 113532	36.7	67.63 N	34.29 E	2.1	9.30E14
33	1990	0621 130954	20.5	67.67 N	33.83 E	2.3	1.70E15
34	1990	0621 231904	15.5	67.67 N	33.66 E	2.2	1.20E15
35	1990	0622 015115	16.5	67.61 N	33.81 E	2.4	2.20E15
36	1990	0624 065848	19.4	67.61 N	33.88 E	2.4	2.20E15
37	1990	0625 062215	16.2	67.56 N	33.82 E	2.3	1.70E15
38	1990	0625 113116	16.1	67.61 N	33.80 E	2.2	1.20E15
39	1990	0625 215128	15.3	67.67 N	33.66 E	2.3	1.70E15
40	1990	0626 052403	19.1	67.72 N	33.30 E	2.4	2.20E15
41	1990	0627 004129	24.4	67.77 N	33.29 E	2.3	1.70E15
42	1990	0627 025428	19.6	67.67 N	33.79 E	2.2	1.20E15
43	1990	0627 051520	23.6	67.59 N	33.99 E	2.4	2.20E15
44	1990	0627 064141	29.0	67.66 N	34.07 E	2.8	7.20E15
45	1990	0628 015919	22.8	67.74 N	33.22 E	2.6	4.00E15
46	1990	0629 041211	19.4	67.69 N	33.75 E	2.8	7.20E15
47	1990	0630 045139	20.4	67.62 N	33.90 E	2.4	2.20E15
48	1990	0630 064224	28.0	67.64 N	34.10 E	2.6	4.00E15
49	1991	0305 000836	23.7	67.55 N	34.00 E	2.1	9.30E14
50	1991	0505 054802	28.5	67.65 N	34.07 E	2.1	9.30E14
51	1991	0815 083545	24.1	67.63 N	33.98 E	2.1	9.30E14
52	1991	1229 151425	27.0	67.70 N	33.96 E	2.1	9.30E14
53	1991	1229 152044	25.0	67.57 N	34.03 E	2.1	9.30E14

Table 7.7.1. Known earthquakes ($M_L > 2.0$) in the Khibiny Massif 1948-1991. The distance to the APA station in Apatity is indicated.
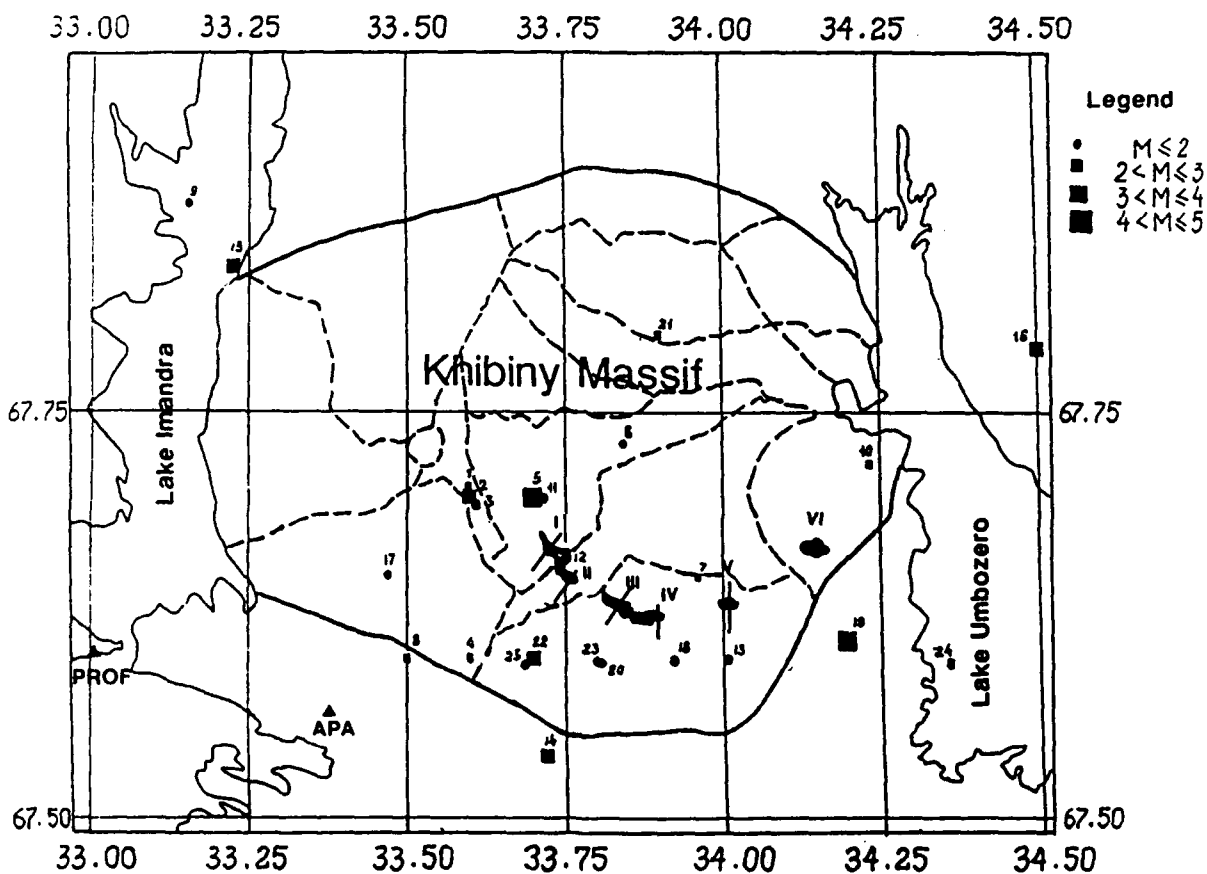
Fig. 7.7.1. The position of mines (I-VI) in the Khibiny Massif together with fault struc-
tures and earthquakes. Mines I, II and III are underground, whereas IV, V and VI are
open-pit mines. The location of the Apatity seismic station (APA) is also shown.
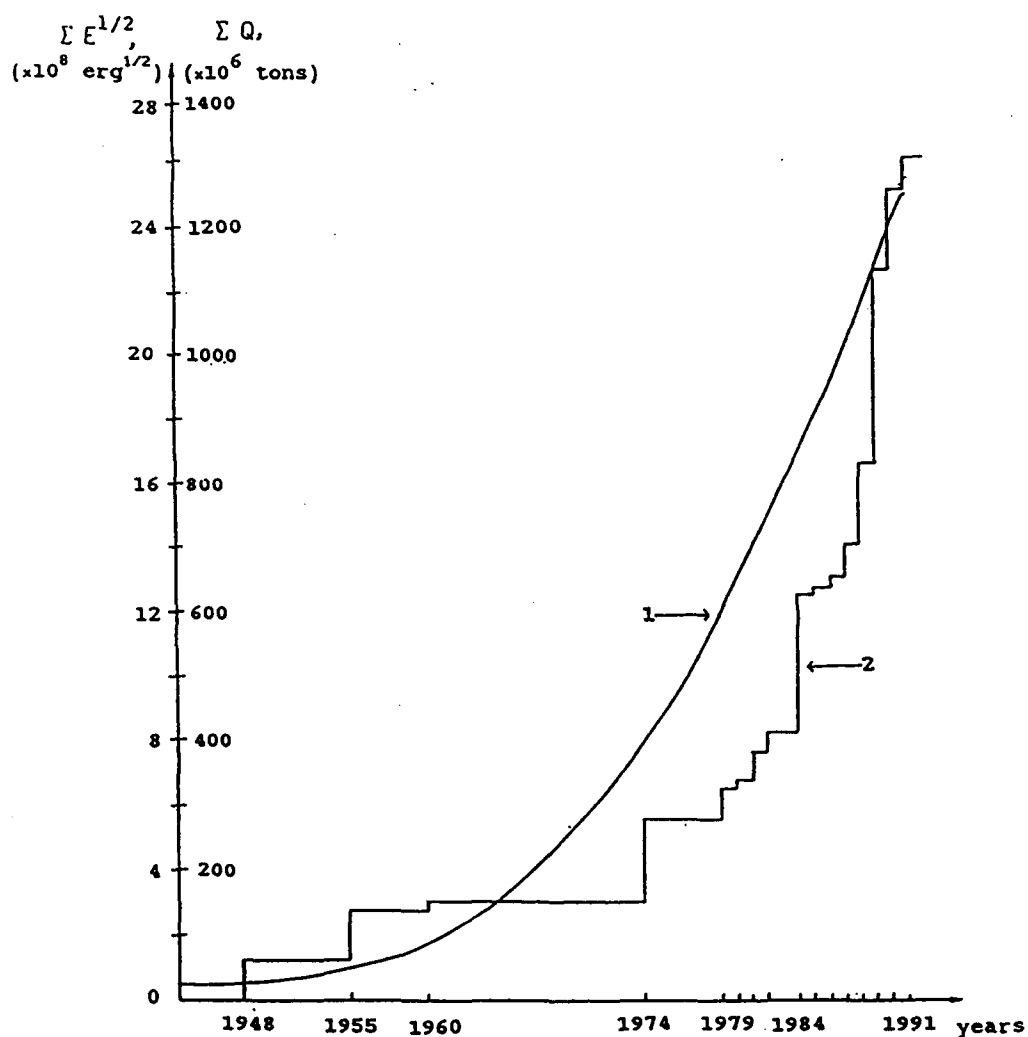
Fig. 7.7.2. Cumulative distributions versus time of extracted masses of the apatite mineral (1) and Benioff's graph of released energy (2) for the Khibiny Massif. Note the similarity between the two graphs.

FKX 15633 beam FR06 At 1989-106:06.35.38.505 snr 1736.8
Phase PN vel 7.70 azi 123.60 rpw 0.760 q 1 a 72273.8 t 0.202 fband 4.0 8.0

FRS.A0.sz	PN PN	89392.
FRS.A1.sz		88069.
FRS.A2.sz		79894.
FRS.A3.sz		105417
FRS.B1.sz		79764.
FRS.B2.sz		68551.
FRS.B3.sz		59069.
FRS.B4.sz		67063.
FRS.B5.sz		64491.
FR06		76405.
FR06		108770

1989-106:06.35.08.505   06.36
                                    16/04/89 09:09:00   NORSAR

Fig. 7.7.3. ARCESS recordings of the 16 April 1989 earthquake (M_L = 4.1) in the Khibiny Massif. The earthquake occurred almost simultaneously with a 240 ton explosion, and it is not possible to visually separate the P phases for the two events.
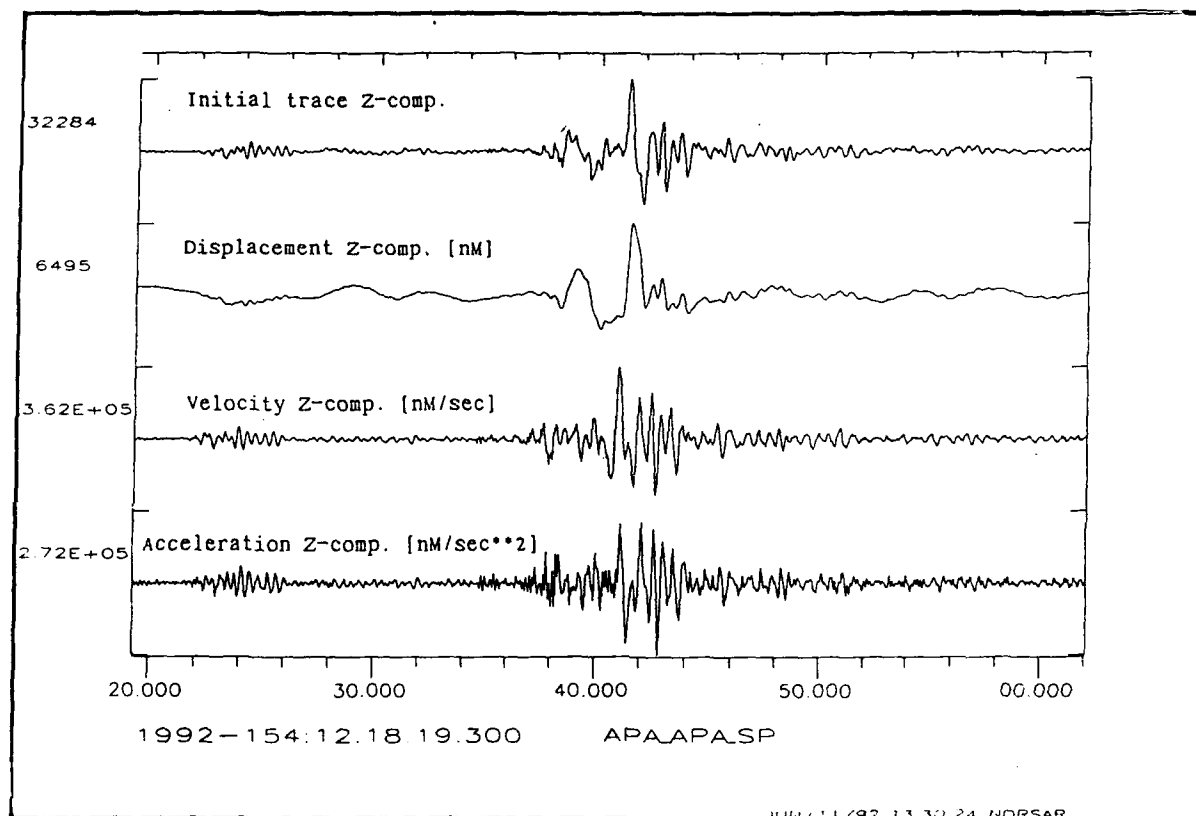
Fig. 7.7.4. A double earthquake in the Khibiny Massif on 2 June 1992 (M_L(ARCESS) = 2.0 and 2.5, respectively). The figure shows APA SPZ recordings, initial trace as well as displacement, velocity and acceleration. These earthquakes were not associated with any mining explosion.